The function of the Notch signalling pathway in pattern formation and head regeneration in *Hydra*



Qin Pan

München, 17. Januar 2025

The function of the Notch signalling pathway in pattern formation and head regeneration in *Hydra*

Dissertation

an der Fakultät für Biologie

der Ludwig-Maximilians-Universität München

vorgelegt von

Qin Pan

München, 17. Januar 2025

Diese Dissertation wurde angefertigt
unter der Leitung von Prof. Dr. Angelika Böttger
im Fachbereich Zell- und Entwicklungsbiologie
an der Fakultät für Biologie
der Ludwig-Maximilians-Universität München.

Erstgutachter: Prof. Dr. Angelika Böttger

Zweitgutachter: Prof. Dr. Christof Osman

Tag der Abgabe: 17.01.2025

Tag der mündlichen Prüfung: 15.07.2025

Eidesstattliche Erklärung

Ich, Qin Pan, erkläre hiermit, dass diese Dissertation mit dem Titel "Die Funktion des

Notch-Signalwegs bei der Musterbildung und Kopfregeneration bei Hydra", die ich zur

Erlangung des Doktorgrades (Doktor rerum naturalium) in Biologie an der Ludwig-

Maximilians-Universität München eingereicht habe, meine Originalarbeit ist. Ich bestätige,

dass diese Dissertation weder ganz noch teilweise für einen anderen Abschluss oder eine

andere Qualifikation bei einem anderen Prüfungsausschuss eingereicht wurde.

München, 17. Januar 2025

Qin Pan

Statutory Declaration

I, Qin Pan, hereby declare that this thesis, titled "The Function of the Notch Signalling

Pathway in Pattern Formation and Head Regeneration in *Hydra*", submitted for the degree

of Doctor of Philosophy (PhD) in Biology at Ludwig-Maximilians-Universität München, is

my original work. I confirm that this thesis has not been submitted, either in whole or in

part, for any other degree or qualification at any other examination board.

Munich, 17. January 2025

Qin Pan

٧

Publications presented in this thesis

- Pan, Q., M. Mercker, A. Klimovich, J. Wittlieb, A. Marciniak-Czochra and A. Bottger (2024). "Genetic interference with HvNotch provides new insights into the role of the Notch-signalling pathway for developmental pattern formation in *Hydra*." <u>Sci Rep</u> 14(1): 8553.
- Moneer, J., S. Siebert, S. Krebs, J. Cazet, A. Prexl, Q. Pan, C. Juliano and A. Bottger (2021). "Differential gene regulation in DAPT-treated *Hydra* reveals candidate direct Notch signalling targets." <u>J Cell Sci</u> 134(15).
- 3. Steichele, M*., L. Sauermann*, **Q. Pan***, J. Moneer, A*. de la Porte, M. Heß, M. Mercker, C. Strube, H. Flaswinkel, M. Jenewein and A. Böttger (2025). "Notch signaling mediates between two pattern-forming processes during head regeneration in *Hydra*." Life Science Alliance 8(1): e202403054. *equal contribution

Statement of my contributions

1. Pan et al. (2024): I conducted all experiments except for *Hydra* embryo injection,

performed by Alexander Klimovich and Jörg Wittlieb, and the establishment of the

mathematical model, which was developed by Moritz Mercker (Fig. 8A). I carried out

all data analyses (Fig. 1 to Fig. 7 and Fig. 8B), drafted the paper and contributed to its

revision.

2. Moneer et al. (2021): I contributed to the data analysis, focusing on sequence

alignment and protein structure identification for a subset of Notch-responsive genes.

of The result my work be accessed can at

https://figshare.com/articles/figure/Figure S3 pdf/14714169?file=28258539.

Additionally, I participated in the revision of this paper.

3. Steichele et al. (2025): I conducted experiments and performed data analyses related

to the entire HyKayak section (Fig. 5 and supplementary Fig. S1, S2). I also

contributed to the RT-qPCR data analyses for Fig. 3 and Fig. 4. Additionally, I

participated in drafting the HyKayak section of this paper and in revising the entire

content.

We hereby confirm the accuracy of the above statements

Qin Pan

Supervisor: Angelika Böttger

ix

Declaration of contributions as a co-first author

The four first authors of the third publication represented in this thesis entitled: "Notch-

signaling mediates between two pattern forming processes during head regeneration in

Hydra" and published in Life Science Alliance 8 (1) 2024

contributed equally as follows:

Mona Steichele: conceptualization, further investigation, methodology, and writing the

original draft. Lara Sauermann: data curation, investigation, methodology, reviewing and

editing of the manuscript. Qin Pan: conceptualization, further investigation, methodology,

data curation, drafting the HyKayak section of the manuscript, reviewing and editing of

the manuscript. Jasmin Moneer: conceptualization, investigation, methodology, reviewing

and editing of the manuscript.

Mona Steichele, Lara Sauermann, and Jasmin Moneer contributed to the *Hydra* treatment

with inhibitors, the observation of the head regeneration phenotypes and organizer

formation abilities after inhibitor treatment, and the RT-qPCR analysis of gene expression

dynamics under inhibitor treatments. Additionally, Lara Sauermann contributed the

regeneration studies of Craspedacusta polyps. Qin Pan conducted all experiments and

performed data analysis for the HyKayak section of the paper.

Angelika Böttger

Mona Steichele

Jasmin Moneer

Lara Sauermann

Qin Pan

χi

Contents

Abbreviations	. 1
Summary	. 3
Zusammenfassung	. 5
1. Introduction	. 7
1.1 The <i>Hydra</i> organism	. 7
1.2 The Wnt signalling pathway	. 9
1.2.1 Signal transduction of the canonical Wnt/β-catenin signalling pathway	. 9
1.2.2 Role of the canonical Wnt/β-catenin signalling pathway in <i>Hydra</i>	11
1.3 The Notch signalling pathway	11
1.3.1 Signal transduction in the Notch signalling pathway	11
1.3.2 The function of Notch in <i>Hydra</i> and other cnidarians	14
2. Aim of this thesis	17
3. Results	19
3.1 Paper I: Genetic interference with HvNotch provides new insights into the role of the Notch-signalling pathway for developmental pattern formation in <i>Hydra</i>	
3.2 Paper II: Differential gene regulation in DAPT-treated <i>Hydra</i> reveals candidate direct Notch signalling targets	49
3.3 Paper III: Notch signalling mediates between two pattern-forming processes during head regeneration in <i>Hydra</i>	77
4. Discussion1	09
4.1 The establishment of NICD-overexpressing and Notch-knockdown transgenic Hydra1	09
4.2 HvNotch function in <i>Hydra</i> budding1	11
4.3 HvNotch function in <i>Hydra</i> axis patterning1	12

4.4 The roles of HvNotch on <i>Hydra</i> head regeneration are context.	xt-dependent 113
4.5 Interactions between HvNotch, Wnt and TGF-β/BMP signalling	ng pathways in <i>Hydra</i>
	116
4.6 The possible inhibitor of <i>HyWnt3</i> expression, HyKayak, is inh	nibited by the Notch
signalling pathway	118
5. Conclusion and outlook	121
6. Reference	123
Acknowledgements	133

Abbreviations

ADAM A Disintegrant and Metalloprotease

ADP Adenosine Diphosphate

ALX aristaless-related gene

APC Adenomatous Polyposis Coli

AP-1 Activator Protein 1

ATP Adenosine Triphosphate

bHLH basic Helix-Loop-Helix

BMP Bone Morphogenetic Protein

bZiP domain basic leucine zipper domain

CnGSC Cnidarian goosecoid

Ck1 Casein kinase I

CnASH Cnidarian Achaete-Scute Homolog

CSL CBF1, Suppressor of Hairless, LAG-1

Co-A Co-activator

DAPT N-[N-(3,5-Difluorophenacetyl)-l-alanyl]-S-phenylglycine t-butyl ester

DMSO Dimethyl Sulfoxide

FISH Fluorescence In Situ Hybridization

GSK-3 Glycogen Synthase Kinase 3

HAS-7 *Hydra* Astacin-7

h hours

Hv Hydra Vulgaris

Hy Hydra

Hes Hairy and Enhancer of Split

iCRT14 inhibitor of β-Catenin-Responsive Transcription

JNK c-Jun N-terminal kinase

LRP Lipoprotein Receptor-related Protein

NR Notch responsive

NOWA Nematocyst Outer Wall Antigen

NICD Notch intracellular domain

prdl proline-rich domain-like

RBPJ Recombination Signal Binding Protein for Immunoglobulin Kappa J

RNA-seq RNA sequencing

RT-qPCR Real-Time quantitative Polymerase Chain Reaction

SAHM1 Stabilized Alpha-Helix of Mastermind 1

shRNA short hairpin RNA

TCF/LEF T-cell factor/Lymphoid enhancer-binding factor

TGF- β Transforming Growth Factor β

TF Transcriptional Factor

Wnt Wingless-related integration site

Summary

The Notch signalling pathway is a highly conserved cell-to-cell communication mechanism in animals. Notch ligands, such as Delta, can regulate the activity of Notch receptors by transactivation in neighbouring cells or cis inhibition within the same cell. This dual regulatory mechanism makes Notch signalling essential for establishing boundaries. In *Hydra*, previous studies using the presentilin inhibitor DAPT have shown that Notch signalling is crucial for defining the parent-bud boundary and for head regeneration following apical decapitation.

In the first part of this thesis (Pan, Mercker et al. 2024), Notch transgenic *Hydra* strains were established to further investigate the function of the Notch signalling pathway. These included NICD-overexpressing and Notch knockdown transgenic *Hydra* strains. NICD-overexpressing transgenic *Hydra* exhibited downregulation of predicted Notch target genes and displayed "Y-shaped" polyps, a phenotype also observed in DAPT-treated *Hydra*. This suggests that NICD-overexpression exerts a dominant-negative effect. Additional phenotypes observed in NICD-overexpressing *Hydra* included "ectopic tentacles", "two-headed", and "multiple heads". Notch-knockdown *Hydra* exhibited similar phenotypes, except for the "multiple heads" form. Instead, an additional "two feet" phenotype was observed. Furthermore, both NICD-overexpressing and Notch-knockdown *Hydra* displayed abnormal head regeneration phenotypes following apical or middle gastric decapitation. These findings confirm that the Notch signalling pathway plays a critical role in body-axis patterning and head regeneration in *Hydra*.

In the second part of this thesis (Moneer, Siebert et al. 2021), a transcriptome analysis of DAPT-treated *Hydra* was conducted, identifying 666 Notch-responsive genes with defined expression patterns in *Hydra*. Among these, genes associated with nematogenesis and head patterning were predominantly downregulated. In addition to *HyHes*, *Sp5* and *HyAlx* were identified as the most promising direct targets of Notch signalling. Furthermore, an upregulated transcriptional factor, HyKayak, was identified, which shows expression in ectodermal head cells and battery cells. This led to the hypothesis that HyKayak might serve as a Notch-dependent regulator of *HyWnt3*, potentially acting as an inhibitor of *HyWnt3*.

The third part (Steichele, Sauermann et al. 2025) describes that *Hydra* head regeneration involves two distinct processes: hypostome regeneration and tentacle patterning. The Notch signalling pathway was found to play a crucial role in regulating the regenerating sequence of these processes. Following apical decapitation, Notch signalling appeared to suppress tentacle fate, probably by inhibiting *BMP5/8b* expression, thereby promoting hypostome fate through the activation of *HyWnt3*. Further experiments confirmed that the loss of HyKayak function, either through shRNA-knockdown or pharmacological treatment, resulted in upregulated expression of *HyWnt3*, suggesting that HyKayak can repress the expression of *HyWnt3*.

Zusammenfassung

Der Notch-Signalweg ist ein hochkonservierter Zell-zu-Zell-Kommunikationsmechanismus, der in tierischen Organismen vorkommt. Notch-Liganden wie Delta können die Aktivität von Notch-Rezeptoren durch Transaktivierung in benachbarten Zellen oder cis-Hemmung innerhalb derselben Zelle regulieren. Dieser duale Regulierungsmechanismus spielt für die Funktion des Notch-Signalweges bei der Ausbildung von Gewebsgrenzen eine Rolle. Bei Hydra haben frühere Studien mit dem Notch-Inhibitor DAPT gezeigt, dass der Notch-Signalweg für die Bildung einer Grenze der Knospe zum Mutterpolypen notwendig ist, welche wiederum gebraucht wird, damit die Knospe einen Fuß bilden und sich vom Mutterpolypen lösen kann. Außerdem ist der Notch signalweg in *Hydra* essenziell für die Kopfregeneration nach apikaler Entfernung des Kopfes.

Im ersten Teil der Arbeit (Pan, Mercker et al. 2024) wurden Notch-transgene Hydra-Stämme etabliert, um die Funktion des Notch-Signalwegs direkt zu untersuchen. Dazu gehörten NICD-überexprimierende und Notch-Knockdown-transgene Hydra-Stämme. NICD-überexprimierende transgene Hydren zeigten eine Herunterregulierung von Notch-Zielgenen sowie "Y-förmige" Polypen, ein Phänotyp, der auch bei DAPT-behandelten Hydra-Polypen beobachtet wurde. Dies deutet darauf hin, dass die NICD-Überexpression einen dominant-negativen Effekt ausübt. Weitere bei NICD-überexprimierenden Hydra polypen beobachtete Phänotypen waren "ektopische Tentakel", "zweiköpfig" und "mehrköpfig". Notch-Knockdown-Hydra-Polypen zeigten ähnliche Phänotypen, mit Ausnahme "mehrköpfigen" Form. Stattdessen wurde ein der zusätzlicher Phänotyp beobachtet. Darüber hinaus "zweifüßiger" zeigten sowohl NICDüberexprimierende als auch Notch-Knockdown-Hydra-Polypen nach Abtrennung des Kopfes an einer apikalen oder mittigen Position abnormale Phänotypen bei der Kopfregeneration. Diese Ergebnisse bestätigen, dass der Notch-Signalweg eine entscheidende Rolle bei der Festlegung der positionellen Werte der Körperachse sowie bei der Kopfregeneration der Polypen spielt.

Im zweiten Teil der Arbeit (Moneer, Siebert et al. 2021) wurde eine Transkriptomanalyse von DAPT-behandelten *Hydra*-Polypen durchgeführt, bei der 666 Notch-regulierte Gene

mit definierten Expressionsmustern identifiziert wurden. Unter diesen waren Gene, die mit der Nematogenese und der Kopfbildung in Zusammenhang stehen, überwiegend herunterreguliert. Neben *HyHes* wurden *Sp5* und *HyAlx* als wahrscheinliche direkte Zielgene des Notch-Signalweges identifiziert. Zusätzlich wurde ein hochreguliertes Gen identifiziert, das den Transkriptionsfaktor HyKayak kodiert und Expression in ektodermalen Kopfzellen und in Batteriezellen zeigt. Dies führte zu der Hypothese, dass HyKayak ein Notch-gesteuerter Regulator von *HyWnt3* ist und möglicherweise als Inhibitor von *HyWnt3* wirkt.

Im dritten Teil (Steichele, Sauermann et al. 2025) wird gezeigt, dass die Regeneration des Hydra-Kopfes zwei unterschiedliche Prozesse umfasst: Hypostomregeneration und Tentakelregeneration. Es wurde festgestellt, dass der Notch-Signalweg entscheidende Rolle bei der Regulierung der Regenerationssequenz dieser Prozesse spielt. Nach apikaler Enthauptung unterdrückt der Notch-Signalweg Tentakelzellbildung, wahrscheinlich durch Hemmung der BMP5/8b-Expression, wodurch die Hypostombildung durch die Aktivierung von HyWnt3 ermöglicht wird. Weitere Experimente bestätigten, dass der Verlust der HyKayak-Funktion, entweder durch shRNA-Knockdown oder durch pharmakologische Behandlung, zu einer Aufregulation der Expression von HyWnt3 führt, was darauf hindeutet, dass HyKayak die Expression von *HyWnt3* unterdrücken kann.

1. Introduction

1.1 The *Hydra* organism

The freshwater polyp *Hydra* belongs to the phylum Cnidaria, a sister group of Bilateria. *Hydra* has a simple body structure with a single oral-aboral body axis. It features a hypostome surrounded by a ring of tentacles at the oral end, and a peduncle ending in a basal disk at the aboral end. The body of *Hydra* consists of two epithelial layers, the ectoderm and the endoderm, which create a cylindrical shape enclosing a gastric cavity for digestion. Epithelial stem cells of both layers can continuously proliferate in the body column, then differentiate into battery cells beyond the tentacle boundaries, or into basal disk cells at the aboral end (David and Campbell 1972, Holstein, Hobmayer et al. 1991, Hobmayer, Jenewein et al. 2012). The extracellular matrix between the two layers is known as mesoglea. Moreover, an interstitial cell lineage is localized in interstitial spaces between epithelial cells. This lineage is composed of multipotent stem cells and their differentiated products, including nematocytes, nerve cells, gland cells, and germ cells in sexually reproducing animals (Campbell and David 1974, David and Gierer 1974).

Hydra epithelial cells in the body column have the potential to divide endlessly. Thus, in a well-fed Hydra, the epithelial cell layers undergo continuous self-renewal in the body column (David and Campbell 1972, Martinez and Bridge 2012). At the ends of the body column, where tentacles or basal disc structures form, these cells become fully differentiated into head and tentacle cells, or peduncle and basal disk cells. These differentiated cells are gradually displaced towards the ends of the tentacles or basal disc, where they are eventually sloughed off. In addition, epithelial cells are also displaced into developing buds, which can detach from the parent once they have developed heads with tentacles and hypostomes, and a mature basal disk. This budding process, the asexual reproduction way of Hydra, takes around three days (Campbell 1967, Otto and Campbell 1977). Hence, adult Hydra cells maintain a steady state with continuous production of new cells and loss of older cells.

Due to the ongoing self-renewal of epithelial cells and interstitial stem cells, *Hydra* can regenerate any missing body parts (Bode 2003). When a *Hydra* is bisected transversely or longitudinally, both parts can regenerate the missing tissues in their original positions.

Additionally, an isolated piece of body column tissue can regenerate a new head at the apical end and a new basal disk at the basal end, indicating the maintenance of the initial polarity (oral-aboral) during the regeneration process. More interestingly, when *Hydra* tissue is dissociated into a cell suspension, the cells can re-aggregate into a cell pellet and subsequently develop into mature polyps within five days (Gierer, Berking et al. 1972).

How are cells organized during the regeneration process? As early as 1909, Ethel Browne demonstrated that specific *Hydra* tissues, such as the peristome tissue, the tip of regenerating tissue, and the head of a young bud that has not yet formed tentacles, could induce the formation of a new *hydra*nth after being grafted into the body of the stock (Browne 1909). In contrast, all other regions of *Hydra* do not have this ability. These observations indicate that these specific tissues have an "organizer" capacity, a term first introduced by Hans Spemann and Hilde Mangold in 1923 to describe a particular tissue from the dorsal blastopore lip of an amphibian gastrula that can induce the formation of a secondary embryo when transplanted to a different region in a host embryo (Spemann and Mangold 2001). Subsequently, similar organizers have been identified in embryonic tissue of other vertebrates, such as primitive nodes in amniotes (Hensen 1876, Waddington 1932, Beddington 1994) or the dorsal shield in zebrafish (Driever 1995, Shih and Fraser 1996).

Additional transplantation experiments on *Hydra* not only supported Browne's results but also offered further insights into the *Hydra* head organizer and head formation (Yao 1945, Webster 1966a, Webster 1966b). As summarized by MacWilliams in 1983, transplanted tissues have demonstrated an increased capacity for forming ectopic heads or *hydra*nths in the absence of the host's head or when placed far away from the host's head (MacWilliams 1983a). Moreover, tissues extracted near the head region of the donor animal exhibit a higher ability to form heads compared to those from more basal regions (MacWilliams 1983b). These results suggested a model based on the existence of two substances: (1) a diffusion-mediated (long-range) head inhibition signal, primarily originating from the head but also present in smaller amounts throughout the body column; (2) a less-diffusible (short-range) head activation signal from the head region. Both signals exhibit concentration gradients from the head to the body column (Gierer and Meinhardt 1972, MacWilliams 1983a, MacWilliams 1983b, Meinhardt 2012). During head

regeneration, the model assumes a localized increase in the head activator at the cutting surface immediately after decapitation, which supports the expansion of the activated zone and the gradual re-establishment of the head inhibitor. Meanwhile, the restored head inhibitor antagonizes the expansion of the head activation zone. This activation-inhibition model may play a crucial role in head formation and axis patterning.

1.2 The Wnt signalling pathway

1.2.1 Signal transduction of the canonical Wnt/β-catenin signalling pathway

The canonical Wnt/ β -catenin signalling pathway is essential for the regulation of cell proliferation and differentiation during embryonic development and in adult tissues. In the absence of a Wnt ligand, a destruction complex composed of axin, APC, CK1 and GSK-3 phosphorylates β -catenin, leading to its ubiquitination and final degradation. As a result, β -catenin cannot accumulate in the cytoplasm or translocate into the nucleus. TCF/LEF transcriptional factors then bind to co-repressors, such as Groucho, thereby preventing the activation of Wnt target genes. In the presence of a Wnt ligand, Wnt binds to the Frizzled transmembrane receptor and its co-receptor LRP. This binding triggers the phosphorylation of LRP by CK1 and GSK-3 and activates Dishevelled proteins. Activated Dishevelled recruits Axin to the membrane, leading to the accumulation of β -catenin in the cytoplasm. β -catenin can then translocate into the nucleus and form a complex with TCF/LEF to activate the transcription of Wnt target genes (see Fig. 1).

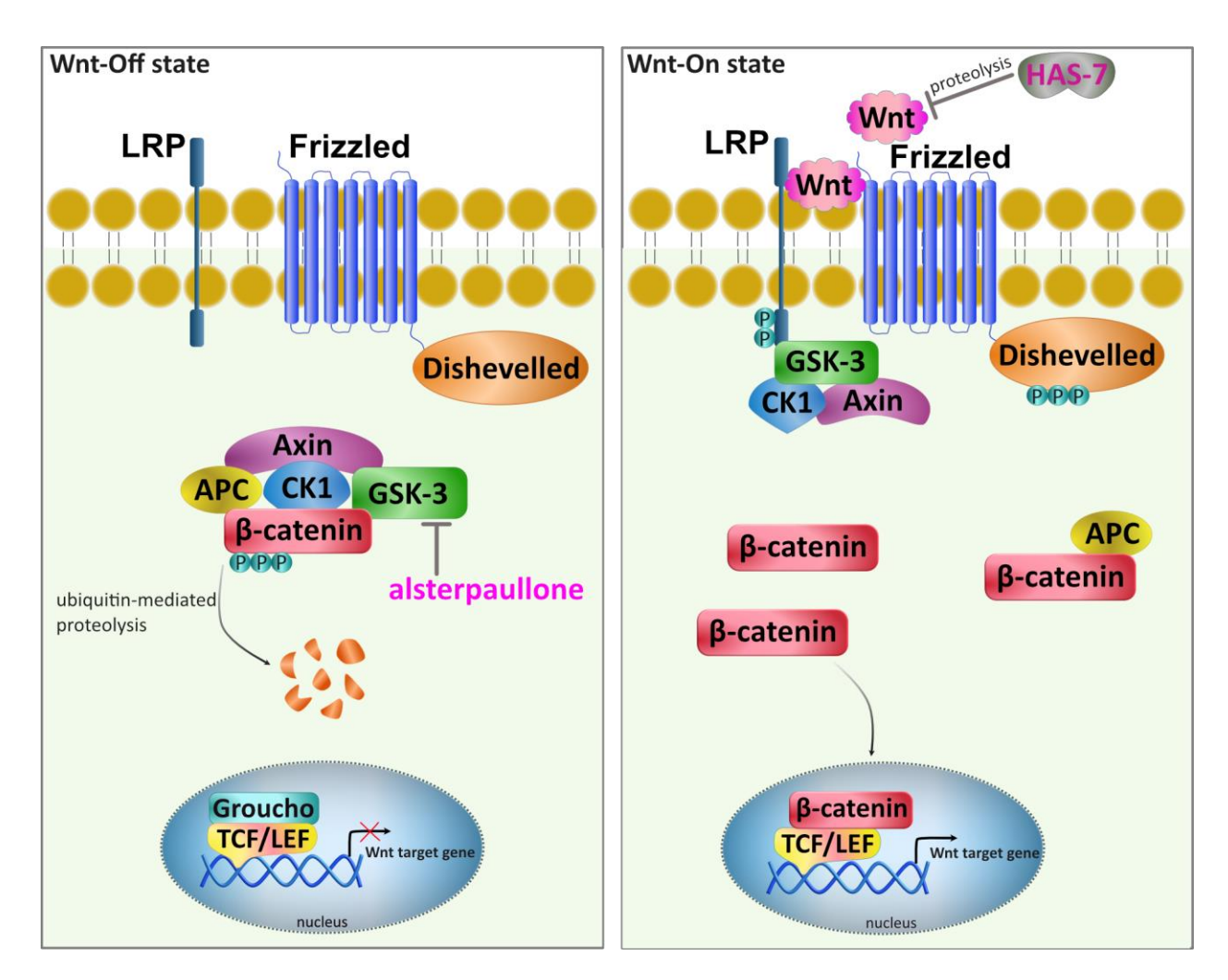


Fig. 1 The canonical Wnt signalling pathway. Left (Wnt-Off state): in the absence of a Wnt ligand, β -catenin is phosphorylated by a protein complex, including Axin, APC, CK1 and GSK-3, leading to its degradation through ubiquitin-mediated proteolysis. In the nucleus, Groucho binds to TCF/LEF, preventing the transcription of Wnt target genes. Right (Wnt-On state): in the presence of a Wnt ligand, Wnt binds to the Frizzled receptor and its co-receptor LRP, leading to the phosphorylation of Dishevelled. LRP is phosphorylated by CK1 and GSK-3 and then recruits Axin to the plasma membrane. The released β -catenin accumulates in the cytoplasm and translocates to the nucleus, where it binds to TCF/LEF and initiates the transcription of Wnt target genes. Alsterpaullone specifically inhibits GSK-3, preventing the phosphorylation of β -catenin (Broun, Gee et al. 2005). HAS-7 (*Hydra* Astacin-7) is an astacin proteinase that regulates the activity of HyWnt3 (Ziegler, Yiallouros et al. 2021).

1.2.2 Role of the canonical Wnt/β-catenin signalling pathway in Hydra

In Hydra, the canonical Wnt/ β -catenin signalling pathway has been reported to be involved in head activation and the establishment of the head organizer (Hobmayer, Rentzsch et al. 2000, Broun, Gee et al. 2005, Lengfeld, Watanabe et al. 2009). Hydra Wnt3 (HyWnt3) has been indicated to be involved in organizer function. It is exclusively expressed at the apical tip of the hypostome during head regeneration and bud formation. HyTcf shows a similar, but more extended expression pattern in the head region compared with HyWnt3. However, $Hy\beta$ -catenin has a relatively lower expression throughout the whole polyp (Hobmayer, Rentzsch et al. 2000).

Abnormal activation of HyWnt3 following treatment with alsterpaullone, a specific inhibitor of GSK-3, leads to a transient increase in the expression of HyTcf and nuclear accumulation of $Hy\beta$ -catenin, resulting in the formation of ectopic tentacles throughout the body column (Broun, Gee et al. 2005, Philipp, Aufschnaiter et al. 2009). Moreover, alsterpaullone-treated body column tissue induces the formation of a second axis when transplanted into a host animal, indicating the presence of head organizer activity in such tissue (Broun, Gee et al. 2005). Additionally, transgenic Hydra strains overexpressing stabilized β -catenin exhibit a multiple-headed phenotype along the body column and acquire a more stable level of head organizer properties in comparison with those treated with alsterpaullone (Gee, Hartig et al. 2010). These results demonstrate that the Wnt signalling pathway has a conserved function in body axis formation in animals from simple organisms like Hydra to complex vertebrates. This raises the question: do other signalling pathways involved in developmental processes in higher animals also have conserved functions in Hydra polyps?

1.3 The Notch signalling pathway

1.3.1 Signal transduction in the Notch signalling pathway

The Notch signalling pathway is highly conserved in multicellular organisms, including the pathway components and signal transduction mechanism. The Notch receptor and its ligands, such as Delta and Jagged in vertebrates, are both transmembrane proteins. When a Notch ligand binds to the Notch receptor on an adjacent cell, it triggers two proteolytic cleavages of the Notch receptor. The first cleavage is mediated by ADAM

metalloprotease, followed by a second cleavage by γ -secretase. This process releases the Notch intracellular domain (NICD), which then translocates to the nucleus. In the nucleus, NICD interacts with DNA-binding proteins from the CSL family (CBF1/RBPJ in mammals, Su(H) in *Drosophila*, and LAG-1 in *C.elegans*) to activate target genes, such as members of the Hes family of transcriptional repressors (Lai 2004, Bray 2006, Kopan and Ilagan 2009). This process is known as the transactivation function of the Notch signalling pathway (see Fig. 2).

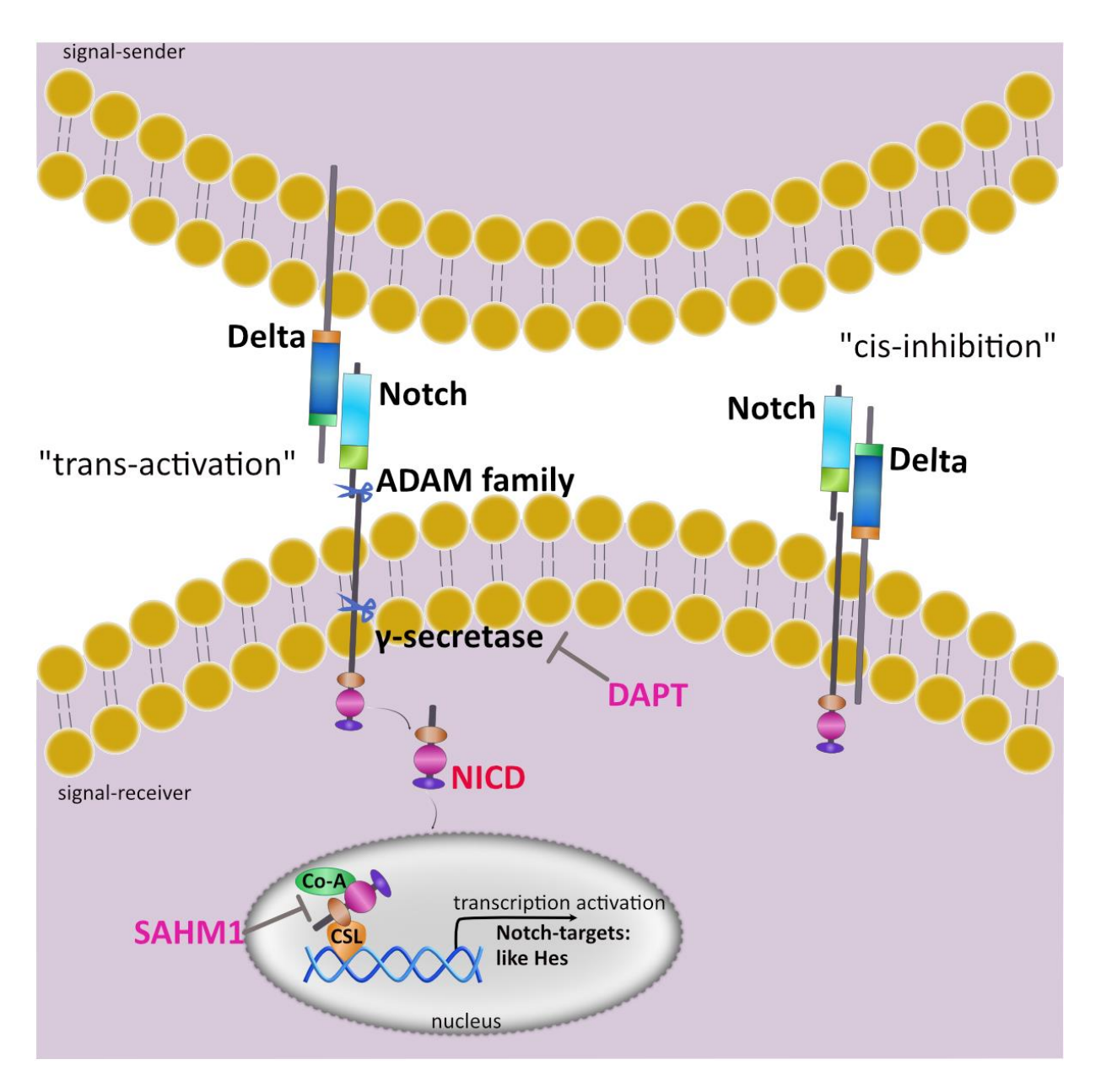


Fig. 2 The Notch signalling pathway. The binding of the Delta ligand on one cell to the Notch receptor on a neighbouring cell triggers two proteolytic cleavages, mediated by the ADAM protease family and γ-secretase, respectively. This process eventually releases the NICD part, which translates into the nucleus. Within the nucleus, NICD interacts with the CSL complex and recruits a co-activator (Co-A) to activate the transcription of Notch target genes, such as *Hes.* This mechanism is referred to as transactivation. DAPT is a γ-secretase inhibitor. SAHM1 prevents the binding of NICD to the co-activator. Cisinhibition occurs when the Delta ligand on one cell binds to the Notch receptor on the same cell.

Additionally, the Notch ligand can inhibit the activity of the Notch receptor within the same cell, a process known as cis-inhibition (Micchelli, Rulifson et al. 1997, Miller, Lyons et al. 2009, Sprinzak, Lakhanpal et al. 2010) (see Fig. 2). This process creates a delicate switch between cells that serve as "signal-sender" (with high ligand concentration and low Notch concentration) and cells that serve as "signal-receiver" (with high Notch concentration and low ligand concentration). When these two cell types interact, the Notch signalling pathway is activated, leading to the formation of sharply defined boundaries between different cell populations (Sprinzak, Lakhanpal et al. 2010, del Álamo, Rouault et al. 2011). In *Drosophila*, studies have shown that Notch signalling is crucial for establishing boundaries between wing vein and intervein, as well as for specifying the differentiation boundary between neurons and epidermal cells in the nervous system (Huppert, Jacobsen et al. 1997, Jose F. de Celis 1997).

1.3.2 The function of Notch in *Hydra* and other cnidarians

Several studies have shown that Notch plays a significant role in various developmental processes, including tissue regeneration in chidarians. In *Hydra vulgaris*, a single Notch receptor and one Jagged ligand have been investigated (Käsbauer, Towb et al. 2007, Prexl, Münder et al. 2011). The protein structures of *Hydra* Notch (HvNotch) and *Hydra* Jagged (HyJagged), along with their signal transduction mechanism, are well conserved. The bHLH transcriptional repressor HyHes is directly activated following the transactivation of HvNotch (Käsbauer, Towb et al. 2007). Inhibition of Notch signalling using DAPT, a y-secretase inhibitor, prevents the differentiation of post-mitotic nematocytes and germ cells (Käsbauer, Towb et al. 2007). Additionally, inhibiting Notch signalling with DAPT results in the formation of irregularly arranged tentacles (Münder, Tischer et al. 2013). Studies on budding *Hydra* have demonstrated that Notch inhibition causes the development of Y-shaped animals due to failed bud detachment (Münder, Käsbauer et al. 2010). These findings indicate that Notch signalling is crucial for establishing tentacle boundaries and the parent-bud boundary. As mentioned above, Hydra is renowned for its remarkable regeneration capabilities, particularly in regenerating new heads. Inhibition of Notch signalling with DAPT blocks the expression of HyWnt3 at the regenerating tip, leading to a failure in head regeneration. This

underscores the crucial role of Notch signalling in this process (Münder, Tischer et al. 2013).

The function of the Notch pathway has also been studied in other cnidarians. In *Hydractinia echinata*, another hydrozoan, Notch signalling is necessary for the development of nematocytes and in the process of tentacle patterning (Gahan, Schnitzler et al. 2017). DAPT treatment results in a reduced number of mature nematocytes and failed regeneration of tentacles after decapitation. In addition, ectopic activation of NICD leads to the formation of ectopic tentacles. In *Nematostella vectensis*, Notch signalling is essential for proper embryonic development and cell fate determination (Marlow, Roettinger et al. 2012). Blocking Notch disrupts endodermal morphogenesis and prevents the differentiation of cnidocytes. Furthermore, Notch signalling is required for tentacle patterning in *Nematostella*, as inhibiting Notch leads to the formation of fused tentacles. Additionally, Notch signalling plays a role in neurogenesis in *Nematostella* embryos, evidenced by an increased expression of neural progenitor cell markers following DAPT treatment (Marlow, Roettinger et al. 2012, Richards and Rentzsch 2015).

2. Aim of this thesis

Previous studies on Notch functions in *Hydra* have mostly relied on pharmacological inhibitors such as DAPT or SAHM1 (Münder, Tischer et al. 2013). However, the short duration of these treatments (typically 48 h) has limited the ability to observe the long-term effects of Notch inhibition. Moreover, although DAPT has been shown to mimic Notch loss-of-function in many model organisms, additional off-target effects of this drug on development cannot be excluded (Moneer, Siebert et al. 2021, Katolikova, Khudiakov et al. 2023).

To address these limitations and further understand the role of the Notch signalling pathway in *Hydra*, I adopted a genetic interference approach. This involved creating transgenic *Hydra* strains that either overexpress NICD or express Notch-knockdown-shRNA (Pan, Mercker et al. 2024). These transgenic lines enabled a more specific investigation of Notch signalling functions over extended periods of time.

In addition, to gain a deeper understanding of the regulatory mechanisms of Notch signalling in *Hydra*, an RNA-seq analysis was performed using polyps treated with 20 µM DAPT. This study examined gene expression differences following 48 h of DAPT treatment and subsequently 3 h and 6 h after DAPT removal. The idea was that 48 h of DAPT treatment would shut down all Notch-mediated transcription. Following the withdrawal of the drug, essentially a Notch run-on experiment, direct target genes of Notch would regain their full transcription levels faster than indirect Notch target genes.

Previous studies have demonstrated that *HyWnt3* expression is significantly downregulated following DAPT treatment, which contributes to failed head regeneration after decapitation (Münder, Tischer et al. 2013). However, there is limited evidence showing that *HyWnt3* is a direct target of Notch signalling (Nakamura, Tsiairis et al. 2011). In this study, we hypothesized the existence of an inhibitor of *HyWnt3* that is regulated by the Notch signalling pathway. Given that known Notch targets, such as HyHes, function as transcriptional repressors, this *HyWnt3* inhibitor should be upregulated when Notch signalling is inhibited.

Through transcriptome analysis, we identified a homolog of the human *c-fos* gene (t5966aep), referred to as the *Hydra-Kayak* gene (*HyKayak*), which was significantly

upregulated upon DAPT treatment and returned to baseline levels 3 h after DAPT withdrawal (Moneer, Siebert et al. 2021). To test our hypothesis, we analysed the expression of *HyWnt3* after blocking the activity of HyKayak through inhibitor treatments and shRNA interference.

3. Results

3.1 Paper I: Genetic interference with HvNotch provides new insights into the role of the Notch-signalling pathway for developmental pattern formation in *Hydra*

Summary of paper I:

In this study, I constructed transgenic *Hydra* strains to investigate the function of the Notch signalling pathway. These included NICD-overexpressing strains, where NICD was overexpressed either in the entire ectoderm or the entire endoderm, and four strains of Notch-knockdown expressing a *Notch*-hairpin-shRNA construct in both epithelial layers.

Surprisingly, ectopic NICD showed a dominant negative effect, as the expression of the predicted Notch-target genes, *HyAlx* and *Sp5* (Moneer, Siebert et al. 2021), was downregulated in NICD-overexpressing *Hydra*. Furthermore, the appearance of the "Y-shaped polyps" phenotype in NICD-overexpressing transgenic *Hydra*, which also appeared in Notch-knockdown transgenic polyps, supported this conclusion. This phenotype closely resembles those observed in DAPT-treated *Hydra*, confirming the function of Notch at parent-bud boundaries. Additionally, I observed phenotypes such as "two- or multi-headed" and "ectopic tentacles" in all strains over extended culture periods, indicating that the Notch signalling pathway might regulate the head activation gradient along the *Hydra* body axis. In regeneration experiments, both NICD-overexpressing and Notch-knockdown transgenic *Hydra* exhibited regeneration defects when cut at the apical or more basal levels.

Overall, the observed phenotypes indicate that the Notch signalling pathway is essential for axis patterning, bud formation, and head regeneration in *Hydra*. These findings also confirm the results from previous studies with DAPT treatment (Münder, Käsbauer et al. 2010, Münder, Tischer et al. 2013).

scientific reports



OPEN

Genetic interference with HvNotch provides new insights into the role of the Notch-signalling pathway for developmental pattern formation in *Hydra*

Qin Pan^{1⊠}, Moritz Mercker², Alexander Klimovich⁰³, Jörg Wittlieb³, Anna Marciniak-Czochra² & Angelika Böttger^{1⊠}

The Notch-signalling pathway plays an important role in pattern formation in *Hydra*. Using pharmacological Notch inhibitors (DAPT and SAHM1), it has been demonstrated that HvNotch is required for head regeneration and tentacle patterning in *Hydra*. HvNotch is also involved in establishing the parent-bud boundary and instructing buds to develop feet and detach from the parent. To further investigate the functions of HvNotch, we successfully constructed NICD (HvNotch intracellular domain)-overexpressing and HvNotch-knockdown transgenic *Hydra* strains. NICD-overexpressing transgenic *Hydra* showed a pronounced inhibition on the expression of predicted HvNotch-target genes, suggesting a dominant negative effect of ectopic NICD. This resulted in a "Y-shaped" phenotype, which arises from the parent-bud boundary defect seen in polyps treated with DAPT. Additionally, "multiple heads", "two-headed" and "ectopic tentacles" phenotypes were observed. The HvNotch-knockdown transgenic *Hydra* with reduced expression of HvNotch exhibited similar, but not identical phenotypes, with the addition of a "two feet" phenotype. Furthermore, we observed regeneration defects in both, overexpression and knockdown strains. We integrated these findings into a mathematical model based on long-range gradients of signalling molecules underlying sharply defined positions of HvNotch-signalling cells at the *Hydra* tentacle and bud boundaries.

The freshwater polyp *Hydra* (Cnidaria) has a simple body plan, comprising a single axis with a hypostome surrounded by a ring of tentacles at the oral end and a peduncle with a basal disk at the aboral end. *Hydra* can reproduce asexually by budding. The entire body consists of three cell lineages: ectodermal epithelial cells, endodermal epithelial cells and interstitial cells. The epithelial cells represent two self-renewing epithelia with continuous proliferation in the body column. At the tentacle boundaries, these cells undergo mitotic exit and differentiate into battery cells, while at the aboral end, they differentiate into peduncle cells^{1,2}. The interstitial cell lineage is located in the spaces between the epithelial cells and consists of multipotent stem cells and their differentiation products, including nematocytes, nerve cells, gland cells, and germ cells^{3–5}.

Due to this ongoing self-renewal, adult *Hydra* polyps harbour all the necessary information for body patterning, enabling an almost unlimited capacity of regenerating lost body parts. In 1909, Ethel Browne performed grafting experiments that demonstrated the ability of *Hydra* head tissue to induce the formation of a new hydranths when transplanted into the body column of recipient polyps. This process involved recruiting recipient tissue into the new head structures and indicated the presence of an "organiser" function of these tissues, a term created by Hans Spemann and Hilde Mangold only in 1923 to describe a tissue in amphibian embryos with similar abilities^{6,7}. Further transplantation studies revealed that the head-forming potential of transplants gradually decreases with their distance from the head of the donor animal but increases when positioned further away from the head in the host animal^{8,9}. These data were interpreted according to a reaction—diffusion model developed by Gierer and Meinhardt in 1972 with two major assumptions: (1) the head organizer produces a self-activating

¹Biocenter, Ludwig-Maximilians-University Munich, Großhaderner Str. 2, 82152 Planegg-Martinsried, Germany. ²Institute of Applied Mathematics, Heidelberg University, Im Neuenheimer Feld 205, 69120 Heidelberg, Germany. ³Zoological Institute, Christian-Albrechts-University of Kiel, Am Botanischen Garten 1-9, 24118 Kiel, Germany. [™]email: pan@Imu.uni-muenchen.de; boettger@zi.biologie.uni-muenchen.de

head activation signal (HA) with a short range, and a long-range inhibition signal (HI). Both signals exist in a gradient pattern from the head to the body column^{8–13}; (2) A head activation gradient is present throughout the whole length of the body column of $Hydra^{14}$. This gradient serves as a slowly changing long-term storage of the body axis gradients and plays a crucial role in the interplay between different pattern formation systems¹⁵.

It has been suggested that canonical Wnt-signalling plays a major role in head activation and that nuclear β -catenin defines the head activation gradient along the Hydra body axis $^{16-18}$. However, ectopic activation of Wnt-signalling using the GSK-3 inhibitor alsterpaullone led to the formation of ectopic tentacles instead of complete ectopic heads, indicating some missing links. We have suggested in previous work that Notch-signalling may also be involved in head activation in $Hydra^{19}$.

The Notch signalling pathway plays a crucial role in cell-fate determination and pattern formation by regulating cell-to-cell communication during development. The Notch receptor and its ligands are both transmembrane proteins. Ligands in one cell trans-activate Notch in a neighbouring cell, inducing two proteolytic cleavages to release the intracellular domain of Notch (NICD) from the membrane to move into the nucleus. NICD then binds to transcriptional regulators of the CSL-family (CBF1, Suppressor of Hairless, Lag2) and co-activates transcriptional targets^{20,21}.

Additionally, ligand and receptor in the same cell mutually inhibit one another^{22–24}. Cells with a high ligand concentration and a low Notch concentration are in a preferentially sending state. Conversely, cells are in a receiver state when the concentration of Notch-receptor is higher than that of ligand. Thus, two mutually exclusive states of Notch activation are created. The activity of Notch reaches its peak when these two states are next to each other, then inducing the formation of a sharp tissue border, which may explain many of the observed tissue patterning functions of Notch-signalling^{24,25}.

The Notch protein (HvNotch), a ligand (HyJagged) and the canonical signal transduction pathway are conserved in *Hydra*. The *Hydra* Hes-family bHLH transcription factor 2 (HyHes) has been shown to be a target for transcriptional activation by NICD^{26,27}. The Notch signalling pathway in *Hydra* plays a critical role in regulating tentacle boundaries and head regeneration after decapitation. Blocking Notch signalling with DAPT in adult *Hydra* leads to the formation of abnormal heads with irregularly arranged tentacles¹⁹. The Notch signalling pathway is also essential for the formation of the parent-bud boundary^{19,28}. When Notch-signalling is inhibited at the parent-bud boundary, the buds fail to form a foot and remain attached to the parent, resulting in the formation of Y-animals. Through a differential gene regulation analysis with Notch-inhibited *Hydra*, the transcriptional repressor HyHes, Sp5 (the putative transcriptional repressor of Wnt3)²⁹ and the tentacle boundary gene HyAlx³⁰ were identified as potential transcriptional target genes for NICD. Moreover, the *Hydra* Fos-homolog Kayak was found to be up-regulated after DAPT inhibition, indicating that it could be a potential target of Notch-induced transcriptional repressors, such as HyHes³¹.

Previous insights into these Notch-functions had been obtained by using the pharmacological inhibitors DAPT or SAHM1. However, drug treatment was always only sustained for 48 h, making it impossible to observe long-term effects of Notch-ablation¹⁹. Additionally, it is important to consider the potential side effects of using pharmacological drugs in animals. Therefore, to further understand the function of the Notch signalling pathway in *Hydra*, an alternative approach involving genetic interference with HvNotch was considered.

Here we created Notch transgenic *Hydra* strains, one overexpressing NICD in either ectodermal or endodermal epithelial cells, and another expressing an interfering HvNotch-hairpin-RNA mediating Notch-knockdown in both epithelial cell layers. We monitored these strains over extended periods of time and compared the phenotypes observed in ectodermal and endodermal NICD-overexpressing polyps and in HvNotch-knockdown polyps. We found similar phenotypes as had been observed after inhibition with DAPT or SAHM1, confirming that HvNotch functions at tissue boundaries. Moreover, we obtained evidence for an additional function of the Notch-signalling pathway in regulating the head activation gradient along the *Hydra* body axis. Finally, we provided an initial mathematic model to explain how HvNotch functions to ensure spatio-temporal timing of Notch-signalling at the parent-bud boundary.

Results

NICD-overexpressing transgenic Hydra

The establishment of NICD (Notch intracellular domain)-overexpressing transgenic Hydra

To create NICD-overexpressing *Hydra*, we cloned the NICD encoding segment of HvNotch into the pHyVec11 vector, which also contains a downstream DsRed-sequence (Fig. 1A). After injecting this plasmid into *Hydra* embryos, we obtained 60 embryos with NICD-pHyVec11 injection and 47 embryos with control-pHyVec11 injection. Only one polyp (named 4# strain) exhibited obvious DsRed signals in the NICD-pHyVec11 group, in comparison to the control with 14 DsRed-positive polyps (supplementary Fig. S1A and Fig. S1B), suggesting a negative effect of NICD-overexpression on embryogenesis. Through the selection of buds with enriched transgenic cell pools and regeneration experiments, we obtained uniformly transgenic *Hydra* strains with NICD-overexpression in the entire ectoderm or in the entire endoderm (Fig. 1B). Both of these transgenic strains displayed more than tenfold higher expression of NICD at the RNA level as measured by RT-qPCR (Fig. 1C). RT-qPCR using primers for detecting mRNA encoding the extracellular part of full length HvNotch transcripts indicated that expression of the endogenous HvNotch was unaffected (Fig. 1C).

The expression level of target genes in NICD-overexpressing transgenic Hydra

RT-qPCR analysis revealed that the predicted Notch-target genes HyAlx and HySp5 both showed a significant downregulation (Fig. 1E, F), whereas HyHes was not significantly affected in NICD-overexpressing polyps (Fig. 1D). Moreover, the expression of the *Hydra* Fos-homolog Kayak (HyKayak) was clearly higher in both NICD-overexpressing strains in comparison with controls (Fig. 1G). These gene expression analyses indicate

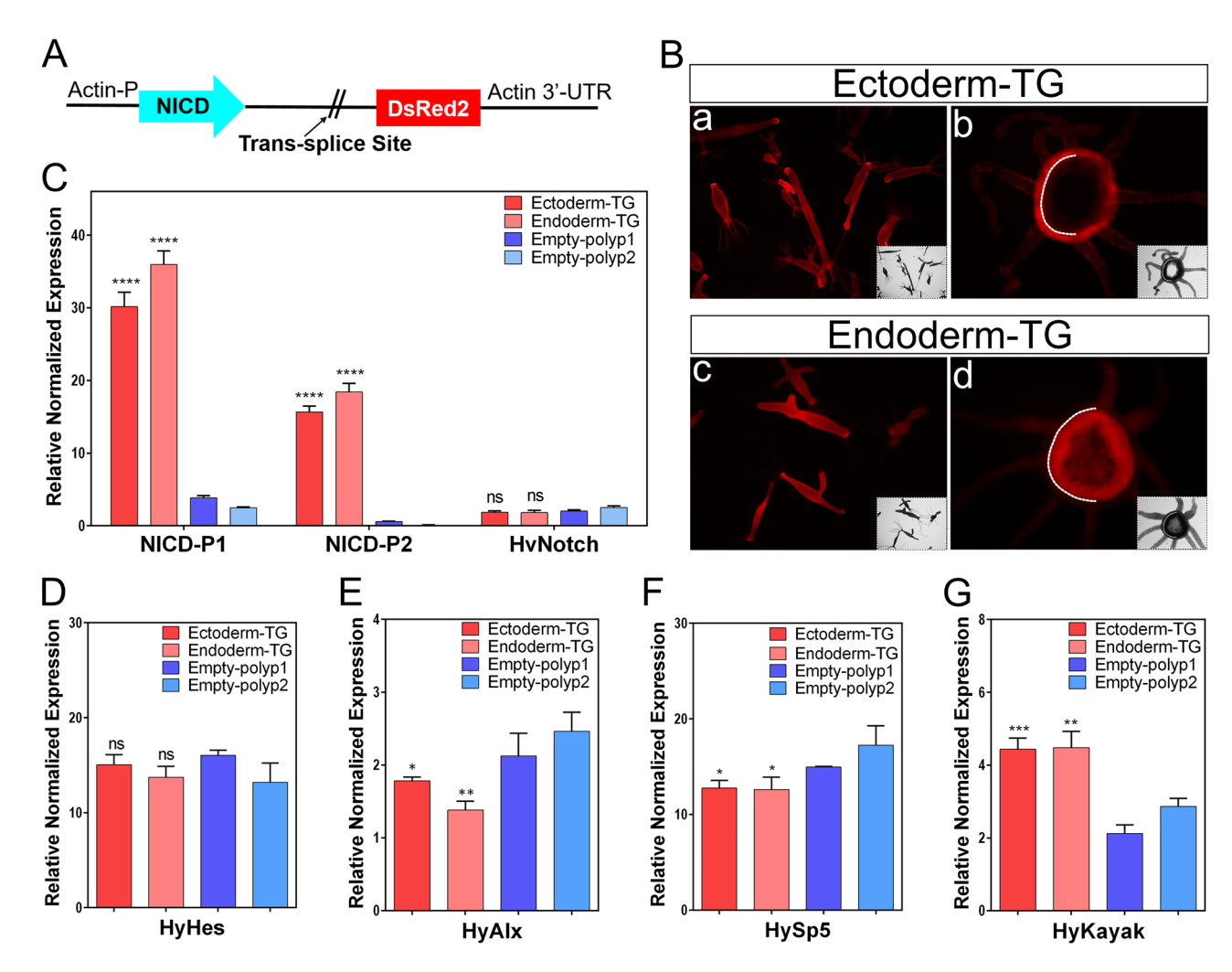


Figure 1. HvNICD-overexpressing transgenic Hydra and the expression of Notch-target genes. (A) Vector pHyVec11 with HvNICD-insert; HvNICD sequence is under the control of the Hydra-actin-promoter. The DsRed-sequence is included in an operon with NICD and expressed independently of HvNICD after transsplice leader addition. (B) Fully transgenic Hydra expressing the transgenes in the whole ectoderm (upper panels, referred to as ectoderm-TG), and in the whole endoderm (lower panels, referred to as Endoderm-TG). a and c are intact animals; b and d are cross sections of polyps; white dotted lines indicate the position of mesoglea. (C) Diagram presents the relative normalized expression of HvNotch and HvNICD, as determined by RT-qPCR with mRNA from Ectoderm-TG and Endoderm-TG polyps in comparison with control groups (empty-polyp1 and empty-polyp2, which were injected by HvNICD-pHyVec11 but did not have DsRed signals); the p-values are related to the average values of empty polyps 1 and 2 (ectoderm-TG: p<0.0001 and endoderm-TG: p<0.0001). Primers for NICD-P1 and NICD-P2 were designed for amplification of HvNICDsequence, primers for HvNotch were designed for amplification of Notch-extracellular domain sequence. (D-G) Diagram presents the relative normalized expression of HvNotch-target genes: HyHes, HyAlx (Ectoderm-TG: p = 0.013 and Endoderm-TG: p = 0.0025), HySp5 (Ectoderm-TG: p = 0.012 and Endoderm-TG: p = 0.022) and HyKayak (Ectoderm-TG: p = 0.0009 and Endoderm-TG: p = 0.002). p-values always related to the average of both control groups. ns (no significance) for p > 0.05; * for $p \le 0.05$; ** for $p \le 0.01$; *** for $p \le 0.01$; *** for $p \le 0.0001$.

that NICD-overexpression leads to similar effects on the expression of potential Notch-target genes, as observed with DAPT-treatment (HyAlx and HySp5 down, HyKayak up, see³¹). This suggests that NICD-overexpression has a dominant negative effect on the transcriptional activity of HvNotch target genes and equals loss-of-function mutants.

Phenotypes of NICD-overexpressing transgenic Hydra

Immediately after obtaining fully transgenic *Hydra* in either the ectoderm or endoderm (referred to as Ectoderm-TG and Endoderm-TG), we did not see any notable phenotypes. Through continuous culture over 5 weeks, we obtained a total of 102 Ectoderm-TG and 94 Endoderm-TG polyps and observed patterning defects (stage 1). These included development of "ectopic tentacles" found in six Ectoderm-TG (Fig. 2A, a, b) and two Endoderm-TG polyps (Fig. 2A, c, d) Furthermore, five Ectoderm-TG polyps exhibited an ectopic head along the body

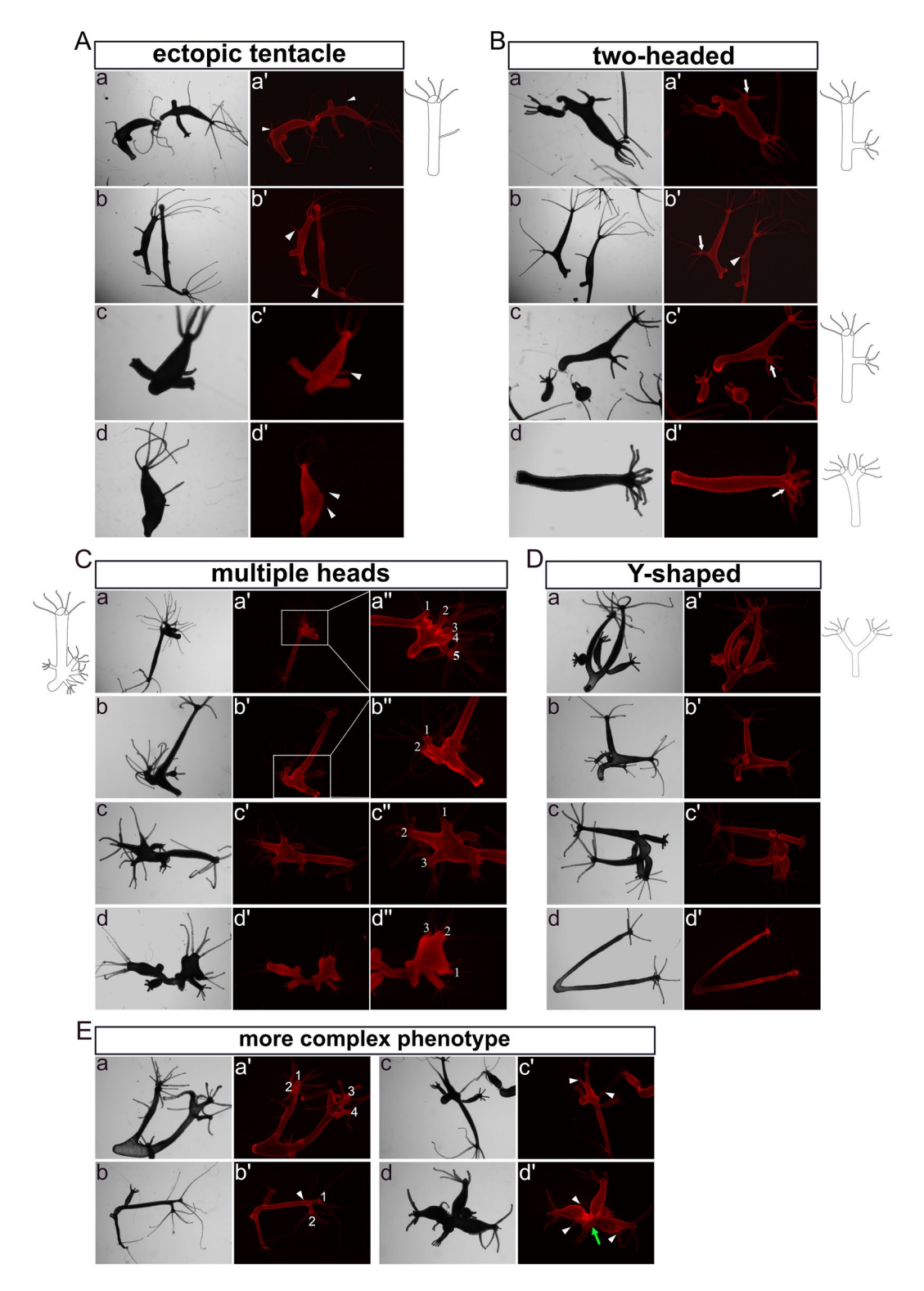


Figure 2. Images and drawings of phenotypes observed in fully transgenic HvNICD-overexpressing *Hydra*. Images labeled with a–d represent light-microscopy, a'–d' display Ds-Red fluorescence. (**A**) "ectopic tentacle" phenotype observed in the initial stage (a, b Ectoderm-TG; c, d Endoderm-TG). (**B**) "two-headed" phenotype appeared in the initial stage (a-d Ectoderm-TG). (**C**) "multiple heads" phenotype after an additional 3 weeks (a-c Ectoderm-TG; d Endoderm-TG; the ectopic heads are numbered). (**D**) "Y-shaped animals" (a-c Ectoderm-TG; d Endoderm-TG). (**E**) combined phenotypes in Ectoderm-TG. Ectopic tentacles are indicated by white triangles, ectopic heads are indicated by white arrows.

column, which occurred near the budding region (Fig. 2B, a, b), in the middle of the body column (Fig. 2B, c) or at the apical end (Fig. 2B, d), (numbers are summarised in supplementary Fig. S9). These phenotypes are similar to those induced with the GSK3- β inhibitor alsterpaullone (ectopic tentacles), transgenic *Hydra* overexpressing stabilised β -catenin (multiple heads along the body column), or Sp5-RNAi transgenic animals ("bouquet" like with two heads at the apical end)^{17,32,33}.

After an additional 3 weeks (stage 2), more "ectopic tentacles" (ten in Ectoderm-TG and seven in Endoderm-TG) and "two-headed" phenotypes appeared (two in Ectoderm-TG and three in Endoderm-TG, supplementary Fig. S2). In addition, "multiple heads" were observed (Fig. 2C, a-c: ectoderm; d: endoderm, for numbers see supplementary Fig. S9). The three "multiple heads" ectoderm-TG polyps from stage 2 were derived from the "two-headed" phenotypes at stage 1. An additional "multiple heads" polyp from endoderm-TG only appeared at stage 2. The maximum were five ectopic heads reminding of a previously described "bouquet"-like phenotype occurring in Sp5 knockdown polyps²⁹. However, in our strains the "bouquet" seemed to appear only on developing buds and not on the parent head. Moreover, the majority of these ectopic heads presented normal hypostomes, while a few displayed incomplete head structures.

Additionally, we observed the presence of "Y-shaped" polyps, which closely resembled the phenotypes of DAPT-treated Hydra²⁸ (Fig. 2D, a-c: ectoderm; d: endoderm). Most of these Y-shaped polyps generated new buds that detached from their parent in a normal manner during the subsequent culture process, suggesting that NICD-overexpression only hindered the detachment of buds at specific time points. We also observed four polyps with more complex phenotypes in Ectodermal-TGs, combining at least two of the aforementioned phenotypes. These included "Y-shaped" animals with "two-headed" (Fig. 2E, a, b), "Y-shaped" polyps with "ectopic tentacles" (Fig. 2E, b-d) and animals with dual "Y-shaped" features probably resulting from repeatedly disrupted bud detachment (Fig. 2E, d).

During the following month (stage 3), these distinctive phenotypes remained observable (numbers see in supplementary Fig. S9). The Ectoderm-TG "ectopic tentacle" polyps exhibited an increase in the number of ectopic tentacles, from having had one or two now possessing more than three in the body column or in the foot region (Fig. 3A). The "multi-headed" phenotype became less intricate, with fewer extra heads/axes compared to the second stage (Fig. 3B, a: ectoderm; b: endoderm). "Two-headed" and "Y-shaped" polyps remained (Fig. 3C, D). It is worth noting that a new type of "Y-shaped" polyps emerged with a shared head and a shared foot (Fig. 3D, a, c: ectoderm; b: endoderm).

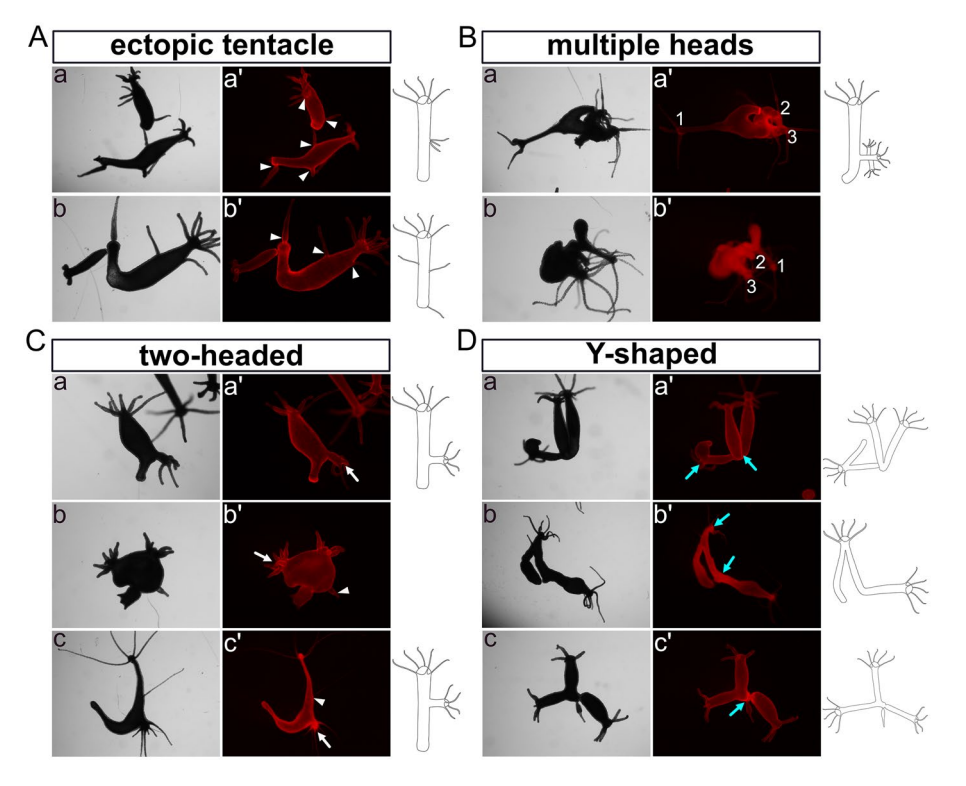


Figure 3. Images and drawings of phenotypes observed in long-term sustained HvNICD-overexpressing transgenic *Hydra*. The images labeled with a–c represent light-microscopy, while a'–c' display Ds-Red fluorescence. (**A**) "Ectopic tentacle" phenotype (a, b Ectoderm-TG; with ectopic tentacles indicated by white triangles). (**B**) "Multiple heads" with less ectopic heads compared to earlier stages (a Ectoderm-TG; b Endoderm-TG; the ectopic heads are numbered). (**C**) "two-headed" polyps with extra heads indicated by white arrows located in the lower part of the body column (a, b Ectoderm-TG; c endoderm-TG). (**D**) "Y-shaped" animals characterized by either shared feet or a shared head, which are indicated by blue arrows (a, c Ectoderm TG; b Endoderm-TG).

In contrast, around 100 empty polyps that were injected with the HvNICD-overexpressing-pHyVec11 but did not display DsRed signals, exhibited a normal morphology. Out of about 100 polyps from the control strain injected with the control-pHyVec11 had occasional instances of polyps (less than 2%) with "ectopic tentacles" during the culture.

NICD-overexpressing Hydra had a normal head regeneration process after apical decapitation, but not after middle gastric sectioning

We proceeded with a head regeneration experiment by removing heads just underneath the tentacle ring (apical regenerates) using *Hydra* that overexpressed NICD but had normal axis pattering. The NICD-overexpressing polyps did not display significant differences in their abilities to regenerate, including regeneration time and patterns of the regenerated heads, in comparison to "empty-polyp" control (supplementary Fig. S3A: 24 h after regeneration; S3B: 72 h after regeneration). We then analysed head regeneration following a cut in the middle of the body column (middle gastric regenerates). We now observed regeneration of two heads or ectopic tentacles while the control groups showed a normal regeneration process (supplementary Fig. S4A and B).

Notch-Knockdown transgenic Hydra

The establishment of Notch-knockdown transgenic Hydra

In order to generate Notch-knockdown *Hydra*, a sequence of the HvNotch-receptor gene (nucleotide 1763-2283) was cloned in both sense and antisense directions into the pHyVec12 vector to be transcribed into a hairpin RNA. In this vector, the *Hydra* actin promoter controls the expression of the HvNotch-hairpin, and an internal sequence allows for the addition of a splice leader between the hairpin and downstream DsRed sequences (Fig. 4A). Consequently, two independent transcripts can be produced: DsRed2-mRNA and Notch-hairpin-RNA³⁴.

After microinjecting the plasmid into embryos, a total of nine polyps displaying mosaic signals developed in the HvNotch-knockdown group and ten polyps in the control group injected with control-pHyVec12, which suggests that Notch-hairpin expression did not have an effect on embryogenesis (supplementary Fig. S5A). Through a series of selection processes, we obtained four transgenic strains (4#, 8#, 11# and 13#), in which Notch-knockdown occurred throughout the ectoderm and endoderm (supplementary Fig.S5A and B). All of these transgenic strains exhibited a significant decrease of approximately threefold in HvNotch expression at the mRNA level compared to the control groups, which included three strains injected with control-pHyVec12 and one strain of polyps injected with Notch-hairpin pHyVec12, but without any DsRed expression (referred to as empty polyps) (Fig. 4B). RT-qPCR did not reveal statistically significant differences in the expression of potential HvNotch-target genes, as shown for HyHes, HyAlx, HySp5 and HyKayak (supplementary Fig. S5C).

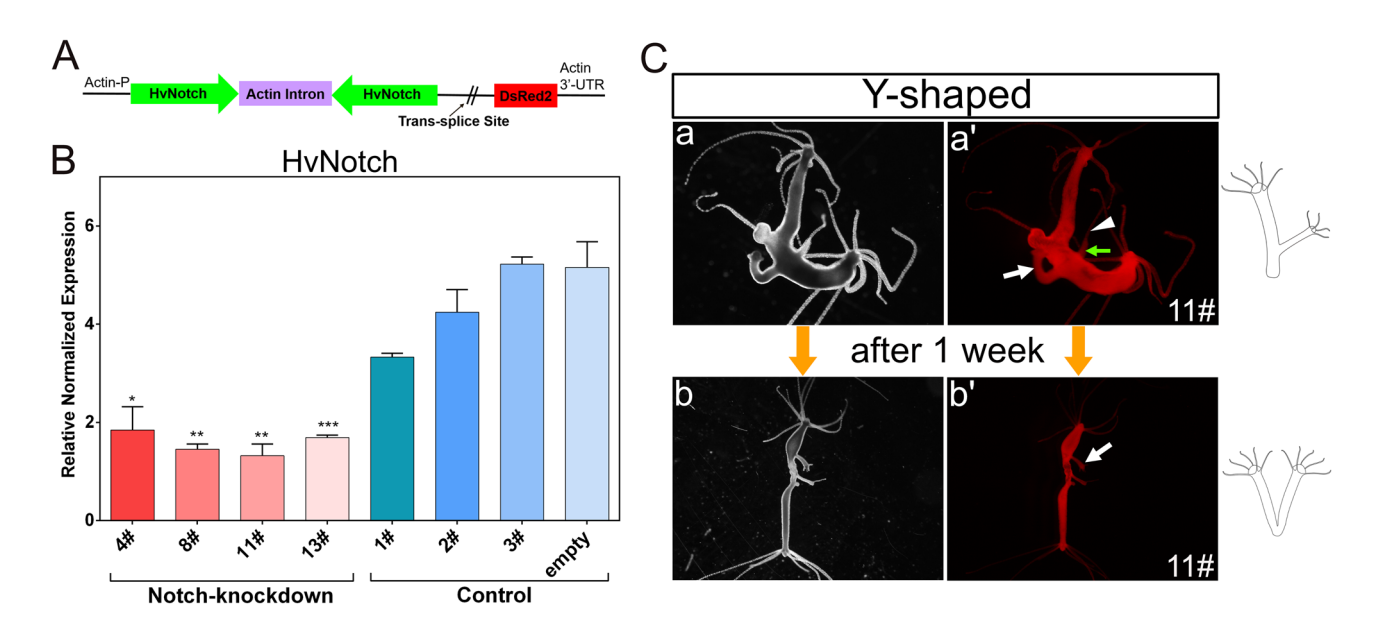


Figure 4. HvNotch-knockdown transgenic *Hydra*. Vector pHyVec12 used for constitutive knockdown of HvNotch. (**A**) The Hairpin structure containing the sequence of HvNotch in sense and antisense orientation is under the control of the actin promoter. DsRed in the same operon is expressed independently after the addition of a splice leader. (**B**) Diagram presents the relative normalized expression of HvNotch, as determined by RT-qPCR with mRNA isolated from four HvNotch-knockdown strains (4#, 8#, 11# and 13#), three control strains (1#, 2#, 3#) injected with control-pHyVec12 and one empty polyp strain injected with HvNotch-hairpin-vector but without DsRed signals. HvNotch showed a significantly lower expression in Notch-knockdown strains in comparison with control groups (4#: p = 0.013; 8#: p = 0.0015; 11#: p = 0.0044; 13#: p = 0.0009). Primers were designed to amplify the extracellular domain of HvNotch sequences. (**C**) "Y-shaped" phenotype in strain 11# was observed in the initial stage (a, a'), the position of the joint moved into the foot region after one week (b, b'). a, b show light microscopy, a', b' show DsRed fluorescence.

Phenotypes of Notch-knockdown transgenic Hydra

Two weeks after obtaining fully transgenic epithelial HvNotch-knockdown strains, we found one "two-headed" polyp and two Y-shaped polyps with ectopic tentacles in the 11# strain. The buds developed in the lower part of the body column and then moved into the foot area within a week (Fig. 4C). There was one case of two-headed polyp, in which the ectopic head initially developed in the lower part of the body column but then moved to the foot area within a week (supplementary Fig. S6A). Unfortunately, this polyp was unable to catch food and subsequently died. We noticed that dying polyps generally had very strong DsRed signals. However, immunofluorescence staining of pan-neuronal antibody (PNab) and acetylated Tubulin indicated that this polyp possessed normal neural nets and nematocyte-capsules (supplementary Fig. S6B).

During the subsequent three months, additional phenotypes began to manifest in all three strains of Notch-knockdown polyps (detailed in supplementary Fig. S10). Over all three strains, in 14 polyps we observed the presence of "ectopic tentacles" on the body column (Fig. 5A), which closely resembled those observed in NICD-overexpressing polyps (Fig. 5A, a). However, it is worth noting that most of these "ectopic tentacles" showed thickening of different lengths at their bases (Fig. 4C, a and Fig. 5A, b–e). Thus, they rather look like a

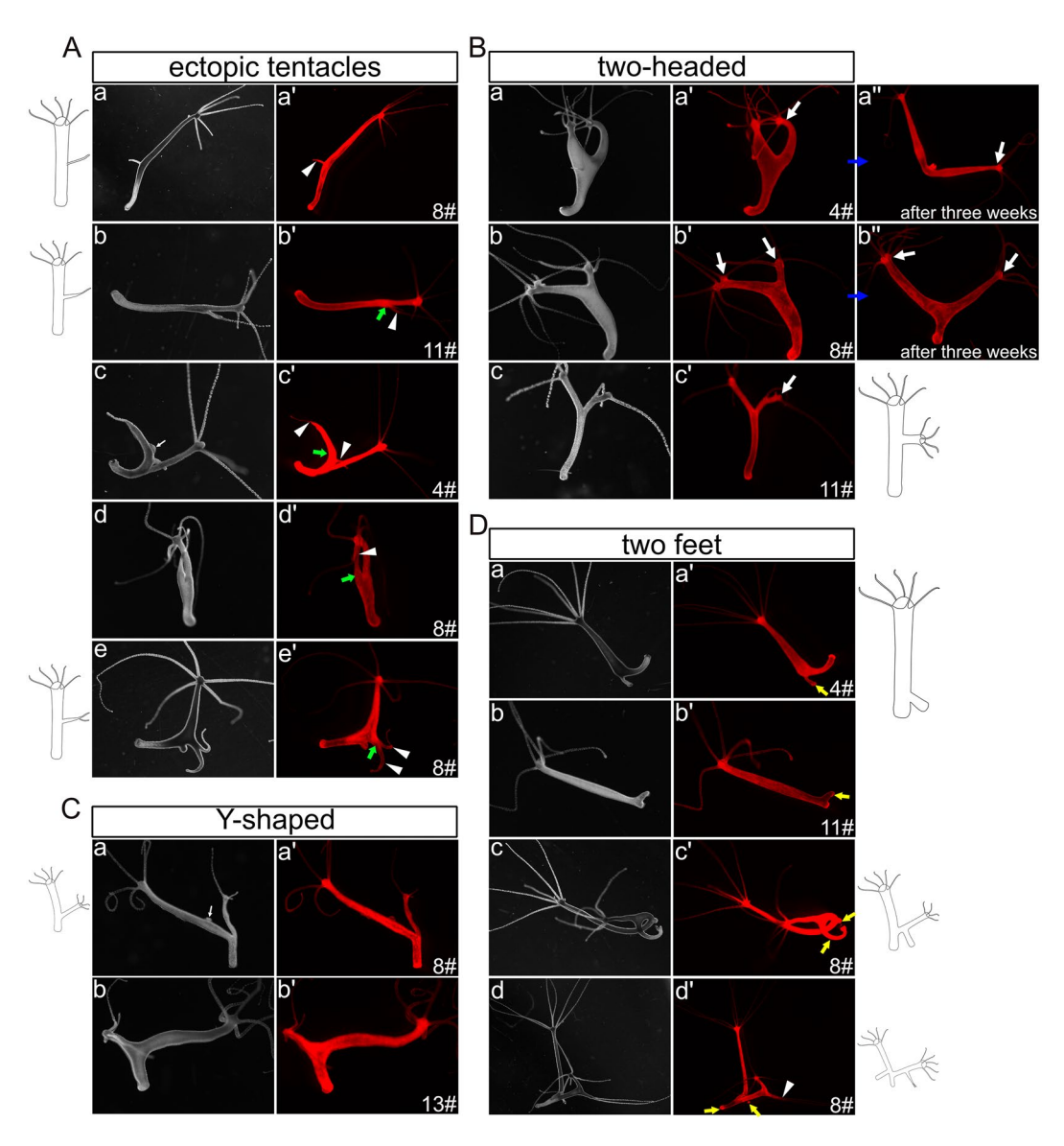


Figure 5. Images and drawings of phenotypes observed in long-term Notch-knockdown transgenic *Hydra*. The images labeled with a–e represent light-microscopy, while a'–e' display Ds-Red fluorescence. (**A**) "Ectopic tentacles" phenotype: a was similar to the phenotypes observed in HvNICD-overexpressing transgenic *Hydra*, b–e showed thickening of different lengths at their bases (ectopic tentacles are indicated by white triangles, thickenings at the bases of ectopic tentacles are shown by green arrows). (**B**) "Two-headed" phenotype: ectopic heads initially located in the oral half of the body column (a–c), and moving into the foot region after three weeks (a", b"). Ectopic heads are indicated by white arrows. (**C**) "Y-shaped" polyps with the joint positioned in the budding zone. (**D**) "Two feet" phenotypes with extra feet indicated by yellow arrows. Two gonads in Fig. 5A-c and Fig. 5C-a were indicated by a thin white arrow.

non-detached bud crowned by one or two tentacles, which is similar to the irregular head structures previously observed in *Hydra* heads and heads of non-detached buds after DAPT-treatment^{19,28}.

Furthermore, we noticed eight more "two-headed" polyps in which the second head positioned well above the budding zone (Fig. 5B, a-c). Later the body column of this second axis became longer and the joining point migrated down towards the foot region (Fig. 5B, a, b). We also observed 17 additional "Y-shaped" animals, in which the second axis had originated in the budding zone (Fig. 5C). Again, we ascribe "Y-shaped" polyps to a failure of bud detachment.

Seven polyps with two feet in the original polyp were detected (Fig. 5D, a, b). Some "Y-shaped" animals had developed two feet (Fig. 5D, c, d). In this case, the bud initially was incapable to form a foot right at the time of detachment but later developed one whilst remaining attached to the parent. We also looked at around 200 empty polyps injected with the Notch-hairpin-pHyVec12 but lacking DsRed signals. We did not notice any abnormal morphology. The control polyps injected with the control-pHyVec12 showed normal morphology during stages 1 and 2.

Most of the Notch-knockdown phenotypes were unstable, with only some simpler traits remaining after 6 months where we still observed two two-headed polyps, two polyps with ectopic tentacles and four Y-shaped animals (supplementary Fig. S7A, B and Fig. S10). However, the control polyps also developed the latter two phenotypes with similar percentage. This did not occur in empty polyps.

Notch-knockdown inhibited the head regeneration process in apical regenerates, but induced regeneration of two heads in middle gastric regenerates

Next, we performed head regeneration experiments with Notch-knockdown polyps, choosing specimens with normal axis pattering. We found that around 20% of the 11# and the 13# strains displayed either non-regeneration or only regenerated a single tentacle. The 4# strain and 8# strains showed abnormal regeneration processes in 11% and 6% of cases, respectively (Fig. 6A, B). However, a small percentage of control polyps also exhibited an abnormal regeneration process (Fig. 6B).

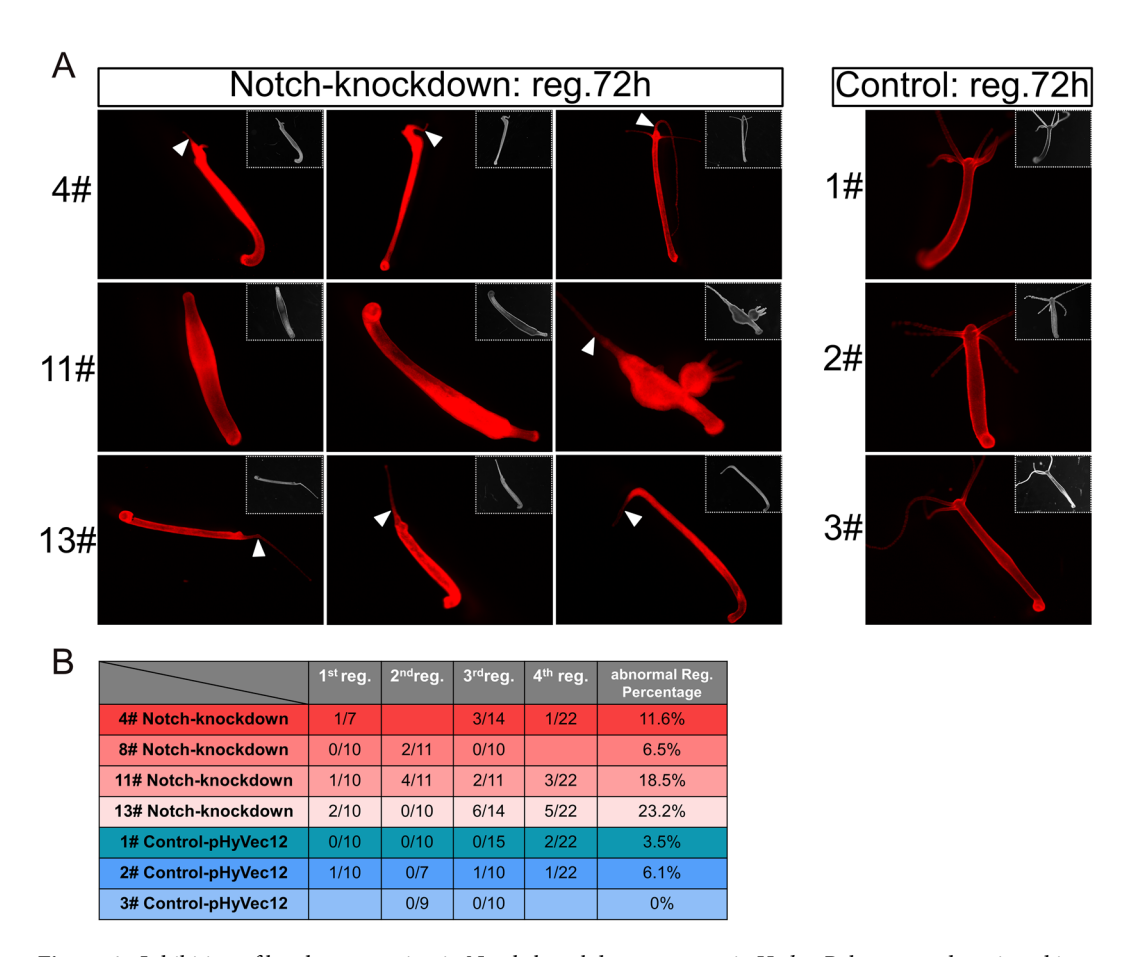


Figure 6. Inhibition of head regeneration in Notch-knockdown transgenic *Hydra*. Polyps were decapitated just underneath the tentacle ring. (**A**) Images depict the DsRed fluorescence and light microscopy (inlets) of polyps from HvNotch-knockdown strains 4#, 11# and 13# 72 h after head removal, compared to control strains 1#, 2# and 3#. Abnormal regeneration involved a complete failure in regenerating head structures observed in strain 11#, or the regeneration of aberrant tentacles, as indicated by white triangles. (**B**) Quantification of abnormal regeneration processes in four consecutive experiments in HvNotch-knockdown and control strains.

We then examined the expression of HyWnt3, a marker of hypostome, and the tentacle boundary gene HyAlx in the regenerating animals 3 days post-decapitation, by in situ hybridization (FISH). We observed that polyps that failed to regenerate or only regenerated a single tentacle displayed a complete absence of HyWnt3 expression (Fig. 7A, a–f). In contrast, normally regenerating polyps exhibited a distinct hypostomal expression pattern of HyWnt3 (Fig. 7A, g–i: Notch-knockdown group; j–l: control).

For HyAlx, most non-regenerated polyps showed a large ring of HyAlx-expression at the regenerating tip (Fig. 7B, a, b). In polyps with a single tentacle, HyAlx was expressed at the base of the regenerated tentacle (Fig. 7B, c–e). In contrast, control polyps with fully regenerated heads displayed normal expression pattern of HyAlx at the base of each tentacle (Fig. 7B, f–h). These changes in the expression patterns of HyWnt3 and HyAlx in Notch-knockdown polyps closely resembled the disturbed regeneration processes previously observed in *Hydra* polyps treated with DAPT or SAHM1¹⁹.

When the animals were cut in the middle of the body column, up to 40% of polyps in strains 8#, 11# and 13# regenerated two heads or ectopic tentacles (supplementary Fig. S8). The control groups exhibited normal regeneration, with the exception of strain 2# where one out of 36 polyps regenerated two heads (supplementary Fig. S8).

A new model for Notch-signalling during budding in Hydra

The phenotypes observed in transgenic *Hydra* polyps with compromised HvNotch-expression or NICD over-expression indicate that Notch-signalling is involved in several fundamental patterning processes in *Hydra*, including budding.

To better understand these processes, we developed an initial mathematical model to illustrate the potential interaction between canonical Wnt- and Notch-signalling in *Hydra* in a simplified way. We concentrated on studying the occurrence of "Y-shaped" animals observed in budding Hydra treated with DAPT28, as well as in NICD-overexpressing and Notch-knockdown transgenic Hydra strains. In previous work with DAPT, we had described a sharp boundary, which is formed at the constriction stage of budding (see budding map³⁵) just before foot formation. Without Notch-signalling, constriction does not occur and a foot is not formed. Even if Notch-signalling is restored later by DAPT removal, the bud does not undergo constriction and instead grows out to result in a "Y-shaped" animal. To analyse this spatio-temporal timing of Notch-induced bud constriction, we followed the ideas of Sprinzak^{24,36}. We coupled a large-scale gradient in the developing bud (e.g., given by β-catenin and/or Wnt-signalling expressed at the tip of the bud) with Notch signalling by assuming a simple positive influence of canonical Wnt signalling (or another large-scale gradient apparent in the developing bud) on the Notch-ligand HyJagged, which is strongly expressed on the parent site of the boundary during the final stages of budding²⁷. Furthermore, we assumed that Notch-signalling was blocked in the body-column of the parent polyp by cis-interactions between HvNotch and HyJagged. Upon simulating this system, we observed the sudden formation of a distinct ring of Notch -signalling in the most basal part of the bud, but only after the bud had reached a certain size (Fig. 8A). Hence, the interplay between both systems is not only able to initiate a locally restricted ring at the future bud-foot, but also to measure the size of the protruding bud to activate HyHesexpression and following constriction at the right moment. In contrast, if Notch-signalling is inhibited in this model, bud outgrowth is not restricted, resulting in the formation of Y-shaped polyps (29 and this work). Interestingly, the same response occurred when we virtually overexpressed β -catenin (Fig. 8A). This is in accordance with previously reported phenotypes of transgenic Hydra overexpressing stabilised β-catenin, where elongated polyps were observed without any visible size limitations on the parent polyp or its buds³².

Discussion

Comparison of NICD-overexpression and Notch-knockdown strains

Previous work to study the function of the Notch-signalling pathway in *Hydra* was based on pharmacological pathway inhibition. It had been described that DAPT reversibly prevented nuclear translocation of NICD and similar phenotypes were obtained with a second Notch-inhibitor SAHM1, which has a completely different mode of action^{19,26–28}. Yet, a direct proof that the observed phenotypes were solely attributable to Notch was lacking. We have now succeeded in establishing transgenic *Hydra* strains. They either expressed NICD in the whole ectoderm or endoderm, or they expressed a Notch-hairpin-RNA in both epithelial layers.

Comparison of NICD-overexpressing strains and Notch-knockdown strains revealed both similarities and important differences. Firstly, all strains showed some patterning phenotypes, such as "Y-shaped" polyps, "ectopic tentacles" and "two-headed". Surprisingly, NICD-overexpression resulted in the down-regulation of potential Notch-target genes, including HyAlx and HySp5. In contrast, HyKayak was upregulated. These findings are consistent with the outcome of 48 h DAPT-treatment on the expression of these genes, supporting the argument of a dominant negative effect of NICD-overexpression, which has also been described in other organisms. Previously, it was reported that overexpression of transgenes mostly composing of the Notch extracellular domain, or the Ram23 plus Ankyrin repeat sequences, have the potential to form non-functional complexes with ligands, and thus sequester endogenous Notch in *Drosophila*^{37–39}.

In Notch-knockdown animals, the expression of HyAlx, HySp5 and HyKayak was not changed significantly. Taken together, these results suggest that NICD-overexpression had a stronger and longer-lasting effect on Notchtarget genes compared to knockdown of endogenous Notch. Correspondingly, the occurrence of transgenic polyps was much lower for NICD-overexpression than for Notch-knockdown. Polyps with NICD in both epithelial layers were not obtained, whereas we established four Notch-knockdown strains. However, the similarities in the observed phenotypes can be attributed to Notch-inhibition (loss-of-function) in both cases.

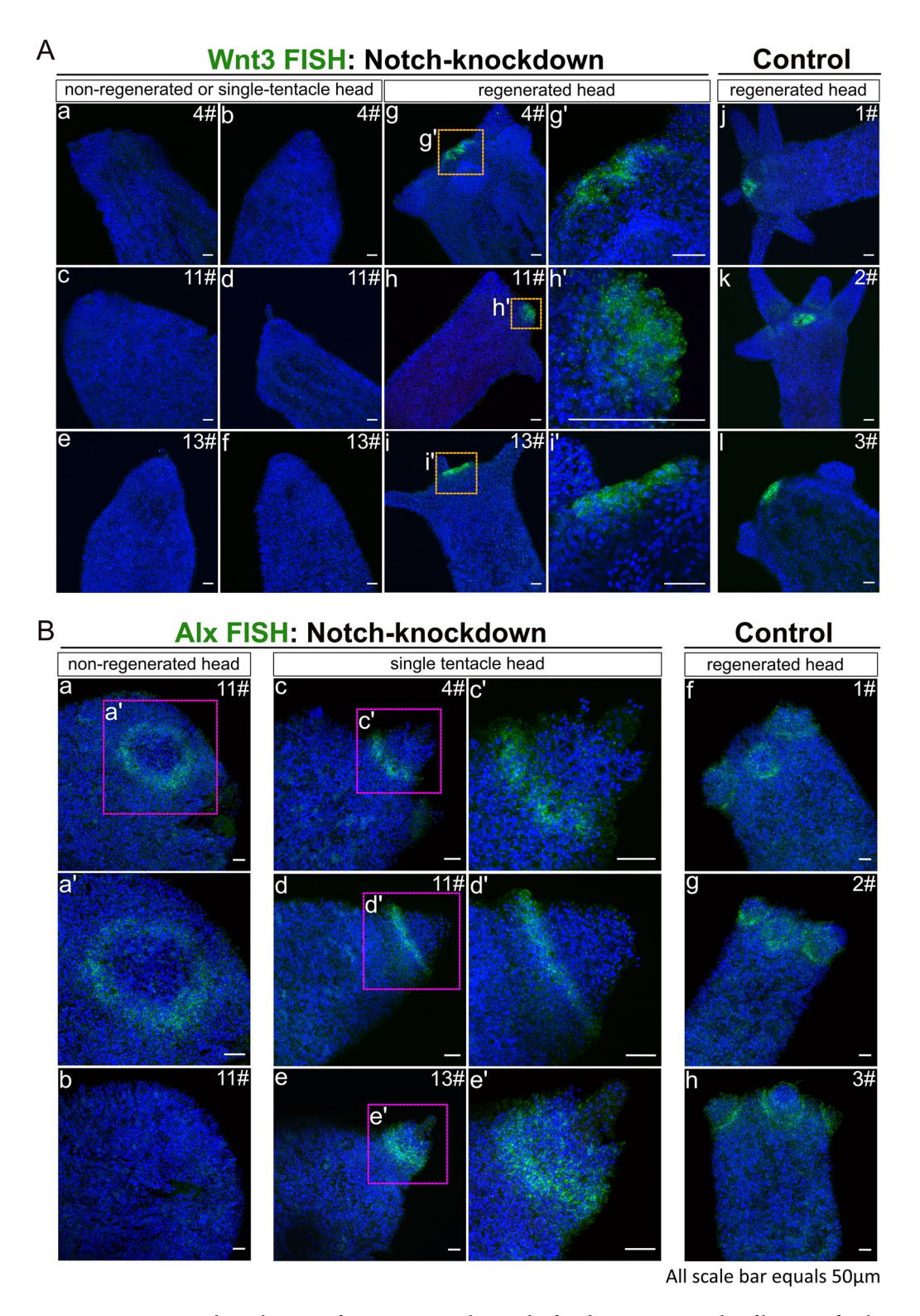


Figure 7. HyWnt3 and HyAlx FISH of regenerating polyps 72 h after decapitation. Stacks of laser-confocal microscopic images. (**A**) Expression of HyWnt3 in abnormally and normally regenerated HvNotch-knockdown polyps (a–f: non-regenerated head or single-tentacle head, g–i: normally regenerated head with enlargements g'–i'). Control polyps 1#, 2# and 3# displayed normal regeneration (j–l). (**B**) Expression of HyAlx in HvNotch-knockdown polyps of strain 11# with non-regenerated heads (a, b and enlargement b'), single-tentacle heads of strains 4#, 11# and 13# (c–e and enlargements c'–e') and control polyps with normally regenerated heads of strains 1#, 2# and 3# (f–h).

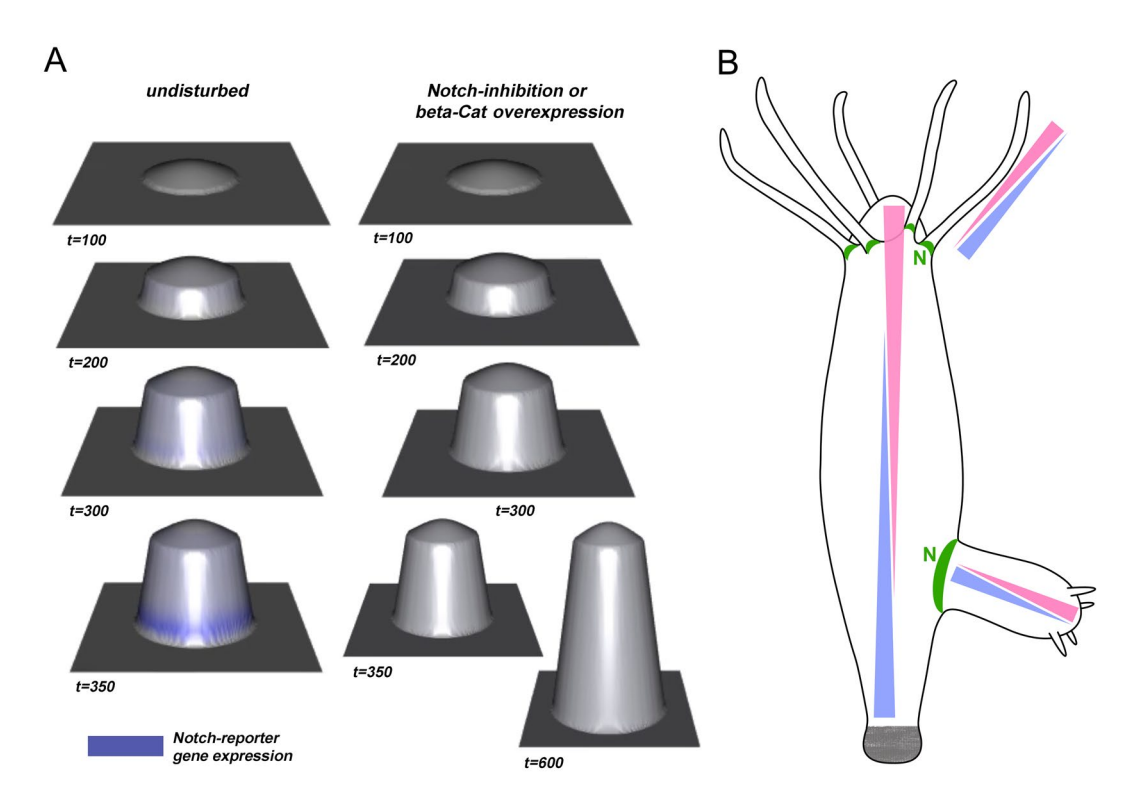


Figure 8. A model for the integration of Notch-signalling with long-range signalling gradients in Hydra. (A) Different simulated virtual time steps and phenotypes during bud-outgrowth when assuming a simple coupling between canonical Wnt- and Notch-signalling. The left-hand side shows the undisturbed system, while the right-hand side shows the impact of inhibiting Notch or overexpressing β-catenin, see also Supplementary Videos VA for undisturbed budding and VB for Notch-inhibition or β-catenin overexpression. (B) Suggested apical-basal gradient displaying pink and basal-apical gradient with blue in different parts of Hydra, including the body column, tentacles and buds. Gradients are supported by published in situ hybridization data, Hobmayer 2000, Fig. 2B and Reinhardt 2004, Figs. 2A and 3D and summarised by Meinhardt 2012. Suggested positions of Notch-signalling (N) are indicated in green based on research by Münder 2010 and Münder 2013.

NICD-overexpression strains

NICD-overexpression revealed the presence of "Y-shaped" animals that had previously been observed after DAPT treatment. Before the bud forms its own foot, HyHes is expressed in a sharp ring of ectodermal cells at the parent-bud boundary. This process is blocked by Notch inhibition, leading to a change in the expression pattern of the *Hydra* FGF-receptor homolog *Kringelchen*⁴⁰. *Kringelchen* now appears in a diffused and broad zone at the base of the bud, covering both parent and bud tissue, rather than in a narrow and sharp band directly adjacent to the HyHes-expressing cells on the side of the parent²⁸. This change prevents foot cell differentiation and bud detachment, resulting in the formation of "Y-shaped" animals²⁸.

We suggest that NICD-overexpression in our transgenic animals inhibits ectodermal HyHes-expression when it is required to establish the parent-bud boundary. As we did not detect a down-regulation of HyHes by RT-qPCR, we furthermore propose that the high level of HyHes expression observed in the whole endoderm⁴¹ of *Hydra* is controlled by other factors in addition to Notch-signalling. This means that HyHes is regulated by Notch mainly in a context dependent manner, such as establishing the parent-bud boundary.

In addition to "Y-animals", we also discovered patterning defects in NICD-overexpressing animals that were not observed with DAPT or SAHM1. These included ectopic tentacles and two- or multi-headed polyps. They reminded of phenotypes seen in animals treated with alsterpaullone or transgenic Hydra with overexpression of stabilised β -catenin^{17,32}, both suggesting an increase of nuclear β -catenin along the body column. Occasionally, multiple heads appeared in a "bouquet" form, which were similar to those previously reported in Sp5-siRNA polyps^{33,42}, which would be consistent with the downregulation of Sp5-levels found in NICD-overexpressing Hydra. However, the ectopic heads and tentacles on the body column indicated a change in the head activation gradient. This was also observed in Notch-knockdown Hydra.

NICD-overexpressing animals regenerated normally (supplementary Fig. S3). Moreover, they did not show aberrant head structures. We attribute this to the fact that NICD was not overexpressed in both epithelial layers, in contrast to the Notch-hairpin-RNA, which did show regeneration phenotypes.

Notch-knockdown strains

All four Notch-knockdown-strains were fully transgenic in both the ectoderm and endoderm. They displayed only 30–50% expression of HvNotch as compared to the average of the control groups. However, the effect on

the expression of Notch target genes here was much lower than in NICD-overexpressing animals. Nevertheless, we did observe some phenotypes in these strains, including "Y-shaped" animals. Moreover, Notch-knockdown affected the heads of the buds, which often displayed irregular tentacle patterns without hypostomes, resembling polyps that had undergone DAPT treatment for several shorter intervals over a longer period of time during consecutive budding processes²⁸. In addition, some aberrant head structures appeared at ectopic sites in Notch-knockdown animals. They were very similar to "ectopic tentacles", but not identical, they rather looked like heads that could only make a tentacle.

Furthermore, Notch-knockdown strains displayed a failure in head regeneration, as observed in the animals treated with DAPT¹⁹ when the heads were cut off just underneath the tentacle ring. In our strains, in around 20% of cases, head regeneration either failed completely, or single tentacles were formed without hypostomes. Upon analyzing the gene expression in these regenerates, we discovered the absence of HyWnt3 when regeneration did not occur. This finding was similar to DAPT or SAHM1 treated regenerates. In contrast, the expression of the tentacle gene HyAlx could be detected in the regenerates of all knockdown animals, albeit not always in the expected ring pattern around the base of developing tentacles. Consequently, regenerates without any tentacles or with a single tentacle expressed HyAlx in a single and often broad ring. This indicated that Notch-knockdown led to a reduction of HyWnt3-expression during head regeneration, while not stopping HyAlx expression. As a result, a proper head could not be formed, only aberrant tentacles appeared occasionally. We explain this with the lack of a lateral inhibition process mediated by HvNotch, which is required for Hydra head regeneration to allow the accumulation of HyWnt-3 expression at the future hypostome and to shift the expression zone of HyAlx to the base of the tentacles. When Notch is missing, the default fate of the regenerating tip is a tentacle fate. However, the lack of HyWnt3 prevents organizer formation and orderly arrangement of tentacles in this case. This idea had been described in our previous investigations on the effects of DAPT and SAHM 1 on Hydra head regeneration¹⁹.

Notch-function in head regeneration is context dependent

Head regeneration had previously been described to be different at apical and basal levels⁴³, It was shown that tentacle markers appeared first in apically cut polyps, while hypostome markers appeared first in basally cut polyps. In middle gastric regenerates, an intermediate result had been observed. Our previous findings had indicated Notch-signalling is required for inhibition of tentacle tissue formation in apical regenerates¹⁹. We now found that Notch is also needed for proper regeneration at more basal levels. Notch-knockdown strains as well as NICD-overexpressing transgenic strains both showed aberrant regeneration by producing two heads, whereby the effect was stronger in the knockdown strains (similar to the observation for apical regeneration and confirming that NICD-overexpression has a dominant negative effect). This suggests that Notch is required for some sort of head inhibition in more basal regenerates. Three days after head removal the "two-headed" regenerates have similarities with the "bouquet" phenotype found in Sp5 knockdown polyps²⁹ and in this study. Whether Sp5 is indeed the target for Notch-signalling in basal regenerates has to be investigated in the future. At this point we conclude that Notch-signalling is necessary to inhibit the tissue that appears first in head regenerates. It has been shown before that the outcome of Notch-signalling is context dependent and often opposing (recently discussed by Vujovici et al⁴⁴). However, in both apical and more basal regenerates HvNotch appears to govern inhibition processes, which seem necessary to balance the hypostomal and the tentacle systems during the regeneration process.

HvNotch function in Hydra patterning and budding

As described for NICD-overexpressing strains, Notch-knockdown strains also exhibited "two-headed" and "ectopic tentacle" phenotypes, as had been observed in animals overexpressing stabilised β -catenin and animals treated with alsterpaullone. Moreover, the knockdown animals sometimes developed two feet, which has not been seen in animals treated with DAPT or SAHM1. This constitutes a newly discovered function of Notch signalling in *Hydra*, suggesting its potential involvement in establishing or stabilising a head and/or foot activation gradient.

The effect of Notch-signalling on *Hydra* head and/or foot activation gradients is not completely unexpected given our previous findings about Notch-target genes in *Hydra*. We had described that epithelial cell genes expressed in the foot were upregulated after 48 h of DAPT treatment, including the BMP pathway component TGF-4 and APCDD1 (a negative regulator of the Wnt signalling pathway)³¹, which could explain the emergence of two-feet phenotype in Notch-knockdown animals. In contrast, head organizer genes including HyWnt7 and the transcription factor HyTCF were downregulated upon DAPT treatment. These changes have the potential to shift the head activation gradient towards the aboral end, which could explain the formation of ectopic heads above the budding zone in NICD-overexpressing and Notch-knockdown transgenic *Hydra*.

Hans Meinhardt has provided a summarised model for Hydra patterning in 2012, which suggested the existence of two opposing gradients of signalling molecules, one reaching from the head to the foot and the other vice versa. These two gradients are initiated by HyWnts and HyBMP5-8b, respectively^{14,45,46}. Moreover, these gradients are repeated in the tentacles with HyWnt5 at the tip and HyBMP5-8b at the base, and in the bud with HyWnt2 initially and later HyWnt3 at the tip, and HyBMP5-8b at the basal end of the bud before the foot is formed (Fig. 8B). We have extended this hypothesis by including Notch-signalling at the boundary between the parent and bud, and at the tentacle borders. In order to explain the formation of the parent-bud boundary, we have developed a mathematical model, where the gradient activity of β -catenin triggers the establishment of Notch-signals in a sharp line at this boundary. This is followed by the constriction and separation of the bud. If these signals fail to occur at the correct length of the bud, we obtain "Y-shaped" animals, indicating strict spatiotemporal requirements for this process. Within this model, the positioning of Notch-signalling depends on the concentration of Notch-receptors and ligands. When the concentrations of HvNotch and HyJagged are equal on

the cell surface, they inhibit Notch-signalling in cis. The transactivation of the pathway occurs at sharp boundaries where cells with free (not cis-inhibited) Notch-receptors touch cells with free Notch ligands. Therefore, this model requires something to establish the gradients of Notch-receptors and its ligands. In *Hydra*, the HyBMP5-8b/HyWnt gradients may be responsible for creating the Notch-activity gradients. In NICD-overexpressing animals, Notch-signalling may be inhibited by interactions between NICD and ligands on the cell membrane, leading to the sequestration of the endogenous HvNotch receptor. In HvNotch-knockdown animals, the gradients of Notch-receptors across the length of the body column might be changed, consequently shifting the positions of the Notch-signal. In both cases, the occurrence of patterning defects can be expected.

Methods *Hydrα* culture

The injected embryos and all transgenic *Hydra* strains were cultured at 18 °C in *Hydra* medium (HM) composed of 0.29 mM CaCl₂, 0.59 mM MgSO₄·7H₂O, 0.50 mM NaHCO₃, 0.08 mM K₂CO3. *Hydra* was regularly fed every 2 days with freshly hatched *Artemia nauplii*.

Plasmid constructions

For NICD-overexpression, 1128 base pairs of HyNotch-NICD (1648-2775 of Notch mRNA) were inserted into the vector pHyVec11 (Addgene plasmid #34794). Expression was driven by the Hydra actin promoter. Downstream of the NICD insert was an intergenic sequence that enables adding of a trans-spliced leader sequence⁴⁷ in front of the DsRed gene sequence to generate two independent transcripts for expressing HvNICD and dsRed. For the construction of the Notch-knockdown plasmid, we designed a hairpin structure using part of the Notch-NICD sequence (1763-2283 nucleotides) in both, the forward and reverse directions, separated by a 433 base pairs actin intron sequence. The entire hairpin sequence was then inserted into the vector pHyVec12 (Addgene plasmid #51851, NCBI KJ472831.1 Hydra Expression Vector pHyVec12). The Notch-Hairpin structure was under the control of the actin promoter. Similar to pHyVec11, the downstream DsRed gene was situated behind an intergenic trans-splice region. After sequencing, the plasmids were isolated from E.coli and purified using the Qiagen Plasmid Maxi kit (QIAGEN, Cat. No. 12162). Subsequently, the plasmids underwent an additional purification step with ethanol and KAc precipitation. Specifically, 10 μl of 2.5 M KAc and 250 μl of 96% ethanol were added to a 100 µl plasmid solution obtained from the Maxi-prep. The mixture was intensively mixed and incubated for 2 h at -20 °C. After incubation, the mixture was centrifuged at 15,000 g for 20 min at 4 °C. The resulting pellet was then washed once with 1 ml of 75% ethanol and air-dried for 30 min to ensure the removal of any residual ethanol. Finally, we resuspended the pellet by adding 50 μL of Nuclease-free water (The resulting concentration was around 2 µg/ml).

Generation of transgenic Hydra

The plasmids were injected into *Hydra* eggs in the lab of Thomas C.G. Bosch, Kiel according to the method described by Wittlieb et al⁴⁸. After 2 weeks of injection, embryos began to hatch. Subsequently, we screened the newly hatched polyps for DsRed signals. Positive hatchlings were fed daily to induce the budding process. Buds exhibiting DsRed-signals were selected. Throughout this procedure, we obtained some polyps with higher concentration of signals on one side. These animals were cut and pieces with more DsRed signals were left to regenerate. In this way we expanded transgenic animal strains and eventually obtained fully transgenic polyps.

RT-qPCR

Total RNA was extracted using the RNeasy plus Mini kit (QIAGEN, Cat. No. A25776). The quality of the RNA was measured using the Agilent 2100 Bioanalyser with the Agilent RNA 6000 Nano kit (Agilent, Cat. No. 5067-1511). Only RNA with RIN value above eight was used for cDNA synthesis with the iScript cDNA synthesis kit (Biorad, Cat. No. 1708891). RT-qPCR was then performed in a 96-well plate using the PowerUp SYBR green master mix (ThermoFisher, Cat. No. 25742) and the CFX96tm real time system from Biorad. The expression level of genes was normalized using reference genes, specifically GAPDH, EF1a and PPIB. The primer sequences used in the RT-qPCR are listed in supplementary Table S1. Statistical significance was determined based on the average value of several control groups using GraphPad Prism 6.01 with a two-tailed *t*-test. The corresponding p-value were expressed in the following manners. ns (no significance) for p > 0.05; * for $p \le 0.05$; ** for $p \le 0.001$; *** for $p \le 0.001$; *** for $p \le 0.001$.

Synthesis of RNA probes

The vector pGEM-T contains M13 primer sites in which an approximately 200 bp insert (e.g. *HyWnt3* and *HyAlx*) was flanked. By performing PCR with M13 primers, the insert was amplified, linearized, and purified from the agarose gel after electrophoresis using a DNA purification kit (Qiagen, Cat. No. 28704). Rib probes were synthesized using SP6 or T7 polymerases together with 500 ng of M13 PCR product, DIG (digoxigenin) RNA labelling mix (Roche, Cat. No. 11277073910). Both, anti-sense (for hybridization) and sense (for control) probes were generated. Next, the DIG-labelled RNA was purification by adding 10% of 3 M sodium acetate and 3 times of ice-cold 100% ethanol. The labelling efficiency of probes was tested by performing a dot plot following the protocol provided by Roche. The probes that exhibited strong signals in the dot blot were considered suitable for subsequent fluorescence in situ hybridization. The primer sequences used for amplification of the inserts are listed in supplementary Table S2. Approximately 25 μg of probes were produced by each synthesis.

Fluorescence in situ hybridization (FISH)

Fluorescence RNA in situ hybridization experiments were carried out according to the previously reported protocol from the laboratory of Celina Juliano⁴¹.

Antibody staining

Polyps were relaxed in 2% Urethane in *Hydra* medium (HM) for 2 min and fixed with 4% PFA in HM for 1 h at room temperature with gentle shaking. Subsequently, the polyps were washed three times with PBS for 5 min each, and then permeabilized with 1% Triton-X100 in PBS for 15 min. Afterwards, the polyps were blocked with a solution of 1% BSA, 0.1% Triton-X100 in PBS for 1 h at room temperature and incubated with diluted anti-Cadherin-antibody (from Prof. Dr. Charles N. David, 1–1000 dilution) and anti-acetylated-Tubulin-antibody (Sigma-Aldrich, Cat.No. T6793, 1–250 dilution) overnight at 4 °C with gentle agitation. On the next day, the polyps were washed three times with PBST (0.1% Tween20) for 10 min each, and incubated with anti-rabbit-Alexa488, anti-mouse-Alexa649 for 2 h at room temperature. Then the polyps were washed again three times with PBST for 10 min each, nuclei were stained with DAPI (Sigma, Cat.No. D9542) at a concentration of 1 µg/ml for 15 min and polyps were mounted on slides with Vectashield anti-fade mounting medium (Biozol, Cat. No. H1000).

Confocal imaging

A series of optical section images were captured along the Z-axis with a Leica TCS SP5-2 confocal microscope. The lasers employed in this study were Diode, Argon and Helium/Neon. After acquisition, the images were processed using ImageJ software.

DAPI nuclear staining was imaged with Diode laser with excitation wavelength at 345 nm and emission at 455 nm. Alexa488 dyes (FISH of Wnt3 and Alx, Cadherin staining) were visualized with an argon laser with excitation at 499 nm and emission at 520 nm. For Alexa 649 (acetylated-Tubulin staining), a Helium–Neon Laser with excitation at 652 nm and emission at 668 nm was used.

Mathematical modelling of Notch signalling

The mathematical discrete model for Notch signalling during bud-outgrowth is chemically based on the MI-model as given in Sprinzak's research²⁴, where β_-D represents β -catenin (or another diffusive gradient related to head identity in *Hydra*). We extend this model by coupling it to the geometrically dynamic situation of an outgrowing bud. In particular, for simulations, we discretize the unit square into 10,000 spatial pixels and define the bud-region by initially a circular region of radius 0.15 in the center of the square, slightly and spherically deformed in z-direction in order to represent the initial bud. For simulations of the bud outgrowth, starting with random initial distribution for all chemical components except β_-D , on the one hand, we simulated the chemical nearest-neighbor network as given by the MI-model for 600 subsequent time steps in the bud-region only. Here, the β -catenin gradient (β_-D) is prescribed in the entire domain circularly decaying from its maximum in the bud tip. On the other hand, mechano-chemical bud outgrowth is simulated by stepwise increasing the bud radius and at the same time moving bud-related pixels a constant amount (for each time step) in z-direction. This eventually leads to a stepwise protruding (slightly conical) bud shape with cells/pixels stepwise moving from the surrounding (budding-region) into the bud region, where newly augmented cells always show lower β -catenin concentrations compared to the cells augmented at the time step before.

Data availability

All data presented in the main manuscript and supplementary files will be provided by the corresponding authors (Angelika Böttger and Qin Pan) upon requests.

Received: 22 December 2023; Accepted: 3 April 2024

Published online: 12 April 2024

References

- 1. Holstein, T. W., Hobmayer, E. & David, C. N. Pattern of epithelial cell cycling in hydra. Dev. Biol. 148, 602-611 (1991).
- 2. David, C. N. & Campbell, R. D. Cell cycle kinetics and development of Hydra attenuata: I. Epithelial cells. J. Cell Sci. 11, 557–568 (1972).
- 3. David, C. N. & Gierer, A. Cell cycle kinetics and development of Hydra attenuata: III. Nerve and nematocyte differentiation. *J. Cell Sci.* 16, 359–375 (1974).
- 4. Campbell, R. D. & David, C. N. Cell cycle kinetics and development of Hydra attenuata: II. Interstitial cells. *J. Cell Sci.* 16, 349–358 (1974)
- 5. Hobmayer, B. et al. Stemness in Hydra—A current perspective. Int. J. Dev. Biol. 56, 509–517 (2012).
- 6. Spemann, H. & Mangold, H. Induction of embryonic primordia by implantation of organizers from a different species. 1923. *Int. J. Dev. Biol.* 45, 13–38 (2001).
- 7. Browne, E. N. The production of new hydranths in Hydra by the insertion of small grafts. J. Exp. Zool. 7, 1-23 (1909).
- 8. MacWilliams, H. K. Hydra transplantation phenomena and the mechanism of Hydra head regeneration: II. Properties of the head activation. *Dev. Biol.* **96**, 239–257 (1983).
- 9. MacWilliams, H. K. Hydra transplantation phenomena and the mechanism of hydra head regeneration: I. Properties of the head inhibition. *Dev. Biol.* **96**, 217–238 (1983).
- 10. Wilby, O. K. & Webster, G. Experimental studies on axial polarity in hydra. J. Embryol. Exp. Morphol. 24, 595-613 (1970).
- 11. Wilby, O. K. & Webster, G. Studies on the transmission of hypostome inhibition in hydra. *J. Embryol. Exp. Morphol.* **24**, 583–593 (1970).
- Takano, J. & Sugiyama, T. Genetic analysis of developmental mechanisms in hydra: XVI. Effect of food on budding and developmental gradients in a mutant strain L4. J. Embryol. Exp. Morphol. 90, 123–138 (1985).
- 13. Gierer, A. & Meinhardt, H. A theory of biological pattern formation. Kybernetik 12, 30-39 (1972).

- Meinhardt, H. Modeling pattern formation in hydra: A route to understanding essential steps in development. Int. J. Dev. Biol. 56, 447–462 (2012).
- 15. Tursch, A. et al. Injury-induced MAPK activation triggers body axis formation in Hydra by default Wnt signaling. Proc. Natl. Acad. Sci. USA. 119, e2204122119 (2022).
- 16. Broun, M. & Bode, H. R. Characterization of the head organizer in hydra. Development 129, 875-884 (2002).
- Broun, M., Gee, L., Reinhardt, B. & Bode, H. R. Formation of the head organizer in hydra involves the canonical Wnt pathway. Development 132, 2907–2916 (2005).
- 18. Hobmayer, B. *et al.* WNT signalling molecules act in axis formation in the diploblastic metazoan Hydra. *Nature* **407**, 186–189 (2000).
- Münder, S. et al. Notch-signalling is required for head regeneration and tentacle patterning in Hydra. Dev. Biol. 383, 146–157 (2013).
- 20. Lai, E. C. Notch signaling: Control of cell communication and cell fate. Development 131, 965-973 (2004).
- 21. Bray, S. J. Notch signalling: A simple pathway becomes complex. Nat. Rev. Mol. Cell Biol. 7, 678-689 (2006).
- 22. Miller, A. C., Lyons, E. L. & Herman, T. G. cis-Inhibition of Notch by endogenous Delta biases the outcome of lateral inhibition. *Curr. Biol.* 19, 1378–1383 (2009).
- 23. Micchelli, C. A., Rulifson, E. J. & Blair, S. S. The function and regulation of cut expression on the wing margin of *Drosophila*: Notch, wingless and a dominant negative role for Delta and serrate. *Development* 124, 1485–1495 (1997).
- 24. Sprinzak, D. et al. Cis-interactions between Notch and Delta generate mutually exclusive signalling states. Nature 465, 86–90 (2010).
- 25. del Álamo, D., Rouault, H. & Schweisguth, F. Mechanism and significance of cis-inhibition in Notch signalling. *Curr. Biol.* 21, R40-47 (2011).
- 26. Käsbauer, T. et al. The Notch signaling pathway in the cnidarian Hydra. Dev. Biol. 303, 376-390 (2007).
- 27. Prexl, A. et al. The putative Notch ligand HyJagged is a transmembrane protein present in all cell types of adult Hydra and upregulated at the boundary between bud and parent. BMC Cell Biol. 12, 38 (2011).
- 28. Münder, S. et al. Notch signalling defines critical boundary during budding in Hydra. Dev. Biol. 344, 331-345 (2010).
- Vogg, M. C. et al. An evolutionarily-conserved Wnt3/beta-catenin/Sp5 feedback loop restricts head organizer activity in Hydra. Nat. Commun. 10, 312 (2019).
- 30. Smith, K. M., Gee, L. & Bode, H. R. HyAlx, an aristaless-related gene, is involved in tentacle formation in hydra. *Development* 127, 4743–4752 (2000).
- 31. Moneer, J. et al. Differential gene regulation in DAPT-treated Hydra reveals candidate direct Notch signalling targets. J. Cell Sci. https://doi.org/10.1242/jcs.258768 (2021).
- 32. Gee, L. et al. Beta-catenin plays a central role in setting up the head organizer in hydra. Dev. Biol. 340, 116-124 (2010).
- 33. Vogg, M. C. *et al.* An evolutionarily-conserved Wnt3/β-catenin/Sp5 feedback loop restricts head organizer activity in Hydra. *Nat. Commun.* **10**, 312 (2019).
- 34. Dana, C. E., Glauber, K. M., Chan, T. A., Bridge, D. M. & Steele, R. E. Incorporation of a horizontally transferred gene into an operon during cnidarian evolution. *PLoS One* 7, e31643 (2012).
- 35. Otto, J. J. & Campbell, R. D. Budding in Hydra attenuata: Bud stages and fate map. *J. Exp. Zool.* **200**, 417–428 (1977).
- 36. Sprinzak, D., Lakhanpal, A., LeBon, L., Garcia-Ojalvo, J. & Elowitz, M. B. Mutual inactivation of Notch receptors and ligands facilitates developmental patterning. *PLoS Comput. Biol.* 7, e1002069 (2011).
- 37. Rebay, I., Fehon, R. G. & Artavanis-Tsakonas, S. Specific truncations of *Drosophila* Notch define dominant activated and dominant negative forms of the receptor. *Cell* 74, 319–329 (1993).
- 38. Jacobsen, T. L., Brennan, K., Arias, A. M. & Muskavitch, M. A. Cis-interactions between Delta and Notch modulate neurogenic signalling in *Drosophila*. Development 125, 4531–4540 (1998).
- 39. Wesley, C. S. & Mok, L. P. Regulation of Notch signaling by a novel mechanism involving suppressor of hairless stability and carboxyl terminus-truncated notch. *Mol. Cell. Biol.* 23, 5581–5593 (2003).
- 40. Sudhop, S. et al. Signalling by the FGFR-like tyrosine kinase, Kringelchen, is essential for bud detachment in Hydra vulgaris. Development 131, 4001–4011 (2004).
- 41. Siebert, S. et al. Stem cell differentiation trajectories in Hydra resolved at single-cell resolution. Science https://doi.org/10.1126/science.aav9314 (2019).
- 42. Mercker, M. et al. β-Catenin and canonical Wnts control two separate pattern formation systems in Hydra: Insights from mathematical modelling. bioRxiv https://doi.org/10.1101/2021.02.05.429954 (2021).
- 43. Technau, U. & Holstein, T. W. Head formation in Hydra is different at apical and basal levels. Development 121, 1273-1282 (1995).
- 44. Vujovic, F., Hunter, N. & Farahani, R. M. Notch pathway: A bistable inducer of biological noise?. *Cell Commun. Signal* 17, 133 (2019)
- 45. Lengfeld, T. et al. Multiple Wnts are involved in Hydra organizer formation and regeneration. Dev. Biol. 330, 186-199 (2009).
- Reinhardt, B., Broun, M., Blitz, I. L. & Bode, H. R. HyBMP5-8b, a BMP5-8 orthologue, acts during axial patterning and tentacle formation in hydra. Dev. Biol. 267, 43–59 (2004).
- 47. Stover, N. A. & Steele, R. E. Trans-spliced leader addition to mRNAs in a cnidarian. *Proc. Natl. Acad. Sci. USA.* **98**, 5693–5698 (2001).
- 48. Wittlieb, J., Khalturin, K., Lohmann, J. U., Anton-Erxleben, F. & Bosch, T. C. Transgenic Hydra allow in vivo tracking of individual stem cells during morphogenesis. *Proc Natl. Acad. Sci. USA* 103, 6208–6211 (2006).

Acknowledgements

We want to express our gratitude to the funding agencies for supporting this work. Q.P. is funded by a CSC-grant (Chinese Scholarship Council), A.B. is funded by the German Research foundation (DFG) project BO1748-12, A.K. is supported by grants from the German Research Foundation (DFG) project KL 3475/2-1 and CRC 1461: "Neurotronics: Bio-Inspired Information Pathways". The drawings in this document were produced using Affinity Designer 2 (version 2.3.0) by Q.P.

Author contributions

A.B. and Q.P. conceived this study. A.K. and J.W. conducted the induction of *Hydra* sexual reproduction, collection and injection of embryos. Q.P. established fully transgenic Hydra, performed all experiments and generated the figures. M. M. and A.M.C developed the mathematics model. Q.P. and A.B. drafted the manuscript. All authors revised and approved the manuscript.

Funding

Open Access funding enabled and organized by Projekt DEAL. Q.P. is funded by a CSC-grant (Chinese Scholarship Council), A.B. is funded by the German Research foundation (DFG) project BO1748-12, A.K. is supported

by grants from the German Research Foundation (DFG) project KL 3475/2-1 and CRC 1461: "Neurotronics: bio-Inspired Information Pathways".

Competing interests

The authors declare no competing interests.

Additional information

Supplementary Information The online version contains supplementary material available at https://doi.org/10.1038/s41598-024-58837-7.

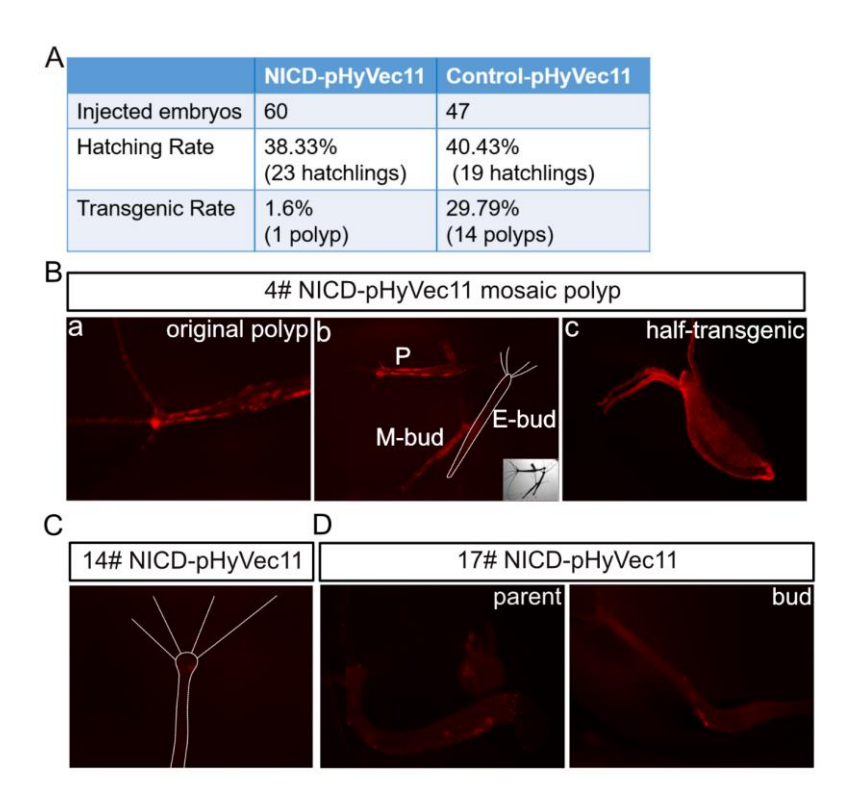
Correspondence and requests for materials should be addressed to Q.P. or A.B.

Reprints and permissions information is available at www.nature.com/reprints.

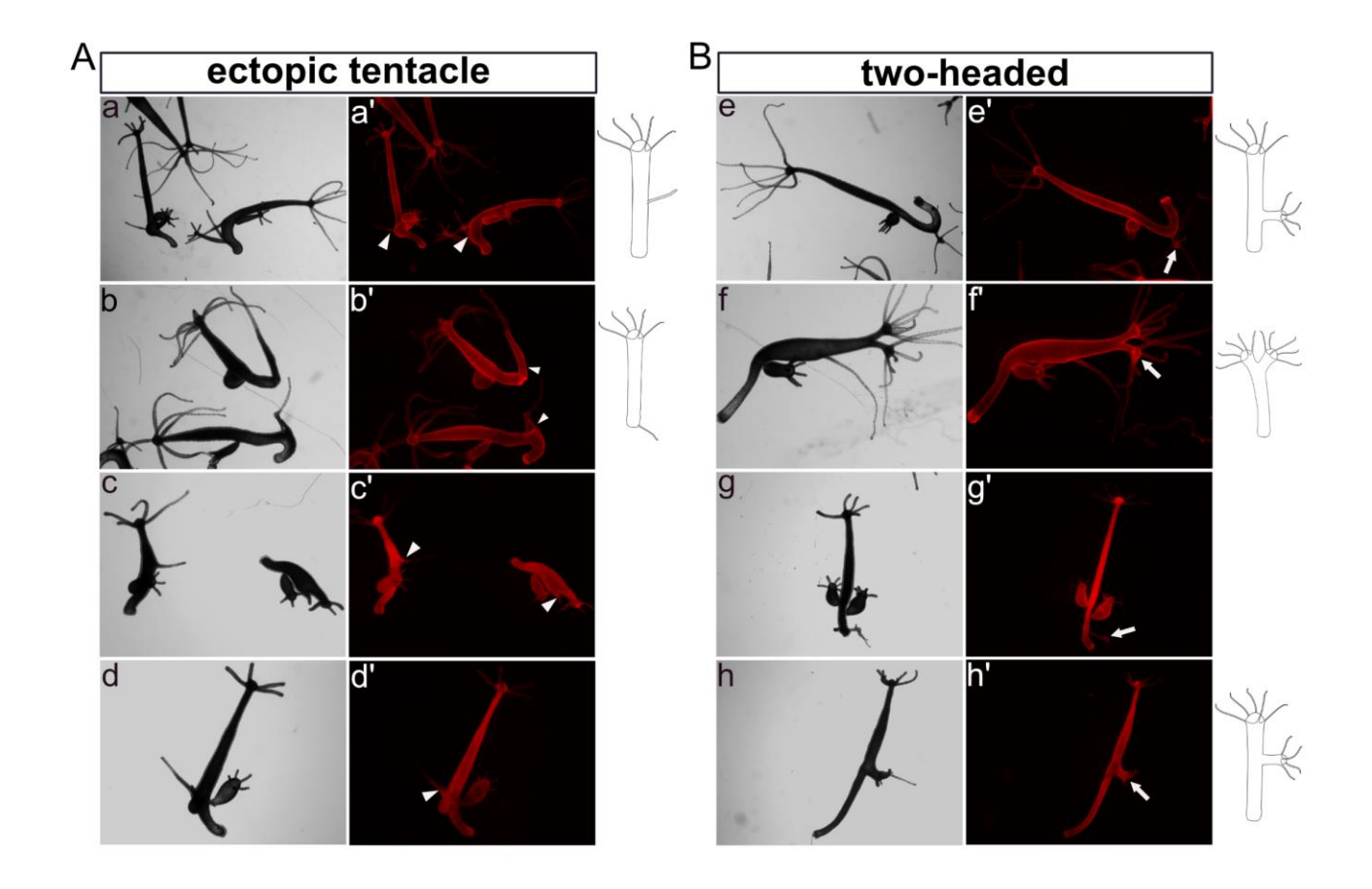
Publisher's note Springer Nature remains neutral with regard to jurisdictional claims in published maps and institutional affiliations.

Open Access This article is licensed under a Creative Commons Attribution 4.0 International License, which permits use, sharing, adaptation, distribution and reproduction in any medium or format, as long as you give appropriate credit to the original author(s) and the source, provide a link to the Creative Commons licence, and indicate if changes were made. The images or other third party material in this article are included in the article's Creative Commons licence, unless indicated otherwise in a credit line to the material. If material is not included in the article's Creative Commons licence and your intended use is not permitted by statutory regulation or exceeds the permitted use, you will need to obtain permission directly from the copyright holder. To view a copy of this licence, visit http://creativecommons.org/licenses/by/4.0/.

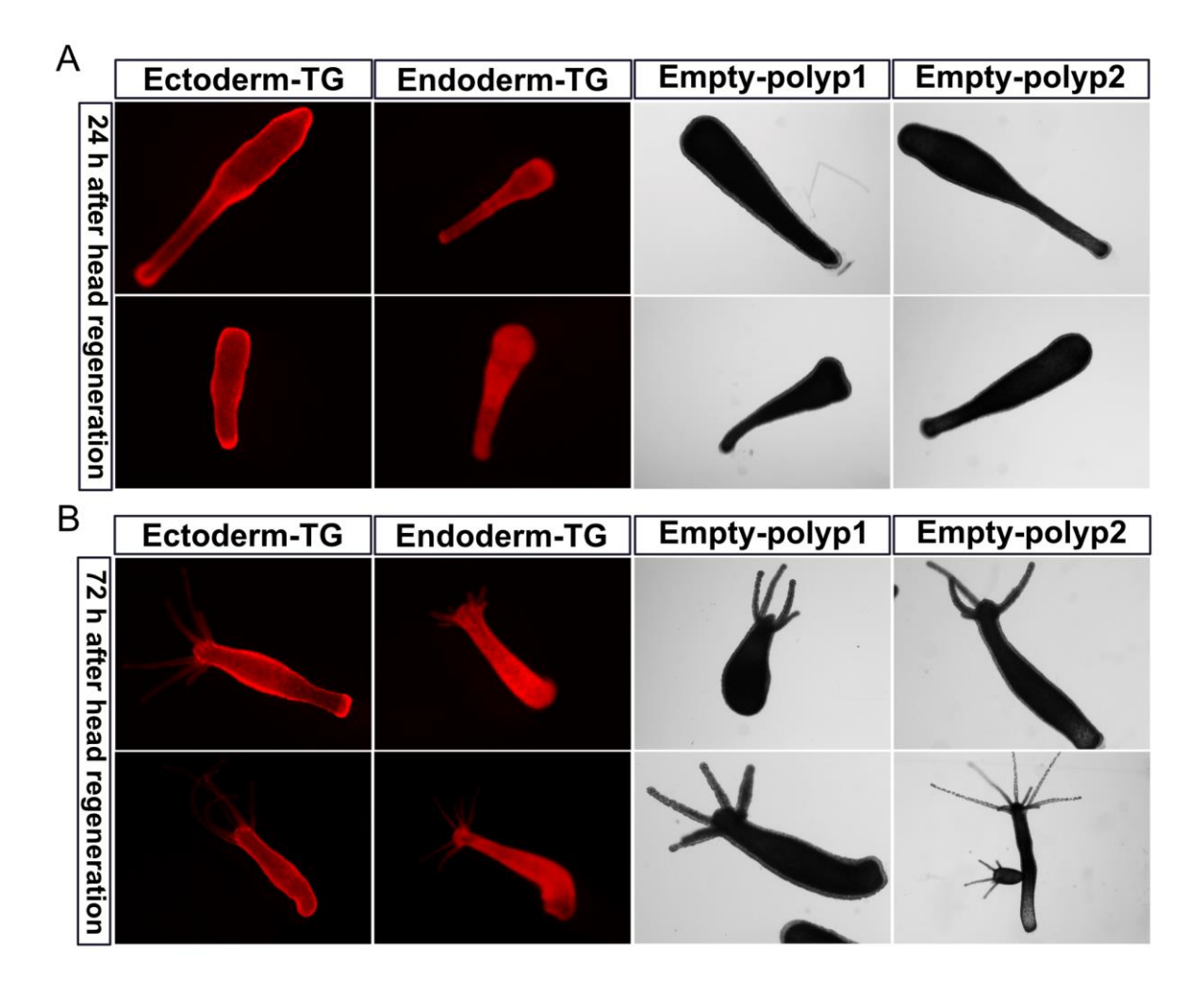
© The Author(s) 2024



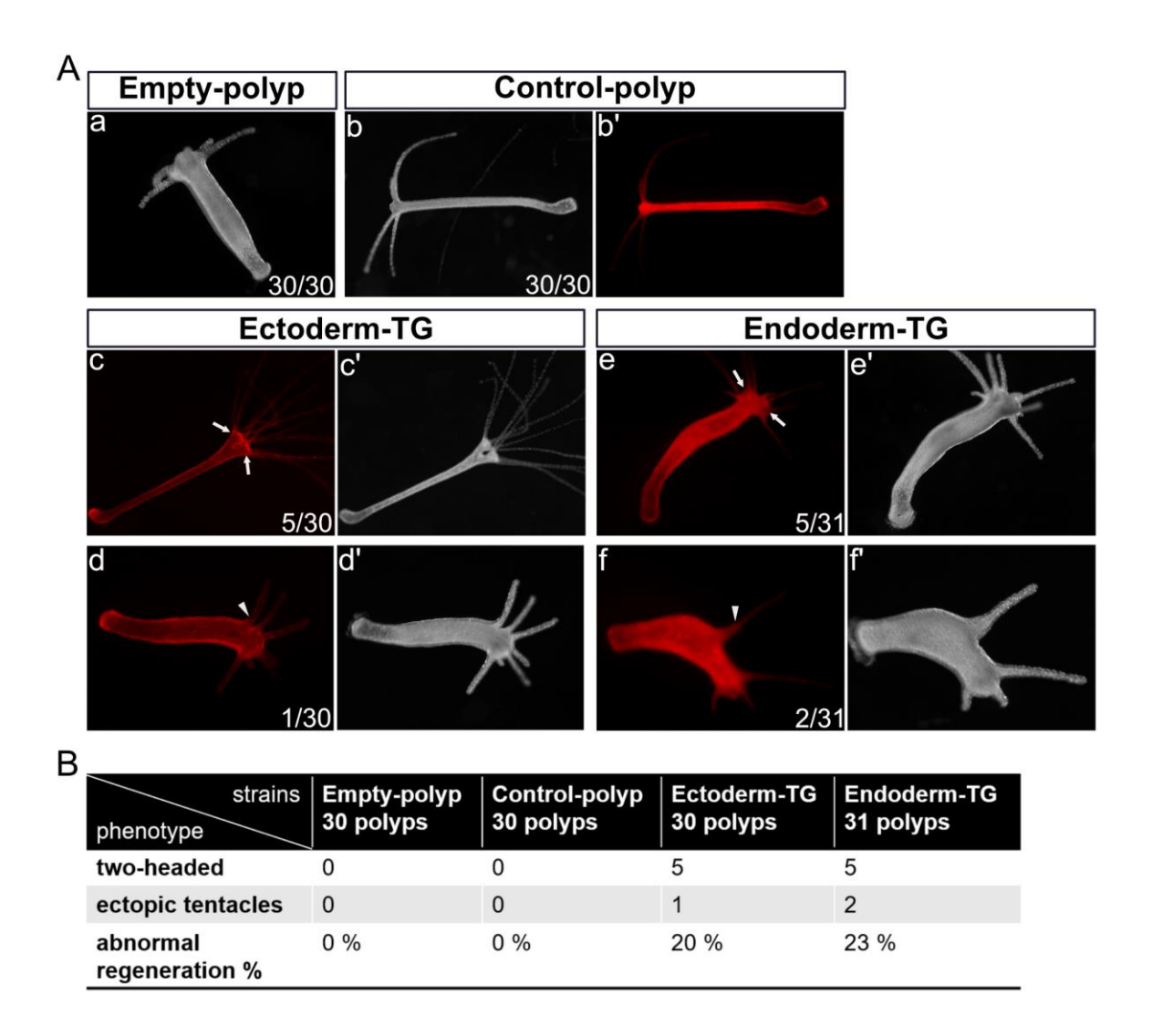
Supplementary Fig. S1 Mosaic HvNICD-overexpressing transgenic *Hydra*. (A) 60 embryos were injected with HvNICD-pHyVec11, resulting in 23 hatchlings. Strain 4# had most promising DsRed signals. 47 embryos were injected with control-pHyVec11, resulting in 19 hatchlings, 14 of which had good DsRed signals. (B) Polyps from strain 4# with mosaic DsRed fluorescence. (B-a) 4# original polyp. (B-b) 4# original polyp with a developing bud and two detached buds. P: parent polyp; M-bud: mosaic bud; E-bud: empty bud means polyps detached from the mosaic parent, but lacking DsRed signals. E-bud is outlined by dotted lines. (B-c) Half-transgenic polyp obtained from 4# mosaic polyp. (C) Strain 14# injected with HvNICD-pHyVec11 with few signals in the head region, migrating away from the head during development. (D) The original polyp and the first bud from strain 17# injected by HvNICD-pHyVec11, both with small number of scattered DsRed positive cells along the body column.



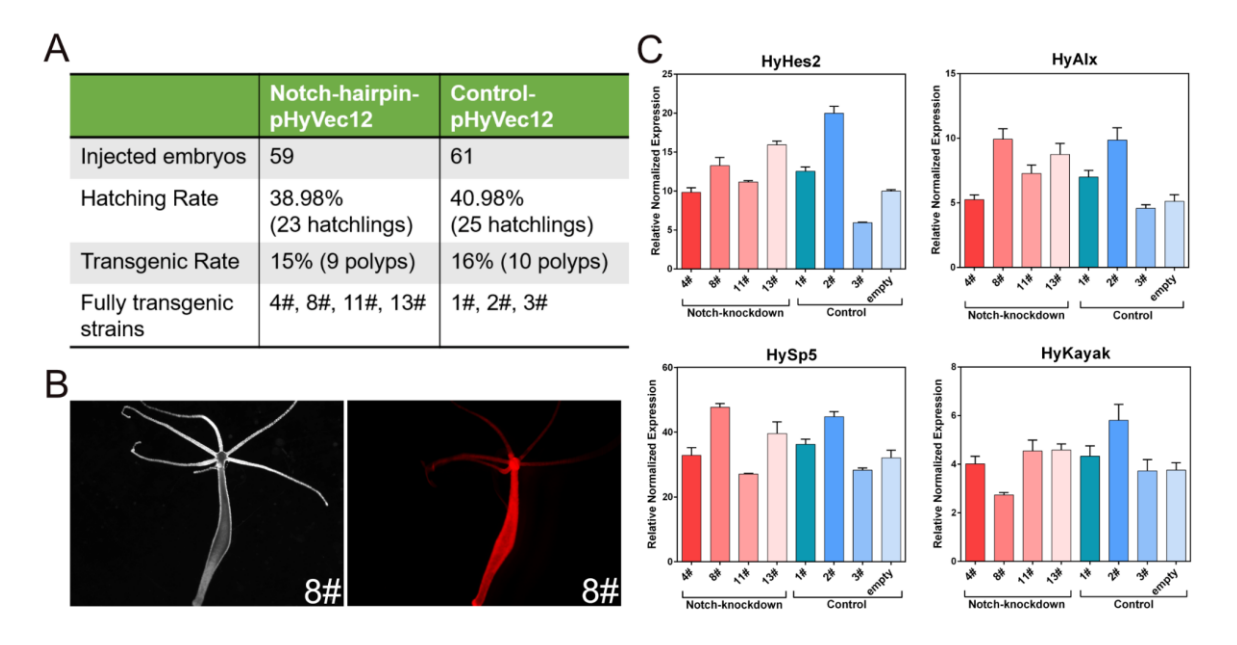
Supplementary Fig. S2 Phenotypes of HvNICD-overexpressing transgenic *Hydra* maintained for a three-week period. (A) "Ectopic tentacles", as indicated by white triangles in the body column (a, b ectoderm-TG; c, d endoderm-TG). (B) "two-headed" phenotype with the extra heads located in different positions along the body column and indicated with white arrows (a, b ectoderm-TG; c, d endoderm-TG).



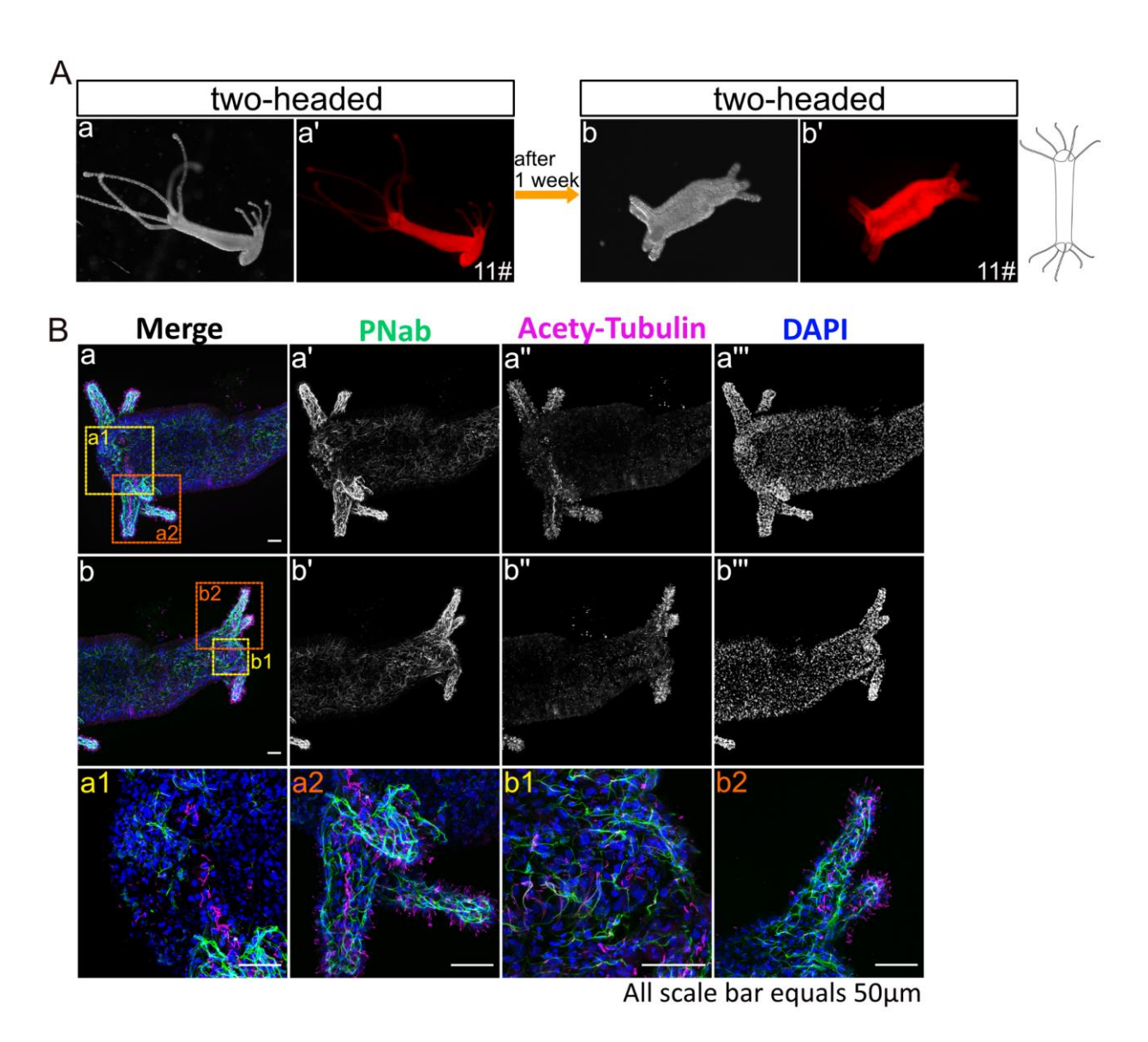
Supplementary Fig. S3 The process of head regeneration in HvNICD-overexpressing transgenic *Hydra* after decapitation below the tentacle ring. Empty polyps were polyps injected with HvNICD-pHyVec11 but without DsRed signals. (A) The regenerating polyps from the ectoderm-TG, endoderm-TG, empty-polyp1 and empty-polyp2 24 h after decapitation. (B) 72 h after head removal, ectoderm-TG, endoderm-TG and two groups of empty polyps show regular head regeneration.



Supplementary Fig. S4 Head regeneration in HvNICD-overexpressing transgenic *Hydra* after decapitation in the middle of the body column. Empty-polyp refers to polyps injected with HvNICD-pHyVec11, but lacking DsRed signals. Control polyp refers to polyps injected with the control-pHyVec11 vector. (A) Normal regenerates in empty-polyp and control-polyp, "two-headed" and "ectopic tentacles" regenerates from Ectoderm-TG and Endoderm-TG 3 days after decapitation. Two heads were indicated with white arrows and ectopic tentacles were indicated with white triangles. (B) Quantification of abnormal regeneration percentages in HvNICD-overexpressing and control groups.

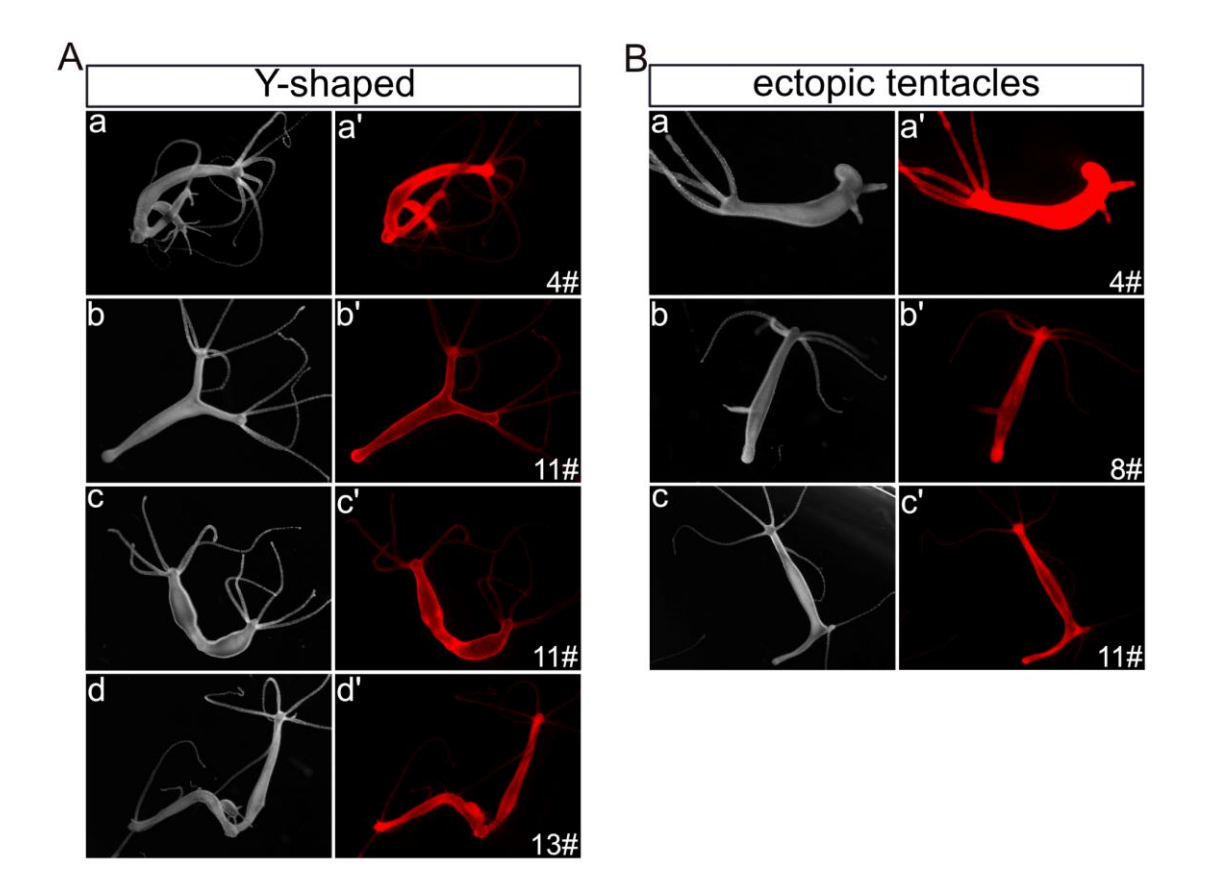


Supplementary Fig. S5 HvNotch-knockdown transgenic *Hydra* and the expression of HvNotch-target genes. (A) 59 embryos injected with HvNotch-hairpin-pHyVec12, produced 23 hatchlings. Among them, nine polyps exhibited mosaic DsRed signals. In the end, four strains (4#, 8#, 11# and 13#) with fully transgenic signals were obtained. 61 embryos were injected with control-pHyVec12, resulting in 25 hatchlings and ten polyps with DsRed signals. From this, we generated three fully transgenic control strains (1#, 2# and 3#). (B) Images of fully transgenic *Hydra* from strain 8# expressing DsRed signals in both epithelial layers. (C) Diagram represents the relative normalized expression of HvNotch-target genes after RT-qPCR with mRNA from indicated Notch-knockdown and control polyps. Data for HyHes2, HyAlx, HySp5 and HyKayak are shown, differences are not statistically significant.

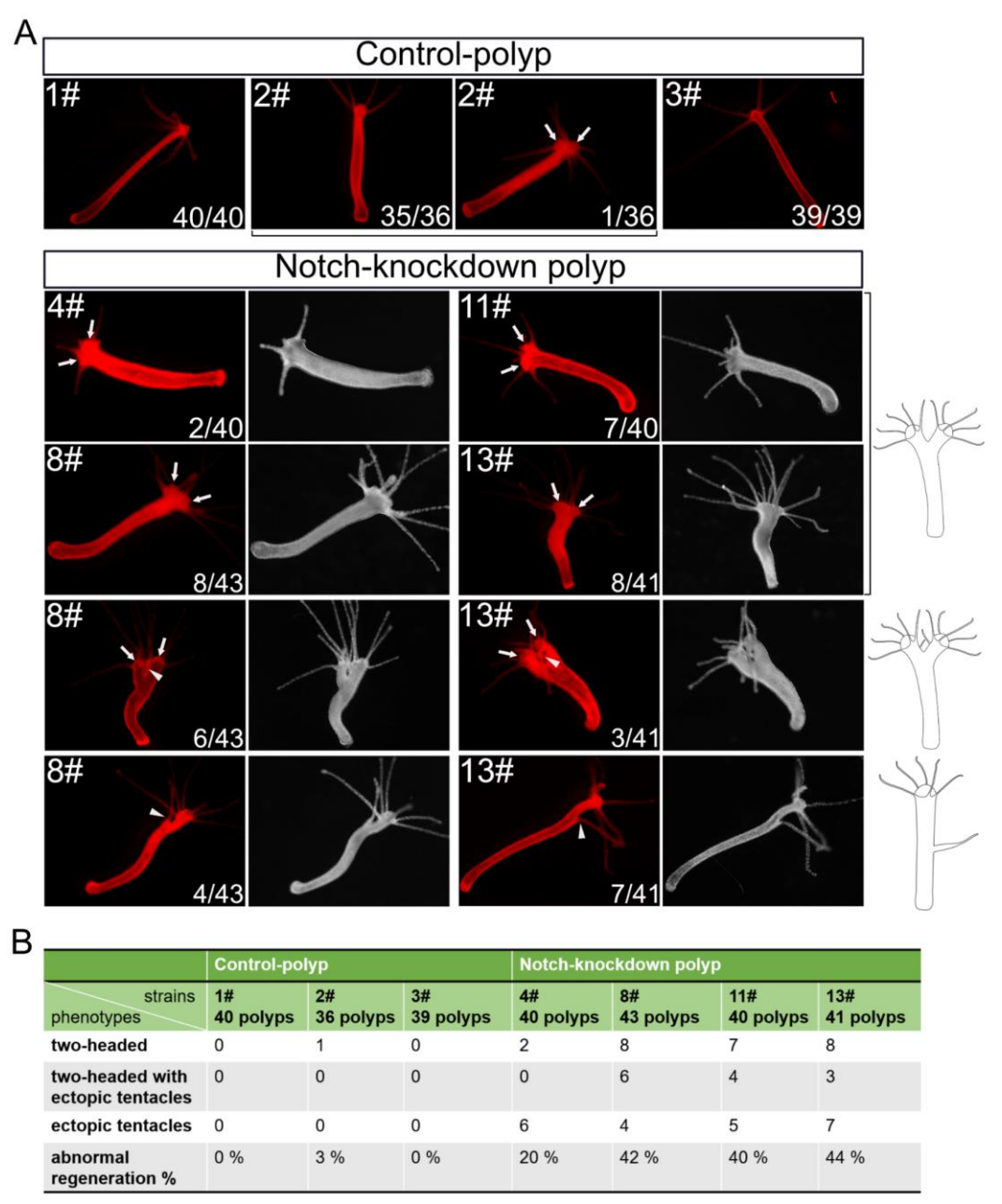


Supplementary Fig. S6 A two-headed polyp from 11# strain of HvNotch-knockdown

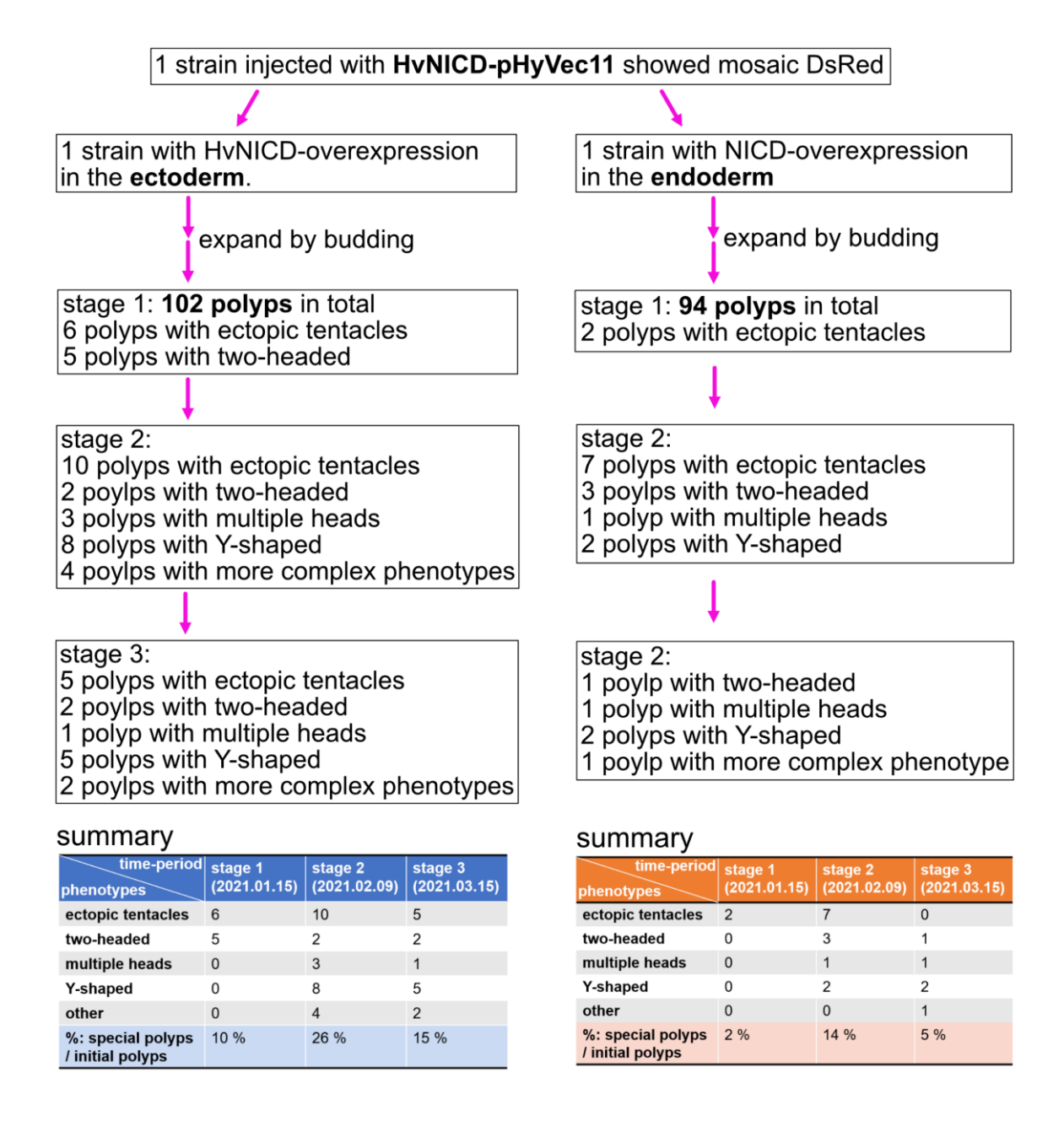
in the initial stage. (A) The development of this two-headed polyp with light-microscopy (a, b) and DsRed-fluorescence images (a', b') taken at the initial stage and after one-week. (B) Confocal laser scanning microscopic images of this two-headed polyp after costaining with pan-neuronal antibody (PNab)(Keramidioti, Schneid et al. 2024) (kind gift of Thomas Holstein) to label nerve cells (black and white images a' and b'), anti-acetylated-tubulin antibodies to label cilia of nematocytes (black and white images a'' and b'') and DAPI for staining of DNA (a''' and b'''); merged images of the left head with the enlargements labeled as a1 and a2, b: merged images of the right head with enlargements labeled as b1 and b2).



Supplementary Fig. S7 The phenotypes observed in HvNotch-knockdown transgenic *Hydra* after 6 months. The images labeled with a-d represent light-microscopy, while a'-d' display Ds-Red fluorescence. (A) "Y-shaped" polyps in strains 4#, 11# and 13#. Most of joining points located in the foot region (a, c, d) while one positioned in the oral half of the body column (b). (B) Strains 4#, 8# and 11# exhibited "ectopic tentacle" phenotype with one or two ectopic tentacles in the body column.



Supplementary Fig. S8 Head regeneration in HvNotch-knockdown transgenic *Hydra* after decapitation in the middle of the body column. (A) Images depict the Ds-Red fluorescence and light microscopy of polyps from HvNotch-knockdown strains 4#, 8#, 11# and 13# 3 days after decapitation, compared to control polyps 1#, 2# and 3#. Abnormal regeneration involved "two-headed" and "ectopic tentacles" observed in all Notch-knockdown strains and 2# control strain (1/36). Two heads were indicated with white arrows and ectopic tentacles were indicated with white triangles. (B) Quantification of abnormal regeneration percentage in HvNotch-knockdown and control polyps.



Supplementary Fig. S9 A summary of observed phenotypes in HvNICD-overexpressing transgenic *Hydra*. Numbers of polyps with described phenotypes at 3 stages (observation time points) are given for Ectoderm-TGs and Endoderm-TGs. Percentage values was calculated by dividing the number of phenotypes at each stage by the number of fully transgenic polyps initially obtained (ectoderm-TG: 102 polyps or endoderm-TG: 94 polyps).

4 strains injected with HvNotch-Hairpin showed mosaic signals

4 strains with HvNotch knockdown in both epithelia: 4#, 8#, 11#, 13#

stage 1 (during the first two weeks after obtaining fully transgenic): 11# strain has 1 polyp with two-headed and 2 Y-shaped polyps with ectopic tentacles

stage 2 (during the subsequent three months): 4# strain: 10 out of 96 polyps showed phenotypes 8# strain: 21 out of 162 polyps showed phenotypes 11# strain: 15 out of 140 polyps showed phenotypes

stage 3 (after six months of culturing these transgenic animals): 1 to 3 polyps out of approximately 200 polyps showed phenotypes

summary

	strain phenotypes	4#: 96 polyps	8#: 162 polyps	11#: 140 polyps	Total number
stage 2	ectopic tentacles	2	7	5	14
	two-headed	1	4	3	8
	Y-shaped	4	7	6	17
	two-feet	3	3	1	7
	%: special polyps / total polyps	10 %	15 %	9 %	12%

	strain phenotypes	4#	8#	11#	13#	Total number	
stage 3	ectopic tentacles	1	1	0	0	2	
	two-headed	0	0	2	0	2	
	Y-shaped	1	0	1	2	4	
	%: special polyps / total polyps (~200 polyps per strain)	around 0.5 % to 1 %					

Supplementary Fig. S10 A summary of observed phenotypes in HvNotch-knockdown transgenic *Hydra*. Numbers of polyps with described phenotypes in strains 4#, 8#, 11# and 13# of HvNotch-knockdown transgenic *Hydra* at indicated stage 2 (approximately three months after obtaining fully transgenic polyps) and stage 3 (after six months).

Supplementary Table S1

RT-qPCR primer		
NICD-P1-Fw	CAAGGCGTCATTTCTGTCAA	
NICD-P1-Rev	ATTGGCATCAAATCCACGAT	
NICD-P2-Fw	TAGAGGTGTTGGATGCACAAG	
NICD-P2-Rev	GGAACTGATTCCTCGCAGAAC	
HvNotch-Fw	TCATCATCTGACAGTGCTTT	
HvNotch-Rev	TAGCTTGCAGCAACTTTAGG	
HyHes-Fw	TGACGGACACAGAAAGACATC	
HyHes-Rev	TGTCGTTTAGACTGTTGTTTATGC	
HyAlx-Fw	GCTCGAGTACAGGTGTGGTT	
HyAlx-Rev	AGCCGAACTACATACTGAGTTACT	
HySp5-Fw	CGTTGCAACCCGAAGATGTC	
HySp5-Rev	TCCGCACCCTGGAATATGAC	
HyKayak-Fw	AACAAGTTGGCTGCTAGAAGATG	
HyKayak-Rev	CATGGTTGTCGTGTTCAATGC	
HyGAPDH-Fw	GACAACCATTCATGCCACAA	
HyGAPDH-Rev	ACAGCTTTTGCAGCTCCAGT	
HyEF1α-Fw	GGTCAAACCAGAGAACATGC	
HyEF1α-Rev	TTCGCTGTATGGTGGTTCAG	
HyPPIB-Fw	ACTGGTAAGGGAATTCTATCCA	
HyPPIB-Rev	TACCATCCAACCATGGAGTT	

Supplementary Table S2

Cloning primers for probes of FISH		
HyAlx-Fw	TCGATTCAACTCTCCCATTTCATC	
HyAlx-Rev	AAGGTCCGTATAGCGTCGATT	
HyWnt3-Fw	TATCTGCGGGAGTTGCGTTT	
HyWnt3-Rev	ACAGGTGTATTCAGGCGTCAT	

Supplementary Table S1 The list of primer sequences used for RT-qPCR.

Supplementary Table S2 The list of primer sequences used to amplify the FISH-probes.

1	Keramidioti, A. <i>et al.</i> A new look at the architecture and dynamics of the <i>Hydra</i> nerve net. <i>Elife</i> 12 , doi:10.7554/eLife.87330 (2024).

3.2 Paper II: Differential gene regulation in DAPT-treated *Hydra* reveals candidate direct Notch signalling targets

Summary of paper II:

This analysis revealed 831 Notch-responsive (NR) genes after DAPT treatment, with the expression patterns of 80% of these genes (666 genes) defined through Hydra single-cell sequencing data (Siebert, Farrell et al. 2019). Among these 666 genes, 315 were associated with the process of nematogenesis, of which 314 were downregulated following DAPT treatment. This includes many genes expressed in post-mitotic nematoblasts, such as *HyDickkopf 3* (t20111aep, a Wnt-inhibitor (Fedders, Augustin et al. 2004)), Spinalin (t38568aep, our transcript encodes a longer Spinalin protein compared to the previously published sequences (Koch, Holstein et al. 1998, Milde, Hemmrich et al. 2009)), Prdl-b (t21636aep, our transcript encodes a more complete protein compared to the Prdl-b in (Gauchat, Kreger et al. 1998)), CnASH (t10853aep, (Grens, Mason et al. 1995) and *NOWA* (t15237aep, (Engel, Pertz et al. 2001) , *Jun* (t17964aep), two Sox-like genes (t23172aep and t23837aep) and three Fox genes (t19720aep, t9145aep and t12948aep) (Moneer, Siebert et al. 2021, sequence alignment of Dickkopf, Spinalin, Prdl-b, Jun, Sox-like and Fox proteins is available in figshare). This downregulation was consistent with the observation that Notch inhibition blocked the nematocyte differentiation process (Käsbauer, Towb et al. 2007). However, most of these genes did not regain their expression 6 h after DAPT removal, except Jun, two Sox-like genes, and two Fox genes (t19720aep and t9145aep). This suggests that Notch may directly regulate the expression of Jun, Sox-like, and Fox genes, potentially influencing nematocyte differentiation.

Compared to the NR genes expressed during nematogenesis, around 170 genes showed specific expression patterns in epithelial cells. Notably, genes involved in tentacle formation and head patterning, such as *Sp5* (t29291aep, a presumed transcriptional repressor of *HyWnt3* (Vogg, Beccari et al. 2019)), *HyAlx* (t16456aep, expressed at tentacle boundaries (Smith, Gee et al. 2000)), *Wnt7* (t28874aep, (Lengfeld, Watanabe et al. 2009)), *Tcf* (t11826aep, (Hobmayer, Rentzsch et al. 2000)), *Otx* (t33622aep, specifically expressed in the hypostome region (Reddy, Gungi et al. 2019)), *Pitx*

(t5275aep, expressed in the endodermal head cells (Reddy, Gungi et al. 2019)) and *CnGSC* (t1216aep, an organizer gene (Broun, Sokol et al. 1999)), were primarily downregulated upon DAPT treatment but restored their expression within 3 h of DAPT removal (Moneer, Siebert et al. 2021, sequence alignment of HyAlx and Otx is available in figshare). These findings suggest that these genes may be potential direct targets of Notch signalling.

Promoter analysis provided further insights, revealing that Sp5 and HyAlx each contain six Notch-responsive RBPJ-binding sites, making them the most likely direct Notch target genes. In addition, Otx and Pitx proteins possess three or four RBPJ-binding sites, respectively (Moneer, Siebert et al. 2021).

One notable exception is the *Hydra-Kayak* gene (t5966aep, referred to as *HyKayak*), which is the ortholog of the mammalian *c-fos* gene. *HyKayak* is expressed in the ectodermal head and battery cells. Interestingly, its expression was significantly upregulated following Notch inhibition with DAPT and returned to baseline levels 3 h after DAPT removal. These results make *HyKayak* an intriguing target for further investigation regarding Notch signalling and head patterning.



RESEARCH ARTICLE

Differential gene regulation in DAPT-treated Hydra reveals candidate direct Notch signalling targets

Jasmin Moneer¹, Stefan Siebert², Stefan Krebs³, Jack Cazet², Andrea Prexl¹, Qin Pan¹, Celina Juliano² and Angelika Böttger^{1,*}

ABSTRACT

In Hydra, Notch inhibition causes defects in head patterning and prevents differentiation of proliferating nematocyte progenitor cells into mature nematocytes. To understand the molecular mechanisms by which the Notch pathway regulates these processes, we performed RNA-seq and identified genes that are differentially regulated in response to 48 h of treating the animals with the Notch inhibitor DAPT. To identify candidate direct regulators of Notch signalling, we profiled gene expression changes that occur during subsequent restoration of Notch activity and performed promoter analyses to identify RBPJ transcription factor-binding sites in the regulatory regions of Notch-responsive genes. Interrogating the available single-cell sequencing data set revealed the gene expression patterns of Notch-regulated Hydra genes. Through these analyses, a comprehensive picture of the molecular pathways regulated by Notch signalling in head patterning and in interstitial cell differentiation in *Hydra* emerged. As prime candidates for direct Notch target genes, in addition to Hydra (Hy)Hes, we suggest Sp5 and HyAlx. They rapidly recovered their expression levels after DAPT removal and possess Notch-responsive RBPJ transcription factorbinding sites in their regulatory regions.

KEY WORDS: Hydra, Notch pathway, Wnt pathway, Axis formation, Nematocyte differentiation

INTRODUCTION

Notch signalling facilitates cell fate decisions and pattern formation by inducing terminal differentiation and mediating lateral inhibition, boundary formation and synchronization of developmental processes in animals. Well-studied examples of Notch-regulated processes include the differentiation of the wing margin and the specification of neurons from neuroectoderm in *Drosophila* embryos and somite formation during vertebrate development (Liao and Oates, 2017; Siebel and Lendahl, 2017). The core components of the Notch pathway include the Notch receptor, the Delta/Serrate/Lag-2 (DSL) ligands and recombining binding protein suppressor of hairless (RBPJ) transcription factors [also called CSL, for CBF1 in mammals, Su(H) in *Drosophila* and

¹Ludwig Maximilians-University Munich, Germany, Biocenter, 82152 Planegg-Martinsried, Großhaderner Str. 2, Germany. ²Department of Molecular and Cellular Biology, University of California, Davis, CA 95616, USA. ³Ludwig-Maximilians-University Munich, Gene Center Munich, Feodor-Lynen-Str. 25 81377 Munich, Germany.

*Author for correspondence (boettger@zi.biologie.uni-muenchen.de)

D J.C., 0000-0002-7331-5631; A.P., 0000-0001-8951-4654; A.B., 0000-0003-3273-9558

Handling Editor: John Heath Received 8 April 2021; Accepted 3 May 2021 Lag-1 in *Caenorhabditis*] (Andersson et al., 2011). Both the DSL ligands and Notch receptors are transmembrane proteins, therefore signalling occurs between directly adjacent cells. Interactions between DSL ligands and Notch receptors result in cleavage of the Notch receptor by presenilin followed by nuclear translocation of the intracellular domain of Notch (NICD) (reviewed in Mumm and Kopan, 2000). NICD works as a transcriptional co-activator of CSL factors.

Direct target genes of Notch signalling have been identified previously (reviewed by Giaimo et al., 2021; Wang et al., 2015). Targets of Notch signalling are activated or repressed in different cell types depending on the composition of transcriptional complexes induced by Notch activity and the epigenetic status at the respective loci. A primary and evolutionarily conserved target of Notch is the Hey-Hes family of transcriptional repressors. Other context-dependent direct target genes of Notch signalling that have been identified include Myc, cyclin D1 and MEK5c in tumour cells (reviewed in Borggrefe and Oswald, 2009). In hematopoietic cells, GATA3, the master regulator for T-cell development, and several Hox genes are direct Notch targets (Fang et al., 2007). Genomewide analysis in *Drosophila* has shown that genes of the epidermal growth factor receptor pathway are direct targets of Notch signalling and it showed that Notch targeted activators and repressors of certain genes at the same time (Krejci et al., 2009). Notch also induces transcription of its own inhibitors, for example, the small Notch-regulated ankyrin repeat protein NRARP (Jarrett et al.,

To reveal the ancestral core regulatory network directed by the highly conserved Notch signalling pathway, we have focused on a cnidarian, the fresh water polyp *Hydra*. As a sister to bilaterian animals, cnidarians hold an informative phylogenetic position. Moreover, *Hydra* provides the unique opportunity to obtain an animal-wide picture of Notch target genes with cell-type resolution due to the recently available single-cell expression map (Siebert et al., 2019).

Hydra polyps have a simple body structure, representing a tube with an oral head structure and an aboral foot. The head consists of the hypostome, with a central mouth opening surrounded by a crest of tentacles. The foot consists of a peduncle, terminating in the basal disc. The body column of the polyp is composed of two epithelial monolayers, termed ectoderm and endoderm, separated by an acellular extracellular matrix, the mesoglea. Ectoderm and endoderm are self-renewing epithelial cell lineages. A third cell lineage, the interstitial cells, resides in interstitial spaces of both epithelia (David and Campbell, 1972; David and Gierer, 1974). It is supported by self-renewing multipotent stem cells, which provide a steady supply of neurons, gland cells and nematocytes. Nematocytes are cnidarian-specific sensory cells, which harbour the nematocyst or cnidocyst used for capturing prey. Epithelial cells divide along the entire body column of the polyps

(Holstein et al., 1991) leading to the displacement of cells towards the oral and aboral ends, and into asexually produced buds. Cells arriving at the base of tentacles or at the basal disc cease cell division and induce differentiation into tentacle or basal disc cells. Buds develop into new polyps and are then released from the parent polyp. Sexual reproduction occurs when interstitial lineage derived germ cells develop into egg and sperm cells (Bosch and David, 1986). Ectodermal tentacle cells are battery cells, where each cell harbours several mature nematocytes. Older cells are shed at the tips of the tentacles and the foot. Owing to continual cell divisions, almost all *Hydra* cells are replaced approximately every 20 days (Otto and Campbell, 1977). Therefore, the homeostatic animal is in a constant state of development requiring the presence of signalling for patterning the body axis and direct cell fate specification (Steele, 2002).

The *Hydra* Notch pathway components include the receptor HvNotch (Hv for *Hydra vulgaris*), the ligand HyJagged (Hy for *Hydra*) and the CSL-homolog, HvSu(H). The basic mechanisms of Notch signalling are conserved in *Hydra*, including regulated intramembrane proteolysis (RIP) through presenilin, followed by nuclear translocation of the NICD (reviewed in Mumm and Kopan, 2000). Moreover, the promoter of the *Hydra* HES-family member *HyHes* can be activated by the HvNotch NICD indicating that *HyHes* is a direct target of Notch signalling (Käsbauer et al., 2007; Münder et al., 2010; Prexl et al., 2011).

The presenilin inhibitor DAPT efficiently blocks nuclear translocation of NICD and phenocopies Notch loss-of-function mutations in *Drosophila* and zebrafish (Geling et al., 2002; Micchelli et al., 2003). In the cnidarians *Nematostella vectensis* and *Hydractinia echinata*, morpholino-mediated knockdown or CRISPR-Cas-mediated mutagenesis of Notch results in comparable phenotypes to those seen upon DAPT treatment in both organisms, with them displaying defects in nematocyte differentiation and tentacle patterning (Gahan et al., 2017; Marlow et al., 2012; Richards and Rentzsch, 2015).

In Hydra, we have shown that DAPT treatment inhibits NICD translocation, which results in four strong effects. First, DAPT blocks post-mitotic differentiation in the nematoblast and germ cell lineages. Early differentiating nematocytes are genetically specified by the expression of the achaete-scute homolog CnASH (Cn for Cnidarian) (Grens et al., 1995; Lindgens et al., 2004) and morphologically by the presence of a post-Golgi vacuole as an element of capsule development. This cell state disappears in DAPT treated animals. Second, DAPT blocks post-mitotic differentiation of female germ cells causing proliferating germ cell precursors to form tumour-like growths (Alexandrova et al., 2005; Käsbauer et al., 2007). Third, DAPT impairs boundary formation at both parent-bud and body column-tentacle boundaries in such a way that the typically sharp gene expression border margins at these structures become diffuse. At the parent-bud boundary this misexpression of the Hydra FGF-R-homolog kringelchen leads to failure of bud foot formation and detachment (Münder et al., 2010; Sudhop et al., 2004). At the base of tentacles, HyAlx expression, which demarcates the tentacle boundaries (Smith et al., 2000), becomes diffuse and we observe malformations of the head structure (Münder et al., 2013). Fourth, DAPT inhibits Hydra head regeneration and regenerating tissue is not able to re-establish an oral organiser as evidenced by lack of Wnt-3 expression. This leads to failure in developing a properly patterned head with hypostome and evenly spaced tentacles (Münder et al., 2013).

To gain a better understanding of the underlying molecular causes of the Notch inhibition phenotypes, we aimed to identify the

transcriptional target genes of Notch signalling. We identified 831 genes that were differentially expressed in response to 48 h of DAPT treatment; 75% of these were downregulated. Single-cell expression data were used to uncover the gene expression patterns at cell-state resolution for the Notch-responsive genes. We found that Notch-responsive genes were expressed in cell states such as differentiating nematocytes and oral cell types, which is consistent with the DAPT-induced phenotypes. To identify potential direct targets of Notch signalling, we also profiled the gene expression changes that occurred immediately after DAPT removal. Investigating the expression dynamics of Notch responsive genes and performing motif enrichment analysis enabled us to predict likely direct targets of Notch signalling in *Hydra*.

RESULTS

Differential gene expression analysis reveals Notchresponsive genes

To identify targets of Notch signalling in *Hydra*, we elucidated transcriptional changes that occur in response to DAPT treatment. We expected that sustained DAPT treatment would result in the misregulation of both direct and indirect Notch targets. We furthermore predicted that direct targets would return to control expression levels after DAPT removal more quickly than indirect targets. We profiled gene expression changes immediately after 48 h of sustained DAPT treatment (0 h time point) to identify all Notch-affected genes. In addition, we profiled gene expression 3 and 6 h after DAPT removal to monitor the recovery of these Notch-affected genes.

To characterise the 3 and 6 h time points after DAPT removal we used reverse transcription quantitative real-time PCR (RT-qPCR) to monitor the expression levels of two genes: (1) *HyHES*, which is a known direct Notch target (Münder et al., 2010), and (2) *CnASH*, which is expressed in post-mitotic differentiating nematoblasts (Lindgens et al., 2004), a cell state that is lost in response to DAPT treatment (Käsbauer et al., 2007). Loss of *CnASH* expression is a secondary (or indirect) effect of Notch inhibition and reestablishment of *CnASH* expression will only occur after DAPT removal once nematogenesis is restored.

As expected, both *HyHES* and *CnASH* were downregulated after 48 h of DAPT treatment. *HyHES* expression returned to normal levels between 5.5 and 8 h after inhibitor removal, whereas *CnASH* expression was still downregulated after 24 h (Fig. S1). RNA-seq was therefore performed on tissue samples collected after 48 h DAPT treatment (0 h) and at the 3 h and 6 h time points after DAPT removal, since the 6 h intervals appeared sufficient to distinguish direct from indirect Notch-targets and the 3 h intervals were added to monitor earliest responses in gene expression after resuming NICD activity. The workflow for this experiment is illustrated in Fig. 1.

Genes that were differentially expressed after 48 h of DAPT treatment (time point 0 h) were referred to as Notch-responsive genes (NR genes). Of the 831 NR genes identified, 624 were downregulated (75%) and 207 were upregulated (25%) (Fig. 2A). Clustering NR genes according to their fold changes (Fig. 2B) at the three time points after DAPT removal (0 h, 3 h, and 6 h) revealed 279 genes (201 down, 78 up) genes with re-established expression levels at 3 h, including the confirmed Notch target *HyHES*. A total of 194 genes (143 down, 51 up) showed re-established expression by 6 h and 313 genes (243 down, 70 up) were still differentially expressed at 6 h, including *CnASH*. A total of 45 genes, including *CnGSC*, were differentially expressed at time points 0 h and 6 h, but not at 3 h (Fig. 2A, 'Other'). In addition, 160 genes were found to be

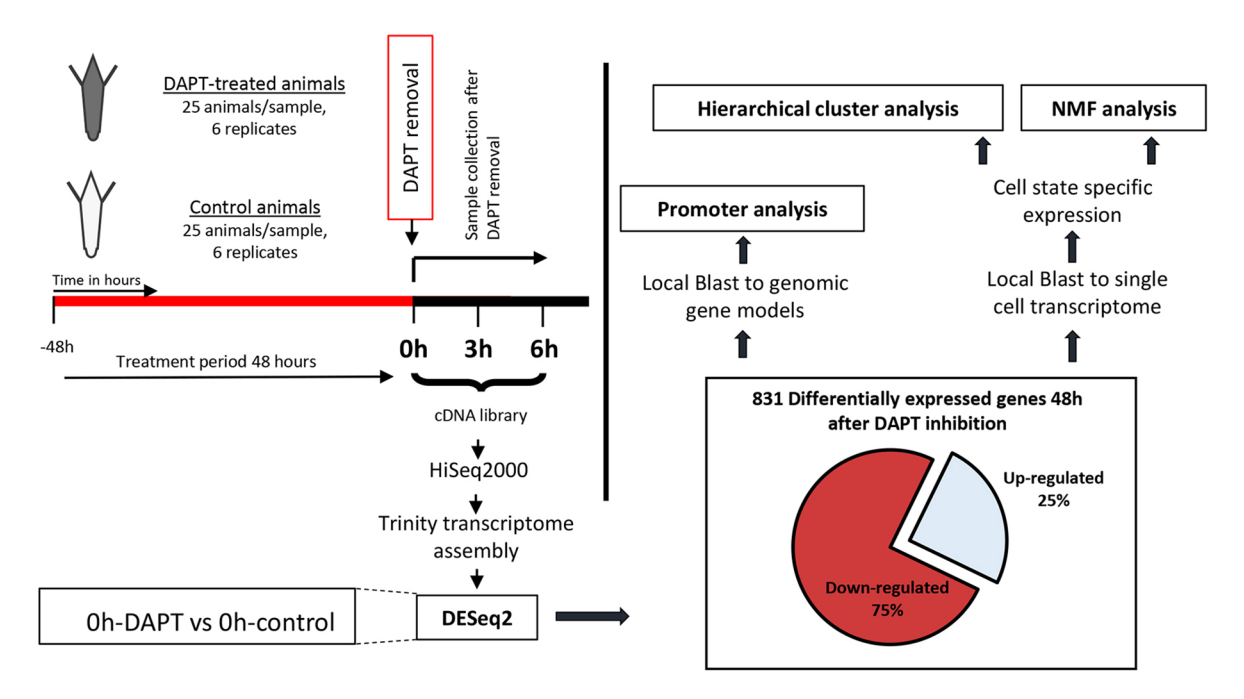


Fig. 1. Overview of the experimental and analysis workflow. *Hydra* polyps were treated with either DAPT or DMSO (control) for 48 h. Thereafter, total RNA for sequencing was collected at three time points. The sample 0 h was taken immediately after 48 h of DAPT treatment. This is also the time point at which DAPT was removed from the samples and total RNA was collected 3 and 6 h after DAPT removal. Six biological replicates for each treatment were collected and processed at the same time point. Pairwise differential gene expression analysis by DESeq2 was performed between DAPT- and DMSO-treated samples for each of the three collection time points. This analysis revealed 831 Notch-responsive genes (NR genes) after 48 h of DAPT treatment (0 h). For these genes we characterized the expression at time points 3 h and 6 h. For 666 NR genes single-cell expression data from homeostatic polyps were available (Siebert et al., 2019) and was used to elucidate expression pattern and cell-state-specific expression using hierarchical cluster and nonnegative matrix factorization (NMF) analysis. Additionally, motif enrichment was performed for the set of NR genes.

differentially expressed at 3 and/or 6 h, but not at 0 h. These were excluded from further analysis.

Overall, these data reveal changes in gene expression caused by inhibition of the Notch pathway, and uncover which changes are rapidly reversed upon relief of this inhibition. This allowed us to explore the cell type-specific effects of DAPT treatment and identify possible direct targets of Notch signalling [the full list of NR genes is available via Figshare (doi:10.6084/m9.figshare.14681343)].

Single-cell expression data demonstrate nematogenesis and epithelial expression of Notch-responsive genes

Next, we elucidated NR gene expression patterns by exploring Hydra single-cell expression data, which were available for 666 (80%) NR genes (Fig. 1). We defined cell state and spatial expression of NR genes on the basis of published cell state annotations (Siebert et al., 2019). Hierarchical cluster analysis revealed groups of genes expressed in specific cell states (Fig. 3): nematoblasts/nematocytes (violet, red, blue and yellow clusters, 315 genes), ectodermal epithelial cells, including battery cells (black cluster, 90 genes), endodermal epithelial cells including tentacle cells (grey cluster, 80 genes), and genes more ubiquitously expressed across cell states (cyan cluster, 79 genes). An additional small subset comprising 102 NR genes included genes with restricted expression in several distinct cell states, such as specific neurons, gland cells, germline cells or ectodermal basal disc cells (green cluster, 102 genes). The majority of these 666 NR genes fell into two broad categories: (1) 47% that were specifically expressed in nematoblasts and nematocysts, and (2) 25% that were specifically expressed in epithelial cells (black and grey cluster, Fig. 3).

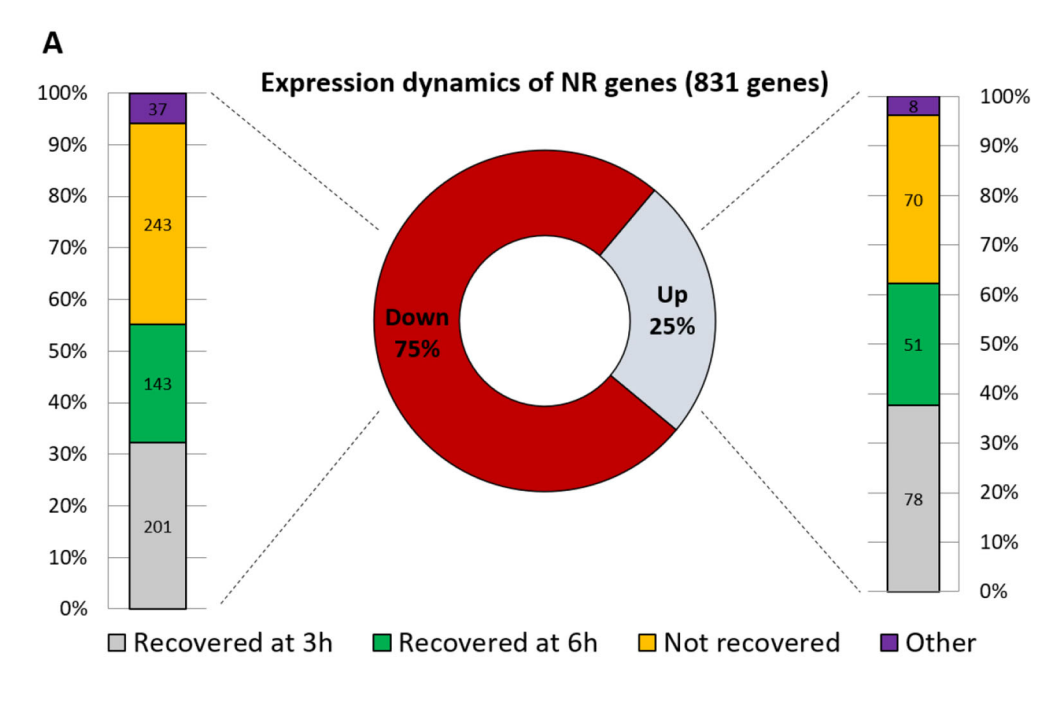
In addition, we performed non-negative matrix factorisation (NMF) on the NR gene set as an unbiased means to uncover

modules of co-expressed genes (metagenes) and identified 23 metagenes. We then visualized metagene expression on the t-distributed stochastic neighbour embedding (tSNE) representation of selected clusterings from Siebert et al. (2019) (Fig. S2). The NMF analysis identified cell-state-specific modules that were consistent with the hierarchical clustering results (Fig. S2; Fig. 3). Interestingly, a single metagene was found to be expressed in female germ line cells, suggesting Notch function during female gametogenesis (Fig. S2G).

Nematoblast and nematocyte expression of NR genes

The largest fraction of NR genes have nematoblast- or nematocytespecific expression. In *Hydra*, this lineage comprises four types of nematocytes, each of which harbours a single capsule (or nematocyst) of the atrichous isorhiza, holotrichous isorhiza, stenotele or desmoneme type. Nematocytes develop from interstitial stem cells via a proliferative amplification phase with incomplete cytokinesis that results in the formation of nests of 4, 8, 16, and 32 nematoblasts. The cells in these nests undergo a final mitosis and start capsule morphogenesis, a process that can be divided into five stages: (1) formation of a growing capsule primordium from a large post-Golgi vacuole, (2) growing of a tubule elongation of the capsule, (3) invagination of the tubule into the capsule, (4) formation of spines inside the invaginated tubule and (5) hardening of the capsule wall. Nests with mature nematocytes break up, and single nematocytes then get incorporated into the battery cells of the tentacles or into epithelial cells of the body column (David and Gierer, 1974; Engel et al., 2002).

As Notch inhibition by DAPT treatment results in a severe block of nematocyte differentiation, which occurs coincident with or immediately after mitotic exit of differentiating nematoblasts



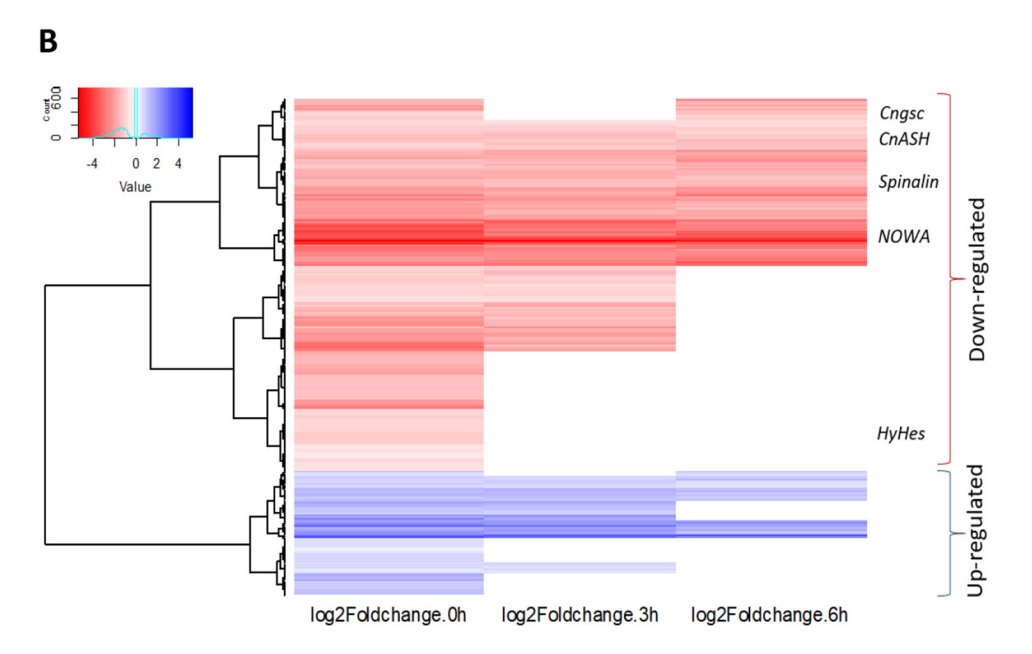


Fig. 2. Differential expression of NR genes post DAPT treatment.

(A) Expression dynamics of differentially expressed NR genes and time points for the recovery of original expression levels. For both up- and down-regulated genes, ~35% recover original expression within the first 3 h ('Recovered at 3h', grey), ~25% recover within 6 h ('Recovered at 6h', green), and ~30-40% do not recover original expression within the time course of the experiment ('Not recovered', yellow). The remaining genes (~5%, 'Other', purple) behave irregularly, e.g. recovered after 3 h, deregulated again after 6 h. (B) Heatmap highlighting expression differences of all 831 NR genes. The colour key refers to the log₂ fold change values. The cyan line in the small diagram indicates the distribution of z-scores. Clustering of NR genes by their log2Foldchange for each time point revealed upregulated (blue) and downregulated (red) genes. No value (white background) means the gene was not differentially expressed at that particular time point and thus had control expression levels. We identified sets of genes that recover their expression by 3 h (e.g. HyHes, differentially expressed at 0 h, thereafter back to control expression level), genes that recover expression by 6 h, and genes that do not recover expression during the course of the experiment, i.e. at 6 h after DAPT removal (e.g. the post-mitotic nematocyte gene markers CnASH, NOWA and Spinalin). A fourth set includes genes that are differentially expressed at 0 h and 6 h, but not at the 3 h time point (e.g. CnGSC).

(Käsbauer et al., 2007), we sought to identify the exact differentiation step that was affected. We therefore performed hierarchical clustering for NR genes with expression in nematoblast or nematocyte cell states (Fig. 3, violet, red, blue and yellow clusters) using the *Hydra* single-cell data (Siebert et al., 2019). The single-cell data revealed four distinct nematocyte differentiation trajectories, and gene expression state changes were identified along these trajectories from stem cells to differentiated nematocytes. Moreover, the single-cell analysis revealed eight distinct nematoblast stages along these four trajectories (nb1 through nb8). Two of these trajectories are annotated as desmoneme and stenotele differentiation, based on marker gene expression (Siebert et al., 2019). In the present study, the clustering of NR genes expressed during nematogenesis revealed that the majority of those genes are strongly expressed in cell states nb4, nb5, nb6, nb7, nb8 and in differentiated nematocytes (nem), with no or much lower

expression in the earlier cell states of interstitial stem cells (ISC.nb), nb1, nb2 and nb3 (Fig. 4A). This was also observed by plotting the expression of the NR gene modules onto the single-cell tSNE representation (Fig. S2) which indicates expression in all three nematocyte types including desmonemes (Fig. S2B), stenoteles (Fig. S2C) and isorhizas (Fig. S2D).

To identify the point in the trajectories in which differentiating nematoblasts transition from proliferating to post-mitotic nematoblasts, we looked at the expression profiles of two genes that mark proliferating nematoblasts: (1) proliferating cell nuclear antigen *PCNA* (t10355aep) and (2) the Zn-finger transcription factor gene zic/odd-paired homolog *Hydra-zic* (*Hyzic*) (t13359aep; Lindgens et al., 2004). *PCNA* expression is seen in states ISC.nb, nb1 and nb2 classifying them as proliferating nematoblasts (Fig. 5A). Nb1 and nb2 express HyZic, confirming that HyZic expression is restricted to proliferative nematoblast states as had

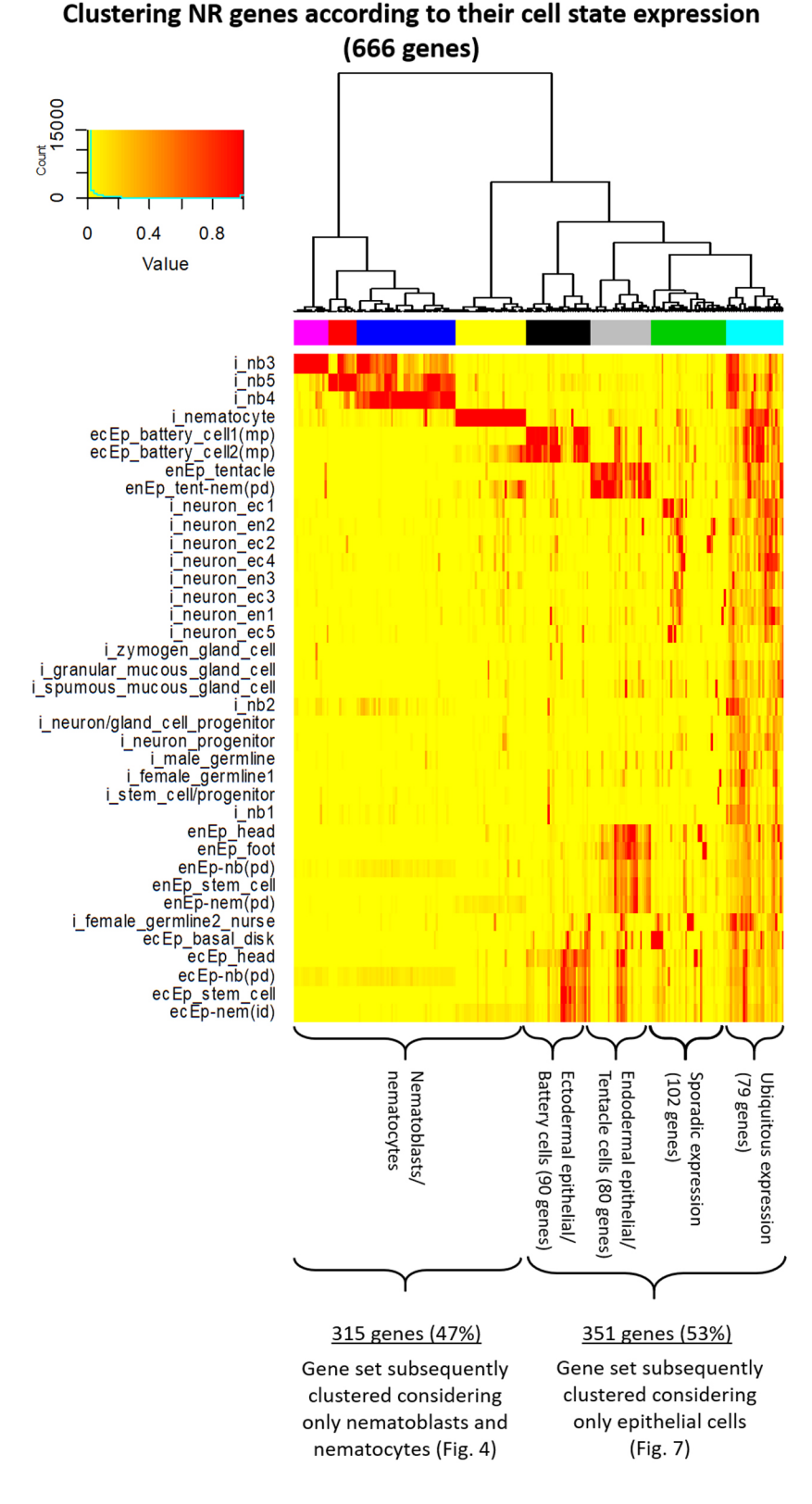
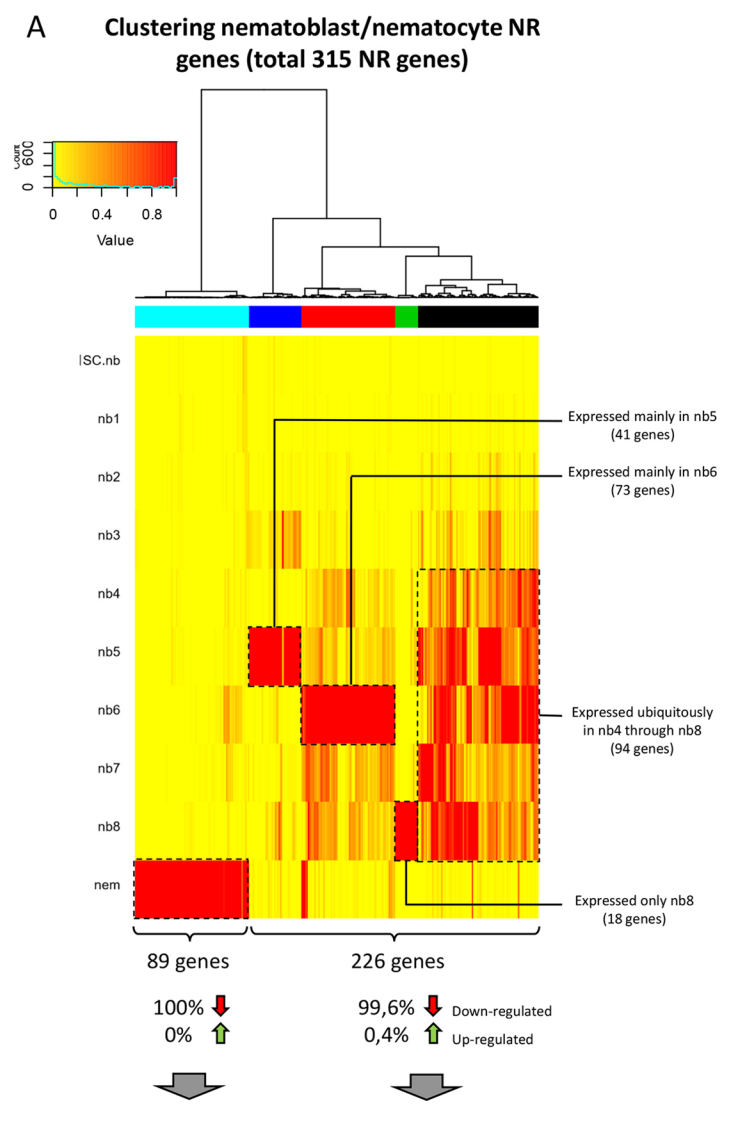


Fig. 3. NR gene expression in homeostatic polyps based on single-cell expression data. Expression data and cell state annotations were retrieved from Siebert et al. (2019). Hierarchical clustering was performed for 666 NR genes using average expression values for each annotated cell state. The colour key refers to cell state expression values. The green line in the small diagram indicates the distribution of z-scores. This revealed expression in nematoblast/nematocyte-specific genes (violet, red, blue and yellow cluster), ectodermal epithelial cell genes including battery cell genes (black), endodermal epithelial cell genes including tentacle genes (grey), genes ubiquitously expressed across a wide range of cell states (cyan) and genes with a sporadic expression (green). Nematoblast/nematocyte genes constituted 47% of the NR genes. i, cell of the interstitial lineage; nb, nematoblast; ecEp, ectodermal epithelial cell; enEP, endodermal epithelial cell; en, endoderm; ec, ectoderm.

been shown before (Lindgens et al., 2004). The absence of PCNA-expression in cell states nb3 and nb4 suggests that these are the earliest post-mitotic nematoblasts producing the nematocyst spine and inner wall protein spinalin (Käsbauer et al., 2007; Koch et al., 1998) and *spinalin* expression is clearly seen in these cells (Fig. 5A). Expression of the early differentiation marker genes

NOWA and *CnASH* become detectable in differentiation states nb5 through nb8 when nematocyst capsules are formed (Fig. 5A,C).

As further evidence that *HyZic* and *CnASH* mark mitotic and post-mitotic stages of nematogenesis respectively, using immunofluorescence we show that CnASH protein is detected in the cytoplasm of nematoblasts that contain vacuoles, which were



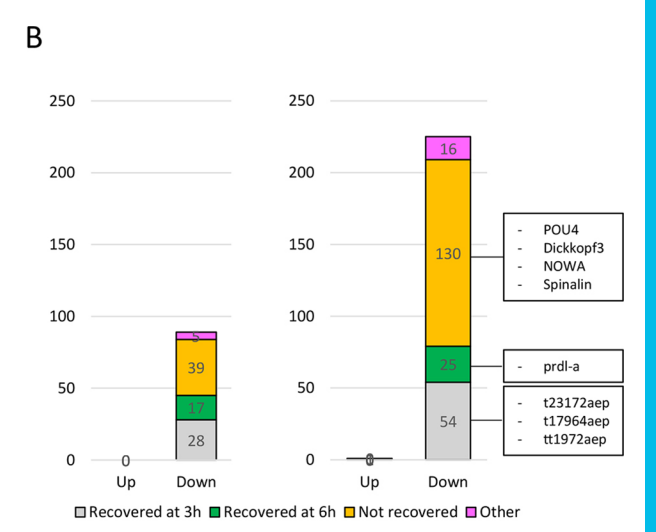


Fig. 4. Hierarchical clustering of NR genes expressed in the nematocyte lineage. (A) NR genes expressed in cells of the nematocyte lineage were clustered separately to reveal their expression in the differentiation states of nematogenesis. This revealed a set of genes only expressed in mature nematocytes (cyan cluster), genes mainly expressed in cell state nb5 (blue), genes mainly expressed in nb6 (red), genes mainly expressed in nb8 (green) and genes expressed ubiquitously in stages nb4 through nb8 (black). Almost all of these genes were downregulated upon DAPT treatment. (B) The majority of both mature nematocyte genes and nematoblast genes did not recover their expression 6 h after DAPT removal (yellow). This includes POU4, Dickkopf3, NOWA and Spinalin. Furthermore, genes are represented that recovered after 3 h (grey), 6 h (green) or that had an irregular recovery profile (magenta).

visualised with anti-NOWA antibody (Engel et al., 2002). By contrast, HyZic protein was detected in the cytoplasm of nematoblasts without visible vacuoles and not found in CnASH positive nematoblasts (Fig. 5B).

Of the 315 NR genes that are expressed in nematoblasts or nematocytes, 314 were downregulated upon Notch-inhibition (Fig. 4A). These downregulated genes include many genes expressed in developing nematocytes such as *POU4* (t11335aep), *Prdl-a* (t21636aep; Gauchat et al., 2004), *HyDickkopf 3* (t20111aep; similar to *HyDKK3*; Fedders et al., 2004), *CnASH* (t10853aep, Grens et al., 1995; Figs 4B and 5B), *NOWA* (t15237aep; Engel et al., 2002) and *Spinalin* (t38568aep; Koch et al., 1998), this gene has now three NCBI entries and encodes a longer protein than initially described [an alignment is available via FigShare (doi:10.6084/m9. figshare.14714169); Fig. 4B]. Using double *in situ* hybridization to detect *POU4* and *HyZic* transcripts, we found mutually exclusive expression of these two genes in differentiating nematocytes, which demonstrates that *POU4* is expressed in post-mitotic

nematocytes (Fig. S3A). Using *in situ* hybridization, we also showed that HyZic-positive nematocytes were not affected by DAPT treatment, whereas *CnASH* and *POU4* expression was lost (Fig. S3B,C). As DAPT treatment causes the disappearance of post-mitotic differentiating nematocytes, which are recognised by their forming of post-Golgi vacuoles (Käsbauer et al., 2007), the seeming loss of *POU* and *CnAsh* expression after DAPT treatment (Fig. S3B, C) is caused by a loss of the developing nematocyte cell states expressing these genes.

More than 50% of the nematoblast-specific NR genes remained downregulated and did not recover their normal expression level within 6 h after the Notch-inhibitor was removed (Fig. 4B). This again suggests that downregulation of nematogenesis genes reflects the loss of cell states and is mainly an indirect effect of the block in this process caused by Notch inhibition. By contrast, some nematocyte-specific putative transcription factors did recover their expression levels quickly after DAPT removal. These included a possible class I member of the HMG box superfamily, similar to

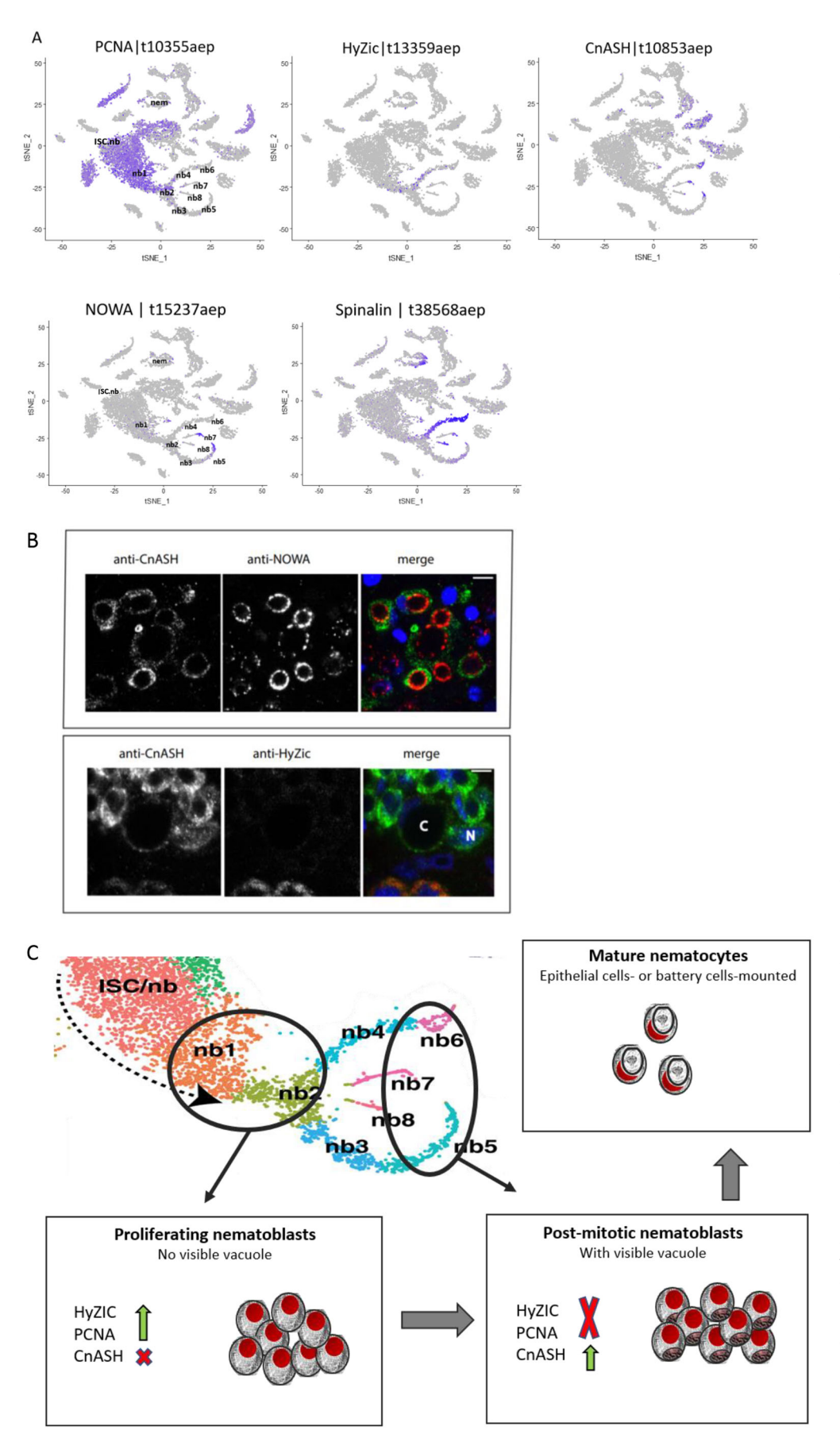


Fig. 5. Homeostatic expression of nematoblast marker genes and proteins. (A) t-Distributed stochastic neighbour embedding (t-SNE) representation showing the interstitial cell state expression of HyZic, PCNA, CnASH, NOWA and spinalin. Cluster labels are provided for cell states of the nematoblast lineage according to Siebert et al. (2019). nb, nematoblast; nem. nematocyte: ISC. interstitial stem cell. Blue dots indicate cells expressing the respective genes. PCNA is expressed in proliferating cells, nematoblast cell states nb1 and nb2. HyZIC is mainly expressed in nb2. This is in accordance with previously published work indicating HyZIC expression in proliferating nematoblasts. CnASH is expressed in nb5, 6, 7, 8, representing post-mitotic nematoblasts lacking PCNA expression. This is in complete agreement with previous work (Lindgens et al., 2004). NOWA encoding an outer capsule protein, is expressed in nb5 and nb7, spinalin, encoding a protein occurring inside the capsule, is expressed in nb4, 5, 6, 7 and 8 and in mature nematocytes (nem), all representing post-mitotic nematoblast stages. (B) Laser confocal microscopic sections of coimmunofluorescence staining with anti-HyZIC, anti-CnASH and anti-NOWA antibodies, in merged images DNA stain DAPI (blue), CnASH (green), HyZIC (red), NOWA (red). Anti-NOWA antibody delineates capsules (upper panel, middle image and red in merged). Co-staining with anti-CnASH antibody indicates signal in cytoplasm of capsule containing cells (upper panel, left hand image and green in merged). Capsule containing CnASHpositive cells (lower panel, left hand side and merged image green) are not stained with anti-HyZIC antibody (lower panel, middle image and merged image red); C, capsule; N, nucleus. Scale bars: 20 µm. (C) Schematic summary of gene expression in the nematoblast lineage indicating a differentiation pathway from interstitial stem cell precursors (ISC/nb) via proliferating PCNA and HyZIC expressing amplifying nematoblast precursors (nb1, nb2) via post-mitotic nematoblasts not expressing PCNA (nb3, nb4) to capsule forming CnASH expressing nematoblasts (nb5, 6, 7, 8), t-SNE representation of cells with clusters labeled by cell state as presented in Siebert et al. (2019) with permission. Images are representative of three experiments.

SOXB3 from *Hydractinia echinata* [t23172aep, XP_012555836.1; an alignment is available via FigShare (doi:10.6084/m9.figshare. 14714169)], a protein with a C-terminal bZIP-Jun-domain [t17964aep; an alignment is available via FigShare (doi:10.6084/m9.figshare.14714169)] and a predicted forkhead box protein I1c-like [t1972aep, an alignment is available via FigShare (doi:10.6084/m9.figshare.14714169)], and (Fig. 4B). Given the rapid recovery of their expression after DAPT removal, these genes may be directly targeted by Notch signalling and possibly play a major role in driving nematogenesis.

In conclusion, our differential gene expression analysis confirms that inhibition of Notch signalling causes a decrease in gene expression in differentiating nematoblast stages, coinciding with the loss of this cell type within 48 h of DAPT treatment (Käsbauer et al., 2007). The gene expression of proliferating nematoblasts remained undisturbed.

Epithelial expression of Notch-regulated genes

About 25% of NR genes for which expression patterns were available had enriched expression in epithelial cells (Fig. 3, black and grey cluster) while the remaining non-nematoblast NR genes showed either sporadic or ubiquitous expression (Fig. 3, cyan and green clusters).

Since previous Notch inhibition studies demonstrated severe malformations of the *Hydra* head structure (Münder et al., 2013), we aimed to elucidate the effect of DAPT treatment on epithelial body column cells and their derivatives (e.g. specialized head and foot cells). Hierarchical clustering using single-cell data for epithelial cells revealed genes that were expressed (1) in all endodermal and ectodermal epithelial cell types along the oral-aboral axis (Fig. 6, grey cluster), (2) mainly in ectodermal epithelial cells (Fig. 6, cyan cluster) and (3) mainly in endodermal epithelial cells (Fig. 6, green cluster). The majority of these epithelial genes from the grey, cyan and green clusters were upregulated in response to DAPT treatment (Fig. 6). These included 36 genes associated with ER, Golgi and endosomal proteins, such as proteins involved in glycosylation like the oligosaccharyl transferase DAD1(t14233aep|DAD1), a negative regulator of cell death (Roboti and High, 2012). Some were involved in redox regulation and unfolded protein response and some were chaperones [see tables on FigShare; full list of NR genes (doi:10.6084/m9.figshare.14681343) and functional annotation of NR genes: (doi:10.6084/m9.figshare.14681319)]. Moreover, membrane proteins, including 12 G-protein coupled receptors, caspase D (t7281aep; Lasi et al., 2010) and the homolog of the ubiquitin-ligase and Notch-modulator mind bomb were also upregulated (t3105aep). Thus, many of the upregulated epithelial genes seem to be involved in stress responses to DAPT treatment. In contrast, Sp5, which is involved in Hydra head patterning (t29291aep; Vogg et al., 2019) was downregulated (Fig. 7A).

Two sets of genes comprised tentacle genes expressed in endodermal tentacle cells (Fig. 6, red cluster) and in ectodermal battery cells (Fig. 6, black cluster). In both sets, the majority of genes were downregulated upon Notch inhibition (88% of battery cell genes and 71% of endodermal tentacle genes). These included a gene encoding a Na⁺ channel in battery cells (t18364aep; Golubovic et al., 2007) and the collagen gene Hcol1 (t14477; Deutzmann et al., 2000) in endodermal tentacle cells (Fig. 7B). The endodermal matrix metalloprotease gene HMMP was upregulated (t16424aep; Leontovich et al., 2000). Both extracellular matrix genes, HMMP and Hcol1, recovered their expression levels within 3 h (Fig. 7B).

Furthermore, small sets of NR genes were specifically expressed in (1) ectodermal head cells, (2) endodermal head cells, and

(3) endodermal foot cells (Fig. 6, included in cyan and green clusters). Another NR gene cluster was expressed in ectodermal basal disc cells (Fig. 6, yellow cluster). These expression patterns also could be seen on tSNE plots after NMF analysis (see Fig. S2I,L,M).

The NR genes expressed in endodermal and ectodermal head cells were largely downregulated and several of these have known functions in head patterning. Of note, HyALX (t16456aep; Smith et al., 2000) is expressed at tentacle boundaries and previous work demonstrated that HvNotch is needed to maintain this expression pattern (Münder et al., 2013). Furthermore, several potential head organizer genes including Wnt7 (t28874aep; Lengfeld et al., 2009). the transcription factor gene TCF (t11826aep; Hobmayer et al., 2000), an Otx-related homeodomain protein (t33622aep), an FGF homolog (t8338aep; annotation confirmed by Monika Hassel, Marburg, Germany) and CnGSC (t1216aep; Broun et al., 1999), were among this downregulated set of head-specific genes (Fig. 7B). Of those, HyALX, CNGSC, Wnt7, FGF and HyTCF recover their normal expression levels within 3 h making these genes candidates for direct targets of Notch signalling. The organizer gene CNGSC was also downregulated and recovered expression after 3 h. However, it was then downregulated again at 6 h. This unusual expression behaviour might indicate the presence of an inhibitory feedback mechanism responding to Notch signalling.

By contrast, the NR genes that were specifically expressed in endodermal foot cells and in ectodermal basal disc cells were largely upregulated in response to Notch inhibition. These include *TGF-4* (t25624aep; Watanabe et al., 2014) and a predicted secreted Wnt inhibitor APCDD1 (t11061aep). Thus, Notch inhibition by DAPT resulted in reciprocal regulation of foot and head genes in *Hydra*, with genes normally expressed at the oral end being downregulated and genes normally expressed at the aboral end being upregulated (Fig. 7B).

These data indicate that Notch signalling regulates gene expression in battery cells and further head patterning genes, including the canonical Wnt signalling components HyWnt7 and HyTCF, whereas the BMP pathway component TGF-4 as well as a secreted Wnt inhibitor, both expressed in the foot, appeared to be negatively regulated by Notch.

Promoter analysis of NR genes reveals likely direct targets of Notch signalling

The differential gene expression analysis revealed sets of genes that showed shared behaviour after Notch inhibition and reactivation after DAPT removal. This suggests shared regulation, and hence we performed a motif enrichment analysis to uncover respective regulatory elements in genes with similar expression dynamics. This analysis was done for the following gene sets: (1) downregulated only at 0 h, (2) downregulated at 0 and 3 h, (3) downregulated at 0, 3 and 6 h, (4) upregulated only at 0 h, (5) upregulated at 0 and 3 h, and (6) upregulated at 0, 3 and 6 h. Regions of open chromatin, as identified by previously published ATAC-seq data, within 5 kb upstream of each gene were considered in the enrichment analysis (see Fig. 8 and Materials and Methods for details) (Siebert et al., 2019).

The group of genes that were downregulated in response to DAPT treatment and then recovered normal expression by 3 h are the best candidates for being direct targets of Notch signalling. If genes are direct targets of Notch signalling, we would expect to find RBPJ-binding sites (Kopan and Ilagan, 2009). In line with our prediction, the RBPJ motif (Bailey and Posakony, 1995) was enriched in NR genes of this group (Table S1; Fig. 8B). Among the 21 genes with RBPJ-binding sites in their regulatory region, *HyAlx* (t16456aep)

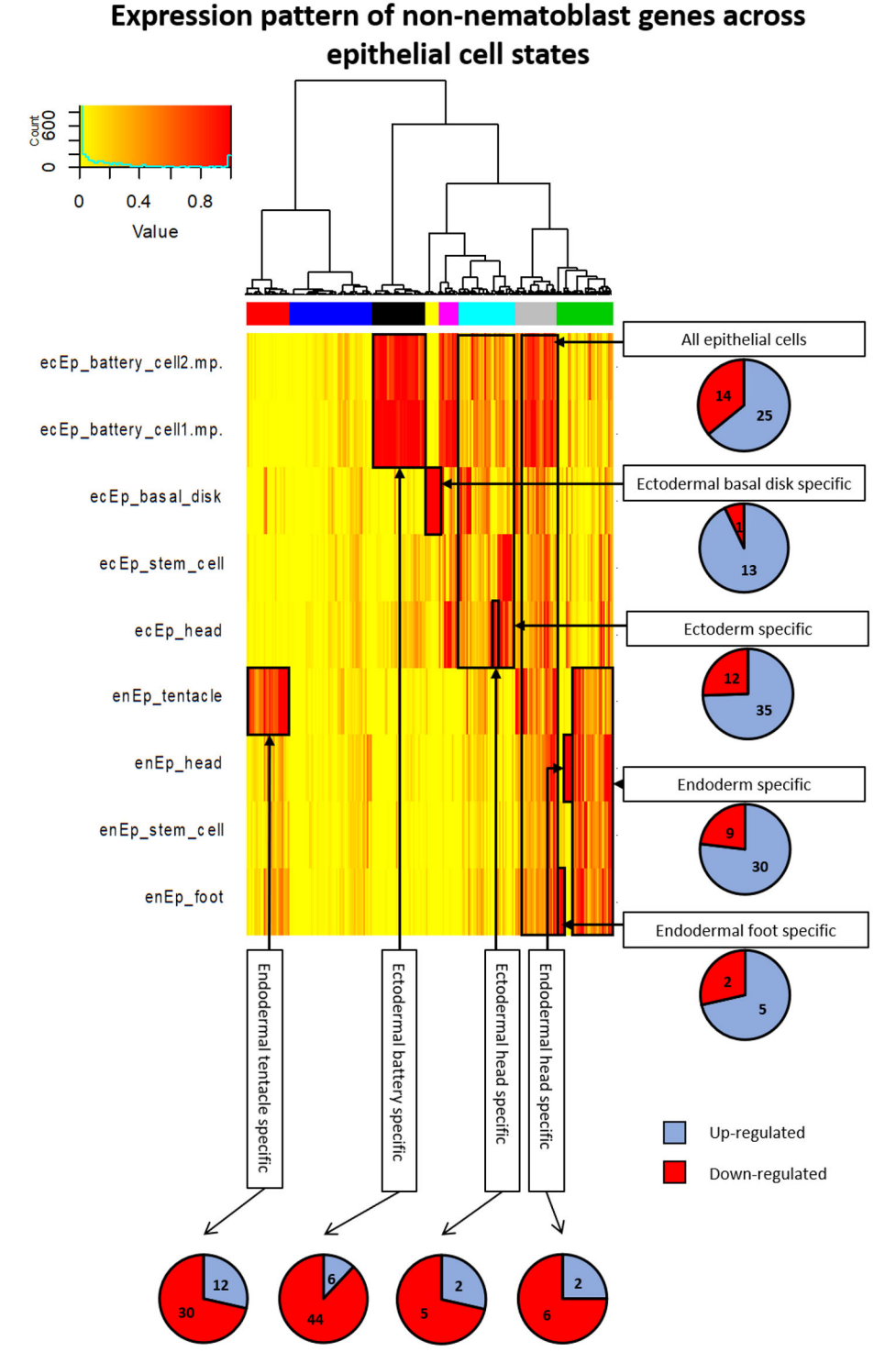


Fig. 6. NR gene subset with expression in epithelial cells. Non-nematoblast NR genes were clustered separately to determine their expression in epithelial cell states. This revealed sets of genes that are most strongly expressed in endodermal tentacle cells (red cluster), ectodermal basal disc cells (yellow), ectodermal battery cells (black), body column ectoderm cells (cyan), body column endoderm cells (green) and all epithelial cells (grey). The analysis also revealed smaller gene sets expressed in endodermal foot cells, endodermal head cells or ectodermal head cells. Tentacle, battery and head-specific genes were mainly downregulated upon DAPT treatment whereas the genes in the remaining clusters were mainly upregulated. The colour key refers to cell state expression values. The green line in the small diagram indicates the distribution of z-scores.

and *Sp5* (t29291aep), with six RBPJ motifs, are the top candidates for direct targets of Notch signalling (Fig. 8D,E; Table S1). We also identified the transcription factors pituitary homeobox 1-like (specifically expressed in head cells of the endoderm, t5275aep) and a homeobox protein of the OTX-family (t33622aep). Putative RBPJ motifs were additionally present in genes encoding potential membrane or extracellular proteins, including a foot-specific secreted frizzled-related protein, a potential regulator of Wnt signalling (t15331aep, annotation provided by Bert Hobmayer, Innsbruck, Austria, personal communication).

In addition to the RBPJ-binding site, we found enrichment of further transcription factor-binding motifs belonging to 10 transcription factor families. Homeobox transcription factors were the most abundant motifs identified and several different HMG, forkhead and bHLH motifs were also found (Table S1). Interestingly, this corresponds with the downregulation of transcription factors that potentially bind to these domains, for example, HyHES (bHLH), Jun (bZIP), FoxP1 (Forkhead), HyAlx, (homeobox, t16456aep), OTX-related (homeobox, t33622aep) and PITX-related factors (homeobox, t5275aep) and three SOX-related

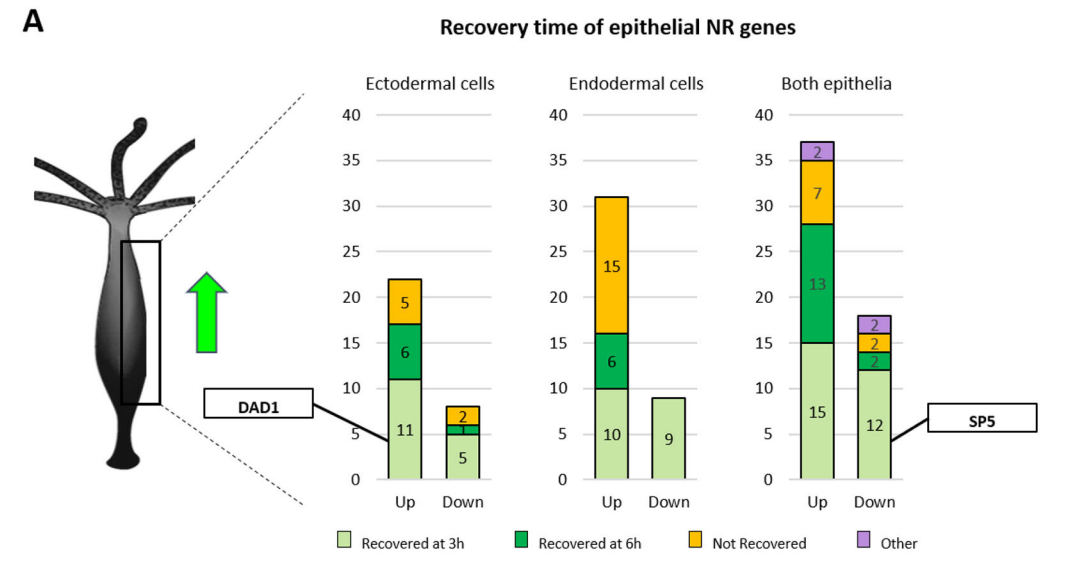
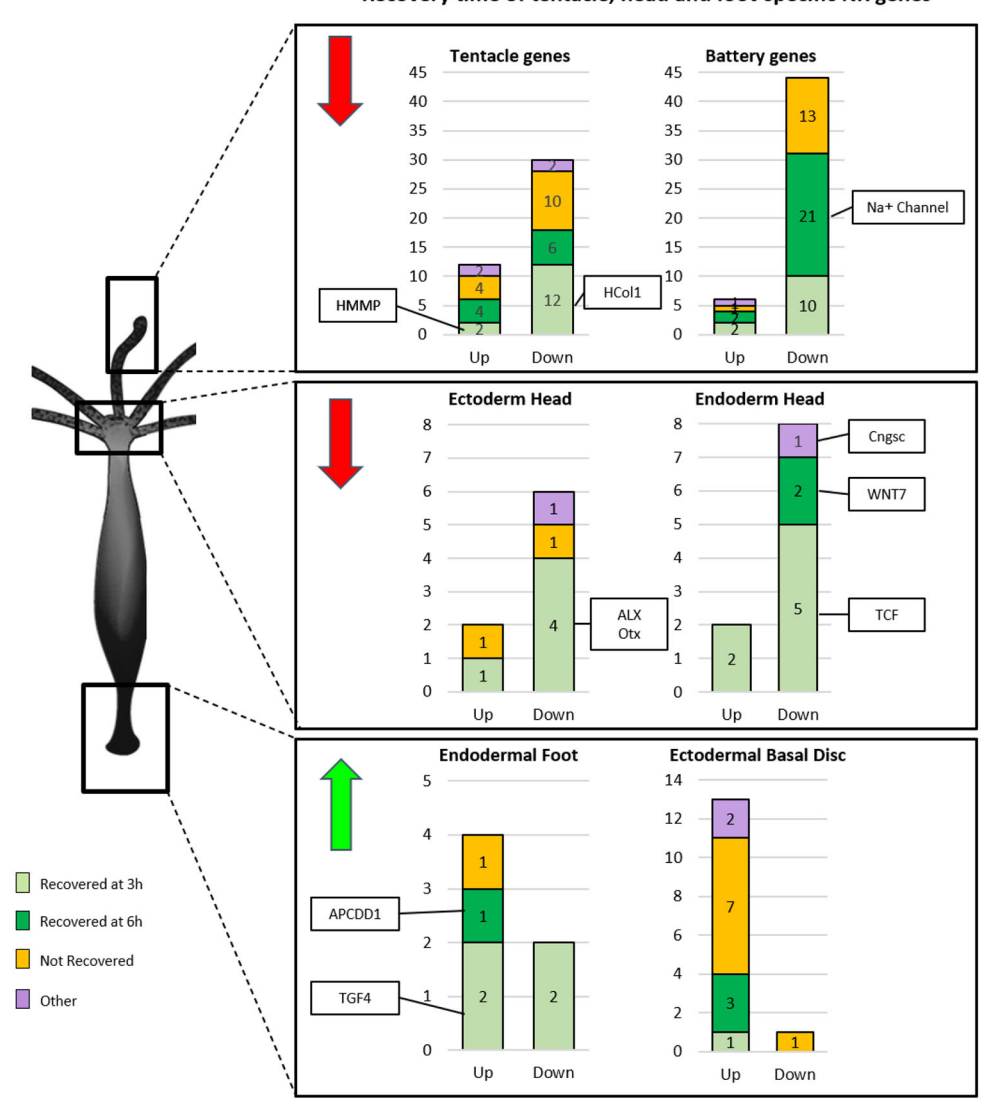


Fig. 7. Recovery time of NR genes. (A) The majority of epithelial NR genes were upregulated upon DAPT treatment. 50% of the upregulated ectodermal-specific NR genes recover expression within the first 3 h post-DAPT removal (light green) and include the apoptosisinvolved gene DAD1. SP5 on the other hand, which is expressed in both epithelia, is downregulated and recovers expression also within the first 3 h. (B) Head-specific fNR genes, including tentacle, battery and ectodermal and endodermal head genes, are mostly downregulated upon DAPT treatment. In contrast, foot-specific genes, including endodermal foot genes and basal disc genes are mostly upregulated. Many of these genes play a predominant role in patterning.

В

Recovery time of tentacle, head and foot-specific NR genes



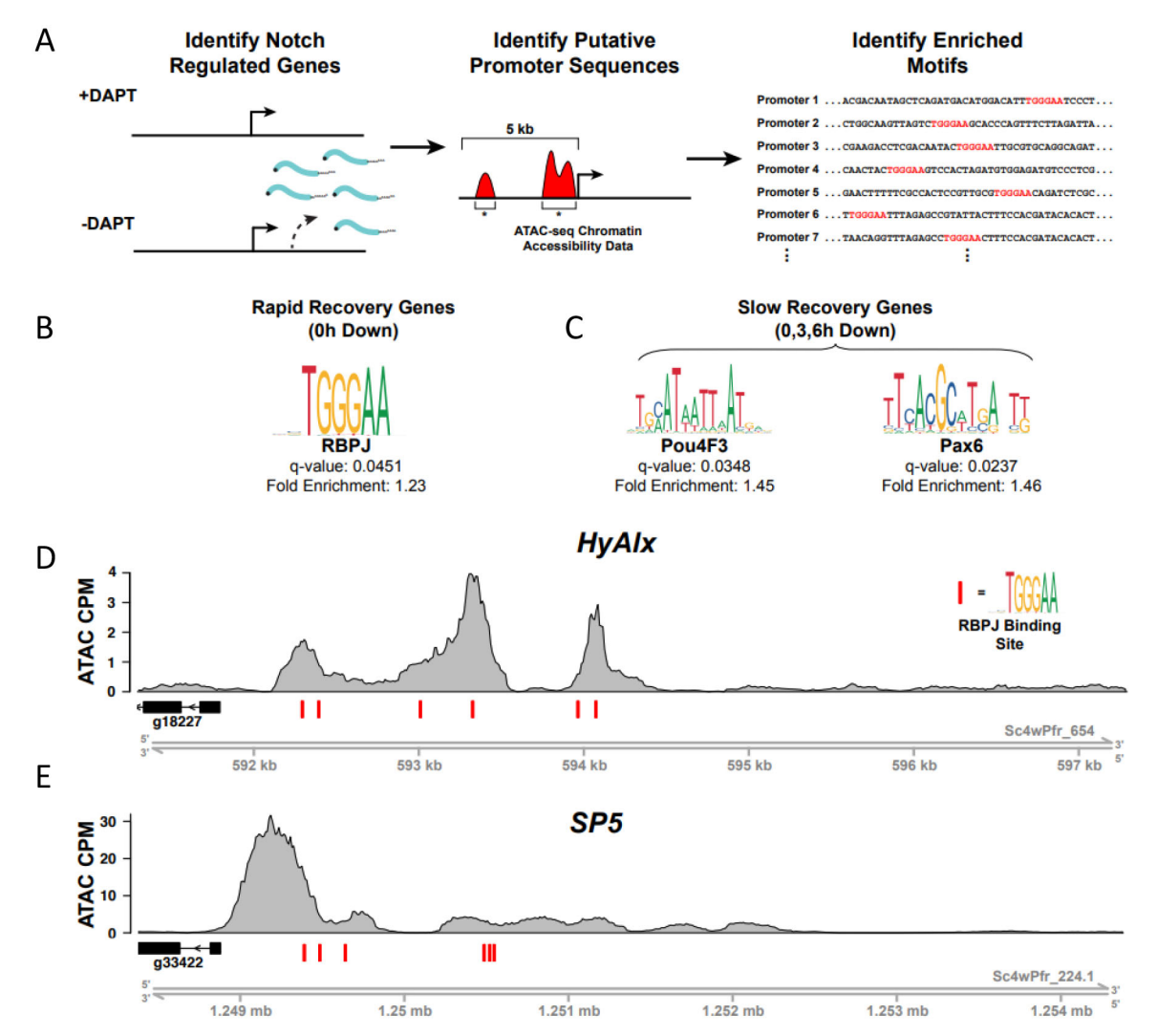


Fig. 8. Motif enrichment analysis of NR gene promoter regions. (A) Workflow of motif enrichment analysis. Putative promoter regions were identified using a previously published ATAC-seq dataset generated using whole wild-type *Hydra* (Siebert et al., 2019). NR gene promoter regions were defined as ATAC-seq peaks that fell within 5 kb upstream of the transcription start site of an NR gene. Using HOMER, NR gene promoters were compared against control peaks that were not associated with NR genes to identify significantly enriched (FDR≤0.05) transcription factor-binding motifs. (B) Notch/RBPJ-binding motifs were significantly enriched in the putative promoters of genes that were downregulated upon DAPT treatment and recovered rapidly following inhibitor removal. (C) Pou and Pax transcription factor binding motifs were significantly enriched in the putative promoters of genes that were downregulated upon DAPT treatment and did not recover their expression over the course of the RNA-seq experiment. Plots of normalized ATAC-seq read density in the 5 kb upstream of (D) HyAlx and (E) SP5 demonstrate the presence of predicted RBPJ-binding sites in the putative promoters of NR genes. Red bars indicate predicted instances of Notch-binding motifs.

proteins (HMG-boxes, t23837aep, t23172aep, t5528aep) [see Tables S1, S2, S3; an alignment and phylogeny is available via FigShare (doi:10.6084/m9.figshare.14714169)]. Therefore, these data reveal the possible components of a gene regulatory network influenced by Notch signalling.

For the group of genes downregulated at all three time points, six enriched motifs were found, most notably POU- and PAX-binding motifs (Fig. 8C; Table S1). The *POU*-gene has previously been implicated in nematocyte differentiation and was found enriched in genes expressed at late stages of nematogenesis (Siebert et al., 2019). *HyPOU4TF-2 like* was downregulated by Notch inhibition at 0 and 3 h (Table S2). The three predicted *Hydra-Pax*-genes [t9974aep, t6559aep and t11467aep, see table (doi:10.6084/m9.figshare. 14681343) and alignment and phylogeny (doi:10.6084/m9.figshare. 14714169) on FigShare] were not amongst the NR genes.

In the group of genes that were upregulated at 0 h, but recovered by 3 h, only the IRF9-binding motif (interferon regulatory factor) was found enriched. For genes that were upregulated at 0 and 3 h, but recovered expression at 6 h, many bZIP-factor-binding motifs were enriched.

As expected, this analysis uncovered RBPJ-binding sites in several NR genes. Of those, and in accordance with their quick recovery after DAPT removal, HyAlx and HySp5, each with six putative RBPJ-sites appeared to be the strongest candidates for direct transcriptional targets of Notch signalling, followed by a negative regulator of Wnt signalling (secreted frizzled-related protein) and the potential transcriptional repressor MAD, which has a hypothetical function in regulating proliferation in epithelia cells.

DISCUSSION

Inhibiting Notch signalling induces a block in nematocyte differentiation and disrupts head patterning in *Hydra* (Münder et al., 2013). Comparable Notch effects have also been described in

two other cnidarian model organisms, namely *Nematostella* and *Hydractinia* (Gahan et al., 2017; Layden and Martindale, 2014; Marlow et al., 2012; Richards and Rentzsch, 2015). In this study, we have identified Notch-regulated (NR) genes by analysing RNA-seq data obtained at different timepoints after treatment of *Hydra* polyps with DAPT. Exploration of the *Hydra* single-cell gene expression atlas (Siebert et al., 2019) revealed sets of genes that were expressed in cell states consistent with observed inhibition phenotypes. Moreover, in many NR genes, we detected binding sites for DNA-binding protein RBPJ – the principal effector of Notch signalling.

Unexpectedly, we detected upregulation of genes encoding heat shock proteins and proteins involved in apoptosis (see table 'Functional annotation of NR genes' at doi:10.6084/m9.figshare. 14681319), hinting at a stress response of the animals to the treatment, which we can attribute to DAPT, as effects of the solvent DMSO should be hidden in our experimental design. Promoter analysis of those upregulated genes revealed enrichment of a Trpcluster motif (IRF9, Table S1). This motif is targeted by the interferon regulatory factor as part of a stress and anti-viral defence pathway in mammals (Jefferies, 2019). Its occurrence and function in *Hydra* genes should be elucidated in the future.

Strikingly, almost half of the Notch-responsive genes were expressed in cells of the nematocyte lineage; 99% of those were downregulated and expressed in post-mitotic nematoblast stages. This reflected Notch regulation of a gene module specific to postmitotic nematoblasts that are in the process of capsule formation. In this module, we find genes that have been previously shown to encode structural capsule proteins, such as minicollagens (Engel et al., 2001), spinalin (Koch et al., 1998), NOWA (Engel et al., 2002), nematogalectin (Zhang et al., 2019), N-col15 (Adamczyk et al., 2008), nematocilin (Hwang et al., 2008) and others. Moreover, we find transcription factors like HyPOU (Siebert et al., 2019) and CnASH (Grens et al., 1995). This is consistent with Notch-inhibition blocking differentiation and the initiation of a transcription programme for capsule formation. We propose that HyPOU is involved in executing this programme, but that it is not a direct Notch target since expression is not re-established within 3 h. In accordance with this hypothesis, motif enrichment analysis identified POU4F DNA-binding motifs in the putative regulatory region of genes that did not recover from DAPT within 6 h. Similarly, CnASH expression does not recover within 6 h, confirming it as an indirect or secondary target (Fig. S1). In contrast, the potential Hydra Jun gene, which encodes a C-terminal bZIP-Jun-domain protein, did recover expression levels fast (Table S2) whereas bZIP-binding motifs appeared to be enriched in promoters of downregulated genes that remained downregulated for 6 h post treatment (Table S1). Recent work in Nematostella had indicated the Jun-homolog Cnido-Jun is involved in driving nematogenesis, as knockdown of Cnido-Jun resulted in loss of expression of NvNcol3 (Nv is Nematostella vectensis) and defects in nematocyte morphology (Sunagar et al., 2018). The mammalian transcription factor JUN is part of the activator-protein 1 (AP-1) transcription factor complex, which responds to numerous extracellular signals including MAP-kinase and cytokine signalling as a reaction to environmental signals. AP-1 is also known as a driver of differentiation in the immune system (reviewed in Katagiri et al., 2021). It is tempting to speculate that Notch controls AP-1-like transcriptional regulation in Hydra (Fig. S4B). This could be a mediator for adjusting nematogenesis in adult animals to nutrient-dependent requirements for nematocyte production from precursors. In starving animals, for instance,

mature nematocytes are not used, thus turnover is low and this governs replenishment (Yaross and Bode, 1978).

Genes that are expressed in nematoblast precursors, including *HyZIC* (Lindgens et al., 2004) and the *Hydra Pax-2A* homolog (19974aep) were not affected by DAPT. This is also true for the *Hydra* homolog of *Myc*, *Hymyc1* (Hartl et al., 2010), the human homolog of which is a Notch target gene in mammals (Giaimo et al., 2021).

Genes that are potentially directly targeted by the NICD would not only be expected to recover their expression level quickly when DAPT treatment is removed and NICD is allowed to enter the nucleus but would be expected to also contain RBDJ sites in their promoter regions. Such binding motifs have been detected in a number of nematocyte-specific genes with unknown function (Table S3). These genes do not encode transcription factors, suggesting that the NICD directly activates the nematocyte differentiation gene complex. Future studies will reveal their role during nematoblast differentiation and also whether they can account for the missing differentiation cue that is directly blocked with DAPT.

However, as an alternative explanation, failure to carry out the nematoblast differentiation programme in our experiments could be caused by missing patterning signals from the *Hydra* head. This hypothesis is suggested because of the strong head phenotypes that we had previously described after DAPT inhibition. The first observable phenotype after 48 h of Notch inhibition was a substantial shortening of the tentacles. Moreover, transplantation experiments with GFP-labelled body column tissue indicated that, during the time of Notch inhibition, cells did not cross the boundary between body column and tentacles (Münder et al., 2013). A 'necklike' structure appeared underneath the tentacle zone, where cells had ceased proliferating, but also did not differentiate into battery cells. In this study, we reveal a cluster of downregulated head-specific genes among the genes that are dysregulated in response to Notch inhibition.

Of particular interest is the aristaless-related gene HyALX, which has six potential RBPJ sites in its putative regulatory region. Our study strongly suggests that Notch signalling directly activates HyALX expression. HyALX has previously been proposed to instruct the specification of tentacle tissue (Smith et al., 2000), and we suggest that HyAlx could play this key role in directing tentacle fate by activating genes with homeobox transcription factor-binding motifs. In support of this, we found that the homeobox motif was enriched in the NR genes downregulated by DAPT that recover their expression quickly after DAPT removal (Table S1). Another potential Notch target with five RBPJ sites in its promoter region is the Max-dimerisation domain (MAD)-encoding MAD gene. This is part of the MYC/Max/MAD network of transcription factors that are involved in the regulation of cell proliferation. MAD forms heterodimers with the bHLH transcription factor MAX, which often mediates repression of proliferative gene activity (Lüscher, 2012). This could also play a role at the tentacle boundary where proliferation of epithelial cells is stopped when they pass into tentacles and become battery cells.

HyALX is expressed in evenly spaced rings at the body column—tentacle boundaries. After release of DAPT inhibition it rapidly recovers expression levels, yet it does not recover a regular expression pattern but becomes expressed in irregular rings, and in extreme cases is in only one ring surrounding the whole animal (Münder et al., 2013). Assuming that NICD acts as a direct activator of HyALX, this indicates that Notch signalling is resumed in the wrong places. Therefore, a feedback mechanism can be suggested,

where the Notch signalling pattern depends on the head organizer, which in turn is co-instructed by Notch signalling.

The potential *Hydra* head organizer gene *CnGSC* (Broun et al., 1999) is downregulated by Notch inhibition and does not recover its activity after 6 h. Furthermore, *Wnt7*, *TCF* and *Sp5*, genes implicated in the canonical Wnt signalling pathway (Broun et al., 1999; Lengfeld et al., 2009; Vogg et al., 2019), are also downregulated. In contrast, we found a small cluster with foot and peduncle genes that were upregulated, including the BMP-pathway gene *TGF-4* (Watanabe et al., 2014). Together, these data may guide the uncovering of molecular pathways responsible for the irregularly shaped heads that develop in polyps after a 48 h period of DAPT treatment (Münder et al., 2013). They also confirm a role of Notch signalling in establishing and maintaining the *Hydra* head organizer, which was previously discovered in transplantation experiments, where the organizer capacity of regenerating *Hydra* head tissue had been inhibited by DAPT (Münder et al., 2013).

The role of Notch signalling for the maintenance of tentacle boundaries can be explained when HyAlx and Sp5 are direct targets for activation by NICD. Expression of HyAlx would then always be maintained by a strong Notch signal at the tentacle boundary. Sp5 would also be expressed in response to this Notch signal to block the activity and expression of canonical Wnts at the boundary. All canonical Wnt genes are expressed in the head outside the tentacle zone. Non-canonical Wnt signalling, on the other hand, does not appear to be affected by NICD and therefore the PCP pathway is active at the boundary and guides movements of cells into tentacles (Fig. S4A).

Conclusion

This study suggests target genes of Notch signalling in Hydra, and provides a resource for the investigation of molecular mechanisms by which HvNotch affects patterning, maintenance of the head organizer and post-mitotic nematocyte differentiation. The expression of the only direct HvNotch target gene, for which experimental evidence is available, HyHes, was also found among NR genes, which quickly recovered original expression levels after DAPT removal. We have identified HyAlx and Sp5 as prime candidates for further direct HvNotch targets involved in head patterning due to their quick recovery after DAPT relief and the presence of RBPJ sites in their promoter regions. A candidate for a direct HvNotch target gene expressed in differentiating nematoblast states and quickly recovering from DAPT treatment is HyJun. As a component of the AP1 transcription complex, it might synchronise nematocyte differentiation as a response to the demand for mature nematocytes depending on usage. Moreover, the impact of HvNotch on regulation of this differentiation step might be conveyed by inducing expression of genes encoding proteins other than transcription factors, for instance genes that are required to form the post-Golgi vacuole. It has to be considered that many genes with as-yet-unknown functions are amongst potential direct Notch targets in nematoblasts.

MATERIALS AND METHODS

Hydra culture

Animals of the strain *Hydra vulgaris* (Basel) were grown in *Hydra* medium (0.1 mM KCl, 1 mM NaCl, 0.1 mM MgSO₄, 1 mM Tris and 1 mM CaCl₂) at 18°C and fed regularly with freshly hatched *Artemia nauplii*.

DAPT treatment

Regularly fed animals were starved for 24 h and incubated in either 20 μ M DAPT with 1% DMSO in *Hydra* medium or in only 1% DMSO in *Hydra* medium (control sample) for 48 h. DAPT and DMSO were renewed every

12 h. Animals were collected, and total RNA was isolated at three different time points: directly at the end of 48 h (0 h), 3 h after DAPT removal (3 h) and 6 h after DAPT removal (6 h). After 48 h incubation, DAPT was removed and replaced with 1% DMSO in *Hydra* medium for the samples 3 h and 6 h. About 25 animals were collected per sample. Six biological replicates were analysed for RNA-seq respectively, two biological replicates (with three technical replicates each) were used for qPCR (Fig. S1).

qPCR

For each sample, total RNA was extracted from 25 whole animals using the RNeasy Mini kit Plus (Qiagen) according to the manufacturer's protocol at time points of 0 h (48 h of DAPT treatment), 2 h, 5.5 h, 8 h, 10 h and 24 h after DAPT removal, for both DAPT-treated and control (1% DMSO only) animals. RNA quality and quantity were assessed using an Agilent Bioanalyzer. RNA with a RIN value of at least 8 was used for cDNA synthesis using the iScript cDNA synthesis kit (BioRad) according to manufacturer's protocol. A non-RNA and non-reverse transcriptase control were included.

Primers for qPCR were designed using the NCBI primer designing tool (https://www.ncbi.nlm.nih.gov/tools/primer-blast/) (*HyHES*, fw 5'-CCCA-CCACCTAGTCCTTCTC-3', rev 5'-TTCTGCTTGGGCAAGTTTGG-3'; *CnASH*, fw 5'-AGACGTTCTAGTCATAGTGTTGTC-3', rev 5'-AGC-CATCATTGACCTGCTTTAC-3') and tested to ensure they amplified the correct fragment from cDNA by gel electrophoresis. Gene-specific primer pairs that yielded one melt peak and a linear standard curve were used for qPCR quantification.

cDNA was diluted 1:25 to ensure the used concentration was within the standard curve of the primers. qPCR with SYBR green detection was performed using an CFX96 Touch Real-Time PCR Detection System (BioRad). Each measurement was performed in three technical replicates. A no template control (NTC) was included. The genes RPL13, $EF1\alpha$ and PPIB served as housekeeping genes and their geomean was used for normalization. The samples were analysed on a 96-well plate in a CFX96 Touch Real-Time PCR Detection System from BioRadRelative expression was calculated as $2^{-}(dCt(\text{test sample})-dCt(\text{reference sample}))$. The error bars represent the s.e.m. (Fig. S1).

Immunohistochemistry

Animals were briefly (1–2 min) relaxed in 2% urethane in *Hydra* medium and fixed immediately after in 2% paraformaldehyde in *Hydra* medium for 1 h. Animals were washed with PBS, permeabilized with 0.5% Triton-X-100/PBS (15 min) and blocked with 0.1% Triton-X-100/1% BSA/PBS (20 min). Primary antibodies were applied overnight at 4°C. After a PBS-wash, animals were incubated with secondary antibodies (2 h), washed again with PBS, counterstained for DNA with DAPI (Sigma, 1 μg/ml) and mounted on slides in Vectashield mounting medium (Axxora).

Whole-mount in situ hybridization

RNA *in situ* hybridization experiments were carried out as previously described (Grens et al., 1995) using digoxigenin labelled RNA probes (Roche) and substrates NBT/BCIP or BM Purple (Roche).

RNA-seq

RNA-seq libraries were prepared for six biological replicates for each experimental condition. cDNA libraries were synthesized from total RNA using the strand-specific SENSE mRNA-Seq Library Prep Kit V2 for Illumina (Lexogen) and the Purification Module with Magnetic Beads (Lexogen). The samples were multiplexed and sequenced on three lanes on Illumina Hiseq2000 with a 100 bp paired end sequencing strategy. Downstream analyses were performed using the Galaxy platform and within R [RStudio Team (2016); version 1.1.463; RCode provided at doi:10. 6084/m9.figshare.14681310]. Illumina adapters and polyA sequences were trimmed and splice leader sequences (Stover and Steele, 2001) were removed from both forward and reverse reads. The tool 'fastqfilter' was used to ensure the paired nature of the filtered dataset, to filter out reads with a quality score lower than 20 and to exclude reads with a read length shorter than 30 bp. Reads that contained 'N's were also removed from the dataset.

De novo transcriptome assembly

All forward and all reverse reads from all sequencing libraries were concatenated. The two resulting files were then used as input to the Trinity (version 2.8.4; Grabherr et al., 2011) *de novo* transcriptome assembler. The assembly was run with the following parameters: -strand-specific library, *in silico* normalisation, -min_contig_length 300, -min_kmer_cov 1, no genome guided mode and no Jaccard Clip options. The resulting reference transcriptome resulted in 62,419 transcripts (43,481 genes) with an average transcript length of 1008b and a median length of 588 bp. A total of 10% of the genes have an average length of 5017 bp and 50% of them are 1495 bp in average. The average GC content of all genes was 34.7%. Transcripts that belonged to the same gene were joined to form SuperTranscripts (tool 'Generate SuperTranscripts from a Trinity assembly'; Galaxy version 2.8.4), which were then used for local Blast search. These were treated as genes models in downstream analyses (see below).

Mapping reads to transcriptome

The processed reads of the 36 RNA-seq libraries (timepoints 0, 3 and 6 h, DAPT and control samples, six replicates) were separately mapped to the *de novo* assembled transcriptome reference, within the Galaxy platform. The reads were mapped as strand-specific and with a maximum insert size of 800. RSEM (Li and Dewey, 2011) – with Bowtie2 (Langmead and Salzberg, 2012; Langmead et al., 2009) as alignment method – was used as the abundance estimation method. The overall alignment rate was >95% for all samples except for one control sample, which had an alignment rate of only 88%. The transcript alignment files of all samples and the gene_to_transcript_map were used as input to generate an expression matrix for all 43,481 assembled genes.

Differential expression analysis

The raw counts were used as input for differential expression (DE) analysis by DESeq2 (version 1.18.1). Genes that were not detected in all 36 samples were excluded from this analysis. DE analysis was performed for each time point separately by comparing the DAPT treatment replicates with those from the control animals (0 h DAPT versus 0 h DMSO, 3 h DAPT versus 3 h DMSO and 6 h DAPT versus 6 h DMSO). Differentially expressed genes at time point 0 h were selected according to their P-adjusted value [Padj(FDR) <0.01]. We refer to this gene set as Notch-regulated genes (NR genes). For each of these NR genes, we investigated whether DE was also identified at time points 3 h and 6 h, thereby applying the same cutoff for DE [Padj(FDR) <0.01].

Blast search

Several blast searches were performed to annotate NR genes. The NCBI Hydra vulgaris protein database (on 2020.02.24) was interrogated using blastx. Sequences with no blast hit or a blast hit with an E-value $>10\times10^{-100}$ were blasted manually. Three types of manual blast searches were performed, NCBI blastn and blastx and NCBI smartBLAST (full list of NR genes on Figshare; doi:10.6084/m9.figshare.14681343). Sequences for which no blast hits were found in either blast search were denoted with 'no blast hit'. This was also the case for sequences, for which a blast hit was found but with an E-value $>10\times10^{-20}$. For the genes that were blasted manually, the NCBI description and accession number was replaced by those of the blast hit with the highest E-value and query cover (for example, if the manual blastn search yielded a better hit than the local blast to the NCBI protein database). The PubMed accession number was added for known Hydra genes. Uniprot was used to search for information about the function and the compartment of the identified sequences, these were denoted as 'unclear' in cases it was unclear or unknown. Multiple alignments were performed for genes with a similar TrinityID and genes with similar/same NCBI description.

Cell state analysis

To make use of the available Hydra single-cell data, we first identified NR genes within the single-cell transcriptome reference using blastn (Siebert et al., 2019) (Transcriptome Shotgun Assembly project; GHHG01000000; see https://www.ncbi.nlm.nih.gov/geo/query/acc.cgi?acc=GSM4009036).

Duplicated hits were removed by keeping the alignments with the highest blast score. Existing Seurat data objects were used to retrieve expression data and cell state annotations (Siebert et al., 2019; and see related data on Dryad at https://doi.org/10.5061/dryad.v5r6077). For hierarchical clustering approaches, average cluster expression was calculated for each cell state (Seurat_2.3.4::AverageExpression). Seurat objectes were then subsetted to the NR gene set and expression was scaled from 0 to 1. Hierarchical clustering was performed using functions stats::dist('euclidian') and stats::hclust('ward.D'). A heatmap (gplots_3.0.0::heatmap.2) with the scaled average expression was generated.

NMF analysis

Normalized expression information was extracted from the whole transcriptome Seurat object for each DE gene with an AEP reference and used for non-negative matrix factorization (NMF) analysis. This analysis was performed as described by Siebert and colleagues (Siebert et al., 2019).

Motif enrichment analysis

To identify putative promoter regions of NR genes, we used a previously published ATAC-seq dataset generated from whole wild-type *Hydra* (Siebert et al., 2019) to locate regions of accessible chromatin (i.e. peaks) within 5 kb upstream of NR gene transcription start sites. We then grouped these NR promoter regions based on the expression dynamics of their putative target genes in our DAPT-treated RNA-seq time course. A total of six sets of NR genes were considered for downstream motif enrichment analyses: (1) genes that were downregulated but recovered by 3 h post-treatment, (2) genes that were downregulated but recovered by 6 h post treatment, (3) genes that were downregulated and remained downregulated at 6 h post treatment, (5) genes that were upregulated but recovered by 6 h post-treatment, and (6) genes that were upregulated and remained upregulated at 6 h post treatment.

For our motif enrichment analysis, we used a curated set of known transcription factor binding motifs provided by the JASPAR database (Fornes et al., 2020). Specifically, we used position weight matrices from the non-redundant vertebrate, insect, nematode and urochordate JASPAR datasets. JASPAR-formatted position weight matrices were converted to HOMER-formatted motifs using the HOMER parseJasparMatrix function. HOMER-formatted motifs require the specification of a score threshold that is used for identifying true motif hits in a query sequence. No such score threshold is included in JASPAR-formatted motifs, so we manually set the threshold to be 40% of the maximum possible score (i.e. the score that would be received by a sequence that perfectly matches the canonical binding sequence) for each motif.

We then used this custom set of HOMER motifs to identify transcription factor-binding motifs that were significantly enriched in each of the six abovementioned NR peak sets. We did this by comparing the NR peak sets to non-NR peaks using a binomial enrichment test as implemented in the HOMER findMotifsGenome function. Motif enrichment results were then filtered using a false discovery rate threshold of ≤0.05.

We found that our raw HOMER results included numerous enriched motifs with highly similar sequences. To simplify these results, we sought to identify and remove redundant motifs from the results tables. To accomplish this, we first generated a matrix of pairwise similarity scores for all motifs in our custom motif set using the HOMER compareMotifs function. These similarity scores were then used to perform hierarchical clustering to identify groups of highly similar motifs. We then reduced the redundancy of our enrichment results by including only the most significantly enriched motif from each motif cluster in the final results table.

To identify putative RBPJ-binding sites in NR promoter regions, we used the HOMER scanMotifGenomeWide function to find sequences that matched the RBPJ and Su(H) binding motifs (JASPAR matrix IDs MA1116.1 and MA0085.1, respectively). In addition, we also made use of a custom Su(H) motif based on a previously reported description of the Su(H) consensus binding site (Bailey and Posakony, 1995). The custom HOMER Su(H) motif was generated using the HOMER seq2profile function; the score threshold was set to be 40% of the maximum possible score.

Plots of ATAC-seq read density and predicted RBPJ-binding sites were generated using the R Gviz package (Hahne and Ivanek, 2016). ATAC-seq reads from individual biological replicates were pooled before generating read density plots.

Acknowledgements

The Galaxy platform of Blum's group at the Gencentre Munich was used for read processing.

Competing interests

The authors declare no competing or financial interests.

Author contributions

Conceptualization: A.B., J.M., C.J., S.S.; Methodology: J.M., S.S., S.K., J.C., A.P.; Software: J.M., S.S., S.K., J.C.; Validation: A.B., J.M., S.S.; Formal analysis: J.M., J.C., A.P., Q.P.; Investigation: A.B., J.M., S.K., J.C., A.P., Q.P.; Resources: J.M.; Data curation: A.B., J.M., J.C., A.P., C.J.; Writing - original draft: A.B., J.M.; Writing - review & editing: J.M., A.B., S.S., C.J.; Visualization: J.M., J.C., A.P., Q.P.; Supervision: A.B.; Project administration: A.B.; Funding acquisition: A.B., C.J.

Funding

This work was funded by Deutsche Forschungsgemeinschaft grant BO1748-12-1 awarded to A.B. and the National Institutes of Health grant R35GM133689 awarded to C.J. Deposited in PMC for release after 12 months.

Data availability

Information available on FigShare comprises the full list of NR genes, doi:10.6084/m9.figshare.14681343; functional annotation of NR genes, doi:10.6084/m9.figshare.14681319; alignment and phylogeny, doi:10.6084/m9.figshare.14714169; Supplementary RCode, doi:10.6084/m9.figshare.14681310; Assembled Trinity SuperTranscripts, doi:10.6084/m9.figshare.14999946.

Peer review history

The peer review history is available online at https://journals.biologists.com/jcs/article-lookup/doi/10.1242/jcs.258768

References

- Adamczyk, P., Meier, S., Gross, T., Hobmayer, B., Grzesiek, S., Bachinger, H.P., Holstein, T.W. and Ozbek, S. (2008). Minicollagen-15, a novel minicollagen isolated from Hydra, forms tubule structures in nematocysts. *J. Mol. Biol.* 376, 1008-1020. doi:10.1016/j.jmb.2007.10.090
- Alexandrova, O., Schade, M., Böttger, A. and David, C. N. (2005). Oogenesis in Hydra: nurse cells transfer cytoplasm directly to the growing oocyte. *Dev. Biol.* 281, 91-101. doi:10.1016/j.ydbio.2005.02.015
- Andersson, E. R., Sandberg, R. and Lendahl, U. (2011). Notch signaling: simplicity in design, versatility in function. *Development* 138, 3593-3612. doi:10. 1242/dev.063610
- Bailey, A. M. and Posakony, J. W. (1995). Suppressor of hairless directly activates transcription of enhancer of split complex genes in response to Notch receptor activity. Genes Dev. 9, 2609-2622. doi:10.1101/gad.9.21.2609
- Borggrefe, T. and Oswald, F. (2009). The Notch signaling pathway: transcriptional regulation at Notch target genes. *Cell. Mol. Life Sci.* **66**, 1631-1646. doi:10.1007/s00018-009-8668-7
- Bosch, T. C. G. and David, C. N. (1986). Male and female stem cells and sex reversal in Hydra polyps. *Proc. Natl. Acad. Sci. USA* 83, 9478-9482. doi:10.1073/ pnas.83.24.9478
- **Broun, M., Sokol, S. and Bode, H. R.** (1999). Cngsc, a homologue of goosecoid, participates in the patterning of the head, and is expressed in the organizer region of Hydra. *Development* **126**, 5245-5254. doi:10.1242/dev.126.23.5245
- David, C. N. and Campbell, R. D. (1972). Cell cycle kinetics and development of Hydra attenuata. I. Epithelial cells. J. Cell Sci. 11, 557-568. doi:10.1242/jcs.11. 2.557
- David, C. N. and Gierer, A. (1974). Cell cycle kinetics and development of Hydra attenuata. III. Nerve and nematocyte differentiation. J. Cell Sci. 16, 359-375. doi:10.1242/jcs.16.2.359
- Deutzmann, R., Fowler, S., Zhang, X., Boone, K., Dexter, S., Boot-Handford, R. P., Rachel, R. and Sarras, M. P.Jr (2000). Molecular, biochemical and functional analysis of a novel and developmentally important fibrillar collagen (Hcol-I) in hydra. *Development* 127, 4669-4680. doi:10.1242/dev.127. 21.4669
- Engel, U., Pertz, O., Fauser, C., Engel, J., David, C. N. and Holstein, T. W. (2001).
 A switch in disulfide linkage during minicollagen assembly in Hydra nematocysts.
 EMBO J. 20, 3063-3073. doi:10.1093/emboj/20.12.3063
- Engel, U., Ozbek, S., Streitwolf-Engel, R., Petri, B., Lottspeich, F. and Holstein, T. W. (2002). Nowa, a novel protein with minicollagen Cys-rich domains, is

- involved in nematocyst formation in Hydra. *J. Cell Sci.* **115**, 3923-3934. doi:10. 1242/ics.00084
- Fang, T. C., Yashiro-Ohtani, Y., Del Bianco, C., Knoblock, D. M., Blacklow, S. C. and Pear, W. S. (2007). Notch directly regulates Gata3 expression during T helper 2 cell differentiation. *Immunity* 27, 100-110. doi:10.1016/j.immuni.2007.04.018
- Fedders, H., Augustin, R. and Bosch, T. C. (2004). A Dickkopf- 3-related gene is expressed in differentiating nematocytes in the basal metazoan Hydra. *Dev. Genes Evol.* 214, 72-80. doi:10.1007/s00427-003-0378-9
- Fornes, O., Castro-Mondragon, J. A., Khan, A., van der Lee, R., Zhang, X., Richmond, P. A., Modi, B. P., Correard, S., Gheorghe, M., Baranasic, D. et al. (2020). JASPAR 2020: update of the open-access database of transcription factor binding profiles. *Nucleic Acids Res.* 48, e87-e92. doi:10.1093/nar/gkaa516
- Gahan, J. M., Schnitzler, C. E., DuBuc, T. Q., Doonan, L. B., Kanska, J., Gornik, S. G., Barreira, S., Thompson, K., Schiffer, P., Baxevanis, A. D. et al. (2017). Functional studies on the role of Notch signaling in Hydractinia development. *Dev. Biol.* 428, 224-231. doi:10.1016/j.ydbio.2017.06.006
- Gauchat, D., Escriva, H., Miljkovic-Licina, M., Chera, S., Langlois, M. C., Begue, A., Laudet, V. and Galliot, B. (2004). The orphan COUP-TF nuclear receptors are markers for neurogenesis from cnidarians to vertebrates. *Dev. Biol.* 275, 104-123. doi:10.1016/j.ydbio.2004.07.037
- Geling, A., Steiner, H., Willem, M., Bally-Cuif, L. and Haass, C. (2002). A gamma-secretase inhibitor blocks Notch signaling in vivo and causes a severe neurogenic phenotype in zebrafish. *EMBO Rep.* 3, 688-694. doi:10.1093/embo-reports/kvf124
- Giaimo, B. D., Gagliani, E. K., Kovall, R. A. and Borggrefe, T. (2021). Transcription factor RBPJ as a molecular switch in regulating the notch response. Adv. Exp. Med. Biol. 1287, 9-30. doi:10.1007/978-3-030-55031-8_2
- Golubovic, A., Kuhn, A., Williamson, M., Kalbacher, H., Holstein, T. W., Grimmelikhuijzen, C. J. and Gründer, S. (2007). A peptide-gated ion channel from the freshwater polyp Hydra. *J. Biol. Chem.* **282**, 35098-35103. doi:10.1074/jbc.M706849200
- Grabherr, M. G., Haas, B. J., Yassour, M., Levin, J. Z., Thompson, D. A., Amit, I., Adiconis, X., Fan, L., Raychowdhury, R., Zeng, Q. et al. (2011). Full-length transcriptome assembly from RNA-Seq data without a reference genome. *Nat. Biotechnol.* 29, 644-652. doi:10.1038/nbt.1883
- Grens, A., Mason, E., Marsh, J. L. and Bode, H. R. (1995). Evolutionary conservation of a cell fate specification gene: the Hydra achaete-scute homolog has proneural activity in Drosophila. *Development* 121, 4027-4035. doi:10.1242/ dev.12112.4027
- Hahne, F. and Ivanek, R. (2016). Visualizing genomic data using gviz and bioconductor. *Methods Mol. Biol.* 1418, 335-351. doi:10.1007/978-1-4939-3578-9 16
- Hartl, M., Mitterstiller, A.-M., Valovka, T., Breuker, K., Hobmayer, B. and Bister, K. (2010). Stem cell-specific activation of an ancestral myc protooncogene with conserved basic functions in the early metazoan Hydra. *Proc. Natl. Acad. Sci. USA* 107, 4051-4056. doi:10.1073/pnas.0911060107
- Hobmayer, B., Rentzsch, F., Kuhn, K., Happel, C. M., von Laue, C. C., Snyder, P., Rothbächer, U. and Holstein, T. W. (2000). WNT signalling molecules act in axis formation in the diploblastic metazoan Hydra. *Nature* 407, 186-189. doi:10. 1038/35025063
- Holstein, T. W., Hobmayer, E. and David, C. N. (1991). Pattern of epithelial cell cycling in hydra. Dev. Biol. 148, 602-611. doi:10.1016/0012-1606(91)90277-A
- Hwang, J. S., Takaku, Y., Chapman, J., Ikeo, K., David, C. N. and Gojobori, T. (2008). Cilium evolution: identification of a novel protein, nematocilin, in the mechanosensory cilium of Hydra nematocytes. *Mol. Biol. Evol.* 25, 2009-2017. doi:10.1093/molbev/msn154
- Jarrett, S. M., Seegar, T. C. M., Andrews, M., Adelmant, G., Marto, J. A., Aster, J. C. and Blacklow, S. C. (2019). Extension of the Notch intracellular domain ankyrin repeat stack by NRARP promotes feedback inhibition of Notch signaling. Sci. Signal. 12, eaay2369. doi:10.1126/scisignal.aay2369
- Jefferies, C. A. (2019). Regulating IRFs in IFN driven disease. Front. Immunol. 10, 325. doi:10.3389/fimmu.2019.00325
- Käsbauer, T., Towb, P., Alexandrova, O., David, C. N., Dall'armi, E., Staudigl, A., Stiening, B. and Böttger, A. (2007). The Notch signaling pathway in the cnidarian Hydra. Dev. Biol. 303, 376-390. doi:10.1016/j.ydbio.2006.11.022
- Katagiri, T., Kameda, H., Nakano, H. and Yamazaki, S. (2021). Regulation of T cell differentiation by the AP-1 transcription factor JunB. *Immunol. Med.* doi:10.1080/ 25785826.2021.1872838.
- Koch, A. W., Holstein, T. W., Mala, C., Kurz, E., Engel, J. and David, C. N. (1998). Spinalin, a new glycine- and histidine-rich protein in spines of Hydra nematocysts. J. Cell Sci. 111, 1545-1554. doi:10.1242/jcs.111.11.1545
- Kopan, R. and Ilagan, M. X. (2009). The canonical Notch signaling pathway: unfolding the activation mechanism. *Cell* 137, 216-233. doi:10.1016/j.cell.2009. 03.045
- Krejci, A., Bernard, F., Housden, B. E., Collins, S. and Bray, S. J. (2009). Direct response to Notch activation: signaling crosstalk and incoherent logic. Sci. Signal. 2, ra1. doi:10.1126/scisignal.2000140
- Langmead, B. and Salzberg, S. L. (2012). Fast gapped-read alignment with Bowtie 2. Nat. Methods 9, 357-359. doi:10.1038/nmeth.1923

- Langmead, B., Trapnell, C., Pop, M. and Salzberg, S. L. (2009). Ultrafast and memory-efficient alignment of short DNA sequences to the human genome. *Genome Biol.* 10, R25. doi:10.1186/gb-2009-10-3-r25
- Lasi, M., Pauly, B., Schmidt, N., Cikala, M., Stiening, B., Käsbauer, T., Zenner, G., Popp, T., Wagner, A., Knapp, R. T. et al. (2010). The molecular cell death machinery in the simple cnidarian Hydra includes an expanded caspase family and pro- and anti-apoptotic Bcl-2 proteins. *Cell Res.* 20, 812-825. doi:10.1038/cr. 2010.66
- Layden, M. J. and Martindale, M. Q. (2014). Non-canonical Notch signaling represents an ancestral mechanism to regulate neural differentiation. *Evodevo* 5, 30. doi:10.1186/2041-9139-5-30
- Lengfeld, T., Watanabe, H., Simakov, O., Lindgens, D., Gee, L., Law, L., Schmidt, H. A., Ozbek, S., Bode, H. and Holstein, T. W. (2009). Multiple Wnts are involved in Hydra organizer formation and regeneration. *Dev. Biol.* 330, 186-199. doi:10.1016/i.vdbio.2009.02.004
- Leontovich, A. A., Zhang, J., Shimokawa, K., Nagase, H. and Sarras, M. P.Jr (2000). A novel hydra matrix metalloproteinase (HMMP) functions in extracellular matrix degradation, morphogenesis and the maintenance of differentiated cells in the foot process. *Development* 127, 907-920. doi:10.1242/dev.127.4.907
- Liao, B.-K. and Oates, A. C. (2017). Delta-Notch signalling in segmentation. Arthropod. Struct. Dev. 46, 429-447. doi:10.1016/j.asd.2016.11.007
- Lindgens, D., Holstein, T. W. and Technau, U. (2004). Hyzic, the Hydra homolog of the zic/odd-paired gene, is involved in the early specification of the sensory nematocytes. *Development* 131, 191-201. doi:10.1242/dev.00903
- Lüscher, B. (2012). MAD1 and its life as a MYC antagonist: an update. Eur. J. Cell Biol. 91, 506-514. doi:10.1016/j.ejcb.2011.07.005
- Marlow, H., Roettinger, E., Boekhout, M. and Martindale, M. Q. (2012).
 Functional roles of Notch signaling in the cnidarian Nematostella vectensis.
 Dev. Biol. 362, 295-308. doi:10.1016/j.ydbio.2011.11.012
- Micchelli, C. A., Esler, W. P., Kimberly, W. T., Jack, C., Berezovska, O., Kornilova, A., Hyman, B. T., Perrimon, N. and Wolfe, M. S. (2003). Gamma-secretase/presenilin inhibitors for Alzheimer's disease phenocopy Notch mutations in Drosophila. *FASEB J.* 17, 79-81. doi:10.1096/fj.02-0394fje
- Mumm, J. S. and Kopan, R. (2000). Notch signaling: from the outside in. *Dev. Biol.* 228, 151-165. doi:10.1006/dbio.2000.9960
- Münder, S., Käsbauer, T., Prexl, A., Aufschnaiter, R., Zhang, X., Towb, P. and Böttger, A. (2010). Notch signalling defines critical boundary during budding in Hydra. *Dev. Biol.* **344**, 331-345. doi:10.1016/j.ydbio.2010.05.517
- Münder, S., Tischer, S., Grundhuber, M., Buchels, N., Bruckmeier, N., Eckert, S., Seefeldt, C. A., Prexl, A., Käsbauer, T. and Böttger, A. (2013). Notch-signalling is required for head regeneration and tentacle patterning in Hydra. *Dev. Biol.* 383, 146-157. doi:10.1016/j.ydbio.2013.08.022
- Otto, J. J. and Campbell, R. D. (1977). Tissue economics of hydra: regulation of cell cycle, animal size and development by controlled feeding rates. *J. Cell Sci.* 28, 117-132. doi:10.1242/jcs.28.1.117
- Prexl, A., Münder, S., Loy, B., Kremmer, E., Tischer, S. and Böttger, A. (2011). The putative Notch ligand HyJagged is a transmembrane protein present in all cell

- types of adult Hydra and upregulated at the boundary between bud and parent. BMC Cell Biol. 12. 38. doi:10.1186/1471-2121-12-38
- Richards, G. S. and Rentzsch, F. (2015). Regulation of Nematostella neural progenitors by SoxB, Notch and bHLH genes. *Development* 142, 3332-3342. doi:10.1242/dev.123745
- **Roboti, P. and High, S.** (2012). The oligosaccharyltransferase subunits OST48, DAD1 and KCP2 function as ubiquitous and selective modulators of mammalian N-glycosylation. *J. Cell. Sci.* **125**, 3474-3484. doi:10.1242/jcs.103952
- Siebel, C. and Lendahl, U. (2017). Notch signaling in development, tissue homeostasis, and disease. *Physiol. Rev.* 97, 1235-1294. doi:10.1152/physrev. 00005.2017
- Siebert, S., Farrell, J. A., Cazet, J. F., Abeykoon, Y., Primack, A. S., Schnitzler, C. E. and Juliano, C. E. (2019). Stem cell differentiation trajectories in Hydra resolved at single-cell resolution. Science 365, eaav9314. doi:10.1126/science. aav9314
- Smith, K. M., Gee, L. and Bode, H. R. (2000). HyAlx, an aristaless-related gene, is involved in tentacle formation in hydra. *Development* **127**, 4743-4752. doi:10. 1242/dev.127.22.4743
- Steele, R. E. (2002). Developmental signaling in Hydra: what does it take to build a "simple" animal? *Dev. Biol.* **248**, 199-219. doi:10.1006/dbio.2002.0744
- Stover, N. A. and Steele, R. E. (2001). Trans-spliced leader addition to mRNAs in a cnidarian. *Proc. Natl. Acad. Sci. USA* **98**, 5693-5698. doi:10.1073/pnas. 10104998
- Sudhop, S., Coulier, F., Bieller, A., Vogt, A., Hotz, T. and Hassel, M. (2004). Signalling by the FGFR-like tyrosine kinase, Kringelchen, is essential for bud detachment in Hydra vulgaris. *Development* 131, 4001-4011. doi:10.1242/dev. 01267
- Sunagar, K., Columbus-Shenkar, Y. Y., Fridrich, A., Gutkovich, N., Aharoni, R. and Moran, Y. (2018). Cell type-specific expression profiling unravels the development and evolution of stinging cells in sea anemone. *BMC Biol.* 16, 108. doi:10.1186/s12915-018-0578-4
- Vogg, M. C., Beccari, L., Iglesias Olle, L., Rampon, C., Vriz, S., Perruchoud, C., Wenger, Y. and Galliot, B. (2019). An evolutionarily-conserved Wnt3/β-catenin/Sp5 feedback loop restricts head organizer activity in Hydra. *Nat. Commun.* 10, 312. doi:10.1038/s41467-018-08242-2
- Wang, H., Zang, C., Liu, X. S. and Aster, J. C. (2015). The role of Notch receptors in transcriptional regulation. *J. Cell. Physiol.* 230, 982-988. doi:10.1002/jcp.24872
- Watanabe, H., Schmidt, H. A., Kuhn, A., Höger, S. K., Kocagöz, Y., Laumann-Lipp, N., Özbek, S. and Holstein, T. W. (2014). Nodal signalling determines biradial asymmetry in Hydra. *Nature* 515, 112-115. doi:10.1038/nature13666
- Yaross, M. S. and Bode, H. R. (1978). Regulation of interstitial cell differentiation in Hydra attenuata. V. Inability of regenerating head to support nematocyte differentiation. *J. Cell Sci.* **34**, 39-52. doi:10.1242/jcs.34.1.39
- Zhang, R., Jin, L., Zhang, N., Petridis, A. K., Eckert, T., Scheiner-Bobis, G., Bergmann, M., Scheidig, A., Schauer, R., Yan, M. et al. (2019). The sialic aciddependent nematocyst discharge process in relation to its physical-chemical properties is a role model for nanomedical diagnostic and therapeutic tools. *Mar. Drugs* 17, 469. doi:10.3390/md17080469

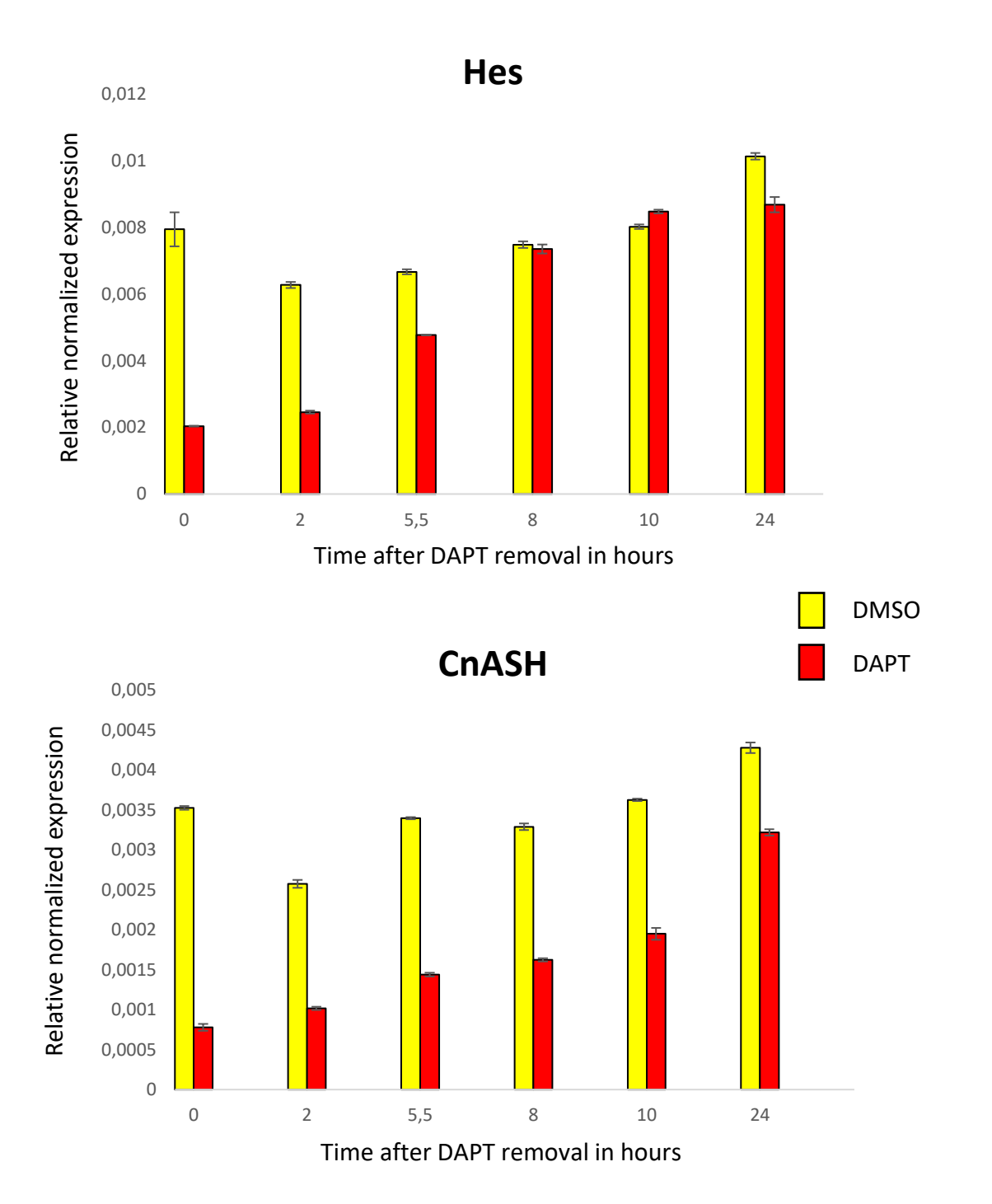
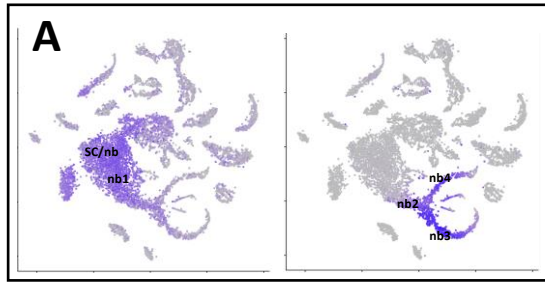
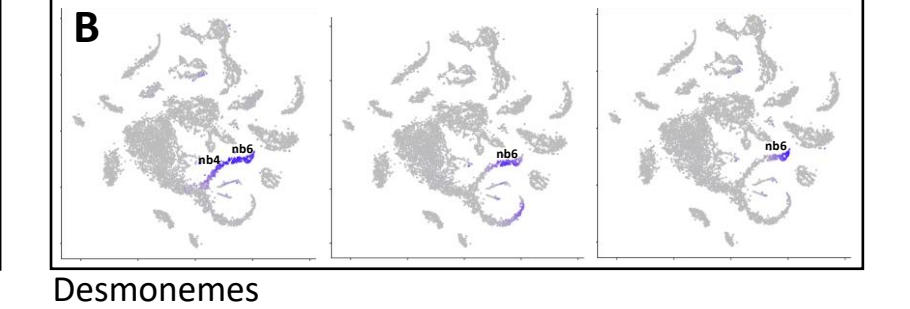


Fig. S1. RT-qPCR measurement of HyHes and HyCnASH upon DAPT removal. Animals were treated with 20 μ M DAPT/1% DMSO or with 1% DMSO as a control for 48 hours. Thereafter, DAPT was removed and all animals were kept in 1%DMSO. RT-qPCR measurements were performed at 0h, 2h, 5,5h, 8h, 10h and 24h post DAPT removal. Expression of HyHES was recovered between 5,5 and 8 hours, whereas expression levels of CnASH were still reduced even 24 hours after DAPT removal. The genes RPL13, $EF1\alpha$, PPIB served as housekeeping genes and their geomean was used for normalization.

Dataset interstitial cell lineage

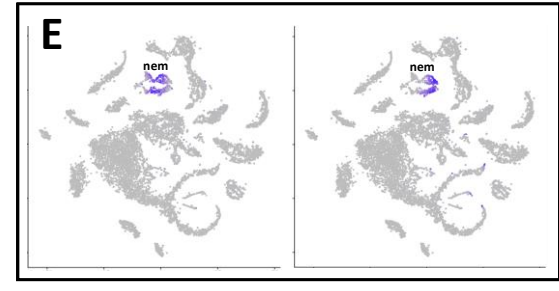




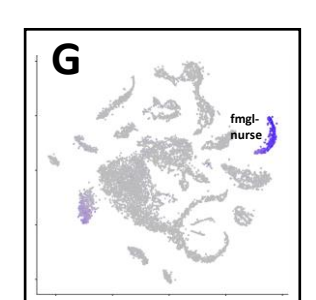
Nematoblast progenitors

D

Stenoteles



Isorhizas

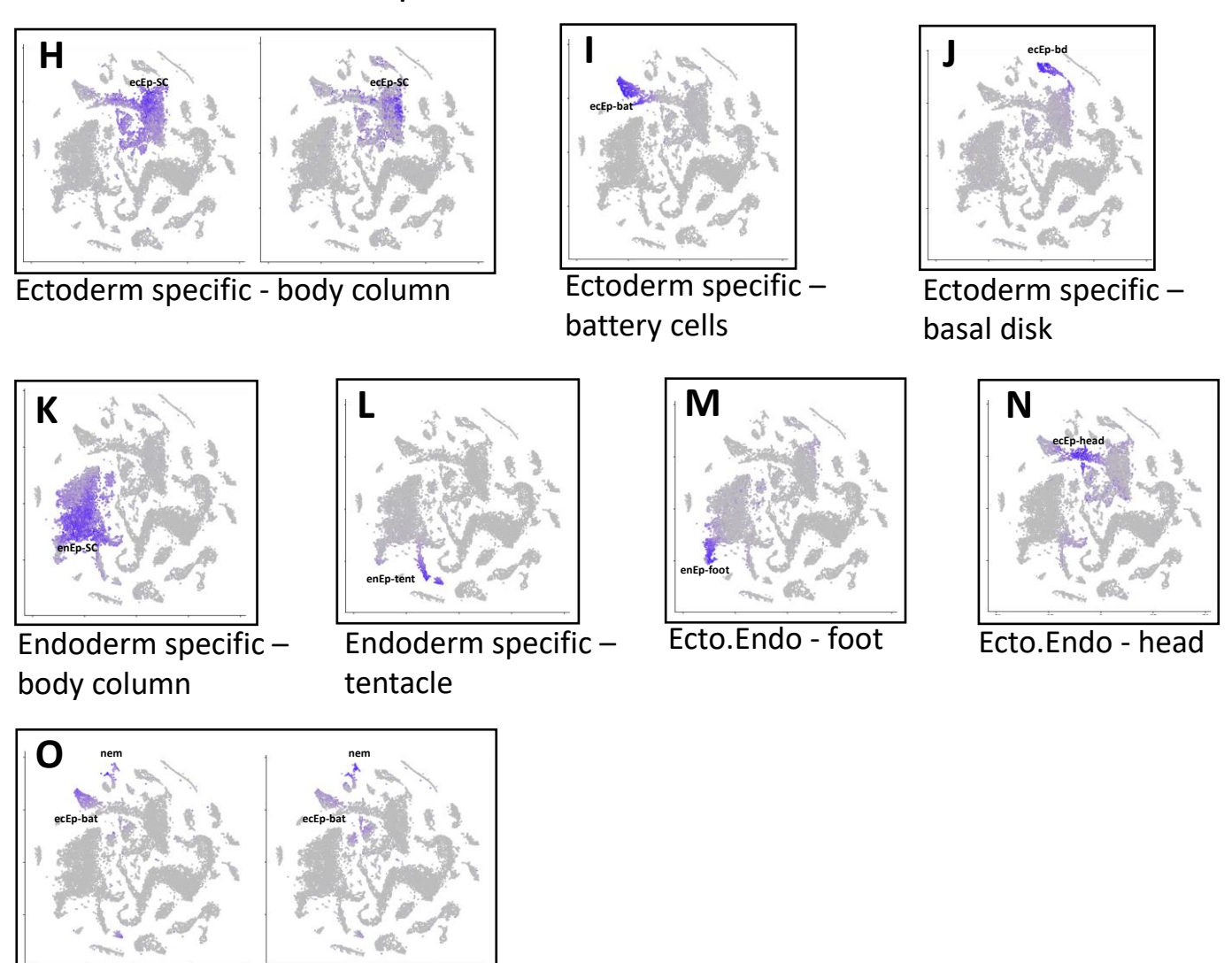


Mature nematocytes

IC derivatives – gland cells

IC derivatives female nurse cells

Dataset whole transcriptome



Ectoderm Battery + Nematocytes

Fig. S2. Metagenes. Metagenes. Non-negative matrix factorization (NMF) was performed in order to identify groups (metagenes) of genes with similar expression patterns. Normalized cell state expression information for the 666 NR-genes with an AEP reference was extracted from the whole-transcriptome dataset (Siebert et al., 2019) and used as input for the NMF analysis. This analysis yielded 23 Metagenes, which were divided into 15 groups, according to the cell types in which the metagenes were expressed. The overall expression of each metagene is displayed on the tSNE plots by blue dots of either the interstitial cell lineage dataset (A-G) or the whole transcriptome dataset (H-O) (Siebert et al., 2019). The grey areas represent the cell states as found and annotated by Siebert et al.. Sc/nb: nematoblast progenitors; nb: nematoblasts (different stages); nem: mature nematocytes; zmg: zymogen gland cells; gmgc: granular mucous gland cell; smgc: spumous mucous gland cell; ecEP: ectodermal epithelial cell; SC: stem cell; bat: battery cell; bd: basal disk; enEP: endodermal epithelial cell; tent: tentacle cell.

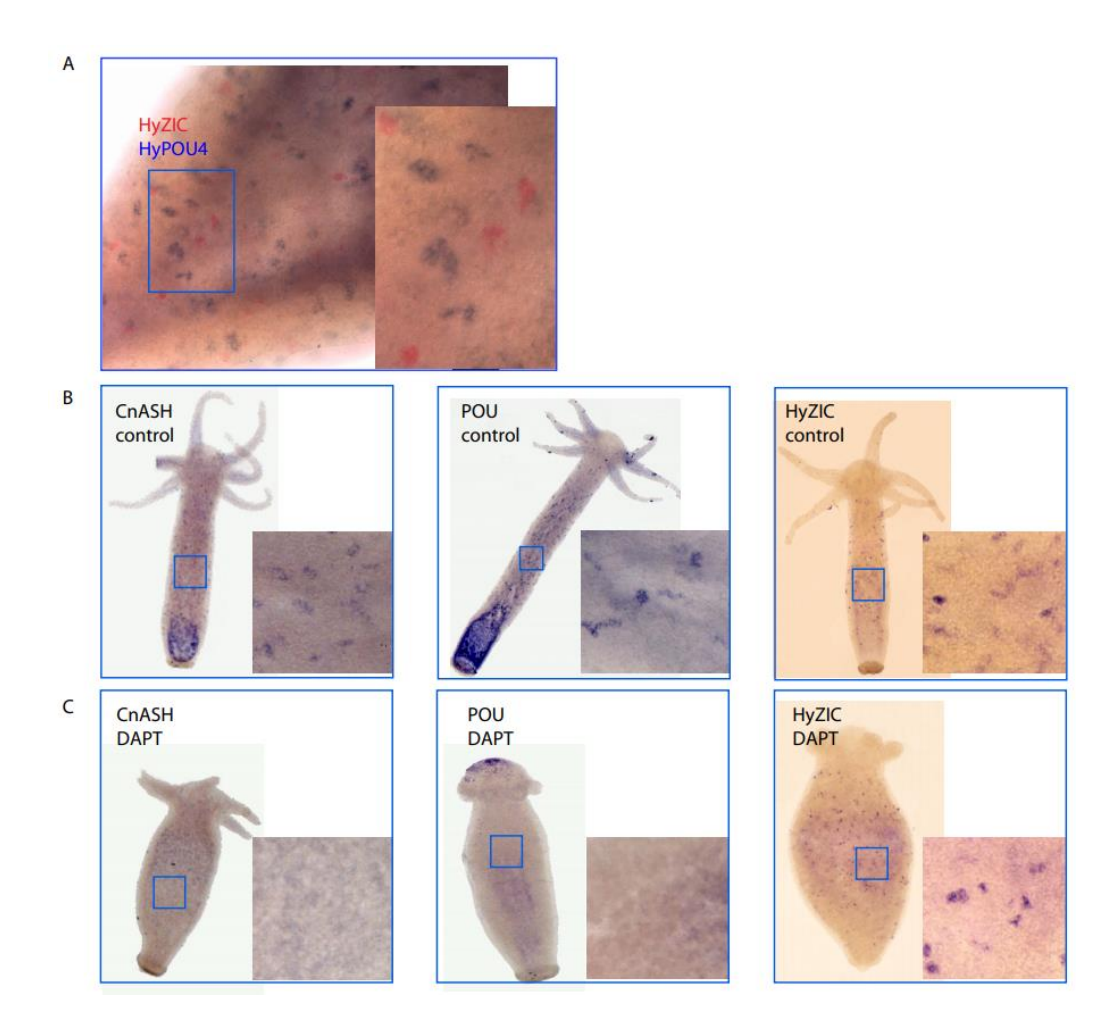


Fig. S3. *In situ hybridization for nematocyte marker genes*. A) Double in situ-hybridisation for expression of *HyZIC (red signals)* and *HyPOU (blue signals)*. B) Whole mount in situ hybridization for *HyZic, CnASH and POU4* in *Hydra* polyps treated for 48 hrs with 1 % DMSO for control (-DAPT). C) Whole mount *in situ hybridization for HyZic, CnASH* and *POU4* in *Hydra* polyps treated for 48 hrs with DAPT. Scale bars 50μm.

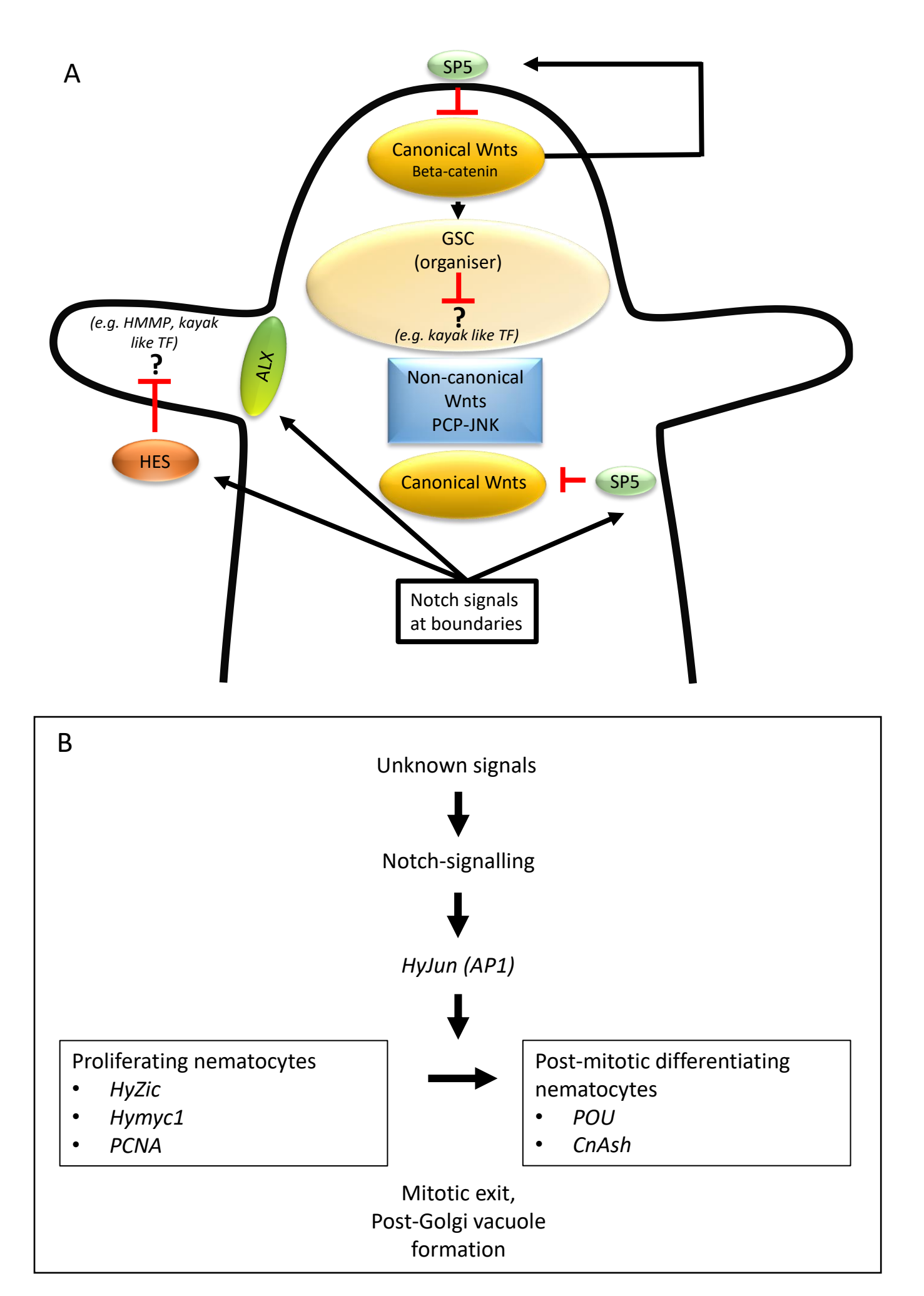


Fig. S4. *Schematic summary.* Hypothetical interactions of Notch regulated genes in A: Head patterning and B: nematocyte differentiation

Table S1. Motifs enriched in the promoters of downregulated genes that recovered by 3 hours post-treatment

Motif ID	Motif Sequence	FDR	Frequency in NR Peaks (n= 173)	Frequency in non-NR Peaks (n= 69267)	Fold Enrichment	Binding TF Class	Potential NR Regulators
ind/MA0228.1	YTAATTA	0.0164	88.44%	75.77%	1.1672	Homeo domain factors	CnAlx (t16456aep); Smith 2000, Fig. S3 OTX1B (t33622aep); Fig. S3 PITX1 (t5275aep); pred. aristaless-like (t16456aep); pred.
TBX1/MA0805.1	AGGTGTGA	0.0164	42.77%	28.26%	1.5134	T-Box factors	
ETV5/MA0765.1	ACCGGAAGTN	0.0183	62.43%	48.04%	1.2995	Tryptophan cluster factors	
FOXP2/MA0593.1	AWGTAAACARA	0.0183	89.02%	77.89%	1.1429	Fork head / winged helix factors	FoxP1 (t19720aep)
CUX1/MA0754.1	TAATCGATAH	0.0183	80.92%	68.34%	1.1841	Homeo domain factors	CnAlx (t16456aep); Smith 2000, Fig. S3 OTX1B (t33622aep); Fig. S3 PITX1 (t5275aep); pred. aristaless-like (t16456aep); pred.
MEF2A/MA0052.3	KCTAWAAATAGA	0.0219	71.68%	58.42%	1.2270	MADS box factors	
SOX10/MA0442.2	NDAACAAAGVN	0.0219	94.22%	85.45%	1.1026	High-mobility group (HMG) domain factors	Sox14(t23172aep); Fig. S3 TF7-like 2 (t11826aep), pred.
D/MA0445.1	TCCATTGTTBT	0.0219	91.33%	81.53%	1.1202	High-mobility group (HMG) domain factors	Sox14(t23172aep); Fig. S3 TF7-like 2 (t11826aep), pred.
Hoxd8/MA0910.1	TAADTAATTAATRGCTW	0.0283	90.75%	81.40%	1.1149	Homeo domain factors	
Ahr::Arnt/MA0006.1	YGCGTG	0.0401	73.41%	61.81%	1.1877	Basic helix-loop-helix factors (bHLH)	HyHES (t3617aep); Münder 2013 TFE3 (t22195aep) Mad-protein (t34122aep)
PAX7/MA0680.1	TAATCGATTA	0.0401	50.29%	38.31%	1.3127	Paired box factors	
cad/MA0216.2	RGCCATAAAAM	0.0401	90.17%	81.46%	1.1069	Homeo domain factors	CnAlx (t16456aep); Smith 2000, Fig. S3 OTX1B (t33622aep); Fig. S3 PITX1 (t5275aep); pred. aristaless-like (t16456aep); pred.
OTX1/MA0711.1	YTAATCCG	0.0401	95.38%	88.36%	1.0794	Homeo domain factors	CnAlx (t16456aep); Smith 2000, Fig. S3 OTX1B (t33622aep); Fig. S3 PITX1 (t5275aep); pred. aristaless-like (t16456aep); pred.
OLIG1/MA0826.1	AACATATGKT	0.0449	30.06%	20.33%	1.4786	Basic helix-loop-helix factors (bHLH)	HyHES (t3617aep); Münder 2013 TFE3 (t22195aep)

							Mad-protein (t34122aep)
NFATC3/MA0625.1	WTTTTCCATT	0.0449	98.84%	93.98%	1.0517	Rel homology region (RHR) factors	
TEAD3/MA0808.1	ACATTCCA	0.0449	55.49%	44.09%	1.2586	TEA domain factors	
Deaf1/MA0185.1	TTCGKS	0.0449	78.61%	68.27%	1.1515	SAND domain factors	
HNF1B/MA0153.2	GTTAATNATTAAY	0.0449	61.27%	49.99%	1.2256	Homeo domain factors	CnAlx (t16456aep); Smith 2000, Fig. S3 OTX1B (t33622aep); Fig. S3 PITX1 (t5275aep); pred. aristaless-like (t16456aep); pred.
NR4A2/MA0160.1	AAGGTCAC	0.0449	79.77%	69.94%	1.1405	Nuclear receptors with C4 zinc fingers	
RBPJ/MA1116.1	BSTGGGAANN	0.0451	57.80%	46.86%	1.2335	Rel homology region (RHR) factors	

Motifs enriched in the promoters of downregulated genes that recovered by 6 hours post-treatment

	P	0_ 0_0	8	8		,	
Motif ID	Motif Sequence	FDR	Frequency in NR Peaks (n=98)	Frequency in non-NR Peaks (n=71913)	Fold Enrichment	Binding TF Class	Potential NR Regulators
FOXP1/MA0481.2	NDGTAAACAGDN	0.0489	98.98%	3% 88.24% 1.1217 Fork head / winged helix factors		Fork head / winged helix factors	FOXI1 (t9145aep); Fig. S3
NKX3-2/MA0122.2	RCCACTTAA 0.0489		93.88%	79.75%	1.1772	Homeo domain factors	

Motifs enriched in the promoters of downregulated genes that remained downregulated by 6 hours post-treatment

Motif ID	Motif Sequence	FDR	Frequency in NR Peaks (n=214)	Frequency in non-NR Peaks (n=73172)	Fold Enrichment	Binding TF Class	Potential NR Regulators
ZIC4/MA0751.1	GACCCCCGCTGYGH	0.0149	7.01%	1.92%	3.6510	C2H2 zinc finger factors	Zinc finger protein 26 like (t11591aep); pred.
Mafb/MA0117.2	AAADTGCTGACD	0.0237	68.69%	55.64%	1.2345	Basic leucine zipper factors (bZIP)	
lin-14/MA0261.1	GAACAC	0.0237	87.85%	77.40%	1.1350	Unknown	
Pax6/MA0069.1	TTCACGCWTGANTT	0.0237	37.38%	25.59%	1.4607	Paired box factors	
POU4F3/MA0791.1	ATGMATAATTAATGAG	0.0348	82.71%	72.22%	1.1453	Homeo domain factors	IRX6-2 (t16018aep) Prdl-b (t21636aep); Gauchat 1998
Deaf1/MA0185.1	TTCGKS	0.0425	77.10%	66.21%	1.1645	SAND domain factors	

Motifs enriched in the promoters of upregulated genes that recovered by 3 hours post-treatment

Motif ID	Motif Sequence	FDR	Frequency in NR Peaks (n=76)	Frequency in non-NR Peaks (n=68746)	Fold Enrichment	Binding TF Class	Potential NR Regulators
IRF9/MA0653.1	AACGAAACCGAAACT	0.0131	7.89%	0.71%	11.1127	Tryptophan cluster factors	

Motifs enriched in the promoters of upregulated genes that recovered by 6 hours post-treatment

Motif ID	Motif Sequence	FDR	Frequency in NR Peaks (n=53)	Frequency in non-NR Peaks (n=71510)	Fold Enrichment	Binding TF Class	Potential NR Regulators
Atf1/MA0604.1	RTGACGTA	0.0143	90.57%	65.01%	1.3932	Basic leucine zipper factors (bZIP)	
Vsx2/MA0180.1	KTTAATTAG	0.0143	83.02%	58.02%	1.4309	Homeo domain factors	
GMEB2/MA0862.1	TTACGTAA	0.0143	90.57%	67.86%	1.3347	SAND domain factors	
EcR::usp/MA0534.1	VAGTTCATTGAMCTT	0.0143	45.28%	22.33%	2.0278	Nuclear receptors with C4 zinc fingers	
Crx/MA0467.1	AAGRGGATTAG	0.0212	69.81%	46.17%	1.5120	Homeo domain factors	
Creb3l2/MA0608.1	GCCACGTGT	0.0212	26.42%	9.77%	2.7042	Basic leucine zipper factors (bZIP)	
HOXC13/MA0907.1	KCTCGTAAAAH	0.0451	77.36%	56.16%	1.3775	Homeo domain factors	
PAX7/MA0680.1	TAATCGATTA	0.0459	60.38%	38.87%	1.5534	Paired box factors	

Motifs enriched in the promoters of upregulated genes that remained upregulated at 6 hours post-treatment

Motif ID	Motif Sequence	FDR	Frequency in NR Peaks (n=78)	Frequency in non-NR Peaks (n=72007)	Fold Enrichment	Binding TF Class	Potential NR Regulators
Crem/MA0609.1	KATGACGTAA	0.0091	64.10%	39.77%	1.6118	Basic leucine zipper factors (bZIP)	

Table S2. Downregulated transcription factors that recovered by 3 hours post-treatment

Trinity ID	AEP ID	Gene Model	log2FC 0h	log2FC 3h	Log2FC 6h	Pubmed Hit	NCBI Accession	NCBI Description	Short Name	DNA Binding Domain
TRINITY_DN7608_c0_g1	t22195aep	Sc4wPfr_552.g10536.t1	-0.326	0	0	NA	CDG71838.1	Hydra vulgaris Microphthalmia- associated transcription factor [Hydra vulgaris]	TFE3	ьнгн
TRINITY_DN10125_c0_g1	t26873aep	Sc4wPfr_1909.g11470.t1	-0.641	0	0	NA	XP_012558352.1	PREDICTED: zinc finger protein 37-like isoform X1 [Hydra vulgaris]	ZSC31	zf-C2H2
TRINITY_DN14709_c0_g1	t5528aep	Sc4wPfr_59.2.g12567.t1	-0.925	0	0	NA	XP_002154370.1	PREDICTED: transcription factor Sox-19a-like [Hydra vulgaris]	HySox19a	HMG box
TRINITY_DN5359_c0_g1	t23172aep	Sc4wPfr_297.g13156.t1	-1.507	0	0	NA	XP_012555836.1	PREDICTED: uncharacterized protein LOC101236863 [Hydra vulgaris], similar to SoxB3 Hydractinia echinata	Sox14	HMG box
TRINITY_DN4294_c0_g1	t20709aep	Sc4wPfr_237.2.g16165.t1	-1.072	0	0	NA	CDG67849.1	Hydra vulgaris Zinc finger protein ZIC 5, partial [Hydra vulgaris]	Zic5-like	zf-C2H2
TRINITY_DN37877_c0_g1	t26616aep	Sc4wPfr_14.g1768.t2	-1.427	0	0	NA	CDG72115.1	Hydra vulgaris Putative transcription factor Ovo-like 1, partial [Hydra vulgaris]	NA	zf-C2H2
TRINITY_DN5649_c0_g1	t16456aep	Sc4wPfr_654.g18227.t1	-1.160	0	0	NA	AAG03082.1	aristaless-like protein [Hydra vulgaris]	CnAlx (Smith, 2000)	Homeobox
TRINITY_DN3178_c1_g1	t17964aep	Sc4wPfr_68.g2328.t1	-1.605	0	0	NA	XP_012567188.1	PREDICTED: uncharacterized protein	Jun	bZIP

								LOC105851038 [Hydra vulgaris]		
TRINITY_DN859_c0_g1	t11826aep	Sc4wPfr_319.g27364.t1	-0.397	0	0	NA	CDG67153.1	Hydra vulgaris Transcription factor 7-like 2 [Hydra vulgaris]	TF7-like 2	HMG box
TRINITY_DN1402_c1_g1	t34122aep	Sc4wPfr_215.1.g29578.t1	-1.010	0	0	NA	CDG70360.1	Hydra vulgaris Max dimerization protein 1 [Hydra vulgaris]	Mad- protein	bнгн
TRINITY_DN5643_c0_g1	t19720aep	Sc4wPfr_396.g3075.t3	-0.481	0	0	NA	XM_012710796.1	PREDICTED: Hydra vulgaris forkhead box protein P1-B-like (LOC100202406), transcript variant X3, mRNA	FoxP1	Forkhead
TRINITY_DN7386_c0_g1	t3617aep	Sc4wPfr_338.1.g31632.t1	-1.036	0	0	NA	XM_004207957.2	Hydra vulgaris Transcription factor HES-2 [Hydra vulgaris]	HyHes (Münder 2013)	ЬНІН
TRINITY_DN2411_c0_g1	t29291aep	Sc4wPfr_224.1.g33422.t1	-1.048	0	0	AXP19710.1	CDG69495.1	Hydra vulgaris Transcription factor Sp5, partial [Hydra vulgaris]	Sp5 (Vogg, 2019)	zf-C2H2
TRINITY_DN19967_c0_g1	t33622aep	Sc4wPfr_224.1.g33440.t1	-0.938	0	0	NA	QCF59210.1	homeobox transcription factor Otx1 [Hydra vulgaris]	OTX1B	Homeobox
TRINITY_DN14675_c0_g1	t5275aep	Sc4wPfr_390.g5621.t1	-1.705	0	0	NA	XP_002164986.2	PREDICTED: pituitary homeobox 1-like [Hydra vulgaris]	PITX1	Homeobox

Downregulated transcription factors that recovered by 6 hours post-treatment

Trinity ID	AEP ID	Gene Model	log2FC 0h	log2FC 3h	Log2FC 6h	Pubmed Hit	NCBI Accession	NCBI Description	Short Name	DNA Binding Domain
TRINITY_DN18625_c0_g1	t9145aep	Sc4wPfr_802.g11764.t1	-2.224	-2.070	0.000	NA	XP_004207988.1	PREDICTED: forkhead box protein I1c-like [Hydra vulgaris]	FOXI1	Forkhead
TRINITY_DN3947_c0_g1	t26993aep	Sc4wPfr_326.g15655.t1	-0.932	-1.103	0.000	NA	CDG68553.1	Hydra vulgaris Fez family zinc finger protein 2, partial [Hydra vulgaris]	FEZ2	zf-C2H2
TRINITY_DN5602_c0_g1	t23837aep	Sc4wPfr_362.g23666.t1	-1.659	-1.409	0.000	NA	XP_012563508.1	PREDICTED: transcription factor	SOX21B	HMG_box

								Sox-21-B-like [Hydra vulgaris]		
TRINITY_DN6990_c0_g1	t11335aep	Sc4wPfr_287.g9045.t1	-1.255	-0.753	0.000	NA	XP_002158636.1	PREDICTED: POU domain, class 4, transcription factor 2- like isoform X2 [Hydra vulgaris]	HyPOU4TF- 2 (Siebert, 2019)	Pou

Downregulated transcription factors that remained downregulated by 6 hours post-treatment

Downregulatea tra	anscripuo	n tactors that rem	amea o	ownre	guiatea	ny o nours po	st-treatment			
Trinity ID	AEP ID	Gene Model	log2FC 0h	log2FC 3h	Log2FC 6h	Pubmed Hit	NCBI Accession	NCBI Description	Short Name	DNA Binding Domain
TRINITY_DN3014_c0_g1	t16018aep	Sc4wPfr_439.g20769.t1	-0.816	-0.567	-0.735	NA	CDG67528.1	Hydra vulgaris Iroquois-class homeodomain protein IRX-2 [Hydra vulgaris]	IRX6-2	Homeobox
TRINITY_DN1167_c0_g1	t12948aep	Sc4wPfr_546.g25835.t1	-3.863	-3.103	-3.221	NA	CDG72033.1	Hydra vulgaris Forkhead box protein N1 [Hydra vulgaris]	FoxN4	Forkhead
TRINITY_DN20727_c0_g1	t11591aep	Sc4wPfr_319.g27294.t1	-2.000	-2.061	-1.572	NA	XP_002157355.1	PREDICTED: zinc finger protein 26-like [Hydra vulgaris]	Zinc finger protein 26 like	zf-C2H2
TRINITY_DN2447_c0_g1	t21636aep	Sc4wPfr_372.g27997.t1	-3.035	-2.765	-1.856	CAA75669	XP_002168027.1	prdl-b protein, partial [Hydra vulgaris]	Prdl-b (Gauchat, 1998)	Homeobox
TRINITY_DN10070_c0_g1	t10853aep	Sc4wPfr_147.g8607.t1	-1.060	-1.212	-0.852	NP_001296673.1	NM_001309744.1	PREDICTED: achaete- scute homolog 1a-like [Hydra vulgaris]	achaete- scute 1a- like	HLH

Upregulated transcription factors that recovered by 3 hours post-treatment

Opregulated transcription factors that recovered by 5 hours post-treatment										
Trinity ID	AEP ID	Gene Model	log2FC 0h	log2FC 3h	Log2FC 6h	Pubmed Hit	NCBI Accession	NCBI Description Sho		DNA Binding Domain
TRINITY_DN1855_c0_g1	t5966aep	Sc4wPfr_224.1.g33377.t3	1.192	0	0	NA	XP_012561111.1	PREDICTED: transcription factor kayak-like [Hydra vulgaris]	NA	bZIP

Upregulated transcription factors that recovered by 6 hours post-treatment

Trinity ID	AEP ID	Gene Model	log2FC 0h	log2FC 3h	Log2FC 6h	Pubmed Hit	NCBI Accession	NCBI Description	Short Name	DNA Binding Domain
TRINITY_DN39755_c0_g1	t14593aep	Sc4wPfr_547.1.g24983.t1	0.937	0.789	0	NA	XP_004205480.1	PREDICTED: zinc finger BED domain- containing protein 4- like [Hydra vulgaris]	NA	zf-BED

Table S3. NR-genes with 3 to 6 RPBJ-motifs in the promoter region

AEP-ID	Minimum distance from TS	Identity/conserved domains	RPBJ- frequency	Expression pattern		
t16456aep	100	CnAlx (Smith2000)	6	EC battery, EC head		
t2316aep	18	Putative sialic acid acetylcholine esterase	6	EN tentacle		
t29291aep	26	Sp5 (Vogg 2019)	6	EC, strong in head		
t15331aep	204	Secreted frizzled-related protein; Bert Hobmayer, Innsbruck, Austria, personal communication	5	EN foot		
t34122aep	19	Max-dimerisation domain, bHLH	5	EC		
t18488aep	47	Shk-domain, pred. toxin	5	Nb 4 through nb 8		
t19736aep	50	Ubiquitin ligase with RING and SH3	4	EC, EN		
t5275aep	21	PITX1, homeobox, Fig. S3	4	EN head		
t17828aep	18	aminopeptidase	4	Nb 4 through nb 8		
t20080aep	98	GPCR	4	Mature nematocytes		
t14454aep	187	Small secreted protein with glycine repeats	3	Nb 6		
t11622aep	354	uncharacterised	3	EN		
t20709aep	13	ZIC5, Zf C2H2-domain	3	neurons		
t28505aep	286	Uncharacterised with collagen binding sites	3	Nb 5		
t25509aep	84	uncharacterised	3	Mature nematocytes		
t25463aep	83	uncharacterised	3	Mature nematocytes		
t26247aep	173	Solute carrier family	3	Nb 4 through n b8		
t6693aep	14	Spry-domain and SOCS- box protein	3	Nb 6		
t23166aep	1470	uncharacterised	3	Mature nematocytes		
t25163aep	8	Helix rich domain	3	Nb 4 through nb		
t33622aep	114	OTX1B like, homeobox, Fig. S3	3	EC head		

3.3 Paper III: Notch signalling mediates between two pattern-forming processes during head regeneration in *Hydra*

Summary of paper III:

This study investigated head regeneration and the expression dynamics of head-related genes during the head regeneration process in *Hydra* following treatment with DAPT and iCRT14, a β-catenin/TCF binding inhibitor (Gonsalves, Klein et al. 2011). The findings indicated that regenerating *Hydra* treated with iCRT14 were able to reform the hypostome and regain organizer activity, unlike DAPT-treated regenerating polyps, which failed to regenerate the hypostome after decapitation. However, iCRT14 treatment completely abolished the regeneration of tentacle tissues. The analysis of gene expression dynamics further revealed that most *HyWnt* genes, including *HyWnt1*, *HyWnt7*, *HyWnt9/10c*, *HyWnt11*, and *HyWnt16*, were inhibited by both DAPT and iCRT14 treatments. Interestingly, *HyWnt3* was specifically blocked by DAPT but not by iCRT14. Conversely, the *HyAlx* gene, expressed at the tentacle boundary, was only partially blocked by DAPT but completely blocked by iCRT14 treatment. These findings suggest that *Hydra* head regeneration involves two distinct processes: hypostome regeneration, regulated primarily by the Notch signalling pathway, and tentacle regeneration, which is highly dependent on canonical Wnt/β-catenin signalling pathways.

Given the reported association between *HyWnt3* expression and organizer formation (Hobmayer, Rentzsch et al. 2000, Broun, Gee et al. 2005), this study highlights the importance of the Notch signalling pathway in maintaining the expression pattern of *HyWnt3* in the hypostome. Nevertheless, the mechanisms by which the Notch signalling pathway influences the expression of *HyWnt3* remain unclear.

To investigate this further, we hypothesized the presence of a *HyWnt3* inhibitor regulated by the Notch signalling pathway. As *HyKayak* was found to be upregulated after Notch inhibition (Moneer, Siebert et al. 2021). Furthermore, *HyKayak* is exclusively expressed in the ectodermal epithelial cells of the head/hypostome, tentacle, and body column regions (Siebert, Farrell et al. 2019). Therefore, we proposed that HyKayak could serve as a potential candidate for inhibiting *HyWnt3*.

To test this hypothesis, the *c-fos* inhibitor T5224 and *HyKayak*-shRNA knockdown were utilized to induce HyKayak loss-of-function in *Hydra*. Notably, both approaches led to a significant upregulation of *HyWnt3* expression, indicating that Hykayak can repress the expression of *HyWnt3*. However, direct evidence of a mechanistic link between HyKayak and *HyWnt3* is still lacking and requires further investigation in future studies.

Research Article









Notch signaling mediates between two pattern-forming processes during head regeneration in *Hydra*

Mona Steichele^{1,*}, Lara Sauermann^{1,*}, Qin Pan^{1,*}, Jasmin Moneer^{1,*}, Alexandra de la Porte¹, Martin Heß¹, Moritz Mercker², Catharina Strube¹, Heinrich Flaswinkel³, Marcell Jenewein¹, Angelika Böttger¹

Hydra head regeneration consists of hypostome/organizer and tentacle development, and involves Notch and Wnt/ β -catenin signaling. Notch inhibition blocks hypostome/organizer regeneration, but not the appearance of the tentacle tissue. β -Catenin inhibition blocks tentacle, but not hypostome/organizer regeneration. Gene expression analyses during head regeneration revealed the Notch-promoting expression of HyWnt3, HyBMP2/4, and the transcriptional repressor genes CnGsc, Sp5, and HyHes, while blocking HyBMP5/8b and the c-fos-related gene HyKayak. β -Catenin promotes the expression of the tentacle specification factor HyAlx, but not of HyWnt3. This suggests HyWnt3 and HyBMP4 as parts of a hypostome/organizer gene module, and BMP5/8, HyAlx, and β -catenin as parts of a tentacle gene module. Notch then functions as an inhibitor of tentacle production to allow regeneration of a hypostome/head organizer. HyKayak is a candidate target gene for HvNotch-induced repressor genes. Inhibiting HvKavak attenuated the expression of HvWnt3. Polyps of Craspedacusta do not have tentacles and thus after head removal only regenerate a hypostome structure. Notch signaling was not needed for head regeneration in Craspedacusta, corroborating the idea of its requirement during Hydra head regeneration to harmonize two co-operating pattern-forming processes.

DOI 10.26508/lsa.202403054 | Received 19 September 2024 | Revised 30 October 2024 | Accepted 30 October 2024 | Published online 12 November 2024

Introduction

The small freshwater polyp *Hydra* belongs to the pre-bilaterian phylum of Cnidaria and consists of a foot, a body column, and a head with a hypostome and a ring of tentacles. Asexual reproduction occurs by budding. Sexual reproduction takes place from fertilized eggs when male and female gametes are formed on the *Hydra* body column (reviewed by Steele [2012]).

Hydra polyps have the capacity for complete regeneration. After being cut into small tissue parts, they will regenerate a head and a foot accurately at the same position as before. This indicates that whole-body pattern information is conserved in the body column during the adult life of Hydra polyps (reviewed by Bode [2003]). Moreover, as observed in 1909 by Ethel Browne, specific Hydra tissues, after transplantation into a host polyp, have the capacity to recruit host tissue to form an ectopic head growing out into a whole new hydranth (Browne, 1909; MacWilliams, 1983). These tissues included "peristome at the base of tentacles," regenerating tips and early buds (according to Ethel Browne). By hypostome-contact grafts, it could be shown later that the tip of the hypostome had the same capability. Less "inductive" capacity was found in the tissue of the tentacle zone (Mutz, 1930; Broun & Bode, 2002). Embryonic amphibian tissue with such inductive capacity had been given the name "organizer" by Hans Spemann, and the region where this tissue was taken from was called "center of organization" (Spemann, 1924; Hamburger, 1969). The Hydra transplantation phenomena were then related to the "organizing" property of the transplanted embryonic tissue (Goetsch, 1926). The "organizer effect" entails a "harmonious interlocking of separate processes that makes up development," or a side-by-side development of structures independently of each other (Spemann, 1935). In addition to inducing the formation of such structures, the organizer must ensure their patterning (Anderson & Stern, 2016). Formation of new hydranths after transplantation of "organizer" tissue involves the side-by-side induction of the hypostome tissue and tentacle tissue. Moreover, it includes the establishment of a regularly organized ring of tentacles with the hypostome doming up in the middle. The function of the Hydra "center of organization" would then be to pattern hypostome/body column and tentacles and to allow for their harmonious re-formation after head removal.

There is an intriguing similarity in gene expression between the amphibian Spemann organizer and the *Hydra* head organizer (Ding et al, 2017). Spemann organizers induce a Wnt3-dependent anterior-posterior axis and a BMP-dependent dorsal-ventral axis

Correspondence: boettger@zi.biologie.uni-muenchen.de

Alexandra de la Porte's present address is Institute of Stem Cell Research, Helmholtz Center Munich, Neuherberg, Germany

¹Biocenter, Ludwig-Maximilians-University Munich, Munich, Germany ²Institute of Applied Mathematics, Heidelberg-University, Heidelberg, Germany ³Center for Molecular Biosystems (BioSysM), Ludwig-Maximilians-Universität München, Munich, Germany

^{*}Mona Steichele, Lara Sauermann, Qin Pan, and Jasmin Moneer contributed equally to this work



(Anderson & Stern, 2016). The Hydra gene HyWnt3 is strongly expressed at the hypostome, at the tip of regenerates after head removal, and at the tip of developing buds, all regions that had been indicated to possess inductive capacity in organizer experiments (Browne, 1909; Mutz, 1930; Broun & Bode, 2002). In addition, the transcriptional repressor goosecoid is expressed in dorsal blastopore lip cells of frog embryos and had originally been considered a universal organizer gene (Anderson & Stern, 2016). In the Hydra head, CnGsc, a goosecoid homolog, is prominently (not solely) expressed in head cells between the hypostome and the tentacle zone (Broun et al, 1999), and thus in the organizer tissue as defined by Ethel Browne.

Hydra has 11 identified Wnt genes, all of which are expressed in the head and/or tentacles. Of those, most are suggested to induce canonical Wnt signaling through nuclear translocation of β -catenin, whereas HyWnt5 and HyWnt8 have been shown to be associated with non-canonical Wnt signaling in the planar cell polarity pathway. In addition, most known mammalian BMP pathway genes have homologs in Hydra. These include Smad, HyBMP5/8b, and HyBMP2/4 (Hobmayer et al, 2001; Reinhardt et al, 2004; Lengfeld et al, 2009; Philipp et al, 2009; Watanabe et al, 2014). Wnt and BMP pathways have been demonstrated to play a role in Hydra regeneration ([Reddy et al, 2019; Reddy et al, 2020] and citations above). After head removal, the expression of Hyβ-catenin and HyTcf is up-regulated earliest, followed by local activation of Wnt genes. Among these, HyWnt3 and HyWnt11 appeared within 1.5 h after head removal, followed by HyWnt1, HyWnt9/10c, HyWnt16, and HyWnt7 (Hobmayer et al, 2001; Lengfeld et al, 2009; Philipp et al, 2009; Gufler et al, 2018; Tursch et al, 2022). Thus, HyWnt3 and HyWnt11 are swiftly induced by injuries. When their activity is sustained, organizers can be formed, which induce ectopic heads when the original organizer tissue (the head) is removed (Cazet et al, 2021; Tursch et al, 2022). Recently, a Wnt3/ β -catenin/Sp5 feedback loop was suggested to be involved in Hydra head patterning (Münder et al, 2013; Vogg et al, 2019; Moneer et al, 2021).

The expression patterns of Wnt and BMP genes can be interpreted as an indication of tentacles, buds, and the main body axis of the polyps being repetitive structures expressing Wnt genes at the apical end and BMP5/8b at the basal end (Meinhardt, 2012; Pan et al, 2024). These could set up opposing signaling gradients to pattern the Hydra body axis and possibly also the bud and tentacle axes. The bud expresses HyWnt2 and later HyWnt3 at the tip and BMP5/8b at the base. The tentacles also express HyBMP5/8b at the base and HyWnt5 at the tip. As Hans Meinhard pointed out, in evolutionary terms the tentacles may therefore be considered as colonialized buds (Meinhardt, 2012). In any case, tentacles and hypostome can be interpreted as independent structures.

Our previous investigations had revealed that the Notch pathway was instrumental for head regeneration and organizer formation by supporting the expression of a strong HyWnt3 signal in regenerating the head tissue. Notch inhibition with the presenilin inhibitor DAPT or the NICD inhibitor SAHM-1 prevented head regeneration and blocked HyWnt3 expression in regenerates, while not preventing the expression of the tentacle boundary gene HyAlx and the tentacle metalloprotease gene HMMP. However, the latter did not obtain their correct expression patterns, and thus, proper tentacles were not formed. Similar experiments using a transgenic Hydra strain expressing an HvNotch-hairpin RNA confirmed the regeneration phenotypes seen with pharmacological inhibitors (Pan et al, 2024). Strikingly, transplantation experiments had revealed that the DAPT-treated regenerating head tissue had lost the capacity to form an organizer (Münder et al, 2010; Münder et al, 2013).

Here, we have further investigated the role of Notch signaling during apical head regeneration. We compared the effect of the Notch inhibitor DAPT with the effect of the β -catenin inhibitor iCRT14 (Gonsalves et al, 2011; Gufler et al, 2018). Although, similar to DAPT, iCRT14-treated animals did not regenerate complete heads, HyWnt3 expression was not blocked and a normal hypostome was regenerated. Accordingly, iCRT14-treated-in contrast to DAPTtreated—regenerating tips retained the ability to form a second axis when transplanted into the body column of an untreated host animal. We also investigated the effect of these inhibitors on the gene expression dynamics of HyWnt and HyBMP genes and transcriptional regulators Hydra Sp5, HyAlx, HyHes, and CnGsc during Hydra head regeneration by qRT-PCR. Our results clearly reveal that the sustained expression of HyWnt3 and hypostome/organizer formation after head removal are controlled by Notch signaling, and not by β -catenin activity. In contrast, the expression of the tentacle specification gene HyAlx and formation of tentacles are dependent on β -catenin activity. In addition, we noted that Notch inhibition increased the expression of HyBMP5/8b, a gene primarily expressed at tentacle boundaries, while blocking the expression of HyBMP2/4, a gene expressed in the head and body column. Moreover, Notch was required for inhibition of the c-fos homolog HyKayak, which we suggest to be a negative regulator of HyWnt3 and a likely candidate for a target of Notch-regulated transcriptional repressors.

We conclude that Notch activity functions in head regeneration to mediate between two independent patterning systems comprising hypostome and tentacle regeneration. In apical regenerates, this probably works through inhibition of the tentacle system in a spatially and temporarily regulated manner. It involves Notchmediated inhibition of *HyBMP5/8b* and direct or indirect activation of HyWnt3 and HyBMP2/4 expression.

Results

Hypostome formation in iCRT14-treated, but not in DAPT-treated, regenerates

Hydra polyps treated either with iCRT14, as described by Gufler et al [2018]; Cazet et al [2021], or with the Notch inhibitor DAPT, as described by Münder et al [2013], fail to regenerate a complete head after decapitation. DAPT blocks Notch intramembrane proteolysis regulated by presenilin and prevents NICD translocation to the nucleus, thus phenocopying loss of Notch function in several organisms including Hydra (Dovey et al, 2001; Geling et al, 2002; Micchelli et al, 2003; Käsbauer et al, 2007; Pan et al, 2024). iCRT14 inhibits the interaction of nuclear β -catenin with TCF in mammalian cell lines and in Hydra (Gonsalves et al, 2011; Gufler et al, 2018).

First, we treated Hydra polyps with 5 µM iCRT14 for 48 h after head removal, and observed that they did not regenerate their heads



during the time of treatment, whereas control animals, treated with 1% DMSO (the solvent for iCRT14 and DAPT), clearly showed regularly spaced tentacle buds at this time point (Fig 1A). iCRT14 and DMSO were then replaced with normal *Hydra* medium. Control animals regenerated heads with long tentacles 24 h later (72 h); however, iCRT14-treated animals did still not show tentacle buds up to 48 h after iCRT14 removal (96 h). For comparison, treatment of head regenerates with DAPT had revealed in our previous study that proper heads could also not be regenerated during the time of treatment. When DAPT was then removed from the medium, irregular heads, dominated by the tentacle tissue, developed in 20% of regenerates (Münder et al, 2013).

To further inspect the morphology of head regenerates treated with DAPT or iCRT14, semithin sections were prepared 48 h after head removal and histologically stained with the Richardson tissue stain. Among other structures, this dye stained the mesoglea dark blue. Fig 1B shows middle sections of polyps. The mesoglea is emphasized by red lines. The hypostome of the polyp can be recognized by a "gap" in the mesoglea. After head removal, the hypostome is regenerated in polyps treated with DMSO and iCRT14, but not with DAPT. Head regeneration of the "watermelon" AEP strain of Hydra vulgaris polyps showed a similar result (Fig 1C). These polyps express GFP in the whole of the ectoderm and red fluorescent protein (dsRed) in the whole of the endoderm (polyps were a kind gift from Rob Steele, UC Irvine). Fig 1C shows optical middle sections obtained by laser scanning microscopy clearly representing a mouth opening. Again, hypostome morphology is recovered in animals after regeneration in DMSO and iCRT14, but not in DAPT. Quantification of regenerated hypostomes and tentacles in DAPT- and iCRT14-treated regenerates in comparison with control animals revealed that 70% of iCRT14-treated animals regenerated an intact hypostome with a detectable mouth opening, whereas tentacles were not formed (Fig 1E). In contrast, DAPTtreated animals did not regenerate a mouth opening, and in 25% of regenerates, aberrant tentacles were observed at the tips of regenerates, as previously described (Münder et al, 2013). The apparent regeneration of a hypostomal mouth opening in iCRT14treated polyps prompted us to perform fluorescence in situ hybridization for HyWnt3 in such regenerates. As shown in Fig 1D, hypostomal *HyWnt3* expression was evident in control regenerates and showed a very similar pattern in regenerates treated with iCRT14. This was different from DAPT-treated regenerates, which do not express HyWnt3 (Münder et al, 2013).

Organizer formation observed in iCRT14-treated regenerates

Previously, we had shown that DAPT-treated regenerating *Hydra* heads lacked organizer activity, as they did not induce the formation of ectopic hydranths when transplanted into the body column of a host animal (Münder et al, 2013). This was in accordance with the loss of *HyWnt3* expression in Notch-inhibited regenerates. We now asked the question whether iCRT14-treated head regenerates would retain organizer properties, as they do express *HyWnt3*. We therefore transplanted regenerating *Hydra* heads (upper 20% of polyps) 24 h after head removal and treatment with iCRT14 or DMSO (for control) into the body column of Evans blue–stained host animals (Fig 2A). Fig 2B shows that 80%

of control regenerates formed ectopic hydranths after transplantation into the body column of the host. Notably, 80% of iCRT14-treated regenerates were also able to form ectopic hydranths and most of them recruited host tissue, indicating organizer activity. This is in accordance with their expression of HyWnt3. From these and previous data, we conclude (1) organizer activity correlates with the presence of HyWnt3 expression; (2) activation of HyWnt3 during the regeneration process is not dependent on β -catenin transcriptional activity; and (3) HyWnt3 must signal via a non-canonical Wnt signaling pathway in iCRT14-treated regenerates.

Comparison of gene expression dynamics during *Hydra* head regeneration in DAPT-treated and iCRT14-treated animals

In order to follow the recovery of head-specific gene expression after head removal, we conducted qRT-PCR analyses from tissue that was left to regenerate. We compared gene expression in regenerates treated with DAPT or with iCRT14, both compounds were administered with 1% DMSO in *Hydra*- medium (HM). For control, the polyps were treated with 1% DMSO in HM without additional compounds.

Effect of Notch inhibition on gene expression dynamics during head regeneration in Hydra

In a previous transcriptome analysis of DAPT-treated *Hydra* polyps, besides *HyHes*, the tentacle boundary gene *HyAlx*, the "organizer" gene *CnGsc*, and the *Hydra Sp5* gene had been suggested to be potential direct Notch target genes (Moneer et al, 2021). The same analysis had revealed that the *fos*-related transcription factor gene *HyKayak* was up-regulated when Notch signaling was blocked.

Here, we performed qRT-PCR analysis to compare gene expression dynamics of these genes during head regeneration 0, 8, 24, 36, and 48 h after head removal. Animals were either treated with 30 μ M DAPT in 1% DMSO, or with 1% DMSO as a control. Time point 0 was measured immediately after head removal. The results of these analyses revealed that HyHes expression was clearly inhibited by DAPT during the first 36 h after head removal (Fig 3A), confirming previously published data that had indicated HyHes as a direct target for NICD (Münder et al, 2010). HyAlx expression levels were slightly up-regulated after 24 h, but later partially inhibited by DAPT (Fig 3B). CnGsc expression under DAPT treatment initially (8 h) was comparable to control levels, but then, it was strongly inhibited (Fig 3C). This corresponds to the observed absence of organizer activity in regenerating Hydra tips (Münder et al, 2013). Interestingly, a similar result was seen for HySp5 expression, which was also normal at 8 h but was then inhibited by DAPT at later time points (Fig 3D). HyKayak, while not affected after 8 h, was strongly overexpressed between 24 and 36 h of regeneration in DAPT-treated polyps in comparison with control regenerates (Fig 3E). However, at the 48-h time point expression appeared normal.

In addition, we tested the expression dynamics of the two *BMP* homologs described in *Hydra*, *HyBMP5/8b* and *HyBMP2/4*. They have mutually exclusive expression patterns in the head. *BMP2/4* is expressed in endodermal and ectodermal epithelial cells of the head, whereas *BMP5/8b* expression is restricted to the base of

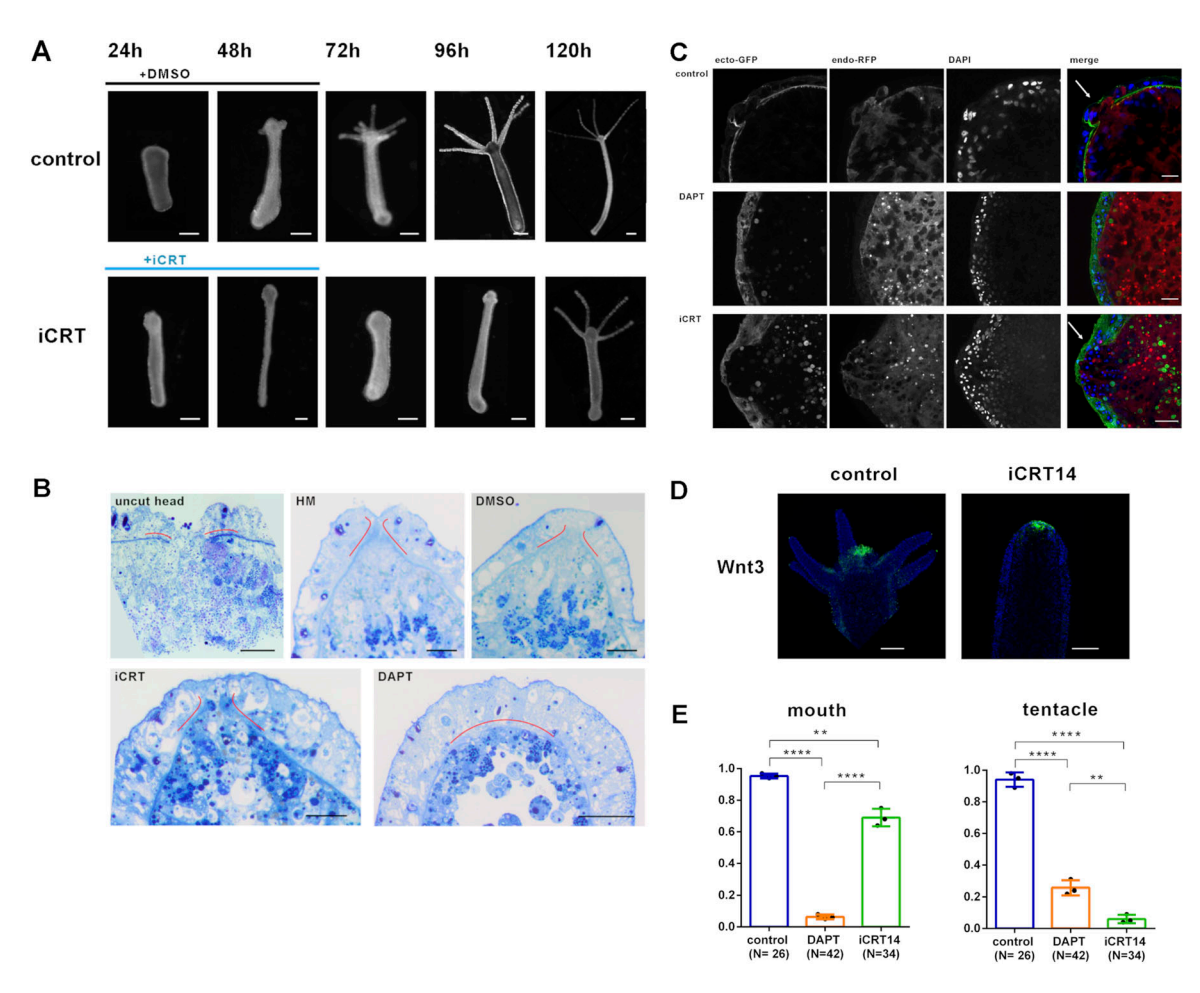


Figure 1. Regeneration of Hydra head structures.

(A) Head regeneration progress of *Hydra* polyps at indicated time points after head removal in control or iCRT14 medium. (B) Semithin sections covering the hypostome region of *Hydra* polyps after the Richardson staining: untreated polyp (uncut head); polyps 48 h after head removal and regeneration in *Hydra* medium (HM); and HM with DMSO (control), DAPT, or iCRT14. The mesoglea appears as a dark blue line, and red lines are added to highlight the mesoglea at the hypostome region. Scale bar: 20 μm. (C) Confocal stack images covering the regenerated hypostome region of *Hydra* polyps of strain AEP "watermelon" 48 h after head removal and regeneration in HM with DMSO (control), DAPT, or iCRT14; GFP present in ectodermal cells, dsRed present in endodermal cells, and DAPI-DNA stain are imaged as indicated. Right-hand panels show merged images. White arrows indicate hypostomal opening in iCRT14-treated and control animals, but not in DAPT-treated polyps. Scale bar: 10 μm. (D) Fluorescence in situ hybridization for *HyWnt3* (green) expression in polyps 48 h after head removal and regeneration in iCRT14 or in DMSO control, as indicated. Scale bar: 100 μm, DAPI in blue. (E) Quantification of regeneration of *Hydra* head structures: mouth and tentacles, 48 h after head removal and regeneration in DMSO control, DAPT, and iCRT14. Data are shown as the mean ± SEM, *P = 0.05, **P = 0.01, ****P = 0.0001.

tentacles and is not found in apical head cells (Reinhardt et al, 2004; Watanabe et al, 2014; Siebert et al, 2019). Interestingly, the two *BMP* genes were conversely affected by Notch inhibition. *HyBMP2/4* expression was blocked with DAPT beginning at 24 h of regeneration (Fig 3F). In contrast, *HyBMP5/8b* expression was drastically increased (Fig 3G).

We had previously shown by in situ hybridization that *HyWnt3* is not expressed in DAPT-treated head regenerates (Münder et al, 2013). This was confirmed now by qRT-PCR measurements, which revealed that *HyWnt3* expression was comparable to the control group 8 h after head removal. However, after this time point, its expression was strongly inhibited by DAPT and almost completely lost after 36 and 48 h (Fig 3H). Eventually, we analyzed most of the *Wnt* genes suggested to engage in canonical Wnt signaling, including *HyWnt1*, *HyWnt7*, *HyWnt9*/10c, *HyWnt11*, and *HyWnt16* (Lengfeld et al,

2009). In the presence of DAPT, these genes all exhibited similar expression levels to the control group 8 h after head removal, but between 24 and 48 h, the expression of *HyWnt1*, *HyWnt7*, *HyWnt9/10*, and *HyWnt16* declined to almost zero (Fig 3I–M). As an exception, *HyWnt11* was only partially inhibited and even appeared up-regulated after 48 h (Fig 3L).

In summary, qRT–PCR analyses showed that Notch signaling during Hydra head regeneration is necessary for activating all HyWnt genes, which are expressed in the Hydra head region and implicated in canonical Wnt signaling. Notch is also necessary for activation of the expression of BMP2/4, a gene expressed in the Hydra head and body column. Moreover, Notch is contributing to the expression of transcriptional repressor genes, HyHes and CnGsc. In contrast, HyBMP5/8b and HyKayak seem to be subject to inhibition by Notch signaling. HyAlx, although previously identified as a Notch target gene, is only partially inhibited by DAPT during head regeneration.

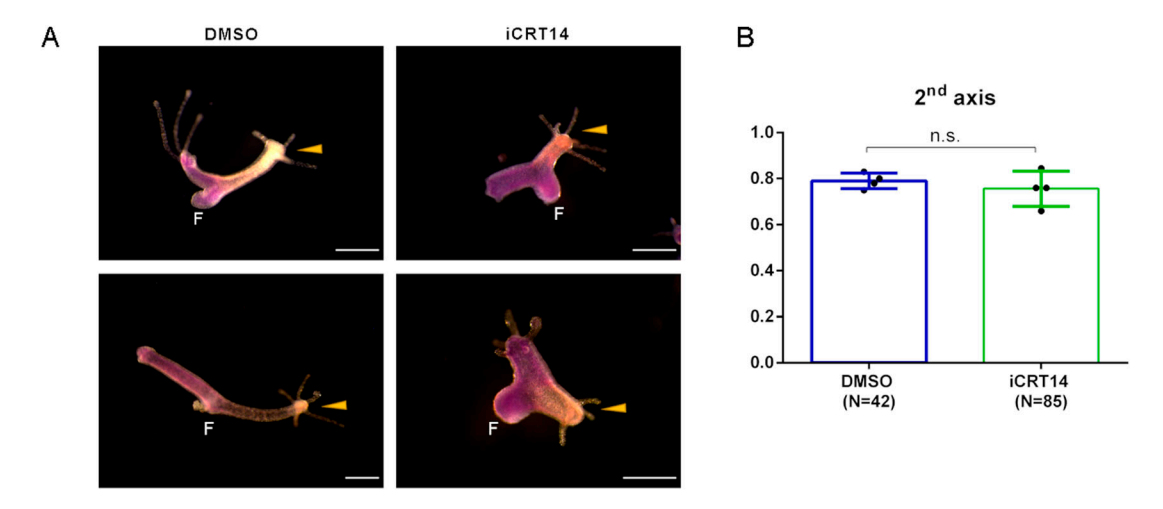


Figure 2. Organizer activity of the regenerating *Hydra* head tissue.

The tissue from the regenerating tip of polyps 24 h after head removal in HM with DMSO (control), or iCRT14 was transplanted into the middle of blue host polyps stained with Evans blue. (A) Microscopic images were taken 48 h after transplantation. Newly formed secondary axes are indicated by yellow arrows. The transplanted tissue appears orange, the host tissue appears blue, and feet are indicated by F. (B) Percentage of transplants forming new axes in HM with DMSO (control), or iCRT14; differences are not significant (n.s.).

Effect of β -catenin inhibition on gene expression dynamics during head regeneration in Hydra

Next, following the same procedure as described for DAPT, we compared the gene expression dynamics of iCRT14-treated regenerates with control regenerates. We found that the expression of the Notch target gene HyHes remained similar to control regenerates up to 24 h, but then was attenuated (Fig 4A), possibly because of the failure of tentacle boundary formation, the tissue where HyHes is strongly expressed. HyAlx expression was completely abolished by iCRT14, consistent with the observation that iCRT14-treated head regenerates did not regenerate any tentacles (Fig 4B). Furthermore, we found that *CnGsc* levels in iCRT14-treated regenerates remained similar to control regenerates up to 24 h, but reached only half of the control levels after 48 h, similar to HyHes (Fig 4C). Sp5 did not significantly respond to iCRT14 treatment (Fig 4D). The expression of HyKayak was decreased at 8 h after head removal in the presence of iCRT14, came back to normal after 36 h, and was suddenly increased after 48 h (Fig 4E), correlating with inhibition of the HyHes repressor. There were no significant changes in the expression dynamics of HyBMP2/4 and HyBMP5/8b between iCRT14-treated regenerates and controls (Fig 4F and G).

Confirming FISH images shown in Fig 1D, *HyWnt3* was not inhibited by iCRT14 during head regeneration; it even appeared slightly up-regulated at the 8-h time point (Fig 4H). In contrast to *HyWnt3*, the expression of all other canonical *HyWnt* genes was inhibited by iCRT14 during head regeneration. *HyWnt1*, *HyWnt7*, and *HyWnt16* were inhibited throughout the whole regeneration period (Fig 4I, J, and M). *HyWnt9/10c* and *HyWnt11* were blocked up to 36 h, but their expression levels returned to control values at 48 h (Fig 4K and L).

In summary, qRT-PCR analyses show that β -catenin transcriptional activity is not required for the expression of *HyWnt3* during head regeneration. However, it is involved in up-regulating the canonical *Wnt* genes *HyWnt1*, *HyWnt7*, *HyWnt9/10*, *HyWnt11*, and *HyWnt16*. Moreover, *HyAlx* expression strongly depends on

 β -catenin activity. The expression of both *HyHes* and *CnGsc* seems strengthened by β -catenin during later regeneration stages, when β -catenin also seems to inhibit *HyKayak* expression. These effects on gene expression may be due to the failure of tentacle development in iCRT14-treated animals. In contrast, *BMP2/4*, *BMP5/8*, and *Sp5* do not appear to be regulated by β -catenin during head regeneration.

From these analyses, we conclude (1) Notch signaling is responsible for the sustained expression of HyWnt3 and all canonical HyWnt genes during head regeneration. In addition, it is required for the expression of BMP2/4 (Broun et al, 1999) and the suggested Hydra organizer gene CnGsc, supporting our previous experiments where DAPT-treated regenerating head tissue did not develop organizer activity (Münder et al, 2013). (2) Notch activity is required for inhibiting HyKayak and HyBMP5/8b gene expression during regeneration, which coincides with DAPT causing down-regulation of the transcriptional repressor and Notch target gene HyHes. (3) β -Catenin transcriptional activity is not necessary to express HyWnt3, acquire organizer activity, and form a new hypostome after head removal. However, β -catenin-dependent transcription is indispensable to express HyAlx and form tentacles.

HyKayak

HyWnt3, albeit inhibited by DAPT specifically during head regeneration, had so far not been indicated as a potential target for Notch-mediated gene activation in Hydra (Münder et al, 2013; Moneer et al, 2021). By analyzing the HyWnt3 promoter region, Nakamura et al found proximal elements similar to Drosophila Su(H) and RBPJ sites (-155 to -143 [Nakamura et al, 2011]). Notch could therefore directly activate Wnt3 expression. However, several repressor genes are Notch-regulated (Moneer et al, 2021). We thus considered the possibility that a repressor of HyWnt3 could be inhibited by Notch signaling, especially at the tip of regenerating heads.

Life Science Alliance

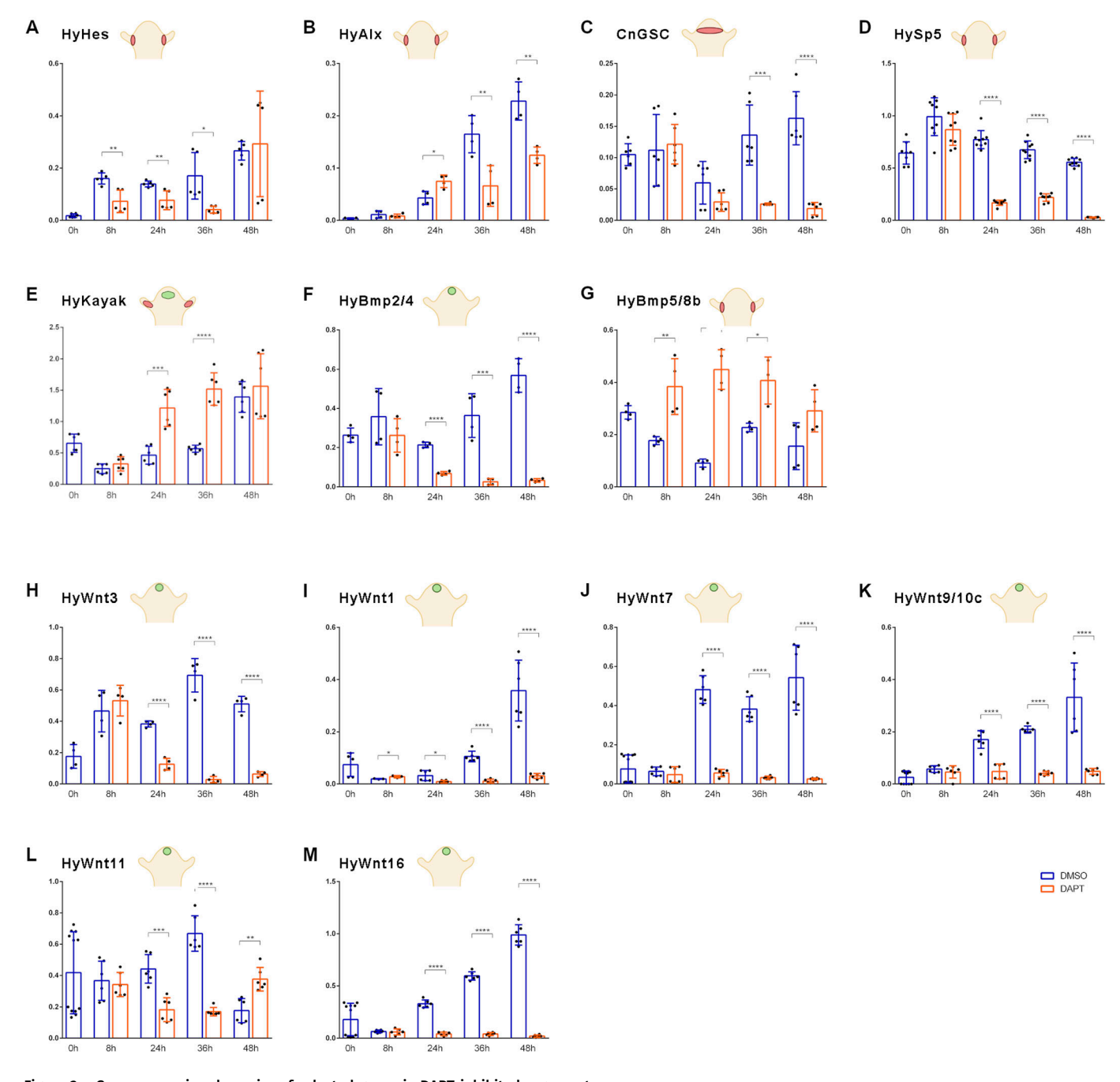


Figure 3. Gene expression dynamics of selected genes in DAPT-inhibited regenerates.

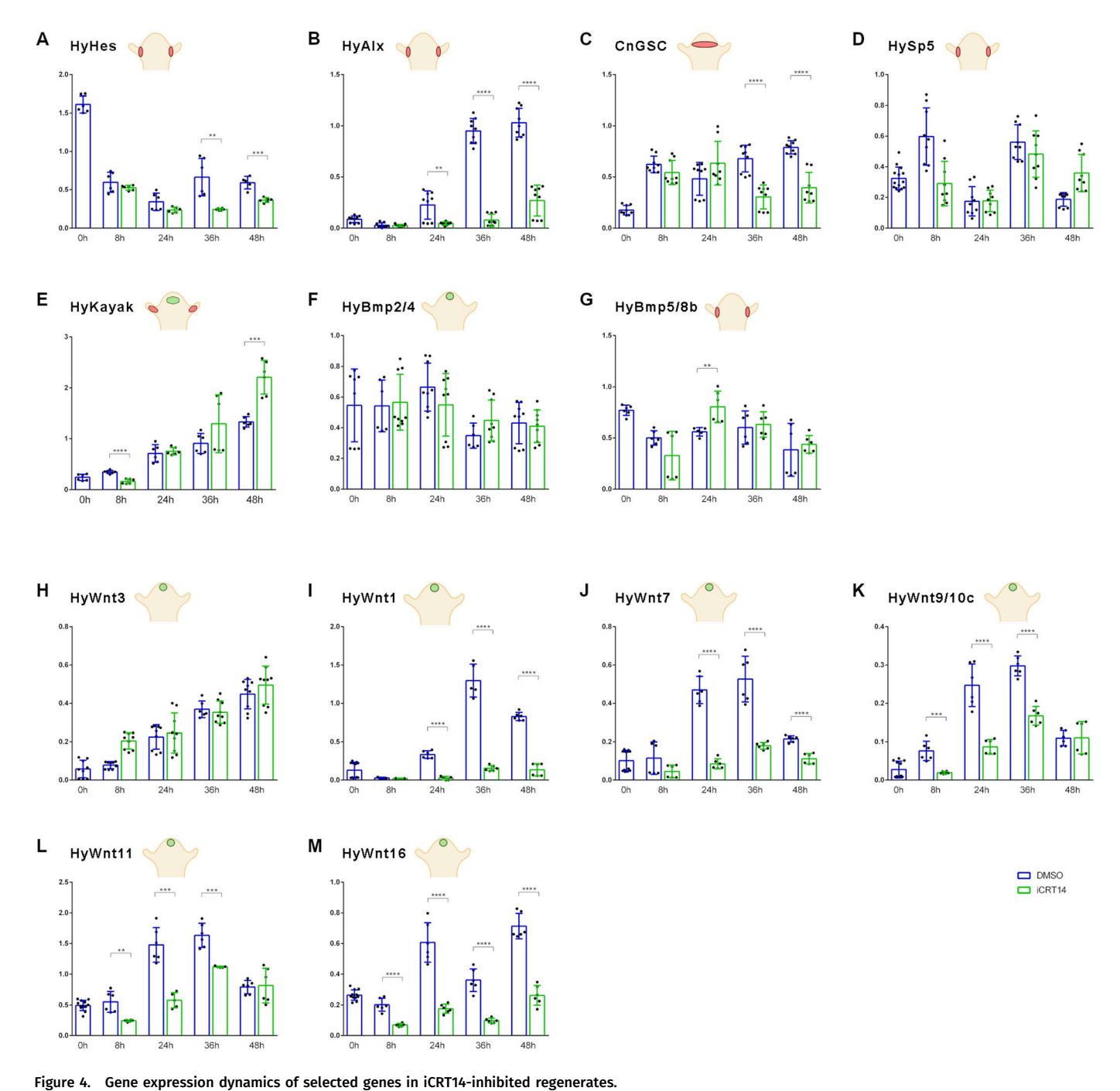
(A, B, C, D, E, F, G) qRT-PCR measurements quantifying the gene expression of (A) HyHes, (B) HyAlx, (C) goosecoid, (D) Sp5, (E) HyKayak, (F) BMP2/4, and (G) BMP5/8b. (H, I, J, K, L, M) HyWnt3, HyWnt1, HyWnt7, HyWnt9/10c, HyWnt11, and HyWnt16 during 48 h of Hydra head regeneration in HM with DAPT (orange) or DMSO control (blue). Hydra cartoons indicate gene expression patterns according to published in situ hybridization data and single-cell sequencing atlas (Broun et al, 1999; Hobmayer et al, 2000; Smith et al, 2000; Reinhardt et al, 2004; Lengfeld et al, 2009; Münder et al, 2010; Watanabe et al, 2014; Siebert et al, 2019; Vogg et al, 2019); Relative normalized expression was calculated against the housekeeping genes GAPDH, RPL13, EF1alpha, and PPIB. Regeneration time is shown on x-axes; t = 0 refers to animals immediately after the head was removed. Data are shown as the mean ± SEM, *P = 0.01, ***P = 0.001, ****P = 0.0001.

According to our previous report, the *Hydra* fos homolog *HyKayak* (t5966aep) was up-regulated after Notch inhibition with DAPT (Moneer et al, 2021). This suggests that *HyKayak* may serve as a potential target gene for Notch-regulated repressors including *HyHes* and *CnGsc*, and in this way, *HyKayak* may be

inhibited when these repressors are activated by Notch signaling.

Analysis of the domain structure and sequence comparison of *HyKayak* with *fos* and *jun* sequences from *Aurelia aurita*, *Stylophora pistillata*, *Caenorhabditis*, *Drosophila*, mouse, and human revealed

Life Science Alliance



(A, B, C, D, E, F, G) qRT-PCR measurements quantifying the gene expression of (A) HyHes, (B) HyAlx, (C) goosecoid, (D) Sp5, (E) HyKayak, (F) BMP2/4, and (G) BMP5/8b. (H, I, J, K, L, M) HyWnt3, HyWnt1, HyWnt7, HyWnt9/10c, HyWnt11, and HyWnt16 during 48 h of Hydra head regeneration in iCRT14 (green) or DMSO for control (blue). Hydra cartoons indicate gene expression patterns according to published in situ hybridization data and single-cell sequencing atlas (Broun et al, 1999; Hobmayer et al, 2000; Smith et al, 2000; Reinhardt et al, 2004; Lengfeld et al, 2009; Münder et al, 2010; Watanabe et al, 2014; Siebert et al, 2019); relative normalized expression was related to the housekeeping genes GAPDH, RPL13, EFTalpha, and PPIB. Regeneration time is shown on x-axes; t = 0 refers to animals immediately after the head was removed. Data are shown as the mean ± SEM, *P = 0.05, **P = 0.01, ***P = 0.001, ****P = 0.0001.

a strong conservation of the bZIP domain (basic leucine zipper domain), which is responsible for DNA binding and dimerization (Fig S1A and B). Phylogenetic analysis showed that *HyKayak* is related to *c-fos* sequences of various species including *Hydra* (Fig S1C). *HyKayak* is expressed in ectodermal cells of the *Hydra* head,

tentacles, and body column, excluding the basal disk (Fig S1D) (Siebert et al, 2019). A second fos gene described by Cazet et al [2021] is expressed in epithelial cells and gland cells (referred to as fos_Cazet). In addition, we identified two transcripts encoding Jun-related proteins, HyJun_nem (t17964aep) expressed

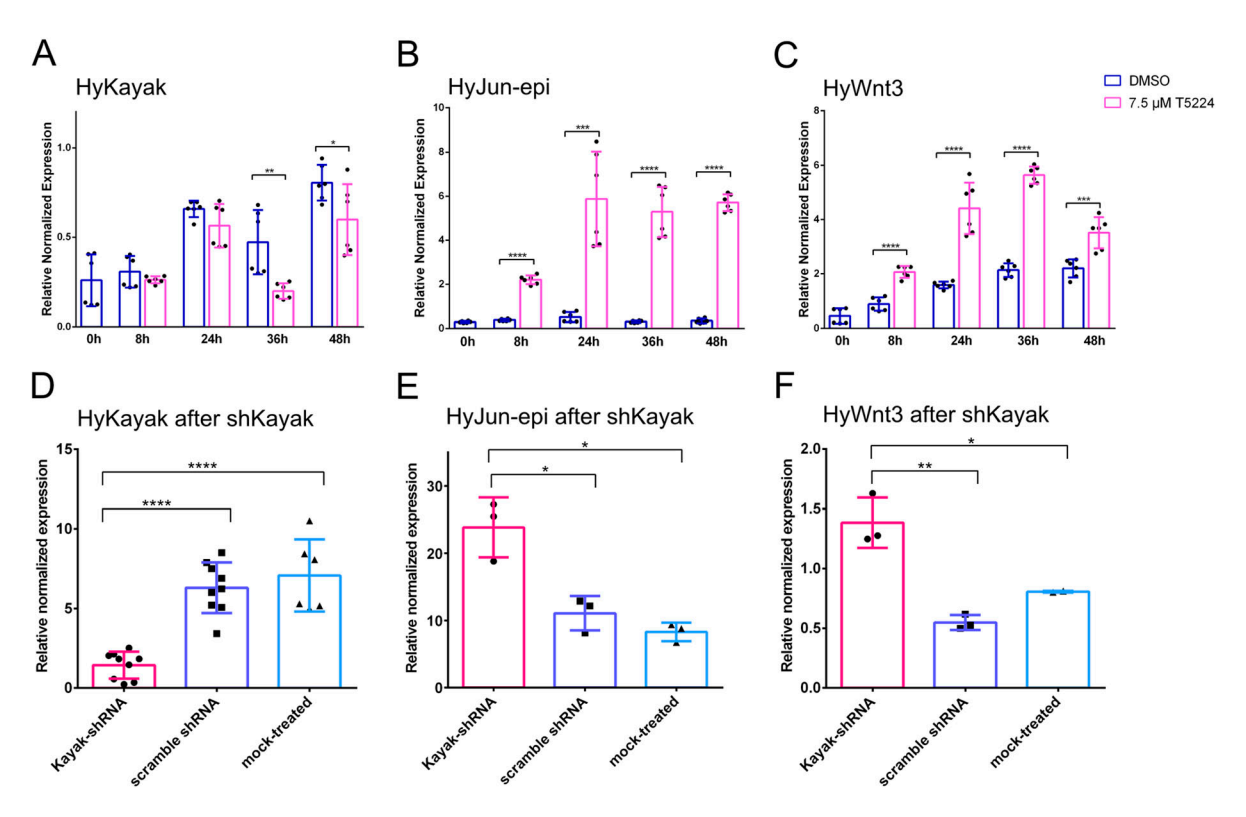


Figure 5. Gene expression dynamics of selected genes in T5224-inhibited regenerates corresponds to gene expression in kayak knockdown polyps. (A, B, C) qRT–PCR measurements quantifying the expression of (A) HyKayak, (B) HyJun_epi, and (C) HyWnt3 for 48 h after head removal in HM with DMSO serving as a control (blue) and HM with 7.5 μM T5224 for inhibition of Fos/AP1 activity (pink). (D, E, F) qRT–PCR measurements quantifying the expression of (D) HyKayak, (E) HyJun-epi, and (F) HyWnt3 after knockdown of HyKayak by shRNA (pink), compared to control knockdown with scramble shRNA (dark blue) and mock knockdown control (light blue). Relative normalized expression was related to the housekeeping genes GAPDH, EF1alpha, and PPIB. Regeneration time is shown on x-axes; t = 0 refers to animals immediately after the head was removed. Data are shown as the mean ± SEM, *P = 0.05, **P = 0.001, ***P = 0.001, ****P = 0.0001.

in nematoblasts 3–5 and HyJun_epi (t19405aep) expressed in all cells, with especially high levels in epithelial cells (Fig S1D). By SDS–PAGE of *Hydra* lysates and staining with anti-*HyKayak* antibody, we found that the *HyKayak* protein remained in the pellet fraction (Fig S1E-a) and only a small percentage could be solubilized after treatment with DNase (Fig S1E-b), suggesting that *HyKayak* is strongly associated with DNA and lending support to its suggested role as a DNA binding protein.

Fos proteins interact with Jun proteins (also bZIP domain proteins) to form the transcriptional regulation complex AP-1 (activator protein 1) (Karin et al, 1997). To test such interactions for the *Hydra* proteins, we performed immunoprecipitation of HyKayak and HyJun_epi-proteins expressed in HEK293T cells. This revealed that HyKayak did not interact with itself, but strongly interacted with the HyJun_epi protein (Fig S2). To investigate the function of HyKayak/AP-1 in *Hydra* head regeneration, we used the Fos/jun inhibitor T5224 to block DNA binding activities of Fos/Jun complexes (Xiong et al, 2022), and analyzed gene expression and phenotypes during *Hydra* head regeneration. This revealed a mild inhibition of *HyKayak* expression in contrast to a strong up-regulation of *HyJun* (Fig 5A and B). In addition, we discovered that *HyWnt3* expression was strongly up-regulated by T5224 (Fig 5C).

To confirm the specificity of the T5224 effect, we knocked down *HyKayak* using shRNA directed against *HyKayak*. We achieved *HyKayak* knockdown by ca. 80% in comparison with control polyps

either mock-treated or treated with scrambled control shRNA (Fig 5D). Moreover, *Kayak* knockdown led to the up-regulation of *HyJun*, consistent with the effects of T5224 treatment (Fig 5E). Importantly, knockdown of *HyKayak* induced an up-regulation of *HyWnt3* (Fig 5F). From these data, we conclude that (1) HyKayak attenuates the expression of *HyWnt3*; (2) HyKayak may work within the AP-1 complex together with Jun-epi; and (3) Notch signaling may block the inhibitory activity of HyKayak on *HyWnt3* by activating repressor genes. With DAPT, HyKayak remains active and inhibits the sustained expression of *HyWnt3* at later stages of head regeneration.

Regeneration of Craspedacusta polyps

Our data dissect the regeneration of Hydra heads into two processes, formation of the hypostome and head and formation of tentacles. For hypostome formation, HyWnt3 is needed, but β -catenin transcriptional activity is dispensable. Notch signaling then appears to be responsible to "organize" these two morphogenetic processes. To test this hypothesis, we asked how the inhibition of Notch signaling might affect regeneration of polyps with a simpler, one-component head. We used polyps of the freshwater hydrozoan Craspedacusta sowerbii. They have a mouth opening that is surrounded by epithelial cells carrying nematocytes, but they do not possess tentacles (Ramos et al, 2017).

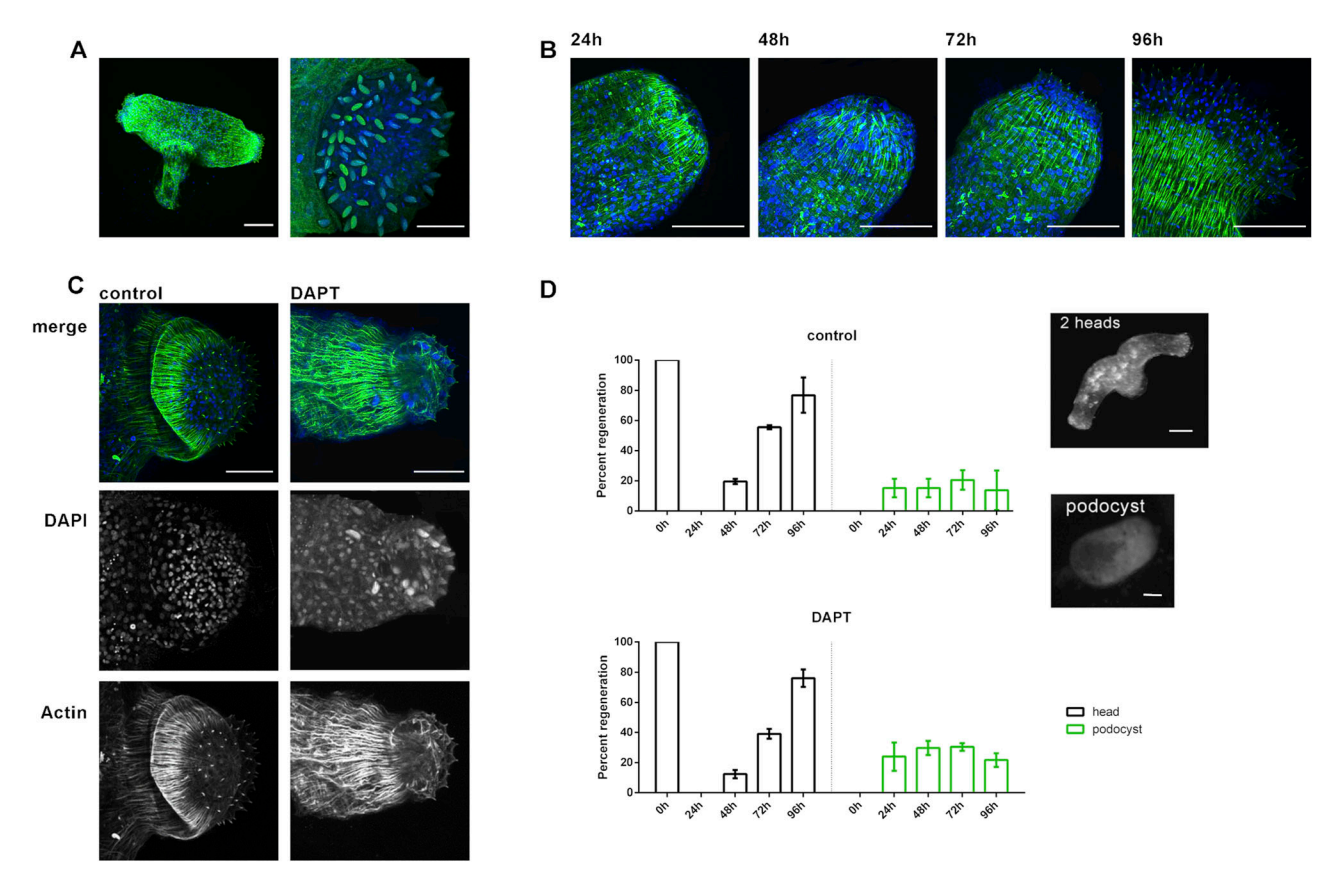


Figure 6. Head regeneration of *Craspedacusta* polyps.
(A) *Craspedacusta* colony with two animals sharing one foot. Scale bar: 100 μm. Magnification of the polyp head with nematocytes surrounding the hypostome. Scale bar: 50 μm. Nematocyte capsules stained with DAPI (green). (B) Regeneration of *Craspedacusta* polyps at 24, 48, 72, and 96 h after head removal with reappearing nematocytes and actin fibers. Scale bar: 50 μm. (C) Regenerated heads 96 h after head removal in HM with DMSO (control) or DAPT as indicated. Scale bar: 50 μm. Actin fibers are shown in green after staining with FITC-phalloidin, and nuclei are shown in blue after staining with DAPI. (D) Percentage of *Craspedacusta* polyps showing normal regeneration with 1, 2, or 3 heads (black) or "podocyst" form (green) at indicated time points after head removal. Representative images of *Craspedacusta* polyps showing a colony with two heads (upper panel) and a podocyst (lower panel). Scale bar: 200 μm.

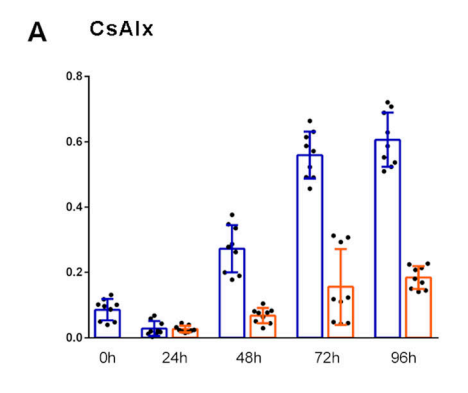
Craspedacusta polyps are shown in Fig 6A. They often occur as mini-colonies with one foot carrying two polyps. Actin fibers are running along the polyp's body column and form a ring where the two polyps separate just above the foot. Actin cushions carrying nematocysts are visible and indicate the positions of capsules along the body column and in a ring surrounding the mouth opening (Fig 6A and B). Additional capsule staining with DAPI (Szczepanek et al, 2002) very clearly reveals the pattern of nematocysts in the head (Fig 6B). When we removed the heads of the polyps, most of them fully regenerated within 96 h (Fig 6B). Some retracted into a podocyst (the "dauerstadium") (Fig 6D). Polyps treated with DMSO or DAPT also completed head regeneration after 96 h (Fig 6C). Quantification of Craspedacusta development after head removal revealed that the similar numbers of proper head regeneration and podocyst formation occurred (Fig 6D). This indicated that Notch signaling was not required for head regeneration in Craspedacusta polyps.

To confirm that DAPT was taken up by the polyps even in the absence of a visible regeneration phenotype, we investigated the effect of the drug under regeneration conditions on the expression of some possible Notch target genes. We choose

homologs of *HyAlx* and *HySp5*, both genes had been identified as Notch target genes in *Hydra* (Moneer et al, 2021), and a homolog of *NOWA*, a gene encoding a protein of the outer nematocyte capsule wall (Figs S3, S4, S5, and S6). In *Hydra*, *NOWA* is down-regulated by DAPT because of the defect in nematocyte differentiation, which occurs when Notch signaling is blocked (Käsbauer et al, 2007; Moneer et al, 2021). The results are shown in Fig 7. DAPT inhibits the expression of *CsSlx* and of *CsSp5* during head regeneration. It also inhibits the expression of homologs of suggested *Hydra* Notch target genes confirms that the drug must have entered the cells in *Craspedacusta* polyps.

Finally, we investigated the expression of the *Craspedacusta Wnt3* gene (Fig 7) and its response to DAPT treatment during head regeneration. We observed a low expression level of *CsWnt3* immediately after head removal (t = 0), which dramatically increased as the head regenerated, suggesting that *Wnt3* is expressed in the head of *Craspedacusta* polyps like its expression in the heads of other cnidarians, including *Hydra*, *Hydractinia*, and *Nematostella* (Hobmayer et al, 2000; Kusserow et al, 2005; Plickert et al, 2006). Consistent with its lack of effect on head regeneration, DAPT also





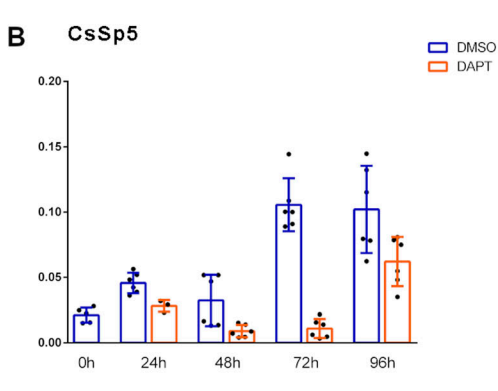
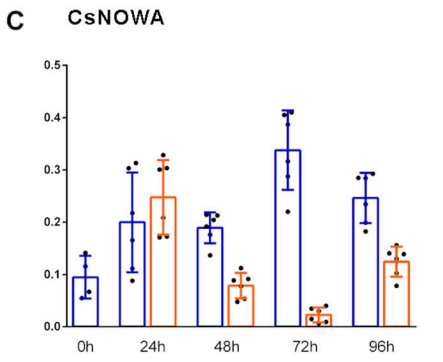
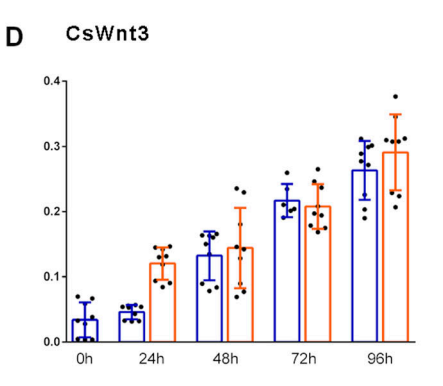


Figure 7. Gene expression dynamics of selected genes in DAPT-inhibited regenerates of *Craspedacusta*.

(A, B, C, D) qRT-PCR measurements quantifying the expression of *Craspedacusta* genes, (A) *CsAlx*, (B) *CsSp5*, (C) *CsNOWA*, and (D) *CsWnt3* during 96 h of head regeneration in DAPT (orange) or DMSO for control (blue). Relative normalized expression related to the housekeeping genes *GAPDH*, *actin*, and *PPIB*. Regeneration time is shown on x-axes; t = 0 refers to animals immediately after the head was removed. Data are shown as the mean ± SEM, *P = 0.05, **P = 0.01, ***P = 0.001, ****P = 0.001, ***P = 0.001, ****P = 0.001, ***P = 0.001





did not inhibit *CsWnt3* expression during this process in *Craspedacusta*. This is opposite to the situation in *Hydra*. If *CsWnt3* would be involved in *Craspedacusta* head regeneration, this could explain the failure of DAPT in disrupting this process.

Discussion

Head regeneration in *Hydra* can be divided into two processes, reformation of a hypostome–body column axis and re-formation of tentacles. We show here that tentacle formation requires β -catenin transcriptional activity, but hypostome regeneration does not. Conversely, hypostome regeneration requires Notch signaling, whereas tentacle tissue does not. By qRT–PCR gene expression analysis, we investigated the expression dynamics of selected genes in response to inhibition of β -catenin transcriptional activity, or of Notch signaling over a regeneration time of 48 h in polyps after heads had been removed at an apical position, just underneath the tentacles.

The results of these gene expression analyses are schematically displayed in Table 1. We distinguish two phases of regeneration, the first 8 h and the time thereafter. With the exception of the direct Notch target gene *HyHes* (Münder et al, 2013; Moneer et al, 2021), the expression of our selected genes is not affected by DAPT 8 h after head removal. This time is allocated to wound healing, and this process appears independent of Notch signals (Cazet et al, 2021). However, over the following time course, expression levels of *HyWnt1*, *HyWnt3*, *HyWnt7*, *HyWnt9/10*, *HyWnt11*, and *HyWnt16*, all implied in canonical Wnt signaling, declined to almost zero in DAPT-

treated polyps. In addition, the potential "organizer" gene CnGsc was inhibited with DAPT corresponding to the observation that Notch-treated regenerates do not acquire organizer activity. Sp5, which was suggested to be part of an inhibition loop for HyWnt3/ β -catenin (Vogg et al, 2019) and a direct Notch target gene (Moneer et al, 2021), was also blocked by DAPT during head regeneration. HyAlx, which has repeatedly been shown to induce differentiation of tentacle tissue (Smith et al, 2000; Broun & Bode, 2002; Broun et al, 2005; Gee et al, 2010; Münder et al, 2013), was only slightly affected by DAPT, corresponding to the detection of irregular tentacles in some regenerates (Münder et al, 2013). However, the lack of organizer activity in such regenerates may be responsible for their failure to produce correct tentacle patterns. We also observed that the expression of HyBMP2/4 is strongly dependent on Notch signaling. Together, these results suggest that Hydra head regeneration requires canonical Wnt and BMP2/4 signaling to produce an organizer and a hypostome, both of which depend on the presence of Notch signaling. In contrast, HyBMP5/8b and HyKayak were upregulated by DAPT, suggesting that Notch was required to inhibit these genes.

We also found that tentacle tissue formation, especially the expression of HyAlx in apical regenerates, was completely blocked with iCRT14. On the contrary, it is known that increasing nuclear β -catenin (and thus its transcriptional activity) by alsterpaullone induces formation of ectopic tentacles, but not hypostomes or even complete heads (Broun et al, 2005). Therefore, the phenotype observed with iCRT14 is obviously caused by a lack of tentacle activation, whereas ectopic activation of β -catenin induces tentacle formation through activation of HyAlx.



Table 1. Summary of changes in gene expression during Hydra head regeneration in medium with Notch and β -catenin inhibitors.

	Groups genes	DAPT treatm	nent	iCRT14 treatment		
		0-8 h	24-48 h	0-8 h	24-48 h	
	Hes	<u> </u>	Û		Û	
Target genes of Notch	Gsc		100		Ŷ	
	Sp5		1111			
	Wnt3		1111	Û		
	Wnt1		1111		111	
	Wnt7		100	Û	111	
Hypostome marker	Wnt9/10c		100	1111	Û	
	Wnt11		ÛÛ	<u>îî</u>	Ŷ	
	Wnt16		1111	1111	111	
	BMP2-4		1111			
Tantaala maskas	Alx				111	
Tentacle marker	BMP5-8		ÛÛ			
Inhibitor	Kayak		ûû	<u>îî</u>	Û	

qRT–PCR results indicating the effect of inhibition of Notch signaling by DAPT (orange) and inhibition of β-catenin transcriptional activity by iCRT14 (green) on expression of HyHes, CnGsc, HySp5, HyWnt3, HyWnt1, HyWnt7, HyWnt9/10c, HyWnt11, HyWnt16, HyBMP2/4, HyBMP5/8, HyAlx, and HyKayak. Gene expression is classified within the initial first 8 h and between 24 and 48 h of regeneration; up-regulation is indicated by blue arrows, and downregulation by yellow arrows. The numbers of arrows refer to the strength of the effect; dotted lines mean no effect.

Most intriguingly, induction of *HyWnt3* expression in apical regenerates was not blocked in the absence of β -catenin transcriptional activity, indicating that *HyWnt3* is not upregulated via β -catenin–dependent autoactivation after head removal, as had been suggested to occur in undisturbed polyps (Nakamura et al, 2011). In contrast to *HyWnt3*, all other canonical *Wnt* genes were down-regulated by iCRT14, at least to some extent, indicating that they were β -catenin–dependent. In the presence of iCRT14, *HyWnt3* must perform its function during head regeneration by signaling through a β -catenin–independent pathway. Remarkably, iCRT-treated tissue regenerated perfect hypostomes with the normal *HyWnt3* expression pattern.

The effect of iCRT14 had also been analyzed in previous studies (Gufler et al, 2018; Cazet et al, 2021; Tursch et al, 2022). All studies showed β -catenin dependency for the down-regulation of head-specific genes in foot regenerates at time points up to 12 h after head removal, including HyWnt3. They also stated a failure of head regeneration in the presence of iCRT14 but, in accordance with our study, did not reveal that HyWnt3 expression at future heads depended on β -catenin. None of these studies analyzed the regeneration of tentacles and hypostomes separately, and they did not report whether the regeneration of hypostomes 48 h after head removal occurred normally upon iCRT14 treatment

Although the tissue left after head removal has the capacity to form both tentacles and hypostome/head, final patterning of the new head involves emergence of hypostome and tentacle structures at distinct locations. A model proposing two independent patterning systems, each comprising an activator and an inhibitor for head and tentacle formation, had been introduced before, when HyAlx was discovered (Smith et al, 2000). After cutting off the head at apical positions, HyAlx first appeared at the tip. This was explained with high tentacle activation potential in this region, leading to a fast establishment of the tentacle system with HyAlx expression and tentacle markers (like HMMP) covering the whole regenerating tip. Tentacle activation is then inhibited by a tentacle inhibitor. Head activation takes over, and the expression of canonical Wnt genes becomes stronger. HyAlx shifts to the emerging tentacle region and finally appears in rings from which tentacles emerge (see Fig 8).

In contrast, budding starts with head activation being established and *HyAlx* is expressed later, always excluding the apical part of the bud. This was attributed to higher head activation potential in the budding region in comparison with tentacle activation activity. Moreover, older regeneration experiments had revealed that apical and basal regenerates differed in the order of appearance of the head and tentacle tissue. The tentacle tissue appeared first in apical regenerates and later in basal ones (Technau & Holstein, 1995).

Here, we have only considered apical regenerates where the heads of the polyps were cut off just underneath the tentacles. We suggest that Notch signaling fulfills a role in tentacle inhibition in this case. Without this inhibition, head activation with the expression of all canonical *Wnt* genes does not occur. However, Notch also affects head regeneration at basal cuts, as we have recently shown by analyzing transgenic *Hydra* with inhibited Notch function. Here, a substantial part of the animals regenerated two heads (Pan et al, 2024). This again confirms the idea that head formation and tentacle formation use two independent patterning systems, and Notch is required to mediate between them. When the tentacle system is activated first, Notch inhibits it to allow emergence of the head system. When the head system emerges first, Notch blocks it to prevent the formation of multiple heads.

How does tentacle inhibition work? It is well established that Notch activates transcriptional repressors, including *HyHes* genes, and thereby suppresses specific cell fates in signal-receiving cells, but allowing those fates in signal-sending cells (Bray, 2006). Our data show that DAPT inhibits the expression of two established transcriptional repressor genes, *HyHes* and *CnGsc*. This poses the question for targets of these repressors, which should be upregulated when Notch signaling is inhibited. We observed this behavior for *BMP5/8b* and *HyKayak*. On the basis of the published *BMP5/8b* expression patterns (Reinhardt et al, 2004), this gene is probably part of the tentacle patterning system.

HyKayak encodes a homolog of Fos proteins, which are components of the AP1 transcriptional complex, as we show by sequence comparison and phylogenetic analysis of the bZIP domain. Moreover, HyKayak interacted with HyJun, but not with itself, similar to the behavior of human c-Fos, which does not form homodimers but instead heterodimerizes with Jun proteins (Kouzarides & Ziff, 1988). Fos is suggested to be a negative regulator of its own

Life Science Alliance

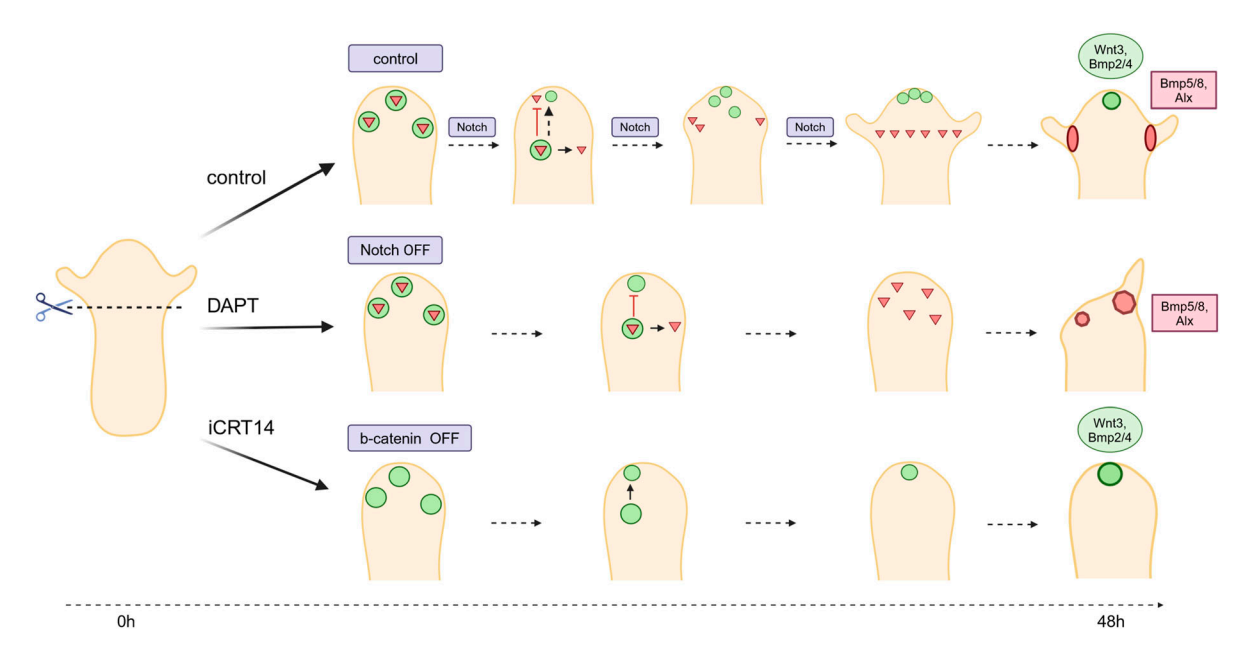


Figure 8. Model for Notch function in Hydra head regeneration in comparison with β -catenin.

Schematic representation of DAPT and iCRT14 effects on Hydra head regeneration. The hypostome is labeled in green; the tentacle boundary is in red. Animals treated with DAPT regenerate tentacle boundary gene expression in irregular patterns and show irregular tentacle morphology. Animals treated with iCRT14 regenerate regular expression patterns of hypostomal genes (HyWnt3) and show normal hypostome morphology. They do not regenerate any HyAlx expression and do not show tentacles. Model for the course of Hydra head regeneration in the presence of Notch signaling (control, upper panel), the absence of Notch signaling (middle panel), and the absence of Wnt/β -catenin signaling (lower panel) are shown. After head removal, the potential to re-form a head (green circles) and tentacles (red triangles) arises in the regenerating tip of the polyp. Notch signaling then mediates inhibition of the tentacle fate in the upper part of the regenerate by repressing HyBMP5/8 and allowing the expression of HyBMP2/4 and HyWnt3 (hypothetically by repressing inhibitors of these genes as indicated by a dotted line). This allows re-establishment of the hypostome and organizer tissue, while confining tentacle development to the lower part of the regenerate (control). With inhibition of Notch (middle panel), tentacle fate is not inhibited in the tip of the regenerate preventing the expression of hypostomal genes (HyWnt3 and HyBMP2/4) and allowing tentacle tissue development in the whole regenerating tip. However, as an organizer does not develop, this tissue cannot be patterned properly (red triangles). Without transcriptional activity of β -catenin, hypostomal genes (Wnt3 and HyBMP2/4) are expressed, whereas tentacle tissue is not induced (no HyAlx). Created with BioRender.

promoter (Sassone-Corsi et al, 1988), and Fos can function as a repressor on cellular immediate-early genes, such as Egr genes (Gius et al, 1990). Both repressions are mediated by the C-terminus of Fos and are independent of Jun (Gius et al, 1990; Ofir et al, 1990). However, the C-terminus of fos is not required for the repression of cardiac transcription and muscle creatine kinase enhancer (Lassar et al, 1989; Li et al, 1992; McBride et al, 1993). Our hypothesis that HyKayak could repress the HyWnt3 gene was confirmed by shRNA-mediated HyKayak knockdown, which resulted in the up-regulation of HyWnt3 expression. In addition, HyJun-epi was also up-regulated. This is in accordance with previously published observations in human prostate cell lines where fos loss of function has resulted in an up-regulation of jun expression (Riedel et al, 2021). Moreover, experiments with pharmacological inhibition of the AP1 complex with T5224 during head regeneration revealed that HyWnt3 and Hylun-epi were strongly up-regulated. We therefore suggest that the Hydra fos homolog HyKayak inhibits HyWnt3 expression and can be a target for a Notch-induced transcriptional repressor (such as HyHes) in the regenerating Hydra head. Nevertheless, we were not able to rescue the DAPT phenotype by inhibiting HyKayak, neither by the inhibitor nor by shRNA treatment, probably because of the strength of the DAPT effect. Therefore, we cannot exclude the possibility that Notch activates HyWnt3 directly, or that it represses unidentified Wnt inhibitors through activation of HyHes or CnGsc.

Different bZIP transcriptional factors (TFs) may have different effects on the expression of Wnt genes, and these effects are context-dependent. In previous research, Cazet et al identified another Hydra fos gene (here referred to as fos cazet), and bZIP TF binding sites in the putative regulatory sequences of HyWnt3 and HyWnt9/10c. They also showed that bZIP TF genes, including jun and fos, were transiently up-regulated 3 h after amputation and hypothesized that bZIP TFs could induce TCF-independent upregulation of HyWnt3 during the early generic wound response (Cazet et al, 2021). In contrast, HyKayak expression continuously increased throughout the entire head regeneration process (Figs 3E and 4E) including the morphogenesis stages (24-48 h postamputation). Another study reported that inhibition of the JNK pathway (which disrupts the formation of the AP-1 complex) resulted in up-regulation of HyWnt3 expression in both head and foot regenerates (Tursch et al, 2022). This result might support our hypothesis, but it only included the first 6 h after amputation. Therefore, it appears that HyKayak and fos_Cazet may have opposing roles in the regulation of Wnt gene expression and are possibly activated by different signaling pathways depending on the stages of regeneration.

The requirement for Notch activity is dependent on the regeneration time. At early time points, it is apparently not required, but between 8 and 48 h after head removal, loss of Notch activity severely impairs the regeneration process (Figs 3 and 8). In



addition, the gene expression dynamics for many of the analyzed genes appears in wave-like patterns in some experiments (see Figs S7 and S8). As we have only measured four time points, we cannot draw strong conclusions from these observations, except that some of the deviations in our data points (e.g., 48-h HyHes) might be due to oscillations. It is tempting to speculate that the gene expression patterns over the time course of regeneration occur in waves. Hes genes, the best-studied Notch target genes, can produce waves of gene expression, for example, during segmentation and as part of the circadian clock (Kageyama et al, 2007). This property is due to the capability of Hes proteins to inhibit their own promoter. Future models for head regeneration in Hydra should consider this potential of the Notch/Hes system. Oscillations in gene expression could explain how the observed local changes in the expression of some genes within the 48 h of head regeneration come about. Examples are HyHes itself and BMP5/8b, both at the beginning strongly expressed at the tip of the regenerate, and later apparently "moving" to the bases of tentacles (Reinhardt et al, 2004; Münder et al, 2013).

Is Notch part of the organizer? The organizer is defined as a piece of tissue with inductive and structuring capacity. Notch is expressed in all cells of Hydra polyps (Prexl et al, 2011), and the overexpression of NICD does not induce second axes all over the Hydra body column (Pan et al, 2024), in contrast to the overexpression of stabilized β -catenin (Gee et al, 2010). Moreover, Notch functions differently during regeneration after apical and basal cuts. Phenotypically during head regeneration in Notch-inhibited polyps, we clearly recognize a missing inhibition of tentacle tissue after apical cuts, and a diminished inhibition of head induction after basal cuts (Pan et al, 2024).

We would thus rather suggest that the organizer activity of the Hydra tissue uses Notch signaling as a mediator of inhibition. As our study of transgenic NICD-overexpressing and Notch knockdown polyps had suggested, the localization of Notch signaling cells depends on relative concentrations of Notch and Notchligand proteins, which are established by gradients of signaling molecules that define the Hydra body axis (Sprinzak et al, 2010; Pan et al, 2024). This is in very good agreement with the greatly accepted "reaction-diffusion model" provided by Alfred Gierer and Hans Meinhardt (Gierer & Meinhardt, 1972; Meinhardt & Gierer, 1974), which suggests a gradient of positional value across the Hydra body column. This gradient may determine the activities of two activation/inhibition systems, one for tentacles and one for the head. When the polyps regenerate new heads, Notch could provide inhibition for either system, depending on the position of the cut.

Head regeneration also occurs in the colonial seawater hydrozoan *Hydractinia*. Colonies consist of stolons, covering the substrate, and connecting polyps, including feeding polyps, which have hypostomes and tentacles, and are capable of head regeneration, similar to *Hydra* polyps. *Wnt3* is expressed at the tip of the head, and by RNAi-mediated knockdown, it was shown that this gene is required for head regeneration (Duffy et al, 2010). In the presence of DAPT, proper head regeneration did not occur, similar to *Hydra*. However, regeneration of the nerve ring around the hypostome was observed, indicating the possibility that hypostomes had been regenerated. Unfortunately, this

study did not include gene expression data, and therefore, it is not clear whether *Wnt3* expression was affected or not (Gahan et al. 2017).

An interesting question was whether regeneration of cnidarian body parts, which are only composed of one structure, also requires Notch signaling. This is certainly true for the *Hydra* foot, which regenerates fine in the presence of DAPT (Käsbauer et al, 2007). Moreover, we tested head regeneration in *Craspedacusta* polyps, which do not have tentacles, and showed that DAPT does not affect this regeneration process. This corroborates our idea that Notch is required for regeneration in cnidarians, when this process involves two pattern-forming processes, which are controlled by different signaling modules. This would be the case for *Hydra* and for *Hydractinia* heads, but not for *Craspedacusta*.

Future studies on expression patterns of the genes that control formation of the *Hydra* head, including *Sp5* and *Alx* in *Craspedacusta*, could provide new insights into the evolution of cnidarian body patterns. *Sp5* and *Alx* appear to be conserved targets of Notch signaling in the two cnidarians we have investigated. *Wnt3*, while being inhibited by Notch inhibition in *Hydra* head regenerates, is not a general target of Notch signaling. It was not affected by DAPT in our comparative transcriptome analysis (Moneer et al, 2021) on uncut *Hydra* polyps, and it was also not affected by DAPT in regenerating heads of *Craspedacusta*.

Materials and Methods

Animal treatment

Hydra polyps were cultured in Hydra medium (HM) (0.29 mM CaCl₂, 0.59 mM MgSO₄, 0.5 mM NaHCO₃, 0.08 mM K₂CO₃ dissolved in Milli-Q water) at a constant temperature of 18°C. They were fed with freshly hatched Artemia nauplii 2–3 times per week, with the exception of 2 d before conducting the experiments. For regeneration experiments, all animals were decapitated at 80% of their body length and left to regenerate for 2 d in HM containing the respective inhibitors dissolved in 1% DMSO. Control animals were left to regenerate in HM with 1% DMSO. Treatments included 35 μ M DAPT/1% DMSO, 5 μ M iCRT14/1% DMSO, or 7.5 μ M T5224 for 8, 24, 36, and 48 h after head removal. Time point 0 refers to animals immediately after the head was cut off. The inhibitor/DMSO-containing medium was renewed every 12–14 h.

C. sowerbii polyps were grown in modified HM (0.29 mM CaCl₂, 0.59 mM MgSO₄, 0.5 mM NaHCO₃, 0.08 mM K₂CO₃ dissolved in Milli-Q water) at 19°C. They were fed with *Brachionus calyciflorus* twice a week. For regeneration experiments, all animals were decapitated at 80% of their body length and left to regenerate for 3–4 d in HM containing the respective inhibitors dissolved in 1% DMSO. Control animals were left to regenerate in HM with 1% DMSO. Treatments included 35 μ M DAPT/1% DMSO or 5 μ M iCRT14/1% DMSO for 8, 24, 36, 48, 72, or 96 h after head removal. Time point 0 refers to animals immediately after the head was cut off. The inhibitor/DMSO-containing medium was renewed every 12–14 h.



Standardizing conditions for qRT-PCR

For quantitative estimates of gene expression dynamics during Hydra head regeneration over time, we performed real-time quantitative RT-PCR (qRT-PCR) experiments. We used a fluorescence-based qRT-PCR method and adhered to the quality standards of the MIQE guidelines (Bustin et al, 2009). After in silico primer design, each primer pair was empirically validated for (1) specificity defined by a single melt peak corresponding to a unique band of expected size, (2) efficiency defined by doubling of the signal in every cycle, and (3) sensitivity defined by a broad linear range, and reproducibility. Primers and gene accession numbers are listed in Table S1. Total RNA was isolated from Hydra polyps, and RNA quality was tested with the Agilent bioanalyzer. Only RNA with an integrity number higher than 8 was used for cDNA synthesis. During head regeneration, mRNA for qRT-PCR was isolated from whole regenerates collected after 8, 24, 36, and 48 h (t = 8, 24, 36, 48). Immediately after head removal, the sample for t = 0 was obtained. All experiments included three biological replicates with three technical replicates each. Quantitative gene expression for each gene was calculated as the ratio of target gene expression to housekeeping gene average (relative normalized gene expression). We plotted the relative normalized gene expression of analyzed genes against the regeneration time points. Housekeeping genes included GAPDH, PPIB, EF1alpha, and RPL13.

Regression analysis of comparative expression levels

To visualize temporal changes in expression levels of different genes, we used appropriate regression methods. In particular, we used generalized additive models (Wood, 2017) enabling the visualization of nonlinear dependencies on the time-dependent variables based on appropriate regression splines (Wood, 2017). Here, we used the Tweedie probability distribution (Kokonendji et al, 2004), which is known to describe non-negative (possibly over-dispersed) data well—in particular if mean values are close to zero. Temporal autocorrelation of model residuals has been investigated based on pacf-plots (Wood, 2017) and was not apparent. The optimal amount of smoothness of regression splines has been estimated separately for each temporal expression pattern based on generalized cross-validation methods (Wood, 2017). For the analysis of expression patterns relative to the control (DMSO) type, the response variable in regression analysis has been defined by dividing separately for each experiment/time point the mean value of the repeated measurements of the treatment of interest (DAPT respectively iCRT) by the mean value of the repeated measurements of the corresponding DMSO treatment from the same experiment/time point.

Semithin sections with the Richardson staining

Animals were fixed with 4% PFA and prepared for semithin sectioning by re-fixation in 1% osmium tetroxide solution for 2 h. Samples were washed with water and dehydrated four times with serial acetone dilutions (30%, 50%, 70%, and 90%, four times 100%).

Finally, they were embedded in Spurr low-viscosity embedding medium standard mix, which was exchanged four times, and dried after each exchange for 24 h at 60°C in a cuboid shape. The resinembedded probes were sectioned with a semidiamond and stained after Richardson on a microscope slide. One drop of color solution (1% azure in H₂O and 1% methylene blue in 1% Na₂B₄O₂ in H₂O mixed 1:1) covering the semithin sections was heated to 80°C for 30 s and cleansed with water. After drying, the slides were analyzed with a brightfield microscope.

Histochemistry of polyps

Polyps were relaxed in 2% urethane and fixed with 4% PFA in HM for 1 h. They were permeabilized with ice-cold 100% ethanol and blocked in 0.1% Triton/1% BSA in PBS. For phalloidin staining, they were incubated with Phalloidin-iFluor 488 (ab176753; Abcam) (1:500) for 1 h, followed by DAPI (1:1,000) staining before mounting on slides with Vectashield. Slides were analyzed with a Leica SP5 point scanning laser confocal microscope equipped with oil-immersion HCX PL APO Lambda Blue 20 × 0.7 and 63 × 1.4 objective lenses. Alexa Fluor 488 fluorochromes were visualized with an argon laser at an excitation wavelength of 488 nm and emission filters of 520-540 nm, and a diode laser at an excitation wavelength of 405 nm and with emission filter at 450-470 nm was used for DAPI. The produced light optical serial sections were stacked with the Image) plugin StackGroom to produce 3D images of the treated polyps. DAPI staining of nematocyte capsules was done according to Szczepanek et al [2002].

Fluorescence in situ hybridization

This experiment was carried out as previously described (Siebert et al, 2019).

Transplantation experiments

Non-budding *Hydra* polyps were pre-treated with 5 μ M iCRT14/1% DMSO in HM for 24 h. After that, they were bisected at 80% of the body column underneath the head and left to regenerate in iCRT14-treated HM for another 24 h. The newly regenerated head region (top 20%) was grafted onto a blue host animal (treated with Evans blue for two weeks) at about 50% of the body column. After 3 h, the rod was removed and the animals were left in HM for another 48 h. Finally, the animals were classified for the presence of newly formed secondary axes displaying a clear hypostome and tentacles. Tissue recruitment was recognized by the blue/white color distribution within the new axes.

ShRNA knockdown

shRNA design and production were done according to Karabulut's protocol (Karabulut et al, 2019). For electroporation, 30 budless Hydra polyps were washed five times with Milli-Q water and incubated for 45 min in Milli-Q water. Then, excess water was removed and replaced with 200 μl of a 10 mM Hepes solution at pH 7.0. The suspended animals were then transferred into a 4-mM-gap electroporation cuvette, and 4 μM of purified shRNA or scramble shRNA



was added to the cuvette. The mixture was mixed by gently tapping the cuvette five times and incubated for 5 min to let animals relax before electroporation. The electroporation was carried out using BTX Electro Cell Manipulator 600 by setting up the condition to 250 V, 25 ms, 1 pulse, 200 μ F capacitance. 500 μ l of restoration medium (80% HM and 20% dissociation medium: 3.6 mM KCl, 6 mM CaCl₂, 1.2 mM MgSO₄, 6 mM sodium citrate, 6 mM sodium pyruvate, 6 mM glucose, 12.5 mM TES, and 50 mg/ml rifampicin, pH 6.9) was added into the cuvette immediately after electroporation. The entire volume of electroporated animals was then transferred into a petri dish. In our experiment, three times of electroporation were done every 2 d to achieve a significant knockdown of HyKayak. And two hairpins of Kayak were used for electroporation at 1:1.

Monoclonal anti-HyKayak antibody

Mice were immunized with fusion protein Hydra_KAYAK-HIS (amino acid of HyKAYAK: 1–111) using a mixture of 50 μg protein, 12 μl Oligo 1,668 (500 pmol/ μl), and 150 μl IFA in a total volume of 400 μl . After 6 wk, a single boost was given with the same mixture except for the IFA, which was omitted. Fusion with Ag8 myeloma cells was performed using standard procedures. Candidate selection was based on positive selection using KAYAK-HIS and negative selection using Hydra_HES-HIS. Hybridoma kayak 3C10-1-1 and 13A4-1-1 were cloned using standard procedures and subsequently grown for antibody production.

Multiple sequence alignment and phylogenetic analysis

The multiple sequence alignment was done using Clustal Omega. The conserved domains were identified by PROSITE. The phylogenetic trees were produced by MEGA. The protein sequences for comparison were retrieved from UniProt and NCBI.

Subcellular fractionation and Western blot

500 Hydra were dissociated into single cells with 10 ml dissociation medium by pipetting. After centrifuge at 2,000g for 10 min, the cellular pellet was resuspended in 500 μ l RIPA buffer (25 mM Tris-HCl, pH 7.5, 150 mM NaCl, 1% NP-40, 1% sodium deoxycholate, 0.1% SDS, 10 ng/ml pepstatin A, 10 ng/ml aprotinin, 10 ng/ml leupeptin, and 0,5 mg/ml Pefabloc) and incubated for 20 min on ice. Subsequently, the mixture was homogenized with a Dounce homogenizer 30 times and then centrifuged for 10 min at 1,000g. The resulting supernatant including cytoplasmic proteins was collected and labeled as CP. The pellet was treated with 500 μ l RIPA buffer and then sonicated at 180 W for 3 min (in rounds of 10-s sonication and 50-s rest on ice for each cycle). After centrifuging at 14,000g for 30 min, the supernatant was collected and labeled as nuclear proteins (NP); the pellet was resuspended with the same volume of RIPA buffer and kept for SDS-PAGE analysis.

For DNase treatment, the pellet from the second centrifuge was resuspended with 500 μ l RIPA buffer supplemented with 200 U/ml DNase, 10 mM CaCl₂, and 10 mM MgCl₂, and incubated at room temperature for 15 min. After centrifuging at 1,000g for 10 min, the supernatant was collected, whereas the pellet was resuspended

in 500 μ l RIPA buffer with 2 M NaCl and incubated on ice for 10 min. Then, the same centrifuge was done, and both the supernatant and pellet were collected for gel analysis. Western blots were stained with the in-house mouse anti-Kayak monoclonal antibody.

Co-immunoprecipitation

HEK293T cells were transferred with C-terminal HA-tagged Kayak and N-terminal GFP-tagged Jun-epi or Kayak using Lipofectamine 2000 (11668030; Thermo Fisher Scientific). The GFP-Trap agarose beads (ABIN509397; ChromoTek) were used for immunoprecipitation as described previously (Webby et al, 2009; Heim et al, 2014). Western blot was stained with the following primary antibodies: mouse anti-GFP antibody (11814460001; Roche) and rabbit anti-HA antibody (H6908; Sigma-Aldrich).

Identification of Craspedacusta genes

Craspedacusta total RNA was extracted from 120 polyps using QIAGEN RNeasy Mini Kit. RNA quality was verified with the Agilent bioanalyzer, the RNA was then reverse-transcribed into cDNA, and cDNA was sequenced with Illumina. The resulting gene sequences were aligned, and by comparison with sequences for HyWnt3, NOWA, HyAlx, and Sp5, the corresponding Craspedacusta cDNA sequences could be identified (CsWnt3, CsNOWA, CsAlx, and CsSp5) and confirmed by sequencing of cDNA clones obtained after qRT-PCR from Craspedacusta total RNA.

Data Availability

All data presented in the main article and supplementary files will be provided by the corresponding author (Angelika Böttger) upon request.

Supplementary Information

Supplementary Information is available at https://doi.org/10.26508/lsa. 202403054.

Acknowledgements

We want to express our gratitude to the funding agencies for supporting this work. A Böttger and L Sauermann are funded by the German Research Foundation (DFG) project BO1748, M Mercker by DFG grant SFB1324, Q Pan is funded by a CSC grant (Chinese Scholarship Council), and L Sauermann is funded by Evangelisches Studienwerk Villigst e.V. Special thanks go to Dr. Herwig Stibor, LMU, for sparking our investigation of Craspedacusta head regeneration. We thank Dr. Stefan Krebs, LMU Munich, for sequencing of Craspedacusta cDNA, Dr. Sergio Vargas, LMU Munich, for bioinformatics sequence analysis and Bianca Sammer for carrying out transplantation experiments. The drawings in this document were produced using Affinity Designer 2 (version 2.3.0) by L Sauermann.



Author Contributions

- M Steichele: conceptualization, investigation, methodology, and writing—original draft.
- L Sauermann: data curation, investigation, methodology, and writing—review and editing.
- Q Pan: conceptualization, investigation, methodology, and writing—review and editing.
- J Moneer: conceptualization, investigation, methodology, and writing—review and editing.
- A de la Porte: investigation and methodology.
- M Heß: resources and methodology.
- M Mercker: data curation, formal analysis, and methodology.
- C Strube: investigation and methodology.
- H Flaswinkel: methodology.
- M Jenewein: conceptualization and methodology.
- A Böttger: conceptualization, supervision, investigation, methodology, project administration, and writing—original draft, review, and editing.

Conflict of Interest Statement

The authors declare that they have no conflict of interest.

References

- Anderson C, Stern CD (2016) Organizers in development. *Curr Top Dev Biol* 117: 435–454. doi:10.1016/bs.ctdb.2015.11.023
- Bode HR (2003) Head regeneration in hydra. *Dev Dyn* 226: 225–236. doi:10.1002/dvdy.10225
- Bray SJ (2006) Notch signalling: A simple pathway becomes complex. Nat Rev Mol Cell Biol 7: 678–689. doi:10.1038/nrm2009
- Broun M, Bode HR (2002) Characterization of the head organizer in hydra. Development 129: 875–884. doi:10.1242/dev.129.4.875
- Broun M, Sokol S, Bode HR (1999) Cngsc, a homologue of goosecoid, participates in the patterning of the head, and is expressed in the organizer region of hydra. *Development* 126: 5245–5254. doi:10.1242/dev.126.23.5245
- Broun M, Gee L, Reinhardt B, Bode HR (2005) Formation of the head organizer in hydra involves the canonical Wnt pathway. *Development* 132: 2907–2916. doi:10.1242/dev.01848
- Browne EN (1909) The production of new hydranths in Hydra by the insertion of small grafts. *JExpZool* 7: 1–23. doi:10.1002/jez.1400070102
- Bustin SA, Benes V, Garson JA, Hellemans J, Huggett J, Kubista M, Mueller R, Nolan T, Pfaffl MW, Shipley GL, et al (2009) The MIQE guidelines: Minimum information for publication of quantitative real-time PCR experiments. *Clin Chem* 55: 611–622. doi:10.1373/clinchem.2008.112797
- Cazet JF, Cho A, Juliano CE (2021) Generic injuries are sufficient to induce ectopic wnt organizers in hydra. *Elife* 10: e60562. doi:10.7554/eLife.60562
- Ding Y, Ploper D, Sosa EA, Colozza G, Moriyama Y, Benitez MD, Zhang K, Merkurjev D, De Robertis EM (2017) Spemann organizer transcriptome induction by early beta-catenin, Wnt, Nodal, And Siamois signals in Xenopus Laevis. Proc Natl Acad Sci U S A 114: E3081–E3090. doi:10.1073/ pnas.1700766114
- Dovey HF, John V, Anderson JP, Chen LZ, de Saint Andrieu P, Fang LY, Freedman SB, Folmer B, Goldbach E, Holsztynska EJ, et al (2001) Functional gamma-secretase inhibitors reduce beta-amyloid peptide

- levels in brain. *J Neurochem* 76: 173–181. doi:10.1046/j.1471-4159.2001.00012.x
- Duffy DJ, Plickert G, Kuenzel T, Tilmann W, Frank U (2010) Wnt signaling promotes oral but suppresses aboral structures in hydractinia metamorphosis and regeneration. *Development* 137: 3057–3066. doi:10.1242/dev.046631
- Gahan JM, Schnitzler CE, DuBuc TQ, Doonan LB, Kanska J, Gornik SG, Barreira S, Thompson K, Schiffer P, Baxevanis AD, et al (2017) Functional studies on the role of notch signaling in hydractinia development. *Dev Biol* 428: 224–231. doi:10.1016/j.ydbio.2017.06.006
- Gee L, Hartig J, Law L, Wittlieb J, Khalturin K, Bosch TC, Bode HR (2010) Betacatenin plays a central role in setting up the head organizer in hydra. *Dev Biol* 340: 116–124. doi:10.1016/j.ydbio.2009.12.036
- Geling A, Steiner H, Willem M, Bally-Cuif L, Haass C (2002) A gamma-secretase inhibitor blocks notch signaling in vivo and causes a severe neurogenic phenotype in zebrafish. *EMBO Rep* 3: 688–694. doi:10.1093/embo-reports/kvf124
- Gierer A, Meinhardt H (1972) A theory of biological pattern formation. *Kybernetik* 12: 30–39. doi:10.1007/BF00289234
- Gius D, Cao XM, Rauscher FJ 3rd, Cohen DR, Curran T, Sukhatme VP (1990)
 Transcriptional activation and repression by fos are independent
 functions: The c terminus represses immediate-early gene expression
 via carg elements. Mol Cell Biol 10: 4243–4255. doi:10.1128/mcb.10.8.42434255.1990
- Goetsch W (1926) "Organisatoren" bei regenerativen prozessen. *Die Naturwissenschaften Heft* 46: 1011–1016.
- Gonsalves FC, Klein K, Carson BB, Katz S, Ekas LA, Evans S, Nagourney R, Cardozo T, Brown AM, DasGupta R (2011) An rnai-based chemical genetic screen identifies three small-molecule inhibitors of the wnt/wingless signaling pathway. *Proc Natl Acad Sci U S A* 108: 5954–5963. doi:10.1073/pnas.1017496108
- Gufler S, Artes B, Bielen H, Krainer I, Eder MK, Falschlunger J, Bollmann A, Ostermann T, Valovka T, Hartl M, et al (2018) β-Catenin acts in a position-independent regeneration response in the simple eumetazoan Hydra. *Dev Biol* 433: 310–323. doi:10.1016/j.ydbio.2017.09.005
- Hamburger V (1969) Hans spemann and the organizer concept. *Experientia* 25: 1121–1125. doi:10.1007/BF01900223
- Heim A, Grimm C, Muller U, Haussler S, Mackeen MM, Merl J, Hauck SM, Kessler BM, Schofield CJ, Wolf A, et al (2014) Jumonji domain containing protein 6 (jmjd6) modulates splicing and specifically interacts with arginine-serine-rich (rs) domains of sr- and sr-like proteins. *Nucleic Acids Res* 42: 7833–7850. doi:10.1093/nar/gku488
- Hobmayer B, Rentzsch F, Kuhn K, Happel CM, von Laue CC, Snyder P, Rothbacher U, Holstein TW (2000) Wnt signalling molecules act in axis formation in the diploblastic metazoan hydra. *Nature* 407: 186–189. doi:10.1038/35025063
- Hobmayer B, Rentzsch F, Holstein TW (2001) Identification and expression of hysmad1, a member of the r-smad family of tgfbeta signal transducers, in the diploblastic metazoan hydra. *Dev Genes Evol* 211: 597–602. doi:10.1007/s00427-001-0198-8
- Kageyama R, Ohtsuka T, Kobayashi T (2007) The hes gene family: Repressors and oscillators that orchestrate embryogenesis. *Development* 134: 1243–1251. doi:10.1242/dev.000786
- Karabulut A, He S, Chen CY, McKinney SA, Gibson MC (2019) Electroporation of short hairpin rnas for rapid and efficient gene knockdown in the starlet sea anemone, nematostella vectensis. *Dev Biol* 448: 7–15. doi:10.1016/j.ydbio.2019.01.005
- Karin M, Liu Z, Zandi E (1997) Ap-1 function and regulation. *Curr Opin Cell Biol* 9: 240–246. doi:10.1016/s0955-0674(97)80068-3
- Käsbauer T, Towb P, Alexandrova O, David CN, Dall'armi E, Staudigl A, Stiening B, Böttger A (2007) The notch signaling pathway in the cnidarian hydra. *Dev Biol* 303: 376–390. doi:10.1016/j.ydbio.2006.11.022



- Kokonendji CC, Doussou-Gbété S, Demétrio CGB (2004) Some discrete exponential dispersion models: Poisson-tweedie and hindedemétrio classes. SORT 28: 201–214.
- Kouzarides T, Ziff E (1988) The role of the leucine zipper in the fos-jun interaction. *Nature* 336: 646–651. doi:10.1038/336646a0
- Kusserow A, Pang K, Sturm C, Hrouda M, Lentfer J, Schmidt HA, Technau U, von Haeseler A, Hobmayer B, Martindale MQ, et al (2005) Unexpected complexity of the Wnt gene family in a sea anemone. *Nature* 433: 156–160. doi:10.1038/nature03158
- Lassar AB, Thayer MJ, Overell RW, Weintraub H (1989) Transformation by activated ras or fos prevents myogenesis by inhibiting expression of MyoD1. Cell 58: 659–667. doi:10.1016/0092-8674(89)90101-3
- Lengfeld T, Watanabe H, Simakov O, Lindgens D, Gee L, Law L, Schmidt HA, Ozbek S, Bode H, Holstein TW (2009) Multiple Wnts are involved in hydra organizer formation and regeneration. *Dev Biol* 330: 186–199. doi:10.1016/j.ydbio.2009.02.004
- Li L, Chambard JC, Karin M, Olson EN (1992) Fos and Jun repress transcriptional activation by myogenin and MyoD: The amino terminus of Jun can mediate repression. *Genes Dev* 6: 676–689. doi:10.1101/gad.6.4.676
- MacWilliams HK (1983) Hydra transplantation phenomena and the mechanism of hydra head regeneration. I. Properties of the head inhibition. *Dev Biol* 96: 217–238. doi:10.1016/0012-1606(83) 90324-x
- McBride K, Robitaille L, Tremblay S, Argentin S, Nemer M (1993) Fos/Jun repression of cardiac-specific transcription in quiescent and growth-stimulated myocytes is targeted at a tissue-specific cis element. *Mol Cell Biol* 13: 600–612. doi:10.1128/mcb.13.1.600-612.1993
- Meinhardt H (2012) Modeling pattern formation in hydra: A route to understanding essential steps in development. *Int J Dev Biol* 56: 447–462. doi:10.1387/ijdb.113483hm
- Meinhardt H, Gierer A (1974) Applications of a theory of biological pattern formation based on lateral inhibition. *J Cell Sci* 15: 321–346. doi:10.1242/jcs.15.2.321
- Micchelli CA, Esler WP, Kimberly WT, Jack C, Berezovska O, Kornilova A, Hyman BT, Perrimon N, Wolfe MS (2003) Gamma-secretase/presenilin inhibitors for alzheimer's disease phenocopy notch mutations in drosophila. FASEB J 17: 79–81. doi:10.1096/fj.02-0394fje
- Moneer J, Siebert S, Krebs S, Cazet J, Prexl A, Pan Q, Juliano C, Bottger A (2021)
 Differential gene regulation in dapt-treated hydra reveals candidate
 direct notch signalling targets. *J Cell Sci* 134: jcs258768. doi:10.1242/
 ics.258768
- Münder S, Käsbauer T, Prexl A, Aufschnaiter R, Zhang X, Towb P, Böttger A (2010) Notch signalling defines critical boundary during budding in hydra. *Dev Biol* 344: 331–345. doi:10.1016/j.ydbio.2010.05.517
- Münder S, Tischer S, Grundhuber M, Buchels N, Bruckmeier N, Eckert S, Seefeldt CA, Prexl A, Käsbauer T, Böttger A (2013) Notch-signalling is required for head regeneration and tentacle patterning in hydra. *Dev Biol* 383: 146–157. doi:10.1016/j.ydbio.2013.08.022
- Mutz E (1930) Transplantationsversuche an hydra mit besonderer berucksichtigung der induktion, regionalität und polarität. Wilhelm Roux Arch Entwickl Mech Org 121: 210–271. doi:10.1007/BF00644951
- Nakamura Y, Tsiairis CD, Ozbek S, Holstein TW (2011) Autoregulatory and repressive inputs localize hydra wnt3 to the head organizer. *Proc Natl Acad Sci U S A* 108: 9137–9142. doi:10.1073/pnas.1018109108
- Ofir R, Dwarki VJ, Rashid D, Verma IM (1990) Phosphorylation of the c terminus of fos protein is required for transcriptional transrepression of the c-fos promoter. *Nature* 348: 80–82. doi:10.1038/348080a0
- Pan Q, Mercker M, Klimovich A, Wittlieb J, Marciniak-Czochra A, Bottger A (2024) Genetic interference with hynotch provides new insights into the role of the notch-signalling pathway for developmental

- pattern formation in hydra. *Sci Rep* 14: 8553. doi:10.1038/s41598-024-58837-7
- Philipp I, Aufschnaiter R, Ozbek S, Pontasch S, Jenewein M, Watanabe H, Rentzsch F, Holstein TW, Hobmayer B (2009) Wnt/Beta-catenin and noncanonical wnt signaling interact in tissue evagination in the simple eumetazoan hydra. *Proc Natl Acad Sci U S A* 106: 4290–4295. doi:10.1073/pnas.0812847106
- Plickert G, Jacoby V, Frank U, Muller WA, Mokady O (2006) Wnt signaling in hydroid development: Formation of the primary body axis in embryogenesis and its subsequent patterning. *Dev Biol* 298: 368–378. doi:10.1016/j.ydbio.2006.06.043
- Prexl A, Münder S, Loy B, Kremmer E, Tischer S, Böttger A (2011) The putative notch ligand hyjagged is a transmembrane protein present in all cell types of adult hydra and upregulated at the boundary between bud and parent. *BMC Cell Biol* 12: 38. doi:10.1186/1471-2121-12-38
- Ramos A, Peronti A, Kondo T, Lemos RNS (2017) First record of craspedacusta sowerbii lankester, 1880 (hydrozoa, limnomedusae) in a natural freshwater lagoon of Uruguay, with notes on polyp stage in captivity. Braz J Biol 77: 87–90. doi:10.1590/1519-6984.05416
- Reddy PC, Gungi A, Ubhe S, Pradhan SJ, Kolte A, Galande S (2019) Molecular signature of an ancient organizer regulated by Wnt/β-catenin signalling during primary body axis patterning in *Hydra*. *Commun Biol* 2: 434. doi:10.1038/s42003-019-0680-3
- Reddy PC, Gungi A, Ubhe S, Galande S (2020) Epigenomic landscape of enhancer elements during hydra head organizer formation. Epigenetics Chromatin 13: 43. doi:10.1186/s13072-020-00364-6
- Reinhardt B, Broun M, Blitz IL, Bode HR (2004) Hybmp5-8b, a bmp5-8 orthologue, acts during axial patterning and tentacle formation in hydra. *Dev Biol* 267: 43–59. doi:10.1016/j.ydbio.2003.10.031
- Riedel M, Cai H, Stoltze IC, Vendelbo MH, Wagner EF, Bakiri L, Thomsen MK (2021) Targeting ap-1 transcription factors by crispr in the prostate. Oncotarget 12: 1956–1961. doi:10.18632/oncotarget.27997
- Sassone-Corsi P, Sisson JC, Verma IM (1988) Transcriptional autoregulation of the proto-oncogene fos. *Nature* 334: 314–319. doi:10.1038/334314a0
- Siebert S, Farrell JA, Cazet JF, Abeykoon Y, Primack AS, Schnitzler CE, Juliano CE (2019) Stem cell differentiation trajectories in hydra resolved at single-cell resolution. *Science* 365: eaav9314. doi:10.1126/science.aav9314
- Smith KM, Gee L, Bode HR (2000) Hyalx, an aristaless-related gene, is involved in tentacle formation in hydra. *Development* 127: 4743–4752. doi:10.1242/dev.127.22.4743
- Spemann H (1924) Über organisatoren in der tierischen entwicklunug. *Die* Naturwissenschaften Heft 48: 1092–1094.
- Spemann H (1935) Nobel lecture. Available at: https://www.nobelprize.org/ prizes/medicine/1935/spemann/lecture/.
- Sprinzak D, Lakhanpal A, Lebon L, Santat LA, Fontes ME, Anderson GA, Garcia-Ojalvo J, Elowitz MB (2010) Cis-interactions between notch and delta generate mutually exclusive signalling states. *Nature* 465: 86–90. doi:10.1038/nature08959
- Steele RE (2012) The hydra genome: Insights, puzzles and opportunities for developmental biologists. *Int J Dev Biol* 56: 535–542. doi:10.1387/iidb.113462rs
- Szczepanek S, Cikala M, David CN (2002) Poly-gamma-glutamate synthesis during formation of nematocyst capsules in hydra. *J Cell Sci* 115: 745–751. doi:10.1242/jcs.115.4.745
- Technau U, Holstein TW (1995) Head formation in hydra is different at apical and basal levels. *Development* 121: 1273–1282. doi:10.1242/dev.121.5.1273
- Tursch A, Bartsch N, Mercker M, Schluter J, Lommel M, Marciniak-Czochra A, Ozbek S, Holstein TW (2022) Injury-induced MAPK activation triggers body axis formation in *Hydra* by default Wnt signaling.



Proc Natl Acad Sci U S A 119: e2204122119. doi:10.1073/pnas.2204122119

Vogg MC, Beccari L, Iglesias Olle L, Rampon C, Vriz S, Perruchoud C, Wenger Y, Galliot B (2019) An evolutionarily-conserved Wnt3/β-catenin/Sp5 feedback loop restricts head organizer activity in Hydra. *Nat Commun* 10: 312. doi:10.1038/s41467-018-08242-2

Watanabe H, Schmidt HA, Kuhn A, Hoger SK, Kocagoz Y, Laumann-Lipp N, Ozbek S, Holstein TW (2014) Nodal signalling determines biradial asymmetry in hydra. *Nature* 515: 112–115. doi:10.1038/nature13666

Webby CJ, Wolf A, Gromak N, Dreger M, Kramer H, Kessler B, Nielsen ML, Schmitz C, Butler DS, Yates JR 3rd, et al (2009) Jmjd6 catalyses lysyl-hydroxylation of u2af65, a protein associated with rna splicing. *Science* 325: 90–93. doi:10.1126/science.1175865

Wood SN (2017) Generalized Additive Models: An Introduction with R, 2nd edn. New York, NY: Chapman & Hall/CRC.

Xiong G, Ouyang S, Xie N, Xie J, Wang W, Yi C, Zhang M, Xu X, Chen D, Wang C (2022) Fosl1 promotes tumor growth and invasion in ameloblastoma. Front Oncol 12: 900108. doi:10.3389/fonc.2022.900108



License: This article is available under a Creative Commons License (Attribution 4.0 International, as described at https://creativecommons.org/licenses/by/4.0/).

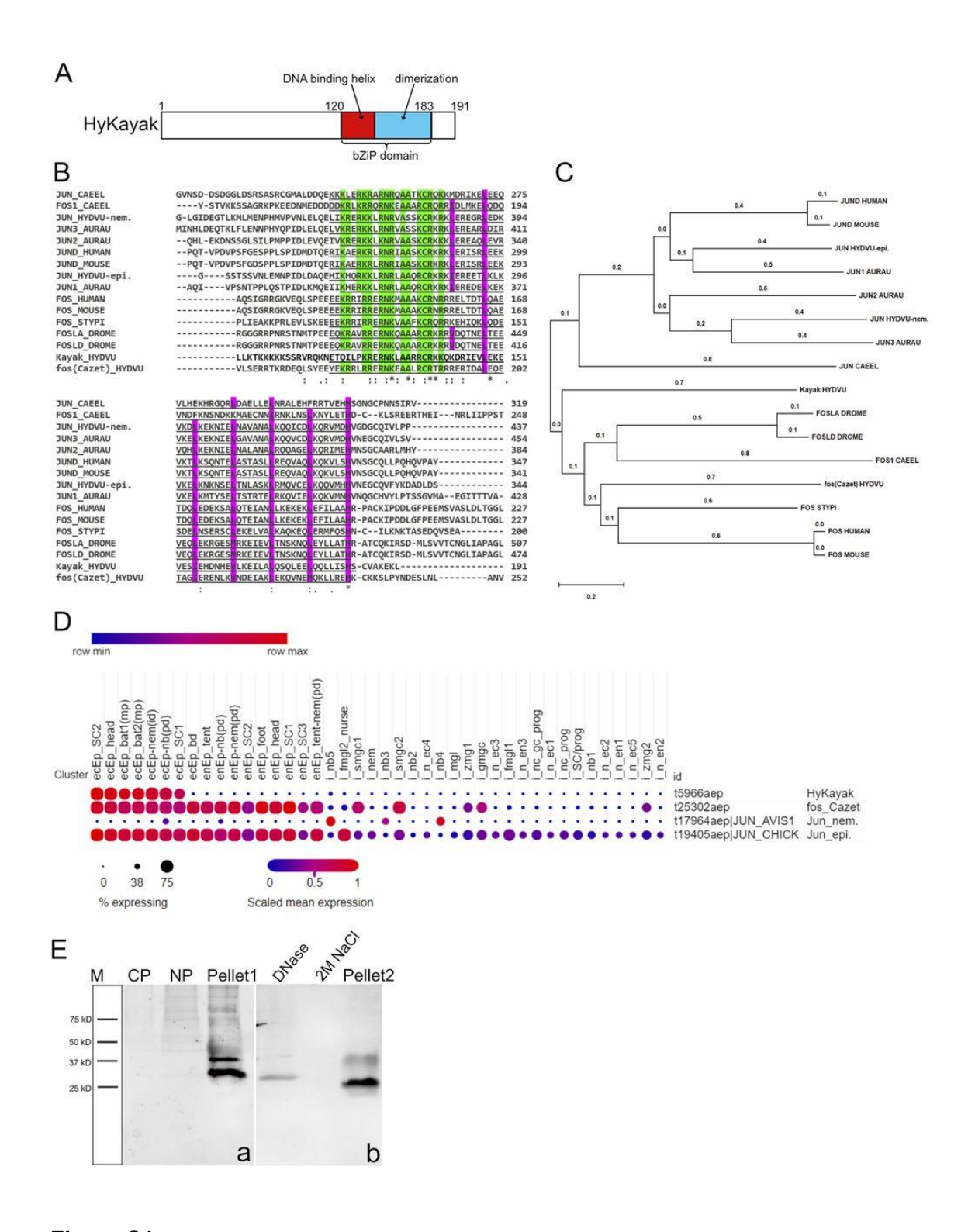


Figure S1.

Kayak gene identification and protein domain structure.

(A) Schematic representation of the HyKayak protein structure (191 amino acids). The bZIP domain with DNA binding and dimerization function is located between amino acids 120 and 183.

(B) Alignment of the protein sequences of Hydra-Kayak, fos-Cazet, Jun-epi, and Jun-nem from *Hydra vulgaris* (HYDVU), FOS and JUN from human, mouse, *Caenorhabditis elegans* (CAEEL), *Aurelia aurita* (AURAU), *Stylophora pistillata* (STYPI), and *Drosophila melanogaster* (DROME); the bZIP domain is underlined, green background indicates amino acids involved in DNA binding, and violet background indicates amino acids of the dimerization interface. (C) Phylogenetic tree based on the alignment of 15 full-length protein sequences affiliated to the FOS and JUN families using MEGA software. Species code: *Aurelia aurita* (AURAU), *Hydra vulgaris* (HYDVU), human, mouse, *Caenorhabditis elegans* (CAEEL), *Drosophila melanogaster* (DROME), *Stylophora pistillata* (STYPI). (D) Dot-plot of the expression patterns for the genes *HyKayak* (t5966aep), *fos_Cazet* (t25302aep), *HyJun_nem* (t17964aep), and *HyJun-epi* (t19405aep) from the single-cell portal (Siebert et al, 2019). (E) Western blot was stained with anti-kayak antibody (in-house). Lysates from Hydra polyps indicating cytoplasmic proteins (CP), nuclear proteins (NP), pellets after centrifugation at 14,000g (Pellet1), supernatant after treatment of pellet with DNase, supernatant after treatment of pellet fraction with 2 M NaCl, and pellet fraction after both treatments (Pellet2).

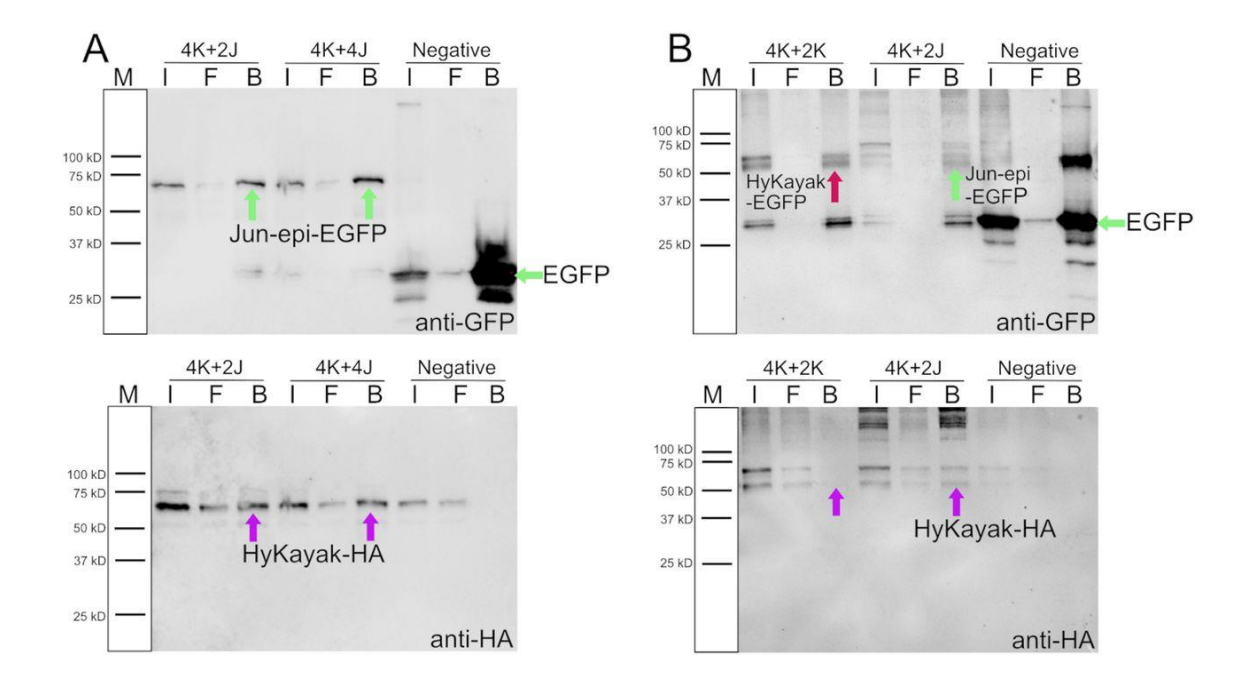


Figure S2.

Kayak Co-immunoprecipitation.

(A) EGFP-tagged Jun-epi was immunoprecipitated with GFP-Trap agarose beads and detected on Western blot using an anti-GFP antibody. Co-precipitation of HA-tagged Kayak was detected on Western blot using an anti-HA antibody in input, flow-through, and beads fractions. 4K + 2J: 4 μM Kayak-HA plus 2 μM Jun-epi-EGFP; 4K + 4J: 4 μM Kayak-HA plus 4 μM Jun-epi-EGFP; negative control: 4 μM Kayak-HA plus 2 μM empty pEGFP-C1 vector. I: input; F: flow-through; B: beads. (B) EGFP-tagged Kayak or Jun-epi were immunoprecipitated by GFP-Trap agarose beads and detected on Western blot using an anti-GFP antibody. Co-precipitation of HA-tagged Kayak was detected on Western blot using an anti-HA antibody in input, flow-through, and beads fractions. 4K + 2K: 4 μM Kayak-HA plus 2 μM Kayak-EGFP; 4K + 2J: 4 μM Kayak-HA plus 2 μM Jun-epi-EGFP, which was used for a positive control; the empty plasmid pEGFP-C1 was used for a negative control.

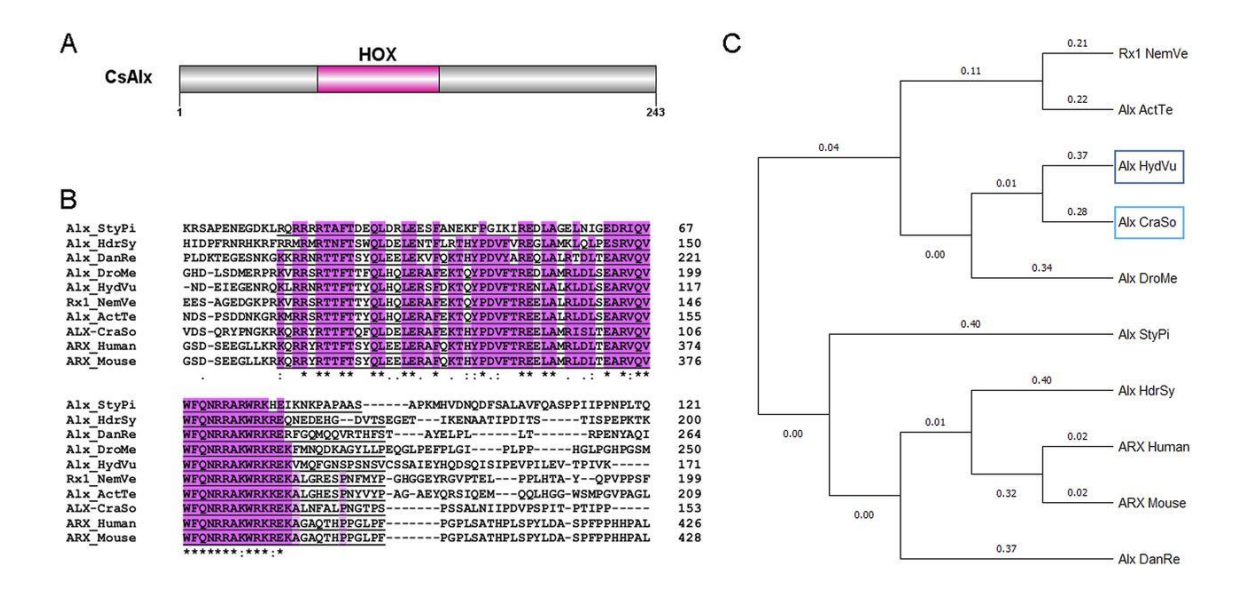


Figure S3.

Craspedacusta CsAlx gene identification and protein domain structure.

(A) Schematic representation of the CsAlx protein structure (243 amino acids). The HOX domain with DNA-binding function is located between amino acids 71 and 133. (B) Alignment of the protein sequences of Alx homologs from *Craspedacusta sowerbii* (CraSo), *Stylophora pistillata* (StyPi)—Acc#: PFX33415.1; *Hydractinia symbiolongicarpus* (HdrSy)—Acc#: XP_057291727.1; *Danio rerio* (DanRe)—Acc#: XP_001340966.1; *Drosophila melanogaster* (DroMe)—Acc#: NP_788420.1; *Hydra vulgaris* (HydVu)—Acc#: AAG03082.1; *Nematostella vectensis* (NemVe)—Acc#: XP_001634166.2; *Actinia tenebrosa* (ActTe)—Acc#: XP_031560466.1; human—Acc#: NP_620689.1; and mouse—Acc#: NP_001292869.1. The HOX domain is underlined, the pink background indicates conserved amino acids involved in DNA binding. (C) Phylogenetic tree based on the alignment of the 10 protein sequences affiliated to the aristaless family using MEGA software.

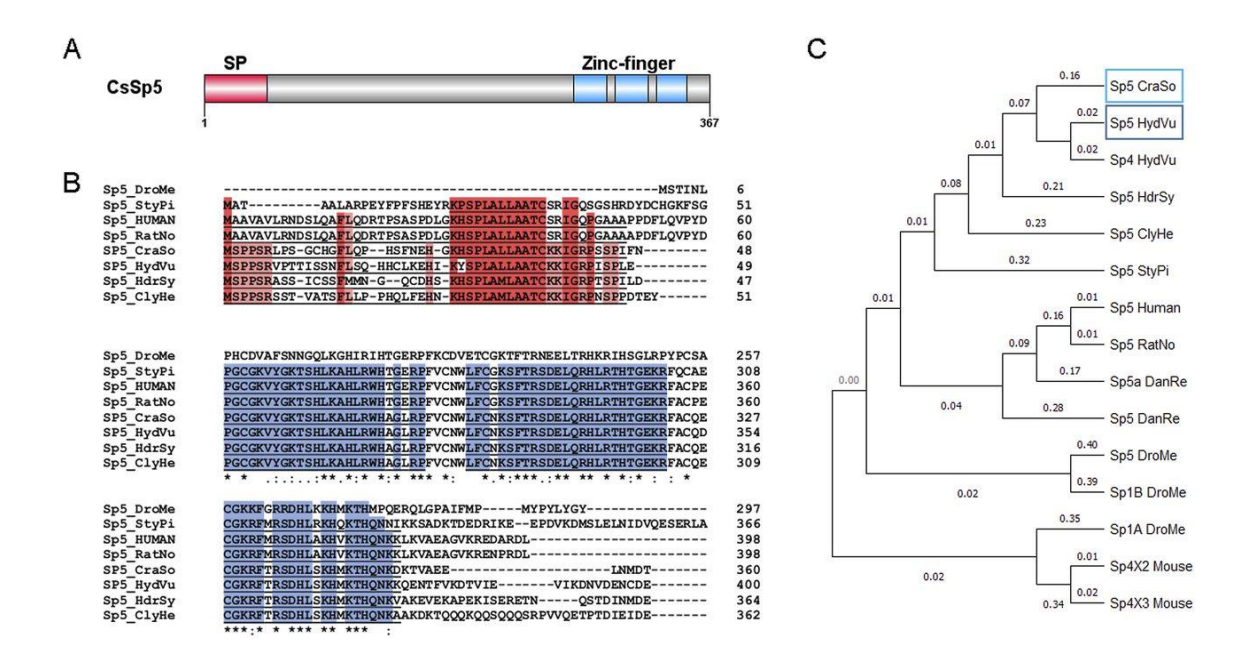


Figure S4.

Craspedacusta CsSp5 gene identification and protein domain structure.

(A) Schematic representation of the CsSp5 protein structure (367 amino acids). At the N-terminus, the signal peptide (SP) is shown in red from amino acids 1 to 46. The three zinc-finger domains with DNA binding function are located at the C-terminus between amino acids 268 and 292, 298 and 322, and 328 and 350 shown in blue. (B) Alignment of the protein sequences of Sp5 homologs from *Craspedacusta sowerbii* (CraSo), Drosophila melanogaster (DroMe)—Acc#: NP_727360.1, NP_651232.1; *Stylophora pistillata* (StyPi)—Acc#: PFX28957.1; *Hydra vulgaris* (HydVu)—Acc#: AXP19710.1; *Hydractinia symbiolongicarpus* (HdrSy)—Acc#: XP_057304028.1; and *Clytia hemisphaerica* (ClyHe)—Acc#: XP_057304028.1. The signal peptide is underlined, the red background indicates conserved amino acids; zinc-finger domains are underlined, the blue background indicates conserved amino acids involved in DNA binding. (C) Phylogenetic tree based on the alignment of the 15 protein sequences affiliated to the transcription factor Sp5 family using MEGA software. Human—Acc#: NP_001003845.1; *Rattus norvegicus* (RatNo)—Acc#: NP_001100022.1; *Danio rerio* (DanRe)—Acc#: NP_919352.1, NP_851304.2; and mouse—Acc#: XP_036013171.1, XP_036013172.1.

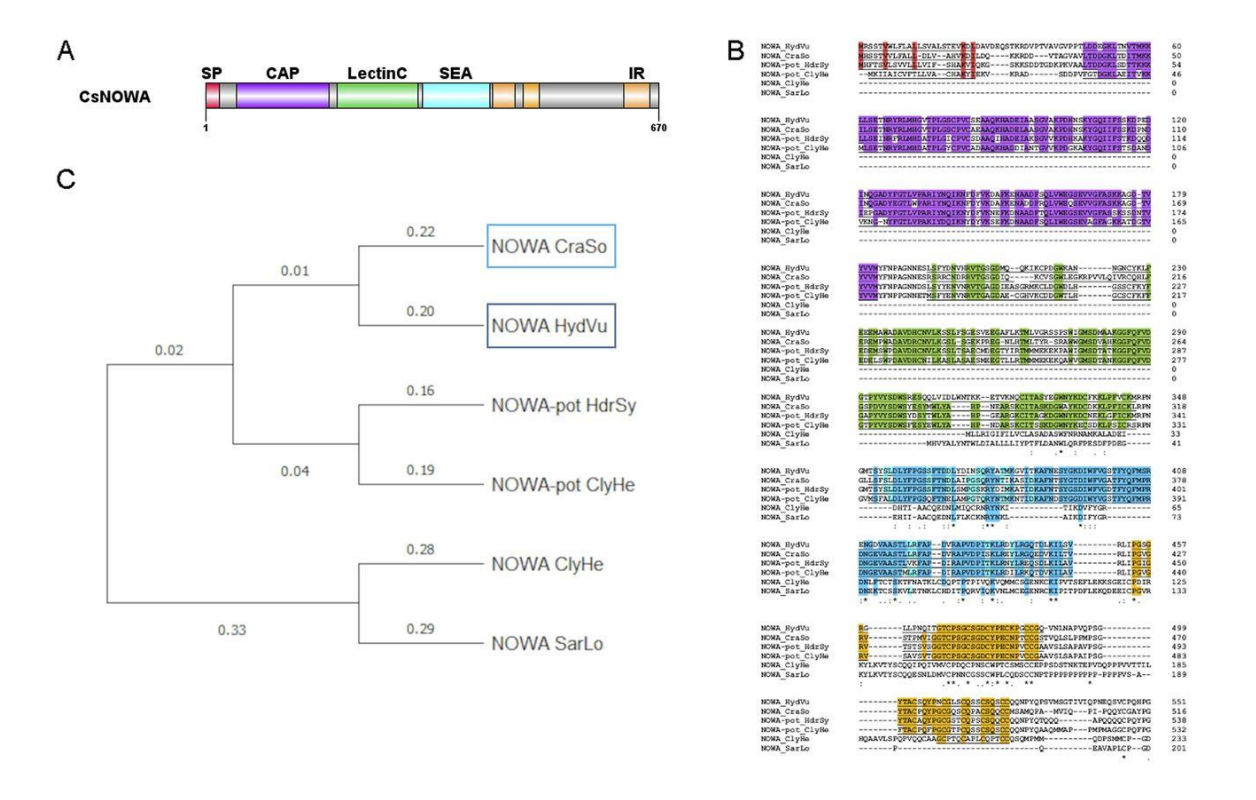


Figure S5

Craspedacusta CsNOWA gene identification and protein domain structure.

(A) Schematic representation of the CsNOWA protein structure (679 amino acids). At the Nterminus, the signal peptide (SP) is shown in red from amino acids (aa) 1 to 20, followed by a CAP domain from 46 to 183 aa in violet, a carbohydrate recognition LectinC domain from 194 to 183 aa shown in green, and a SEA domain for membrane interaction shown in blue from 321 to 420 aa. The three internal repeats at the C-terminus are shown in orange between amino acids 424 and 457, 470 and 493, and 618 and 656. (B) Alignment of the protein sequences of NOWA vulgaris (HydVu)—Acc#: homologs from Craspedacusta sowerbii (CraSo), Hydra AAN52336.1; Hydractinia symbiolongicarpus (HdrSy)—Acc#: XP 057312482.1; Clytia hemisphaerica (ClyHe)—Acc#: XP 066935203.1 and precursor Acc#: ABY71251.1; and Sarsia lovenii (SarLo)—Acc#: WVX52206.1. The signal peptide is underlined, the red background indicates conserved amino acids; CAP domains are underlined, violet background indicates conserved amino acids; LectinC domains are underlined, green background indicates conserved amino acids; SEA domains are underlined, the blue background indicates conserved amino acids; internal repeats are underlined, orange background indicates conserved acids. (C) Phylogenetic tree based on the alignment of the 6 protein sequences affiliated to the nematocyte-producing antigen family using MEGA software.

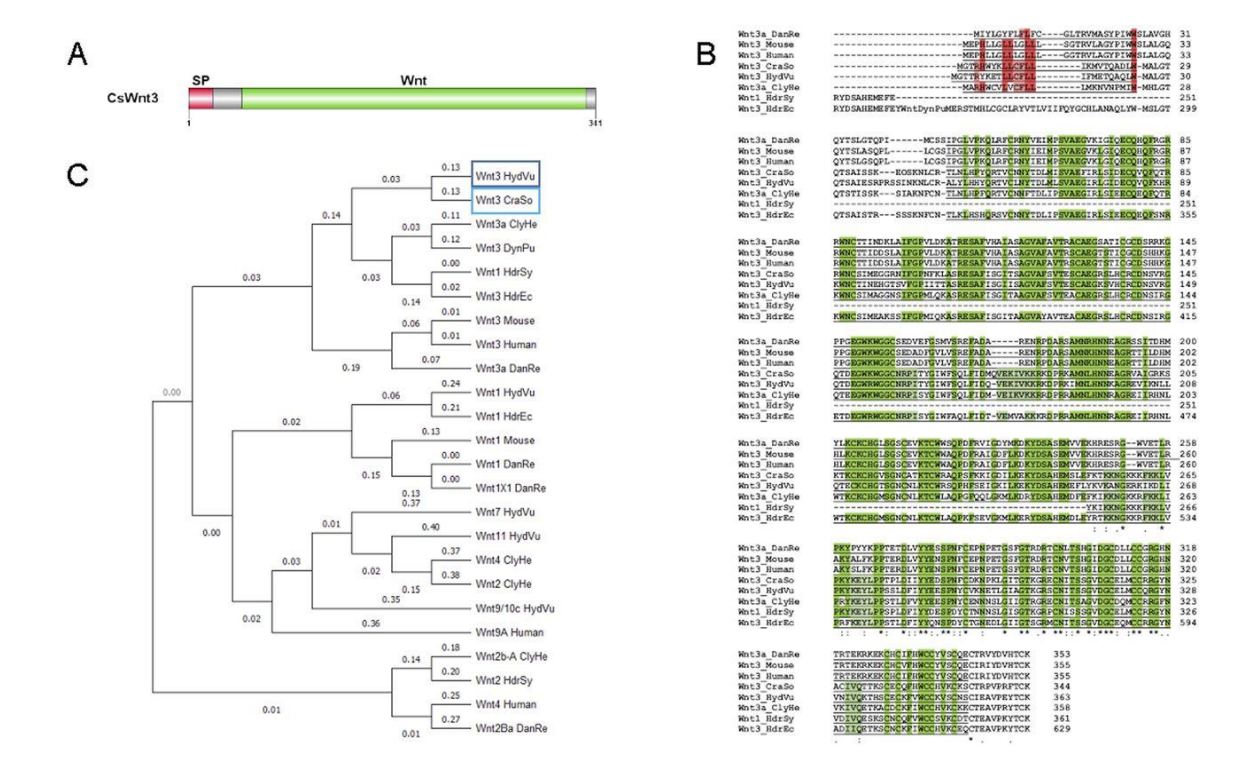


Figure S6.

Craspedacusta CsWnt3 gene identification and protein domain structure.

(A) Schematic representation of the CsWnt3 protein domain structure (341 amino acids). The Nterminal signal peptide (SP) is shown in red from amino acids (aa) 1 to 21, followed by the Wnt domain from 45 to 333 aa in green. (B) Alignment of the protein sequences of Wnt3 homologs from Craspedacusta sowerbii (CraSo), Danio rerio (DanRe)—Acc#: XP 005163717.1; mouse— NP 110380.1; Hydra Acc#: NP 033547.1; human—Acc#: vulgaris (HydVu)—Acc#: CDG70667.1; Clytia hemisphaerica (ClyHe)—Acc#: XP 066919214.1; Hydractinia symbiolongicarpus (HdrSy)—Acc#: XP 057304029.1; and Hydractinia echinata (HdrEc)—Acc#: CAK50826.1. The signal peptide is underlined, the red background indicates conserved amino acids; Wnt domains are underlined, green background indicates conserved amino acids. (C) Phylogenetic tree based on the alignment of the 24 protein sequences affiliated to the Wnt3 family using MEGA software. Hydra vulgaris: Wnt1—Acc#: BAH23782.1; Wnt7—Acc#: BAH23781.1; Wnt11—Acc#: BAH23776.1; Clytia hemisphaerica (ClyHe)—Acc#: AFI99119.1, AFI99118.1; Dynamena XP 066919469.1, pumila (DynPu)—Acc#: QBC65507.1; Hydractinia symbiolongicarpus (HdrSy)—Acc#: AIA10263.1; Hydractinia echinata (HdrEc)—Acc#: AIU99839.1; mouse—Acc#: NP 067254.1; human—Acc#:

NP_110388.2, KAI4085194.1; and *Danio rerio* (DanRe)—Acc#: NP_001188327.1, XP_005162280.1, NP_878296.1.

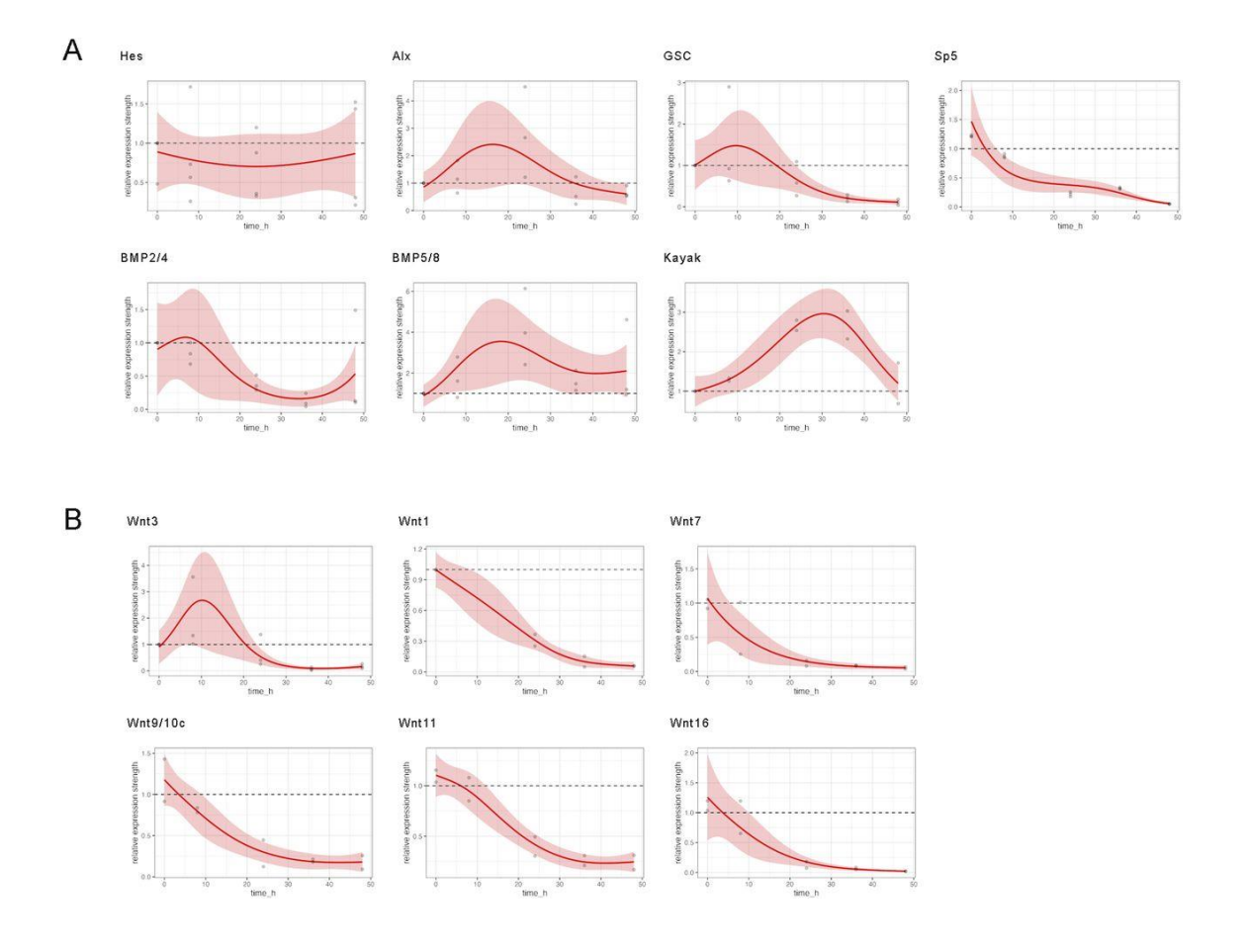


Figure S7.

GAM-based visualization of relative gene expression dynamics of DAPT-treated regenerates.

GAM-based visualization of gene expression as measured by qRT–PCR in DAPT-treated animals relative to control animals (y-axis) depending on the time after head removal (x-axis). Gray points show raw data (quotients of mean values of DAPT-treated relative to DMSO-treated animals), the colored lines show the smooth GAM-based estimates, and color-shaded areas are 95% confidence bands. Gene expression was followed for 48 h after head removal in DMSO control and DAPT. For time point 0, polyps were used immediately after head removal without any exposure to inhibitor or control medium. (A) *HyHes*, *HyAlx*, *CnGsc*, *HySp5*, *HyKayak*, *HyBMP2/4*, and *HyBMP5/8*. (B) *HyWnt3* and *HyWnt1*, *HyWnt7*, *HyWnt9/10c*, *HyWnt11*,

and *HyWnt16* during 48 h. Relative normalized expression was related to the housekeeping genes *GAPDH*, *RPL13*, *EF1α*, and *PPIB*.

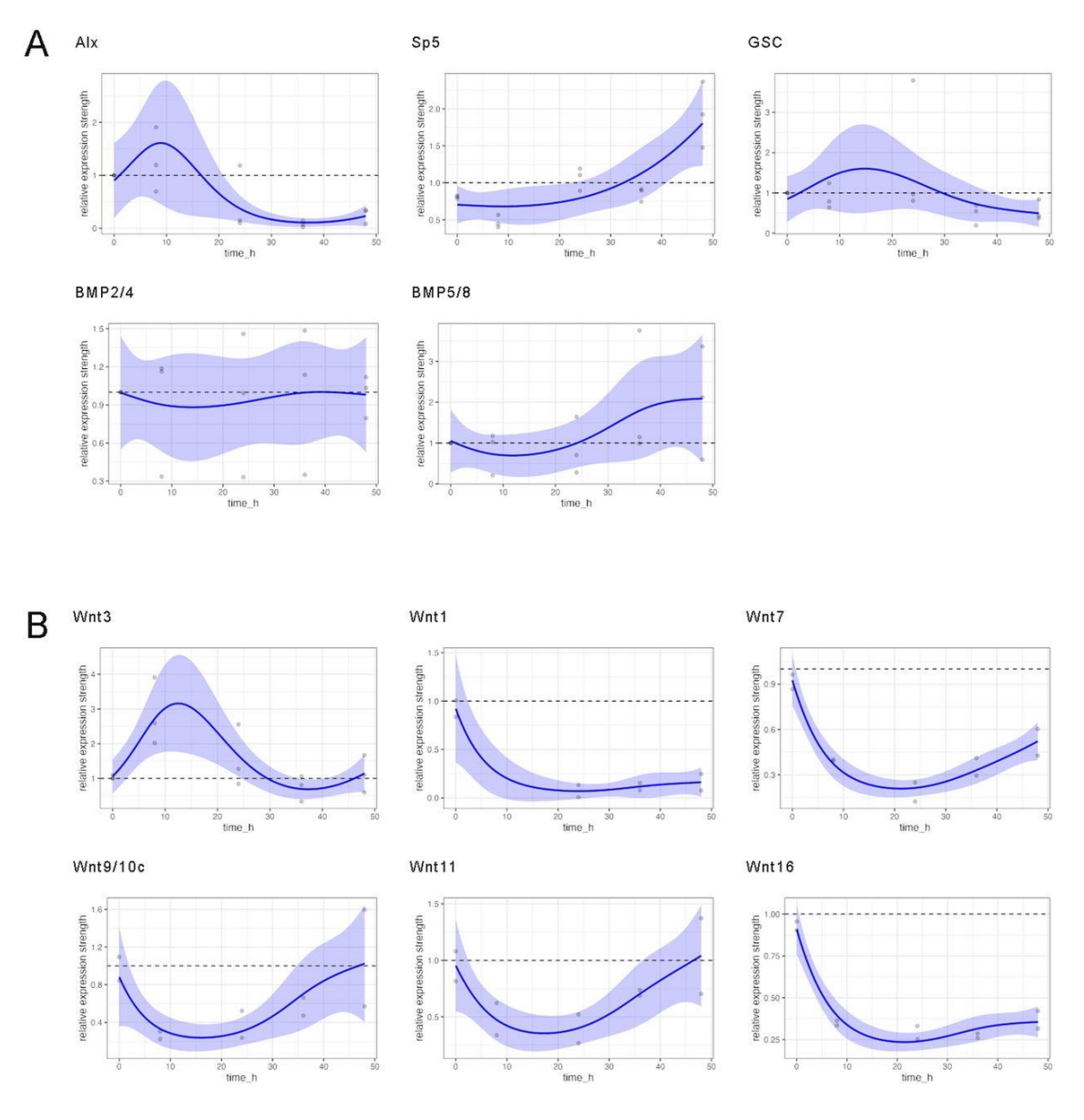


Figure S8.

GAM-based visualization of relative gene expression dynamics of iCRT14-treated regenerates.

GAM-based visualization of gene expression as measured by qRT–PCR in iCRT14-treated animals relative to control animals (y-axis) depending on the time after head removal (x-axis). Gray points show raw data (quotients of mean values of iCRT14-treated relative to DMSO-treated animals), the colored lines show the smooth GAM-based estimates, and color-shaded areas are 95% confidence bands. Gene expression was followed for 48 h after head removal in DMSO control and iCRT14. For time point 0, polyps were used immediately after head removal without any exposure to inhibitor or control medium. (A) *HyAlx*, *CnGsc*, *HySp5*, *HyBMP2/4*,

and *HyBMP5/8*. (B) *HyWnt3* and *HyWnt1*, *HyWnt7*, *HyWnt9/10c*, *HyWnt11*, and *HyWnt16* during 48 h. Relative normalized expression was related to the housekeeping genes *GAPDH*, *RPL13*, *EF1a*, and *PPIB*.

4. Discussion

4.1 The establishment of NICD-overexpressing and Notch-knockdown transgenic *Hydra*

Previous research on the role of the Notch signalling pathway in *Hydra* relied on pharmacological inhibition with DAPT or SAHM1. DAPT inhibits the nuclear translocation of NICD after receptor activation by blocking the proteolytic activity of presenilin (Geling, Steiner et al. 2002). SAHM1 targets the transcriptional activation function of the NICD-CSL complex by competing with mastermind-like co-activators (Moellering, Cornejo et al. 2009). It has been previously shown that DAPT treatment of *Hydra* polyps inhibited the translocation of NICD to the nucleus (Käsbauer, Towb et al. 2007). Moreover, SAHM1 has been shown to block the transcriptional activation of a *HyHes* reporter gene (Münder, Tischer et al. 2013). As a result of DAPT treatment, the post-mitotic differentiation of nematocytes and the development of female germ cells have been interrupted. Moreover, DAPT or SAHM1 treatment resulted in irregularly distributed tentacles in adult *Hydra*. It also prevented head regeneration after decapitation (Münder, Tischer et al. 2013), but not the regeneration of feet (Münder, Käsbauer et al. 2010). However, direct evidence that the observed phenotypes were due to Notch inhibition was lacking.

Therefore, I constructed NICD-overexpressing and Notch-knockdown transgenic *Hydra* in this study. I received one strain with mosaic transgenic signals from 23 hatchlings injected with NICD-pHyVec11. From this strain, two fully transgenic strains were developed: one with ectodermal transgene expression and another with endodermal transgene expression. On the other hand, of 23 Notch-hairpin-shRNA injected hatchlings, nine strains showed transgenic signals, which eventually generated four fully transgenic strains expressing the Notch-hairpin construct in both the entire ectoderm and the endoderm. After establishing fully transgenic *Hydra* strains, I detected the expression of Notch and its potential targets. Surprisingly, the NICD-overexpressing *Hydra* strains, which exhibited over tenfold upregulation of *NICD*, displayed a downregulation of potential Notch targets, including *Sp5* and *HyAlx*. In contrast, the *c-fos-like* gene *HyKayak* was upregulated. These results are consistent with those detected in DAPT-treated polyps, indicating that NICD-overexpression exerts a dominant negative effect. A similar

phenomenon has been reported in studies of Notch transgenes in *Drosophila*. For instance, the overexpression of the Notch intracellular domain lacking the C-terminal sequence, primarily the Ram23 domain and Ankyrin repeats, in middle-stage *Drosophila* embryos suppressed SuH-dependent Notch signalling by reducing the availability of full-length Notch and SuH (Wesley and Mok 2003, LeComte, Wesley et al. 2006). Additionally, the overexpression of the Notch extracellular domain in adult *Drosophila* also produced a dominant negative effect by forming non-functional complexes with Notch ligands, thereby sequestering the endogenous Notch receptors (Rebay, Fehon et al. 1993, Jacobsen, Brennan et al. 1998, LeComte, Wesley et al. 2006).

In contrast, the expressions of *Sp5*, *HyAlx*, and *HyKayak* in Notch-knockdown polyps did not show a significant difference. This might have been due to the relatively low levels of Notch downregulation (30% to 50%) achieved by using only a single Notch-hairpin construct.

I further compared the phenotypes of NICD-overexpressing and Notch-knockdown transgenic *Hydra*. Interestingly, phenotypes like "two-headed", "ectopic tentacles", and "Y-shaped" were observed in both NICD-overexpressing and Notch-knockdown strains. This similarity of phenotypes further confirms the dominant negative effect after overexpressing NICD. Except for the above-mentioned shared phenotypes, I also observed the "multiple heads" phenotype in NICD-overexpressing strains and the "two-feet" phenotype in Notch-knockdown strains, respectively. This indicates that there are also differences between NICD-overexpressing polyps and Notch-knockdown polyps, despite NICD overexpression causing some loss-of-function effects.

Overall, it appeared that the generation of NICD-overexpressing transgenic *Hydra* was more challenging compared to Notch-knockdown transgenic *Hydra*. As four strains of Notch-knockdown *Hydra* with transgenes in both epithelial layers were successfully obtained, only one strain of NICD-overexpressing *Hydra* was generated, which expressed NICD in either the ectoderm or the endoderm, but not in both. In addition, NICD-overexpressing transgenic *Hydra* exhibited more pronounced and complex effects on Notch downstream targets, observed phenotypes, as well as the difference in head regeneration (discussed below) in comparison to Notch-knockdown *Hydra*.

4.2 HvNotch function in *Hydra* budding

The *Hydra* bud can form a foot and then detach from the parent when reaching a certain length. Foot formation requires a constriction process happening at the base of the bud. During this process, *kringelchen*, the *Hydra* homolog of the FGF-receptor (Sudhop, Coulier et al. 2004), is expressed in a narrow, ring-like band at the parent-bud boundary. The matrix metalloprotease *MMP-A3* is expressed in the same cells as *kringelchen*, while *HyHes* is expressed transiently at the constriction stage of budding (stage 8 according to Otto and Campbell 1977) in the ectodermal epithelial cells at the base of the bud, adjacent to the *kringelchen*-expressing cells (Münder, Käsbauer et al. 2010). Previous research demonstrated that Notch inhibition with DAPT completely abolished the expression of *MMP-A3* and *HyHes* at the parent-bud boundary, and disturbed the expression pattern of *kringelchen*, which instead showed a diffused and expansive expression zone across the parent and bud. Consequently, foot formation of buds and further bud detachment were prevented, leading to the appearance of Y-shaped animals in DAPT-treated *Hydra* (Münder, Käsbauer et al. 2010).

In our experiments, all strains of NICD-overexpressing and Notch-knockdown transgenic *Hydra* showed Y-shaped animals, similar to those in 48 h DAPT-treated *Hydra* (Pan, Mercker et al. 2024). This indicates that NICD-overexpression or Notch-knockdown can inhibit the expression of the *HyHes* gene at the parent-bud boundary, resulting in a "Y-shaped" phenotype.

Downregulation of total *HyHes* expression in either NICD-overexpressing or Notch-knockdown polyps was not detected by RT-qPCR, indicating the existence of HvNotch-independent regulation mechanisms on *HyHes* expression in *Hydra*. As reported in other organisms, the expression of *Hes* genes can also be regulated by different signalling pathways in a Notch-independent manner. For example, the expression of *Hes1* and *Hes5* can be regulated by the Sonic Hedgehog (Shh) pathway in mouse retinal progenitor cells (Wall, Mears et al. 2009) and multipotent mesodermal cells (Ingram, McCue et al. 2008), which appears to be independent of functional RBPJ-k factors. *Hes1* expression in mouse P19 cells (embryonic teratocarcinoma cell lines) can also respond to hypoxia independently of the Notch pathway (Zheng, Narayanan et al. 2017). Moreover, Human

Hes1 expression in endothelial cells can be regulated by the c-Jun N-terminal kinase (JNK) pathway (Curry, Reed et al. 2006). Thus, the regulation of Notch on Hes expression obviously depends on the cellular and developmental context. In addition, it was reported that the Notch signalling crosstalks with other signalling pathways, such as the Wnt/β-catenin and the TGF-β/BMP pathways, to regulate the expression of Notch receptors, ligands, as well as its target gene Hes1 (Blokzijl, Dahlqvist et al. 2003, Shimizu, Kagawa et al. 2008, Guo and Wang 2009, Kurpinski, Lam et al. 2010, Li, Jia et al. 2012, Borggrefe, Lauth et al. 2016).

4.3 HvNotch function in *Hydra* axis patterning

Hydra has an organizing centre in the apical hypostome, which we call the "head organizer" according to the properties of the Spemann-Mangold organizer. Hydra organizer tissue can induce the formation of the second axis after being transplanted into the body of a host polyp (Browne 1909, Bode 2012). In addition, the Hydra organizer produces a head activation gradient and a head inhibition gradient along the body column (MacWilliams 1983a, MacWilliams 1983b). These two gradients together allow Hydra to form a head only at the apical end, thus producing a single body axis by inhibiting the formation of additional heads in other regions. The canonical Wnt/β-catenin signalling pathway is critical for this process (Hobmayer, Rentzsch et al. 2000, Broun, Gee et al. 2005).

Treating *Hydra* with alsterpaullone, which inhibits GSK-3 and thus activates nuclear translocation of β-catenin in the absence of a Wnt signal, induces transient ectopic expression of *HyWnt3* in spots along the body column and subsequently the formation of an "ectopic tentacles" phenotype (Broun, Gee et al. 2005). This phenotype was also seen in both NICD-overexpressing and Notch-knockdown transgenic animals (Pan, Mercker et al. 2024). Further research has shown that β-catenin-overexpressing transgenic polyps exhibit "organizer" activity in the body column tissue, resulting in "two-head", or "multiple heads" phenotypes with a normal *HyWnt3* expression pattern at the tip of each hypostome (Gee, Hartig et al. 2010). Moreover, HyWnt3-overexpressing *Hydra*, HAS-7 (*Hydra* astacin-7 protein, a member of the astacin proteinase family with HyWnt3-specific proteolytic activity) knockdown *Hydra*, as well as our transgenic *Hydra* strains all showed

these two phenotypes (Ziegler, Yiallouros et al. 2021, Pan, Mercker et al. 2024). The ectopic heads in these multiple-headed animals were mostly located in the middle part of the body column or at the budding region. Occasionally, I observed that some ectopic heads appeared near the original head as a "bouquet", which was like the recently reported phenotype in Sp5 (a transcriptional repressor of *HyWnt3*) siRNA-silenced animals (Vogg, Beccari et al. 2019, Pan, Mercker et al. 2024). This result is consistent with the downregulation of *Sp5*, as shown by RT-qPCR in NICD-overexpressing *Hydra*.

In addition, I observed a "two-feet" phenotype in Y-shaped Notch-knockdown animals, which has also been previously reported in β-catenin-overexpressing animals. It is noted that additional feet are formed in "multiple-head" animals with a huge size, which eventually leads to the separation of such colony-like animals (Gee, Hartig et al. 2010). In addition, the "two-feet" phenotype was also observed in double-headed animals after *HAS-7* siRNA knockdown (Ziegler, Yiallouros et al. 2021). Here, the formation of two feet in Y-shaped animals also led to their separation into two polyps. In addition, I observed "ectopic foot" phenotypes in Notch-knockdown polyps with a normal axis/a single head, which was not reported before in *Hydra*.

Taken together, the appearance of phenotypes such as "ectopic tentacles", "two-headed", "multiple heads" and "two feet" in our NICD-overexpressing or Notch-knockdown transgenic Hydra lines indicated that abnormal expression of Notch on Hydra disrupted its axis patterning. This effect was similar to the phenotypes observed following HyWnt3 or β -catenin overexpression in Hydra. These observations suggested that the Notch signalling pathway may interact with the canonical Wnt/β -catenin signalling pathway in Hydra, which is further discussed below.

4.4 The roles of HvNotch on Hydra head regeneration are context-dependent

Our latest studies in *Hydra* have shown that *Hydra* head regeneration involves two separate processes: hypostome regeneration and tentacle regeneration. After decapitation, DAPT treatment inhibited the expression of *Wnt* genes and blocked hypostome regeneration, while tentacle regeneration still occurred occasionally and irregularly (Münder, Tischer et al. 2013, Steichele, Sauermann et al. 2025). In contrast, iCRT14 treatment, which inhibits the interaction between β-catenin and TCF, only

suppressed the expression of HyAlx and prevented tentacle regeneration, whereas hypostome regeneration and organizer formation remained unaffected (Steichele, Sauermann et al. 2025). These results suggest that Notch signalling is essential not only for the expression of HyWnt3 at the tip of the hypostome but also for maintaining the specific expression pattern of HyAlx at the tentacle boundary. Notably, since HyAlx expression is also dependent on the canonical Wnt/ β -catenin signalling pathway, this indicates that both the Notch and canonical Wnt/ β -catenin signalling pathways are crucial for the head regeneration process in Hydra.

Additionally, research on *Hydra* head regeneration has reported that the appearing order of hypostome and tentacle regeneration varies depending on the position of amputation (Technau and Holstein 1995). In apical regenerates, in which the cut is made just underneath the tentacle ring, tentacle markers appear first. In more basal regenerates (cut at 70% - 80% of the body column), the hypostome markers are expressed slightly earlier. For the middle gastric regenerates (cut at 50% of the body column), an intermediate state is produced.

In apical regeneration, NICD-overexpressing transgenic animals regenerated a normal and functional head 48 h after decapitation. In contrast, Notch-knockdown animals exhibited either complete non-regeneration or regeneration of a single tentacle in around 20% of cases, resembling the regeneration defects observed in DAPT-treated *Hydra*. Furthermore, fluorescence in-situ hybridisation (FISH) of *HyWnt3* revealed that *HyWnt3* expression was abolished in these 20% of regenerates. However, *HyAlx* was expressed as a large ring at the apical tip or the base of the regenerated single tentacle in non-regeneration polyps or polyps with aberrant tentacles (Pan, Mercker et al. 2024). These changes in the expression patterns of *HyWnt3* and *HyAlx* are similar to those in DAPT-treated regenerating *Hydra* (Münder, Tischer et al. 2013).

We assumed that the Notch signalling pathway can inhibit the initial signal that appears following decapitation during head regeneration. After apical decapitation, tentacle markers are expressed first. Notch signalling then suppresses the tentacle fate of cells in the regenerating tip, possibly through *BMP5/8b*, which allows *HyWnt3* to be exclusively expressed at the tip and promotes the formation of a new hypostome. Meanwhile, this

process facilitates the redistribution of *HyAlx*-expressing cells to the base of newly emerging tentacle buds, thereby establishing the tentacle boundaries. This coordination between hypostome formation and subsequent tentacle development is termed "longranging help" (Münder, Tischer et al. 2013).

When Notch signalling is inhibited with DAPT or interfered with by RNAi, tentacle fate is activated at the regenerating tip, while *HyWnt3* expression and hypostome fate are suppressed. This disruption prevents the separation of supposed hypostome and tentacle precursor cells, causing the expression of *HyAlx* as a large ring at the regenerating tip. Consequently, this leads to the formation of non-regenerating polyps or polyps with a single tentacle, as observed through *HyAlx*-FISH staining in Notch-knockdown regenerating *Hydra*.

In middle gastric regeneration, where animals were cut in the middle of the body column, we observed the formations of "two-headed" and "ectopic tentacles" phenotypes in both NICD-overexpressing and Notch-knockdown polyps three days post-amputation (Pan, Mercker et al. 2024). The presence of these common phenotypes in middle gastric regeneration further supports our conclusion that NICD overexpression produces a dominant-negative effect in *Hydra*. Additionally, Notch-knockdown strains displayed a higher incidence of irregular regeneration, occurring in 40% of cases compared to 20% in NICD-overexpressing strains. Combined with the results from apical regeneration, this suggests that the impact on head regeneration is consistently stronger in Notch-knockdown strains than in NICD-overexpressing strains, regardless of the position of the amputation.

In the middle gastric regenerates, the signals for hypostome and tentacle regeneration appear randomly and can sometimes emerge simultaneously. When hypostome signals appear first, Notch signalling prevents the overexpression of *HyWnt3*, ensuring the formation of a single hypostome/head followed by evenly spaced tentacles. However, upon Notch inhibition, these head formation signals are derepressed, leading to the formation of "two-headed" regenerates. This phenotype is highly similar to the "bouquet" phenotype observed in Sp5-RNAi regenerates (Vogg, Beccari et al. 2019). Furthermore, if hypostome and tentacle signals appear simultaneously and at comparable levels, Notch

inhibition may activate both fates. This would result in the formation of two-headed polyps with ectopic tentacles located close to the head structures, as seen in Notch-knockdown strains.

In summary, Notch interference affects *Hydra* head regeneration differently depending on whether the cut is made just below the tentacles or at the middle-gastric levels. This suggests that the function of the Notch signalling pathway in *Hydra* head regeneration is context-dependent, a phenomenon also observed in other organisms. One possible explanation for this variability is the extensive network of downstream responsive genes regulated by Notch.

The studies of genome-wide differential transcriptome analyses across various organisms have identified a considerable variety of Notch target genes. They include genes associated with the differentiation process of murine embryonic stem cells (Meier-Stiegen, Schwanbeck et al. 2010, Schwanbeck, Martini et al. 2011), genes identified in different human T-ALL cell lines (Palomero, Lim et al. 2006, Dohda, Maljukova et al. 2007, Chadwick, Zeef et al. 2009), and those found in *Drosophila* myogenic cells under different treatments (Krejci, Bernard et al. 2009). These findings support the context-specific nature of Notch signalling. Moreover, Notch target genes comprise both transcriptional activators and repressors, which can sequentially activate or repress secondary targets, thereby contributing to the complex and diverse functions of the Notch pathway in various biological contexts. Additionally, crosstalk reactions between the Notch signalling pathway and other pathways, such as BMP, Wnt, Hedgehog, and MAPK-ERK, further increase Notch-responsive diversity by co-regulating the expression of common targets or mutually controlling core components within these pathways (Andersson, Sandberg et al. 2011).

4.5 Interactions between HvNotch, Wnt and TGF-β/BMP signalling pathways in *Hydra*

In *Hydra*, various lines of evidence have suggested interactions between the Notch signalling pathway and the Wnt and TGF-β/BMP signalling pathways, which appeared to be especially important for *Hydra* axis patterning and head regeneration. For instance, similar phenotypes have been observed in Notch-transgenic, HyWnt3-overexpressing,

and β -catenin-overexpressing *Hydra* lines (Gee, Hartig et al. 2010, Ziegler, Yiallouros et al. 2021, Pan, Mercker et al. 2024). Additionally, alterations in downstream gene expression patterns following Notch inhibition further support these interactions.

As reported by Moneer et al (2021), a comparative transcriptome analysis of DAPT-treated *Hydra* has revealed that Wnt signalling components, including *HyWnt7* (a Wnt ligand according to Lengfeld, Watanabe et al. 2009) and *Tcf7-like 2* (a key transcriptional factor in the Wnt signalling pathway according to Hobmayer, Rentzsch et al. 2000), were downregulated after a 48 h DAPT treatment and quickly recovered their expression levels 3 h after DAPT removal. Furthermore, during the head regeneration process following apical head removal, DAPT treatment almost completely abolished the expression of most canonical *Wnt* genes, including *HyWnt1*, *Wnt3*, *Wnt7*, *Wnt9/10c*, *Wnt11* and *Wnt16* (Steichele, Sauermann et al. 2025). *BMP2/4*, expressed in epithelial cells of the *Hydra* head (Watanabe, Schmidt et al. 2014), was also significantly downregulated after DAPT treatment. By contrast, *BMP5/8b*, expressed at the base of *Hydra* tentacles (Reinhardt, Broun et al. 2004), was upregulated considerably.

These findings suggest that Notch signalling can potentially regulate the expression of key components within the Wnt and TGF-β/BMP signalling pathways, including ligands and downstream transcription factor genes. Since canonical *Wnt* genes and *BMP2/4* are primarily expressed in the *Hydra* head and play a crucial role in *Hydra* axis patterning (Lengfeld, Watanabe et al. 2009, Watanabe, Schmidt et al. 2014, Siebert, Farrell et al. 2019), changes in the expression levels of these genes by Notch inhibition could explain the reasons behind the failure of head regeneration when Notch activity is blocked. Moreover, these changes in gene expression may shift the head activation gradient, potentially leading to the formation of ectopic heads or tentacles on the upper part of the body column.

In addition, transcriptome analysis upon DAPT treatment demonstrated that foot-expressing genes, such as *HmaTGF3* (the ligand in the TGF-β signalling pathway according to Watanabe, Schmidt et al. 2014) and *APCDD1* (a negative regulator of Wnt signalling according to Shimomura, Agalliu et al. 2010), were both upregulated after 48 h of Notch inhibition. These findings indicate that the Notch signalling pathway can affect

foot formation by regulating the expression of components of the TGF- β and Wnt signalling pathways. It also provides insight into the formation of a "two feet" phenotype in Notch-knockdown animals.

Therefore, we propose that the head regeneration and axis patterning phenotypes observed in Notch loss-of-function transgenic animals result from disrupted interactions between the Notch signalling pathway and both the canonical Wnt signalling pathway and the TGF- β /BMP pathway.

4.6 The possible inhibitor of *HyWnt3* expression, HyKayak, is inhibited by the Notch signalling pathway

HyWnt3 is expressed at the tip of the hypostome and is known to play a critical role in establishing the Hydra head organizer (Hobmayer, Rentzsch et al. 2000). The transcriptome analysis and RT-qPCR results on DAPT-treated polyps both demonstrated that most head-expressing genes, including HyWnt3, are significantly downregulated after Notch inhibition, directly contributing to the failed head regeneration after decapitation (Münder, Tischer et al. 2013, Moneer, Siebert et al. 2021). However, there is no evidence to suggest that HyWnt3 is a direct target of Notch, although an analysis of the proximal elements of the HyWnt3 upstream promoter identified a single RBPJ binding site (Nakamura, Tsiairis et al. 2011). Therefore, the activation of HyWnt3 by Notch might be indirect. Here, we hypothesized the existence of HyWnt3 repressors, which might be under the control of the Notch signalling pathway. This seems plausible, given that the most prominent Notch-target genes, like Hes-family members, encode transcriptional repressors. If HyHes would repress an inhibitor of HyWnt3 expression, HyWnt3 could be indirectly upregulated by Notch-signalling under certain circumstances. Conversely, in the presence of Notch inhibition, such repressors of HyWnt3 would be upregulated.

By analysing the upregulated Notch-responsive genes following DAPT treatment, we found a gene, t5955aep, which encodes a *Hydra* homolog of the proto-oncogene *fos*, referred to as *HyKayak*. *HyKayak* expression was upregulated after DAPT treatment and recovered to baseline levels 3 h after DAPT removal (Moneer, Siebert et al. 2021). This suggests that *HyKayak* might be regulated by a Notch target, such as HyHes.

HyKayak has a highly conserved basic leucine zipper domain (bZiP domain), which consists of a basic region responsible for the sequence-specific DNA binding and a leucine zipper region that mediates dimerization. In addition, HyKayak was found to form heterodimers with HyJun (t19405aep) but did not form homodimers with itself. This behaviour is similar to that of human Fos, which typically dimerizes with Jun to form the AP-1 (activating protein 1) complex (Kouzarides and Ziff 1988, Karin, Liu et al. 1997).

The Fos-Jun heterodimer is primarily known for trans-activating target genes by binding to TPA-responsive element (TRE) or cAMP response elements (CRE). However, studies have shown that Fos can also act as a repressor for itself and several immediate-early genes, like *Egr-1* and *Egr-2*, under serum stimulation conditions, which is dependent on several sites within the 5' regulatory sequence and the C-terminal region of c-Fos (Sassone-Corsi, Sisson et al. 1988, Wilson and Treisman 1988, Gius, Cao et al. 1990, Ofir, Dwarki et al. 1990). Moreover, Fos proteins with a deletion of the bZiP domain maintain the repression function, indicating that this repression function does not need interaction with Jun proteins (Gius, Cao et al. 1990). In addition to immediate-early genes, Fos can also repress the transcriptional activity of muscle-specific genes like *myogenin* and *MyoD* by binding to their bHLH regions (Lassar, Thayer et al. 1989, Li, Chambard et al. 1992, Barutcu, Elizalde et al. 2022). Furthermore, Fos inhibits the promoter activity of the cardiac-specific gene *ANF*, but this inhibition does not rely on the DNA-binding activity of AP-1 or the C-terminal region of Fos (McBride, Robitaille et al. 1993). These studies demonstrate that the function of Fos is flexible and context-dependent.

In our model, we hypothesized that HyKayak might inhibit the expression of *HyWnt3*, which was first supported by the presence of CRE sites in the regulatory sequence of *HyWnt3* (Cazet, Cho et al. 2021). Furthermore, *HyKayak* interference using shRNA resulted in an upregulation of *HyWnt3* expression. We also noted that *HyJun* (t19405aep) was upregulated following *HyKayak* interference. This observation is similar to previous studies in human prostate cells, where Fos knockdown led to the upregulation of *Jun* (Riedel, Cai et al. 2021). In addition, treating regenerating *Hydra* with the AP-1 complex inhibitor T5224, which inhibits the DNA binding activity of AP-1, significantly upregulated the expression of both *HyWnt3* and *HyJun* during the entire regeneration process. Together, these experiments support the role of HyKayak in repressing *HyWnt3*. The

T5224 treatment further suggests that this inhibitory effect may depend on the DNA-binding activity of the AP-1 complex.

However, *Hydra* that was treated with T5224 or underwent *Hykayak* interference displayed normal head regeneration. This indicates that the upregulation of *HyWnt3* resulting from HyKayak knockdown is not sufficient to induce the regeneration of multiple heads, as observed in Sp5 knockdown *Hydra* (Vogg, Beccari et al. 2019). Furthermore, when regenerating *Hydra* was treated together with both DAPT and T5224 or with DAPT alongside *HyKayak* interference, *HyWnt3* expression did not return to baseline levels, and the failed head regeneration was not rescued. This suggests the possibility of other unidentified repressors of *HyWnt3* that may cooperate with HyKayak.

In addition to HyKayak, there is another Fos protein in *Hydra*, referred to as Fos_Cazet (t25302aep) (Cazet, Cho et al. 2021). HyKayak is expressed in the ectodermal cells of the head, tentacle, and body column regions, while Fos_Cazet is uniformly expressed in the entire ectoderm and endoderm, as well as in gland cells (Siebert, Farrell et al. 2019). Previous studies have shown that bZiP transcription factors (TFs), including *Fos_Cazet* and *HyJun* (t19405aep), are transiently upregulated 3 h post-amputation in *Hydra*. Furthermore, bZiP TFs are considered promising positive regulators of early generic injury-responsive genes, such as *wntless*, *Wnt3*, *Wnt9/10*, and *Sp5*, as these genes all contain CRE sites in their regulatory sequences (Cazet, Cho et al. 2021). In contrast, *HyKayak* expression continuously increased throughout the regeneration process, up to 48 h after decapitation. This hints at separate roles for HyKayak and Fos_Cazet in regulating *HyWnt3* expression. Additionally, recent research on the JNK pathway has demonstrated that inhibiting this pathway, which reduces the formation and activity of the AP-1 complex, leads to an upregulation of *HyWnt3* expression within the first 6 h post-amputation (Tursch, Bartsch et al. 2022).

Given these findings, it seems reasonable to assume that HyKayak-HyJun dimers act as repressors of *HyWnt3*. Therefore, the interference with *HyKayak* alone is insufficient to induce a substantial increase in *HyWnt3* expression and to promote further regeneration phenotypes, such as the formation of multiple heads.

5. Conclusion and outlook

In *Hydra*, the Notch signalling pathway has been reported to play a role in the establishment of parent-bud boundaries and the head regeneration process of apical regenerates. In my research, I confirmed these findings by creating NICD-overexpressing and Notch-knockdown transgenic *Hydra* strains, which showed phenotypes similar to those observed in DAPT- or SHAM1-treated *Hydra*, including Y-shaped animals and failed head regeneration following apical decapitation. Furthermore, I found that the disruption of HvNotch functions generated a different effect in apical versus more basal regenerates, probably by inhibiting signals related to tentacle fate or hypostome fate. Notably, the Notch transgenic *Hydra* strains displayed features like "ectopic tentacle", "two-headed", "multiple heads" and "two feet" animals, suggesting a potential new role for HvNotch in axis patterning by maintaining activation gradients for head and foot development (see Fig. 3A). This notion was supported by comparative transcriptome and RT-qPCR data upon DAPT treatment, in which the head-expressing genes were mainly downregulated, whereas foot-expressing genes were upregulated (see Fig. 3B).

In addition, according to the transcriptome analysis, we identified a transcription factor gene, *HyKayak*, which is a *Hydra* homolog of *c-fos*. Since *HyKayak* expression was found to be upregulated after DAPT treatment, with its levels returning to normal 3 h after DAPT removal, we hypothesized that HyKayak may be a target of Notch-responsive repressors and could function as a *HyWnt3* inhibitor. In my studies using inhibitor treatment during the head regeneration process, I observed that *HyWnt3* expression was increased following the suppression of HyKayak's DNA-binding activities. Furthermore, targeted shRNA interference of *HyKayak* also led to an increase in *HyWnt3* expression, further supporting our hypothesis (see Fig. 3C). However, direct evidence of the interaction between HyKayak and *HyWnt3* could not be provided within the scope of this thesis. Moreover, the upregulation of *HyWnt3* expression observed in my experiments did not result in obvious regenerative phenotypes, suggesting the possibility of an unidentified repressor of *HyWnt3*. Therefore, further investigation into the role of HyKayak in *Hydra* patterning and its underlying mechanisms is warranted in future research.

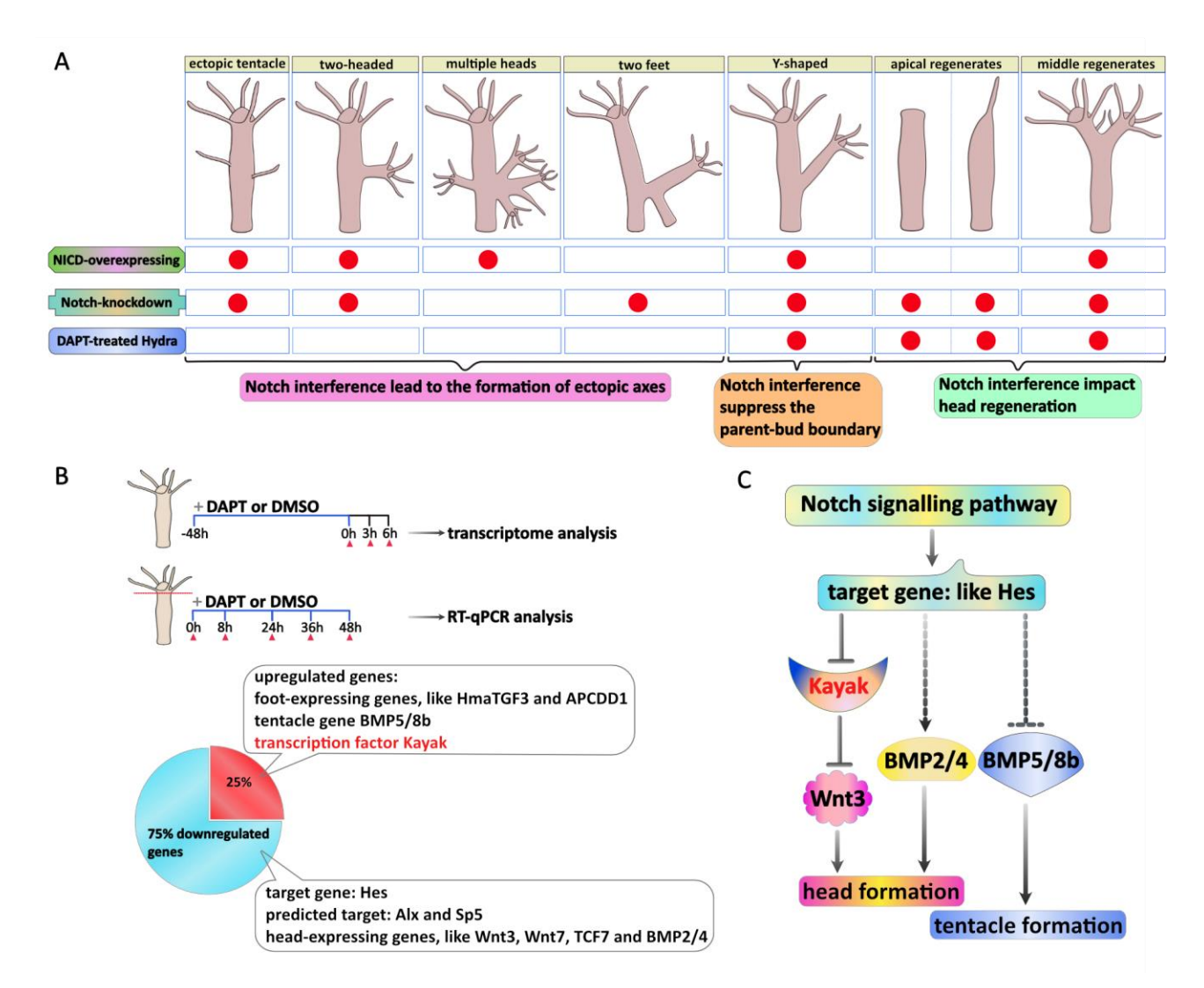


Fig. 3 Summary of key findings. (A) The Notch signalling pathway plays a role in axis patterning, formation of the parent-bud boundary, and head regeneration in *Hydra*. (B) *HyKayak* is identified as one of the upregulated genes following DAPT treatment. (C) Proposed model of the interaction between the Notch signalling pathway, Wnt genes, and BMP genes in *Hydra*.

6. Reference

Andersson E.R., Sandberg R. and Lendahl U. (2011). "Notch signaling: simplicity in design, versatility in function." Development 138(17): 3593-3612.

Barutcu A.R., Elizalde G., Gonzalez A.E., Soni K., Rinn J.L., Wagers A.J. and Almada A.E. (2022). "Prolonged FOS activity disrupts a global myogenic transcriptional program by altering 3D chromatin architecture in primary muscle progenitor cells." Skelet Muscle 12(1): 20.

Beddington R.S. (1994). "Induction of a second neural axis by the mouse node." Development 120(3): 613-620.

Blokzijl A., Dahlqvist C., Reissmann E., Falk A., Moliner A., Lendahl U. and Ibanez C.F. (2003). "Cross-talk between the Notch and TGF-beta signaling pathways mediated by interaction of the Notch intracellular domain with Smad3." J Cell Biol 163(4): 723-728.

Bode H.R. (2003). "Head regeneration in Hydra." Dev Dyn 226(2): 225-236.

Bode H.R. (2012). "The head organizer in Hydra." Int J Dev Biol 56(6-8): 473-478.

Borggrefe T., Lauth M., Zwijsen A., Huylebroeck D., Oswald F. and Giaimo B.D. (2016). "The Notch intracellular domain integrates signals from Wnt, Hedgehog, TGFbeta/BMP and hypoxia pathways." Biochim Biophys Acta 1863(2): 303-313.

Bray S.J. (2006). "Notch signalling: a simple pathway becomes complex." Nature Reviews Molecular Cell Biology 7(9): 678-689.

Broun M., Gee L., Reinhardt B. and Bode H.R. (2005). "Formation of the head organizer in hydra involves the canonical Wnt pathway." Development 132(12): 2907-2916.

Broun M., Sokol S. and Bode H.R. (1999). "Cngsc, a homologue of goosecoid, participates in the patterning of the head, and is expressed in the organizer region of Hydra." Development 126(23): 5245-5254.

Browne E.N. (1909). "The production of new hydranths in Hydra by the insertion of small grafts." J Exp Zool 7: 1-23.

Campbell R.D. (1967). "Tissue dynamics of steady state growth in Hydra littoralis. II. Patterns of tissue movement." J Morphol 121(1): 19-28.

Campbell R.D. and David C.N. (1974). "Cell cycle kinetics and development of Hydra attenuata. II. Interstitial cells." J Cell Sci 16(2): 349-358.

Cazet J.F., Cho A. and Juliano C.E. (2021). "Generic injuries are sufficient to induce ectopic Wnt organizers in Hydra." Elife 10.

Chadwick N., Zeef L., Portillo V., Fennessy C., Warrander F., Hoyle S. and Buckle A.M. (2009). "Identification of novel Notch target genes in T cell leukaemia." Mol Cancer 8: 35.

Curry C.L., Reed L.L., Nickoloff B.J., Miele L. and Foreman K.E. (2006). "Notch-independent regulation of Hes-1 expression by c-Jun N-terminal kinase signaling in human endothelial cells." Lab Invest 86(8): 842-852.

David C.N. and Campbell R.D. (1972). "Cell cycle kinetics and development of Hydra attenuata. I. Epithelial cells." J Cell Sci 11(2): 557-568.

David C.N. and Gierer A. (1974). "Cell cycle kinetics and development of Hydra attenuata. III. Nerve and nematocyte differentiation." J Cell Sci 16(2): 359-375.

del Álamo D., Rouault H. and Schweisguth F. (2011). "Mechanism and significance of cisinhibition in Notch signalling." Curr Biol 21(1): R40-47.

Dohda T., Maljukova A., Liu L., Heyman M., Grander D., Brodin D., Sangfelt O. and Lendahl U. (2007). "Notch signaling induces SKP2 expression and promotes reduction of p27Kip1 in T-cell acute lymphoblastic leukemia cell lines." Exp Cell Res 313(14): 3141-3152.

Driever W. (1995). "Axis formation in zebrafish." Curr Opin Genet Dev 5(5): 610-618.

Engel U., Pertz O., Fauser C., Engel J., David C.N. and Holstein T.W. (2001). "A switch in disulfide linkage during minicollagen assembly in Hydra nematocysts." EMBO J 20(12): 3063-3073.

Fedders H., Augustin R. and Bosch T.C. (2004). "A Dickkopf-3-related gene is expressed in differentiating nematocytes in the basal metazoan Hydra." Dev Genes Evol 214(2): 72-80.

Gahan J.M., Schnitzler C.E., DuBuc T.Q., Doonan L.B., Kanska J., Gornik S.G., Barreira S., Thompson K., Schiffer P., Baxevanis A.D. and Frank U. (2017). "Functional studies on the role of Notch signaling in Hydractinia development." Dev Biol 428(1): 224-231.

Gauchat D., Kreger S., Holstein T. and Galliot B. (1998). "prdl-a, a gene marker for hydra apical differentiation related to triploblastic paired-like head-specific genes." Development 125(9): 1637-1645.

Gee L., Hartig J., Law L., Wittlieb J., Khalturin K., Bosch T.C. and Bode H.R. (2010). "beta-catenin plays a central role in setting up the head organizer in hydra." Dev Biol 340(1): 116-124.

Geling A., Steiner H., Willem M., Bally-Cuif L. and Haass C. (2002). "A gamma-secretase inhibitor blocks Notch signaling in vivo and causes a severe neurogenic phenotype in zebrafish." EMBO Rep 3(7): 688-694.

Gierer A., Berking S., Bode H., David C.N., Flick K., Hansmann G., Schaller H. and Trenkner E. (1972). "Regeneration of hydra from reaggregated cells." Nat New Biol 239(91): 98-101.

Gierer A. and Meinhardt H. (1972). "A theory of biological pattern formation." Kybernetik 12(1): 30-39.

Gius D., Cao X.M., Rauscher F.J., 3rd, Cohen D.R., Curran T. and Sukhatme V.P. (1990). "Transcriptional activation and repression by Fos are independent functions: the C terminus represses immediate-early gene expression via CArG elements." Mol Cell Biol 10(8): 4243-4255. Gonsalves F.C., Klein K., Carson B.B., Katz S., Ekas L.A., Evans S., Nagourney R., Cardozo T., Brown A.M. and DasGupta R. (2011). "An RNAi-based chemical genetic screen identifies three small-molecule inhibitors of the Wnt/wingless signaling pathway." Proc Natl Acad Sci U S A 108(15): 5954-5963.

Grens A., Mason E., Marsh J.L. and Bode H.R. (1995). "Evolutionary conservation of a cell fate specification gene: the Hydra achaete-scute homolog has proneural activity in Drosophila." Development 121(12): 4027-4035.

Guo X. and Wang X.F. (2009). "Signaling cross-talk between TGF-beta/BMP and other pathways." Cell Res 19(1): 71-88.

Hensen V. (1876). "Beobachtungen über die Befruchtung und Entwicklung des Kaninchens und Meerschweinchens." Z. Anat. Entw. Gesh. 1: 353–423.

Hobmayer B., Jenewein M., Eder D., Eder M.K., Glasauer S., Gufler S., Hartl M. and Salvenmoser W. (2012). "Stemness in Hydra - a current perspective." Int J Dev Biol 56(6-8): 509-517.

Hobmayer B., Rentzsch F., Kuhn K., Happel C.M., von Laue C.C., Snyder P., Rothbacher U. and Holstein T.W. (2000). "WNT signalling molecules act in axis formation in the diploblastic metazoan Hydra." Nature 407(6801): 186-189.

Holstein T.W., Hobmayer E. and David C.N. (1991). "Pattern of epithelial cell cycling in hydra." Dev Biol 148(2): 602-611.

Huppert S.S., Jacobsen T.L. and Muskavitch M.A. (1997). "Feedback regulation is central to Delta-Notch signalling required for Drosophila wing vein morphogenesis." Development 124(17): 3283-3291.

Ingram W.J., McCue K.I., Tran T.H., Hallahan A.R. and Wainwright B.J. (2008). "Sonic Hedgehog regulates Hes1 through a novel mechanism that is independent of canonical Notch pathway signalling." Oncogene 27(10): 1489-1500.

Jacobsen T.L., Brennan K., Arias A.M. and Muskavitch M.A. (1998). "Cis-interactions between Delta and Notch modulate neurogenic signalling in Drosophila." Development 125(22): 4531-4540. Jose F. de Celis S.B., Antonio Garcia-Bellido (1997). "Notch signalling regulates veinlet expression and establishes boundaries between veins and interveins in the Drosophila wing " Development 124: 1919-1928.

Karin M., Liu Z. and Zandi E. (1997). "AP-1 function and regulation." Curr Opin Cell Biol 9(2): 240-246.

Käsbauer T., Towb P., Alexandrova O., David C.N., Dall'armi E., Staudigl A., Stiening B. and Bottger A. (2007). "The Notch signaling pathway in the cnidarian Hydra." Dev Biol 303(1): 376-390.

Käsbauer T., Towb P., Alexandrova O., David C.N., Dall'armi E., Staudigl A., Stiening B. and Böttger A. (2007). "The Notch signaling pathway in the cnidarian Hydra." Dev Biol 303(1): 376-390.

Katolikova N.V., Khudiakov A.A., Shafranskaya D.D., Prjibelski A.D., Masharskiy A.E., Mor M.S., Golovkin A.S., Zaytseva A.K., Neganova I.E., Efimova E.V., Gainetdinov R.R. and Malashicheva A.B. (2023). "Modulation of Notch Signaling at Early Stages of Differentiation of Human Induced Pluripotent Stem Cells to Dopaminergic Neurons." Int J Mol Sci 24(2).

Keramidioti A., Schneid S., Busse C., Cramer von Laue C., Bertulat B., Salvenmoser W., Hess M., Alexandrova O., Glauber K.M., Steele R.E., Hobmayer B., Holstein T.W. and David C.N. (2024). "A new look at the architecture and dynamics of the Hydra nerve net." Elife 12.

Koch A.W., Holstein T.W., Mala C., Kurz E., Engel J. and David C.N. (1998). "Spinalin, a new glycine- and histidine-rich protein in spines of Hydra nematocysts." J Cell Sci 111 (Pt 11): 1545-1554.

Kopan R. and Ilagan M.X. (2009). "The canonical Notch signaling pathway: unfolding the activation mechanism." Cell 137(2): 216-233.

Kouzarides T. and Ziff E. (1988). "The role of the leucine zipper in the fos-jun interaction." Nature 336(6200): 646-651.

Krejci A., Bernard F., Housden B.E., Collins S. and Bray S.J. (2009). "Direct response to Notch activation: signaling crosstalk and incoherent logic." Sci Signal 2(55): ra1.

Kurpinski K., Lam H., Chu J., Wang A., Kim A., Tsay E., Agrawal S., Schaffer D.V. and Li S. (2010). "Transforming growth factor-beta and notch signaling mediate stem cell differentiation into smooth muscle cells." Stem Cells 28(4): 734-742.

Lai E.C. (2004). "Notch signaling: control of cell communication and cell fate." Development 131(5): 965-973.

Lassar A.B., Thayer M.J., Overell R.W. and Weintraub H. (1989). "Transformation by activated ras or fos prevents myogenesis by inhibiting expression of MyoD1." Cell 58(4): 659-667.

LeComte M., Wesley U.V., Mok L.P., Shepherd A. and Wesley C. (2006). "Evidence for the involvement of dominant-negative Notch molecules in the normal course of Drosophila development." Dev Dyn 235(2): 411-426.

Lengfeld T., Watanabe H., Simakov O., Lindgens D., Gee L., Law L., Schmidt H.A., Ozbek S., Bode H. and Holstein T.W. (2009). "Multiple Wnts are involved in Hydra organizer formation and regeneration." Dev Biol 330(1): 186-199.

Li B., Jia Z., Wang T., Wang W., Zhang C., Chen P., Ma K. and Zhou C. (2012). "Interaction of Wnt/beta-catenin and notch signaling in the early stage of cardiac differentiation of P19CL6 cells." J Cell Biochem 113(2): 629-639.

Li L., Chambard J.C., Karin M. and Olson E.N. (1992). "Fos and Jun repress transcriptional activation by myogenin and MyoD: the amino terminus of Jun can mediate repression." Genes Dev 6(4): 676-689.

MacWilliams H.K. (1983a). "Hydra transplantation phenomena and the mechanism of hydra head regeneration. I. Properties of the head inhibition." Dev Biol 96(1): 217-238.

MacWilliams H.K. (1983b). "Hydra transplantation phenomena and the mechanism of Hydra head regeneration. II. Properties of the head activation." Dev Biol 96(1): 239-257.

Marlow H., Roettinger E., Boekhout M. and Martindale M.Q. (2012). "Functional roles of Notch signaling in the cnidarian Nematostella vectensis." Dev Biol 362(2): 295-308.

Martinez D.E. and Bridge D. (2012). "Hydra, the everlasting embryo, confronts aging." Int J Dev Biol 56(6-8): 479-487.

McBride K., Robitaille L., Tremblay S., Argentin S. and Nemer M. (1993). "fos/jun repression of cardiac-specific transcription in quiescent and growth-stimulated myocytes is targeted at a tissue-specific cis element." Mol Cell Biol 13(1): 600-612.

Meier-Stiegen F., Schwanbeck R., Bernoth K., Martini S., Hieronymus T., Ruau D., Zenke M. and Just U. (2010). "Activated Notch1 target genes during embryonic cell differentiation depend on the cellular context and include lineage determinants and inhibitors." PLoS One 5(7): e11481.

Meinhardt H. (2012). "Modeling pattern formation in hydra: a route to understanding essential steps in development." Int J Dev Biol 56(6-8): 447-462.

Micchelli C.A., Rulifson E.J. and Blair S.S. (1997). "The function and regulation of cut expression on the wing margin of Drosophila: Notch, Wingless and a dominant negative role for Delta and Serrate." Development 124(8): 1485-1495.

Milde S., Hemmrich G., Anton-Erxleben F., Khalturin K., Wittlieb J. and Bosch T.C. (2009). "Characterization of taxonomically restricted genes in a phylum-restricted cell type." Genome Biol 10(1): R8.

Miller A.C., Lyons E.L. and Herman T.G. (2009). "cis-Inhibition of Notch by endogenous Delta biases the outcome of lateral inhibition." Curr Biol 19(16): 1378-1383.

Moellering R.E., Cornejo M., Davis T.N., Del Bianco C., Aster J.C., Blacklow S.C., Kung A.L., Gilliland D.G., Verdine G.L. and Bradner J.E. (2009). "Direct inhibition of the NOTCH transcription factor complex." Nature 462(7270): 182-188.

Moneer J., Siebert S., Krebs S., Cazet J., Prexl A., Pan Q., Juliano C. and Böttger A. (2021). "Differential gene regulation in DAPT-treated Hydra reveals candidate direct Notch signalling targets." J Cell Sci 134(15).

Münder S., Käsbauer T., Prexl A., Aufschnaiter R., Zhang X., Towb P. and Böttger A. (2010). "Notch signalling defines critical boundary during budding in Hydra." Dev Biol 344(1): 331-345. Münder S., Tischer S., Grundhuber M., Büchels N., Bruckmeier N., Eckert S., Seefeldt C.A., Prexl A., Käsbauer T. and Böttger A. (2013). "Notch-signalling is required for head regeneration and tentacle patterning in Hydra." Dev Biol 383(1): 146-157.

Nakamura Y., Tsiairis C.D., Ozbek S. and Holstein T.W. (2011). "Autoregulatory and repressive inputs localize Hydra Wnt3 to the head organizer." Proc Natl Acad Sci U S A 108(22): 9137-9142. Ofir R., Dwarki V.J., Rashid D. and Verma I.M. (1990). "Phosphorylation of the C terminus of Fos protein is required for transcriptional transrepression of the c-fos promoter." Nature 348(6296): 80-82.

Otto J.J. and Campbell R.D. (1977). "Budding in Hydra attenuata: bud stages and fate map." J Exp Zool 200(3): 417-428.

Otto J.J. and Campbell R.D. (1977). "Tissue economics of hydra: regulation of cell cycle, animal size and development by controlled feeding rates." J Cell Sci 28: 117-132.

Palomero T., Lim W.K., Odom D.T., Sulis M.L., Real P.J., Margolin A., Barnes K.C., O'Neil J., Neuberg D., Weng A.P., Aster J.C., Sigaux F., Soulier J., Look A.T., Young R.A., Califano A. and Ferrando A.A. (2006). "NOTCH1 directly regulates c-MYC and activates a feed-forward-loop transcriptional network promoting leukemic cell growth." Proc Natl Acad Sci U S A 103(48): 18261-18266.

Pan Q., Mercker M., Klimovich A., Wittlieb J., Marciniak-Czochra A. and Bottger A. (2024). "Genetic interference with HvNotch provides new insights into the role of the Notch-signalling pathway for developmental pattern formation in Hydra." Sci Rep 14(1): 8553.

Philipp I., Aufschnaiter R., Ozbek S., Pontasch S., Jenewein M., Watanabe H., Rentzsch F., Holstein T.W. and Hobmayer B. (2009). "Wnt/beta-catenin and noncanonical Wnt signaling interact in tissue evagination in the simple eumetazoan Hydra." Proc Natl Acad Sci U S A 106(11): 4290-4295.

Prexl A., Münder S., Loy B., Kremmer E., Tischer S. and Böttger A. (2011). "The putative Notch ligand HyJagged is a transmembrane protein present in all cell types of adult Hydra and upregulated at the boundary between bud and parent." BMC Cell Biol 12: 38.

Rebay I., Fehon R.G. and Artavanis-Tsakonas S. (1993). "Specific truncations of Drosophila Notch define dominant activated and dominant negative forms of the receptor." Cell 74(2): 319-329.

Reddy P.C., Gungi A., Ubhe S., Pradhan S.J., Kolte A. and Galande S. (2019). "Molecular signature of an ancient organizer regulated by Wnt/beta-catenin signalling during primary body axis patterning in Hydra." Commun Biol 2: 434.

Reinhardt B., Broun M., Blitz I.L. and Bode H.R. (2004). "HyBMP5-8b, a BMP5-8 orthologue, acts during axial patterning and tentacle formation in hydra." Dev Biol 267(1): 43-59.

Richards G.S. and Rentzsch F. (2015). "Regulation of Nematostella neural progenitors by SoxB, Notch and bHLH genes." Development 142(19): 3332-3342.

Riedel M., Cai H., Stoltze I.C., Vendelbo M.H., Wagner E.F., Bakiri L. and Thomsen M.K. (2021). "Targeting AP-1 transcription factors by CRISPR in the prostate." Oncotarget 12(19): 1956-1961. Sassone-Corsi P., Sisson J.C. and Verma I.M. (1988). "Transcriptional autoregulation of the proto-oncogene fos." Nature 334(6180): 314-319.

Schwanbeck R., Martini S., Bernoth K. and Just U. (2011). "The Notch signaling pathway: molecular basis of cell context dependency." Eur J Cell Biol 90(6-7): 572-581.

Shih J. and Fraser S.E. (1996). "Characterizing the zebrafish organizer: microsurgical analysis at the early-shield stage." Development 122(4): 1313-1322.

Shimizu T., Kagawa T., Inoue T., Nonaka A., Takada S., Aburatani H. and Taga T. (2008). "Stabilized beta-catenin functions through TCF/LEF proteins and the Notch/RBP-Jkappa complex to promote proliferation and suppress differentiation of neural precursor cells." Mol Cell Biol 28(24): 7427-7441.

Shimomura Y., Agalliu D., Vonica A., Luria V., Wajid M., Baumer A., Belli S., Petukhova L., Schinzel A., Brivanlou A.H., Barres B.A. and Christiano A.M. (2010). "APCDD1 is a novel Wnt inhibitor mutated in hereditary hypotrichosis simplex." Nature 464(7291): 1043-1047.

Siebert S., Farrell J.A., Cazet J.F., Abeykoon Y., Primack A.S., Schnitzler C.E. and Juliano C.E. (2019). "Stem cell differentiation trajectories in Hydra resolved at single-cell resolution." Science 365(6451).

Smith K.M., Gee L. and Bode H.R. (2000). "HyAlx, an aristaless-related gene, is involved in tentacle formation in hydra." Development 127(22): 4743-4752.

Spemann H. and Mangold H. (2001). "Induction of embryonic primordia by implantation of organizers from a different species. 1923." Int J Dev Biol 45(1): 13-38.

Sprinzak D., Lakhanpal A., Lebon L., Santat L.A., Fontes M.E., Anderson G.A., Garcia-Ojalvo J. and Elowitz M.B. (2010). "Cis-interactions between Notch and Delta generate mutually exclusive signalling states." Nature 465(7294): 86-90.

Steichele M., Sauermann L., Pan Q., Moneer J., de la Porte A., Heß M., Mercker M., Strube C., Flaswinkel H., Jenewein M. and Böttger A. (2025). "Notch signaling mediates between two pattern-forming processes during head regeneration in Hydra." Life Sci Alliance 8(1): e202403054. Sudhop S., Coulier F., Bieller A., Vogt A., Hotz T. and Hassel M. (2004). "Signalling by the FGFR-like tyrosine kinase, Kringelchen, is essential for bud detachment in Hydra vulgaris." Development 131(16): 4001-4011.

Technau U. and Holstein T.W. (1995). "Head formation in Hydra is different at apical and basal levels." Development 121(5): 1273-1282.

Tursch A., Bartsch N., Mercker M., Schluter J., Lommel M., Marciniak-Czochra A., Ozbek S. and Holstein T.W. (2022). "Injury-induced MAPK activation triggers body axis formation in Hydra by default Wnt signaling." Proc Natl Acad Sci U S A 119(35): e2204122119.

Vogg M.C., Beccari L., Iglesias Ollé L., Rampon C., Vriz S., Perruchoud C., Wenger Y. and Galliot B. (2019). "An evolutionarily-conserved Wnt3/β-catenin/Sp5 feedback loop restricts head organizer activity in Hydra." Nat Commun 10(1): 312.

Waddington C.H. (1932). "Experiments on the Development of Chick and Duck Embryos, Cultivated in vitro." Philosophical Transactions of the Royal Society of London. Series B, Containing Papers of a Biological Character 221: 179-230.

Wall D.S., Mears A.J., McNeill B., Mazerolle C., Thurig S., Wang Y., Kageyama R. and Wallace V.A. (2009). "Progenitor cell proliferation in the retina is dependent on Notch-independent Sonic hedgehog/Hes1 activity." J Cell Biol 184(1): 101-112.

Watanabe H., Schmidt H.A., Kuhn A., Hoger S.K., Kocagoz Y., Laumann-Lipp N., Ozbek S. and Holstein T.W. (2014). "Nodal signalling determines biradial asymmetry in Hydra." Nature 515(7525): 112-115.

Webster G. (1966a). "Studies on pattern regulation in hydra. 3. Dynamic aspects of factors controlling hypostome formation." J Embryol Exp Morphol 16(1): 123-141.

Webster G. (1966b). "Studies on pattern regulation in hydra. II. Factors controlling hypostome formation." J Embryol Exp Morphol 16(1): 105-122.

Wesley C.S. and Mok L.P. (2003). "Regulation of Notch signaling by a novel mechanism involving suppressor of hairless stability and carboxyl terminus-truncated notch." Mol Cell Biol 23(16): 5581-5593.

Wilson T. and Treisman R. (1988). "Fos C-terminal mutations block down-regulation of c-fos transcription following serum stimulation." EMBO J 7(13): 4193-4202.

Yao T. (1945). "Studies on the Organizer Problem in Pelmatohydra Oligactis: I. The Induction Potency of the Implants and the Nature of the Induced Hydranth." Journal of Experimental Biology 21(3-4): 147-150.

Zheng X., Narayanan S., Zheng X., Luecke-Johansson S., Gradin K., Catrina S.B., Poellinger L. and Pereira T.S. (2017). "A Notch-independent mechanism contributes to the induction of Hes1 gene expression in response to hypoxia in P19 cells." Exp Cell Res 358(2): 129-139.

Ziegler B., Yiallouros I., Trageser B., Kumar S., Mercker M., Kling S., Fath M., Warnken U., Schnolzer M., Holstein T.W., Hartl M., Marciniak-Czochra A., Stetefeld J., Stocker W. and Ozbek S. (2021). "The Wnt-specific astacin proteinase HAS-7 restricts head organizer formation in Hydra." BMC Biol 19(1): 120.

Acknowledgements

I would like to express my deepest gratitude to my supervisor, Prof. Dr. Angelika Böttger, for giving me this valuable opportunity to study in her lab. Thank you for your professional guidance and useful suggestions on my projects. And thank you for your patience and support in both my work and personal life. During times when I faced challenges with my experiments, you offered me not only advice for resolving these issues but also encouragement and trust, which filled me with energy and confidence to continue my PhD studies. Moreover, thank you for your assistance in publishing my papers and for the financial support you provided after my scholarship ended. I truly appreciate all the time, help, and support you have given me.

I would also like to extend my sincere thanks to Prof. Dr. Charles David for your professional advice and kind help with my experiments. Thank you for your patience and for taking the time to discuss my projects with me. It has been a pleasure to meet and work with you, a pioneer who has made great contributions to *Hydra* research.

I also extend my sincere thanks to Dr. Tamara Mikeladze-Dvali and Prof. Dr. Nicolas Gompel for serving as members of my Thesis Advisory Committee. I am greatly appreciative of your support, valuable suggestions, and warm assistance over the past five years.

Additionally, I would like to thank my wonderful colleagues for creating such a nice atmosphere. Nikoleta Raguz, thank you for teaching me new experimental techniques and sharing your great ideas. Lara Sauermann, thank you for your constant help with my projects and personal matters. I still remember how you patiently taught me to handle *Hydra* when I first joined the lab. Astrid Heim, thank you for your technical support and for ensuring the smooth operation of our lab. Catharina Strube, I am grateful for the opportunity to supervise your master's thesis, and I am happy to have worked with you.

I would also like to acknowledge the contributions of our collaborators: Dr. Heinrich Flaswinkel for helping with the production of Kayak antibodies, and Dr. Aleksandr Klimovich for your help with microinjections.

I would also like to acknowledge the six examiners of my PhD examination committee: Prof. Dr. Angelika Böttger, Dr. Tamara Mikeladze-Dvali, Prof. Dr. Wolfgang Enard, Prof. Dr. Martin Heß, Prof. Dr. Christof Osman and Prof. Dr. Herwig Stibor. Thank you for your time in serving as my examiners and for your support.

I am grateful to the China Scholarship Council (CSC) for providing financial support for my PhD studies, and to the Graduate School Life Science Munich (LSM) for offering a platform to participate in various interesting courses and activities.

Lastly, I would like to thank my friend Jin Qiu for her warm companionship, my boyfriend Zhaoyu Du for his unwavering support and encouragement, and my parents for always being by my side.